



**HAL**  
open science

# Improvement of the production of a secondary metabolite with potent anticancer activity in cyanobacterium *Nostoc* sp. ATCC 53789, using abiotic stress : phytochemical investigation of this strain

Alexandros Polyzois

## ► To cite this version:

Alexandros Polyzois. Improvement of the production of a secondary metabolite with potent anticancer activity in cyanobacterium *Nostoc* sp. ATCC 53789, using abiotic stress : phytochemical investigation of this strain. Pharmacology. Université Paris Cité, 2020. English. NNT : 2020UNIP5019 . tel-03870703

**HAL Id: tel-03870703**

**<https://theses.hal.science/tel-03870703>**

Submitted on 24 Nov 2022

**HAL** is a multi-disciplinary open access archive for the deposit and dissemination of scientific research documents, whether they are published or not. The documents may come from teaching and research institutions in France or abroad, or from public or private research centers.

L'archive ouverte pluridisciplinaire **HAL**, est destinée au dépôt et à la diffusion de documents scientifiques de niveau recherche, publiés ou non, émanant des établissements d'enseignement et de recherche français ou étrangers, des laboratoires publics ou privés.

# Université de Paris

École doctorale MTCl (n° 563)

*(CiTCoM, UMR CNRS 8038)*

*Équipe Produits Naturels Analyse et Synthèse*

Improvement of the production of a secondary metabolite with potent anticancer activity in cyanobacterium *Nostoc* sp. ATCC 53789, using abiotic stress. Phytochemical investigation of this strain.

Par Alexandros Polyzois

Thèse de doctorat de Pharmacognosie

Dirigée par Sylvie Michel

Présentée et soutenue publiquement le 16 Décembre 2020

Devant un jury composé de:

Olivier Grovel  
Muriel Gugger  
Diana Kirilovsky  
Sylvie Michel

Pr, Faculté de Pharmacie, Université de Nantes  
Chercheur de Recherche Expert (HDR), Institut Pasteur Paris  
DR, CNRS, Institut de biologie Intégrative de la cellule- CEA  
Pr, UMR CNRS 8038, Faculté de Pharmacie, Université de Paris

Rapporteur  
Rapporteuse  
Examinatrice  
Examinatrice



Except where otherwise noted, this is work licensed under <https://creativecommons.org/licenses/by-nc-nd/3.0/fr/>



## Acknowledgments

This PhD thesis is the outcome of the effort and support of people who were by my side on this long journey to whom I am extremely grateful.

First and foremost, I would like to express my sincere gratitude to my supervisor Prof. Sylvie Michel for the continuous support of my PhD. Professor Sylvie Michel with her mentorship provided me the freedom of developing my ideas and at the same time the support and guidance to put them in order and work efficiently. We spent countless time discussing the project in congresses around Europe, in the lab, and in her office, where the door was always open to welcome me, answer my questions, and support me in work as well as importantly in the difficulties that I faced in the process.

My sincere thanks also go to Dr. Diana Kirilovsky, who hosted me at her lab, and under her supervision, I conducted a major part of the experiments. Without her contribution to the experimental plan and her extended reviewing of my writings, this work would not be accomplished.

I would like to extend my thanks to Prof. Xavier Cachet, who introduced me to molecular networks with patience and method. His expertise in the field let me understand in-depth several aspects of the subject and developed coherent techniques.

I want to warmly thank Prof. Olivier Grovel and Dr. Muriel Gugger for taking the time to review my thesis. Their productive feedback and intriguing comments were significant for the completion of this work.

I am deeply grateful to Dr. Hanh Dufat for her contribution to the development of quantification methodologies and extraction processes. Chouaha Bouzidi for her insightful comments and suggestions on HPLC. Dr. Cyril Colas (Institut de Chimie Organique et Analytique, ICOA UMR 7311 CNRS Université d'Orléans) for his contribution to UHPLC-ESI-Q-TOF-HRMS<sup>2</sup> analysis. Dr. Ellie Duran and Dr. Quoc Dang Thai for their assistance on the photobioreactor's instrumentation. I am also grateful for having been supported by the work of Alexandre Zucal, Olivier Hermet, Jennifer Bodin, the great technicians that made our work in the lab a lot more efficient.

I would like to acknowledge the European Union's Horizon 2020 research and innovation programme for funding this project and providing me the Marie Skłodowska-Curie fellowship. The consortium not only offered the grant for my research activity but permitted me to have an overall view on the research field of cyanobacterial biotechnological applications through a series of seminars, workshops, and congresses throughout Europe. Working together with the SE2B team made these meetings unforgettable and the outcome even more productive.

I could not have imagined that I could go through that 3-year period without the support of my labmates. From Paris Descartes lab Camille, Kedmany, Andrea, Efi, Evgeniayour daily support and all the small moments changed the lab routine. Julia the Brazilian sweets that you prepared from time to time and Maxime, your music choices gave a joyful spirit in the lab. Especially, I like to thank Tsvetelina for her support, she finished her project first and was an example of how to work with method and not give up.

Officemates from CEA, you will always have a special place in my memories. You welcomed me from the first day. Fernando, Pablo you made me feel in a short period like part of your lab and you taught me how a good team can collaborate and have fun inside the lab and in free time.

The project was a unique chance to appreciate all the love of my friends and family. In the beginning, they were the reason for continuing my studies, as they were an inspiration, believed in me, and made me think that everything is achievable. Then, they were always supportive of my choice throughout these years. The distance made their support even more present. They visited me at every chance, and every time I returned home it was a spontaneous reason to celebrate. For your constant support and unconditional love, I love you all dearly.

Improvement of the production of a metabolite with potent anticancer activity in cyanobacterium *Nostoc* sp. ATCC 53789, using abiotic stress. Phytochemical investigation of this strain.

Cyanobacteria is one of the most ancient and largest groups of bacteria on Earth. They produce a range of compounds useful for human and its activities, from biofuels to nutrition. They also, however, produce secondary metabolites with toxic effect, the cyanotoxins. The study of these toxins may lead to novel pharmaceutical agents. We examined the cyanotoxin cryptophycin-1, as it has been reported to possess significant anticancer properties. It interacts with tubulin's *Vincadomain* and disrupts the microtubule's dynamics leading to apoptosis. Unfortunately, despite its high potency, its synthesis provides insufficient yield for industrial use. However, stressing cyanobacteria by modification of the culture's environmental conditions, can be a means for increasing metabolite's production yield. Our work was performed with *Nostoc* sp. ATCC 53789 which is currently the only commercially available strain among the three species producing this metabolite. We examined a range of abiotic culture parameters in relation to light conditions (photoperiod, intensity, wavelength), pH, temperature and medium composition. Then, the synergic effect of combined conditions was evaluated, as well as the effect of high-scale cultivation in a photobioreactor. Growth was measured and metabolite concentration was calculated through an HPLC method, developed for small-volumes quantification. Growth and toxin's productivity curves were then drawn. It was concluded that orange-red constant light of medium intensities provided the optimum yield. Nitrates were also needed in medium, while the strain performed better at 25°C and in a pH range 8.5-9.0. Moreover, the combined conditions were shown to have a positive synergic effect, while the cultivation in a photobioreactor increased significantly the obtained yield, even if the growth rate was lower. In addition to the examination of cryptophycin-1, the total molecular fingerprint of the strain was examined by molecular networks from UHPLC-ESI-Q-TOF-HRMS<sup>2</sup> analysis. Finally, these results indicate the presence of 9 cryptophycin-analogues and their respective proportions in *Nostoc* sp. ATCC 53789, unidentified in this strain to this date. Through the molecular networks' aspect, the analogues were observed to be mostly expressed in the late exponential phase and under the developed combined optimal culture conditions, the major analogues seemed to be overexpressed. The results of this work set the grounds for further research and industrial exploitation in the field of novel cyanobacterial anticancer agents.

**Keywords:** Cryptophycin; *Nostoc* sp. ATCC 53789; cyanotoxin; abiotic stress; photobioreactor; molecular networking; UHPLC-HRMS<sup>2</sup>

Amélioration par stress abiotique de la production d'un métabolite secondaire présentant une puissante activité antitumorale chez une cyanobactérie : *Nostoc* sp. ATCC 53789. Investigation phytochimique de la souche.

Les cyanobactéries sont un des plus anciens et des plus grands groupes de bactéries sur la terre. Elles produisent de nombreux composés utiles pour l'homme et ses activités, allant des biofuels jusqu'aux nutriments. Certaines espèces produisent cependant des métabolites secondaires toxiques comme les cyanotoxines. L'étude de ces toxines peut conduire à de nouveaux agents pharmaceutiques doués d'un intérêt thérapeutique. Parmi ces composés, la cryptophycine-1 est un composé qui s'est montré posséder des propriétés antitumorales significatives confirmées par des essais cliniques. Le mécanisme d'action fait intervenir une interaction avec le domaine Vinca de la tubuline. La dynamique des microtubules est détruite conduisant à l'entrée en apoptose des cellules. Malheureusement, malgré l'intérêt thérapeutique et la grande puissance de ce composé, sa production industrielle n'est pas évidente, en particulier par synthèse totale. La culture sous stress biotique ou abiotique des cyanobactéries en modifiant les conditions de culture peut apparaître comme un moyen d'accroître le rendement de production des métabolites. Notre travail a porté sur la souche *Nostoc* sp. ATCC 53789 qui est actuellement la seule souche commerciale disponible parmi les trois souches productrices de ce métabolite. Nous avons donc étudié les effets d'une gamme de paramètres abiotiques sur la croissance de la souche en culture et la production de cryptophycine. L'effet de la lumière : photopériode, intensité, longueur d'onde a tout d'abord été étudié. L'influence d'autres facteurs comme le pH, la température et la composition des milieux de culture a également été évaluée. Enfin, les différents paramètres de culture optimisés ont été appliqués à une production en photobioréacteur afin de déterminer si lors d'une culture à plus large échelle, un effet de synergie pouvait être observé. Pour chacun des paramètres étudiés, la croissance de la biomasse est appréciée par mesure de la densité optique ou de sa masse et la production de cryptophycine déterminée, selon une méthode HPLC mise au point afin permettre la mesure de petites concentrations en cryptophycine. Les courbes de croissance de la biomasse et de production de cryptophycine ont ainsi pu être tracées. Les rendements optimums ont été obtenus avec un éclairage par une lumière orange-rouge avec une exposition constante à une lumière d'intensité moyenne. Pour la croissance de *Nostoc* sp. la présence de nitrates dans le milieu est nécessaire et cette croissance est meilleure si la souche est cultivée à une température de 25 degrés à un pH compris entre 8.5-9.0. L'application de l'ensemble des conditions optimales a permis de constater un effet synergique positif. La culture en photobioréacteur, en appliquant les conditions optimales combinées, montrent une augmentation significative de la production de cryptophycine avec

cependant, une croissance plus lente de la souche. Enfin, la dernière partie de ce travail, se propose d'établir, en dehors de la présence de cryptophycine -1 déjà établie, une première approche phytochimique de la souche *Nostoc* sp. ATCC 53789. Des extraits réalisés à partir de biomasses obtenues dans différentes conditions de culture ont été soumis à des analyses UHPLC-ESI-Q-TOF-HRMS<sup>2</sup>. Les données obtenues ont permis de construire des réseaux moléculaires permettant d'observer la présence d'analogues de série cryptophycine. Neuf analogues potentiels de série cryptophycine non encore identifiés dans cette souche, à ce jour, ont pu être mis en évidence. Ces derniers sont principalement produits en phase exponentielle tardive. Dans les conditions optimisées, la production des dérivés de série cryptophycine semblent surexprimée. Les résultats de ce travail jettent les bases d'une recherche approfondie sur l'exploitation industrielle de cyanobactéries pour la production d'agents anticancéreux.

**Mots-clés:** Cryptophycine; *Nostoc* sp. ATCC 53789; cyanotoxine; abiotic stress; photobioréacteur; réseaux moléculaires; UHPLC-HRMS<sup>2</sup>



## Contents

|   |    |
|---|----|
| Acknowledgments .....   | 3  |
| Contents .....  | 8  |
| Table of figures .....  | 11 |
| Table of tables .....   | 13 |
| List of abbreviations .....   | 14 |
| General introduction .....  | 17 |
| 1 Chapter 1 - Cyanobacterial physiology, Cyanotoxin of interest- cryptophycin.....  | 22 |
| 1.1 Cyanobacterial treat and threats .....  | 22 |
| 1.1.1 Applications of Cyanobacterial products in people’s lives (biofuels, agriculture, nutrition, food supplements, cosmeceuticals)..... | 22 |
| 1.1.2 Cyanotoxins .....   | 24 |
| 1.2 Physiology of cyanobacteria.....  | 28 |
| 1.2.1 Cyanobacterial cells.....   | 28 |
| 1.2.2 Heterocysts.....  | 31 |
| 1.2.3 Akinetes.....   | 32 |
| 1.2.4 Hormogonia.....   | 33 |
| 1.2.5 Taxonomy of the producing strain .....  | 33 |
| 1.3 Phytochemical Profile of cyanobacteria.....   | 34 |
| 1.3.1 Proteins.....   | 34 |
| 1.3.2 Carbohydrates & Polysaccharides .....   | 35 |
| 1.3.3 Lipids.....   | 35 |
| 1.3.4 Other compounds.....  | 36 |
| 1.4 Historical development & Natural occurring analogues .....  | 37 |
| 1.4.1 Detection on <i>Nostoc</i> sp. MB5357, focus on antifungal activity .....   | 37 |
| 1.4.2 Detection on <i>Nostoc</i> sp. GSV 224, focus on cytotoxic activity .....   | 38 |
| 1.4.3 Detection on <i>Nostoc</i> sp. ASN_M .....  | 38 |
| 1.4.4 Naturally occurring analogues.....  | 39 |
| 1.5 Cryptophycin’s mechanism of action .....  | 42 |
| 1.5.1 Affinity of cryptophycin for <i>Vinca</i> domain .....  | 43 |
| 1.5.2 Cryptophycin’s activity comparing to known anticancer drugs .....   | 44 |
| 1.5.3 Mechanism of action at the molecular level.....   | 45 |
| 1.6 Structure activity relationship of cryptophycin-analogues .....   | 47 |
| 1.6.1 Structure activity relationship of natural occurring analogues.....   | 47 |
| 1.6.2 Structure activity relationship of synthetic analogues.....   | 48 |
| 1.6.3 Case of Cryptophycin-52 .....   | 49 |
| 1.7 Gene cluster .....  | 51 |
| 1.7.1 Cryptophycin’s gene cluster .....   | 51 |

|       |  |     |
|-------|--|-----|
| 1.7.2 | Genome sequence of <i>Nostoc</i> sp. ATCC 53789 .....  | 52  |
|       | Conclusion - Chapter 1 .....   | 54  |
| 2     | Chapter 2 - Optimizing culture conditions for cryptophycin overproduction.....                                 | 58  |
| 2.1   | Review on the culture parameters.....  | 58  |
| 2.1.1 | Light photoperiod.....   | 59  |
| 2.1.2 | Light wavelength .....   | 60  |
| 2.1.3 | Light intensity .....  | 61  |
| 2.1.4 | Medium's composition.....  | 63  |
| 2.1.5 | The effect of pH.....  | 65  |
| 2.1.6 | The effect of temperature.....   | 66  |
| 2.2   | Review on photobioreactors and photoacclimation.....   | 69  |
| 2.2.1 | Introduction to photoacclimation .....   | 69  |
| 2.2.2 | Photobioreactors.....  | 71  |
| 2.3   | Personal work: involved techniques and methods in cyanobacterial culture .....                                 | 73  |
| 2.3.1 | Working under sterile conditions.....  | 73  |
| 2.3.2 | Growth observations.....   | 75  |
| 2.3.3 | Microscopic observations.....  | 77  |
| 2.4   | Personal work: involved techniques in cryptophycin's quantification method.....                                | 78  |
| 2.4.1 | Development of extraction and quantification method of cryptophycin from small volumes.....                    | 78  |
| 2.5   | Overproduction of cryptophycin through optimizing the culture conditions of <i>Nostoc</i> sp. ATCC 53789 ..... | 81  |
| 2.5.1 | Light intensity experiment.....  | 82  |
| 2.5.2 | Photoperiod experiment .....   | 85  |
| 2.5.3 | Wavelength experiment.....   | 87  |
| 2.5.4 | pH experiment.....   | 88  |
| 2.5.5 | Medium's composition experiment .....  | 90  |
| 2.5.6 | Temperature experiment.....  | 92  |
| 2.5.7 | Combined set of optimal conditions .....   | 93  |
| 2.5.8 | Cryptophycin production on scale-up conditions .....   | 95  |
|       | Conclusion – Chapter 2.....  | 100 |
| 3     | Chapter 3 - Examination of strain's phytochemical profile through molecular networks study                     | 104 |
| 3.1   | Review of applied cryptophycin's isolation and purification processes .....                                    | 104 |
| 3.2   | Personal work on cryptophycin isolation-purification process.....  | 106 |
| 3.2.1 | Occupation of dry biomass.....   | 106 |
| 3.2.2 | Extraction method development .....  | 109 |
| 3.2.3 | Development of two purification methods for the study of cryptophycin and strain's phytochemical profile.....  | 112 |

|       |  |     |
|-------|--|-----|
| 3.3   | Personal work: Phytochemical investigation through UHPLC-ESI-Q-TOF-HRMS <sup>2</sup> analysis and molecular networking ..... | 120 |
| 3.3.1 | Introduction in molecular networking bioinformatic approach .....  | 120 |
| 3.3.2 | UHPLC-ESI-Q-TOF-HRMS <sup>2</sup> method development .....   | 122 |
| 3.3.3 | Parametrization of the softwares involved in the molecular networking .....  | 123 |
| 3.3.4 | Results on cryptophycin's analogues in <i>Nostoc</i> sp. ATCC 53789 .....  | 125 |
| 3.3.5 | Results on general phytochemical profile of <i>Nostoc</i> sp. ATCC 53789.....  | 129 |
|       | Conclusion – Chapter 3.....  | 133 |
|       | General conclusion and future perspectives.....  | 134 |
|       | Annexes – Instrumentation of used equipment and techniques.....  | 137 |
|       | High Performance Liquid Chromatography.....  | 137 |
|       | Column Chromatography .....  | 139 |
|       | Thin-layer Chromatography .....  | 140 |
|       | Mass spectrometry (MS) .....   | 141 |
|       | Bibliographic References.....  | 144 |
|       | Résumé des travaux.....  | 157 |

## Table of figures

|   |     |
|---|-----|
| Figure 1.1: Structure Nostocyclopeptide M1 .....  | 37  |
| Figure 1.2: Time culture's growth, in packed cell volume, and cry production in a fermentor.....          | 38  |
| Figure 1.3: Structures of Cry-1 and -53, indicating the four units cyclic sequence A, B, C, D.....        | 39  |
| Figure 1.4: Demonstrating the Cry selectivity in <i>Vinca</i> domain .....                                | 43  |
| Figure 1.5: Cry inhibits MTP polymerization for longer period comparing to Vinblastine, Colchicine .      | 45  |
| Figure 1.6: Ring-shape formation after Cry-tubulin interaction .....                                      | 46  |
| Figure 1.7: Comparative depiction of the bound to bovine $\beta$ -tubulin .....                           | 47  |
| Figure 1.8: The Cry gene cluster and the deduced PKS/NRPS assembly line.....                              | 52  |
| Figure 2.1: Photoacclimation development, measured as ratio of OD <sub>680</sub> /OD <sub>735</sub> ..... | 71  |
| Figure 2.2: Instrumentation of bubble column photobioreactor.....   | 72  |
| Figure 2.3: Instrumentation of airlift photobioreactor with .....   | 72  |
| Figure 2.4: Sterility tests using petri-dishes of agar with Trypticase-Soja .....                         | 74  |
| Figure 2.5: The culture containers differ in size, shape and the top.....                                 | 74  |
| Figure 2.6: Optical density to dry biomass .....  | 76  |
| Figure 2.7: Filaments with vegetative cells .....   | 77  |
| Figure 2.8: Filaments with heterocysts .....  | 78  |
| Figure 2.9: Culture of long filaments with vegetatives, and short filaments which are hormogonia...       | 78  |
| Figure 2.10: Extraction and quantification process from small volumes of culture .....                    | 80  |
| Figure 2.11: Calibration curve to translate AUC value into "µg/in sample of 20 mL" .....                  | 81  |
| Figure 2.12: Light intensity experiment instrumentation of MC1000 multi-incubator. ....                   | 83  |
| Figure 2.13: The effect of light intensity on growth and Cry production.....                              | 83  |
| Figure 2.14: Photoperiod experiment instrumentation on Brunswick Innova 4340.....                         | 85  |
| Figure 2.15: The effect of light photoperiod on growth and Cry production.....                            | 86  |
| Figure 2.16: The effect of light wavelength on growth and Cry production.....                             | 87  |
| Figure 2.17: Observation of cultures after 7 days inoculation with Tris and Glycylglycine buffers.....    | 89  |
| Figure 2.18: The effect of pH on growth and Cry production.....   | 89  |
| Figure 2.19: The effect of medium's composition on growth and Cry production.....                         | 91  |
| Figure 2.20: The effect of temperature on growth and Cry production.....                                  | 92  |
| Figure 2.21: The effect of combined conditions on growth and Cry production.....                          | 94  |
| Figure 2.22: 15 L photobioreactor with cylindrical main chamber. ....                                     | 96  |
| Figure 2.23: Metal jacket with water circulation system the bottom of the photobioreactor.....            | 96  |
| Figure 2.24: The effect of scale-up cultivation on growth and Cry production.....                         | 98  |
| Figure 3.1: Schematic representation of the dry biomass occupation process.....                           | 107 |
| Figure 3.2: Isolation of dry biomass process .....  | 108 |
| Figure 3.3: Comparison of extraction solvent systems <i>via</i> HPLC quantification .....                 | 109 |
| Figure 3.4: Comparative HPLC-chromatograms for the extraction of Cry-1.....                               | 110 |
| Figure 3.5: Extraction process from high-scale volumes.....   | 111 |
| Figure 3.6: Extraction-purification method.....   | 112 |
| Figure 3.7: TLC on first OPC.....   | 114 |
| Figure 3.8: TLC on second OPC.....  | 116 |
| Figure 3.9: Comparative chromatogram of Cry-1 standard to FR.140-217 .....                                | 117 |
| Figure 3.10: Absorption spectrum of peak at ret.time 22.85 min .....                                      | 117 |
| Figure 3.11: TLC of flash column chromatography .....   | 119 |
| Figure 3.12: Proposed fragmentation pathway .....   | 127 |
| Figure 3.13: Cry cluster A and B .....  | 128 |
| Figure 3.14: Comparison of Cry content in relation to culture condition .....                             | 129 |

---

|   |     |
|---|-----|
| Figure 3.15: Comparison of Cry content in late exponential phase to log phase .....               | 129 |
| Figure 3.16: Total molecular network of the examined samples.....                                 | 131 |
| Figure 3.17 Comparative chromatogram of OPT_1.2 and OPT_0.2.....                                  | 132 |
| Figure 3.18 Focus on the part of cluster-complex H. comparison of OPT_0.2 and OPT_1.2 .....       | 132 |
| Figure 3.19 Focus on the part of cluster-complex H. comparison of augmenting polarity fractions . | 132 |
| Figure 4.1 : HPLC system illustration .....   | 137 |
| Figure 4.2 : OPC instrumentation.....   | 140 |
| Figure 4.3: Instrumentation of electrospray ionization source.....                                | 142 |

## Table of tables

|  |     |
|--|-----|
| Table 1.1: Categorization of cyanotoxins, and representative structures .....                      | 27  |
| Table 1.2: Taxonomy of <i>Nostoc</i> sp. ....  | 33  |
| Table 1.3: Structures of natural occurring Cry analogues in relation to the Units A, B, C, D. .... | 41  |
| Table 1.4: Toxicity of Cry analogues in KB, LoVo, and SKOV3 cell lines .....                       | 42  |
| Table 1.5: Toxicity of cryptophycin in comparison to vinblastine, colchicine and taxol .....       | 45  |
| Table 2.1: Gradient mode H <sub>2</sub> O/MeCN.....  | 79  |
| Table 2.2: BG11 & BG11o composition .....  | 90  |
| Table 3.1: Review of cryptophycin's isolation procedures.....                                      | 106 |
| Table 3.2: Comparison of extraction solvent systems .....  | 110 |
| Table 3.3: List of examined cultures.....  | 110 |
| Table 3.4: List of examined extracts and respective yields .....                                   | 111 |
| Table 3.5: List of "MIX_A" fractionation.....  | 113 |
| Table 3.6: List of grouped fractions.....  | 113 |
| Table 3.7: Gradient mode solvent system.....   | 114 |
| Table 3.8: Fractionation of A2_FR.63-65.....   | 115 |
| Table 3.9: Gradient mode solvent system.....   | 118 |
| Table 3.10: Grouped fractions of B_BG11.....   | 118 |
| Table 3.11: Gradient mode solvent system.....  | 122 |
| Table 3.12: MZmine and GNPS settings .....   | 124 |
| Table 3.13: Review of Cry-analogues, detected in <i>Nostoc</i> sp. GSV 224 .....                   | 125 |
| Table 3.14: Hypothesis of detected compounds.....  | 127 |
| Table 3.15: Cry-analogues' proportions in the two producer strains .....                           | 128 |

## List of abbreviations

|       |  |          |  |
|-------|--|----------|--|
| AcOEt | Ethyl acetate  | MeOH     | Methanol                                     |
| ADDA  | (2S,3S,8S,9S)-3-amino-9-methoxy-2,6,8-trimethyl-10-phenyldeca-4,6-dienoic acid | MS       | Mass spectrometry                            |
| ADP   | Adenosine diphosphate  | MTD      | Maximum tolerated dose                       |
| ATP   | Adenosine triphosphate   | MTP      | Microtubule protein                          |
| AUC   | Area under the curve   | MUFA     | Monosaturated fatty acids                    |
| AW    | Artificial seawater  | NADPH    | Nicotinamide adenine dinucleotide phosphate  |
| Car   | Carotenoid   | Ncp      | Nostocyclopeptide                            |
| Chl   | Chlorophyll  | Nif      | Nitrogen fixation gene cluster               |
| CID   | Collision induced dissociation   | NOD      | Noduarin                                     |
| Crp   | Cryptophycin's gene cluster  | NRP      | Nonribosomal peptides                        |
| Cry   | Cryptophycin   | NSCLC    | Non-small cell lung cancer                   |
| CV    | Column-volume  | NW       | Natural seawater                             |
| CYN   | Cylindrospermopsin   | OD       | Optical density                              |
| DAD   | Diode-array detector   | ODS      | Octadecyl-silica                             |
| DBC   | Dry biomass calculation  | OOSS     | Oxalic acid soluble substance                |
| DCM   | Methylene chloride   | OPC      | Open column chromatography                   |
| DLT   | Dose limiting toxicity   | PBR      | Photobioreactor                              |
| DNA   | Deoxyribonucleic acid  | PHB      | Poly- $\beta$ -hydroxybutyrate               |
| EPA   | Eicosapentaenoic acid  | Pheo     | Pheophytin                                   |
| EPS   | Extracellular polysaccharides  | PK       | Polyketides                                  |
| ESI   | Electrospray ionization  | PKS      | Polyketides synthetase                       |
| EtOH  | Ethanol  | PLFA     | Polar lipids                                 |
| FA    | Fatty acid   | PP       | Protein phosphatase                          |
| FBMN  | Feature Based Molecular Networking   | PPB      | Pheophorbide                                 |
| FR.   | Fraction   | PS       | Photosystem                                  |
| GDP   | Guanosine 5'-diphosphate   | Psb      | PhotosystemII protein                        |
| GLA   | $\gamma$ -linolenic acid   | PSP      | Paralytic shellfish poisoning                |
| GLFA  | Glycolipids  | PUFA     | Polyunsaturated fatty acid                   |
| GNPS  | Global Natural Products Social Molecular Networking                            | Q        | Quadrupole                                   |
| GTP   | Guanosine 5'-triphosphate  | RNA      | Ribonucleic acid                             |
| HEP   | Heterocyst envelope polysaccharide   | ROS      | Dangerous species of oxygen                  |
| HEPES | N-2-hydroxyethylpiperazine-N'-2-ethanesulfonic acid                            | Rpm      | Rounds per minute                            |
| HGL   | Heterocyst specific glycolipid   | Ret.time | Retention time                               |
| HIV   | Human immunodeficiency viruses   | SAR      | Structure-activity-relationship              |
| HPLC  | High-performance liquid chromatography   | STX      | Saxitoxin                                    |
| HRMS  | High resolution mass spectrometry  | T        | Temperature                                  |
| IC50  | half maximal inhibitory concentration  | TGA      | Triglycerides                                |
| L:D   | Light:Dark   | TLC      | Thin-Layer Chromatography                    |
|       |  | TMH      | Transmembrane $\alpha$ -helix                |
|       |  | TOF      | Time of flight                               |
|       |  | UHPLC    | Ultra high performance liquid chromatography |

|            |                               |           |                                |
|------------|-------------------------------|-----------|--------------------------------|
| LC         | Liquid chromatography         | UV        | Ultraviolet                    |
| <i>m/z</i> | Mass-to-charge ratio          | Vis       | Visible                        |
| MC         | Microcystin                   | VS        | Vanillin-sulfuric acid reagent |
| MeCN       | Acetonitrile (methyl cyanide) | $\lambda$ | Wavelength                     |





## General introduction

Nowadays, cancer is the second leading cause of death. For instance, it was responsible for more than 6 thousand deaths in the United States in 2019, while it is estimated that 1 in 6 deaths is due to cancer (Siegel R.L. 2019). The general betterment of patients' life-quality and the treatment of the disease were always a primary goal for the medicinal society. Indeed, the pharmaceutical industry invests in cancer research 5.3– 6.4 € billion annually, mainly in Europe and the United States. At the same time, the economic cost of cancer in 2010 was estimated at approximately 1.16 US\$ trillion (Knaul F.M. *et al.* 2014). Natural products consist of a significant source for the development of novel anticancer agents (Da Rocha A.B. *et al.* 2001, Gordaliza M. 2007). Numerous marine products and several cyanobacterial compounds have been examined in that direction (Luesch H. *et al.* 2002, Simmons T.L. *et al.* 2005).

One of these prominent compounds is the cyanobacterial toxin cryptophycin. Cryptophycin-1, which is the major analogue of cryptophycins group, was firstly isolated in 1990 (Schwartz R.E *et al.* 1990), and its high potency was soon demonstrated (Golakoti T. *et al.* 1994). Indeed, it interacts with tubulin's *Vinca* domain leading to apoptosis (Smith C.D. and Zhang X. 1996). Inspired by that significant biological activity, the research on the field continued in the following years, while a synthetical analogue, cryptophycin-52, was tested in Clinical Phase I and II (Edelman M.J. *et al.* 2003). Though, despite the studies on chemical synthesis the process until today provides insufficient yield for industrial exploitation (Moore R.E *et al.* 1996). The metabolite's isolation from the natural producer microorganism is an alternative solution. However, as cyanotoxins are expressed in low quantities, it would be necessary to develop a set of culture conditions which would enable the maximization of metabolite's production.

There are only three strains which naturally produce that cyanotoxin, while only one - *Nostoc* sp. ATCC 53789 - is commercially available. Few studies have been done for the specific species regarding its culture conditions as well as its phytochemical profile. Specifically, there is not identified any more cryptophycin analogue than cryptophycin-1.

The thesis' objective is to increase cryptophycin's production by forming the optimal set of abiotic culture parameters. Then, as until today few are known for the specific strain, we aim to examine its phytochemical profile, and how this is affected by the developed conditions. So, the main experimental session is divided into two parts.

In the first part, we optimized the culture conditions, and we tested the scale-up adaptation in photobioreactor cultivation. A collaboration with Dr. Diana Kirilovsky's lab (CNRS, Institut de biologie Intégrative de la cellule- CEA) permitted the use of specialized culture facilities. It also enabled us to focus on the cyanobacterial photosynthetic apparatus and to explain the obtained results.

Furthermore, a collaboration with Phycosource (Garges-Les-Gonesse, France) allowed us to work with high-scale photobioreactors, and to understand how the strain would behave under industrial production.

In the second part, it was studied the general phytochemical profile of the strain through molecular networks aspect from UHPLC-ESI-Q-TOF-HRMS<sup>2</sup> analysis. That analysis was conducted in collaboration with Institut de Chimie Organique et Analytique (ICOA UMR 7311 CNRS Université d'Orléans), and Dr. Cyril Colas.

It was further examined, through comparative interpretation of the networks, how that profile changes during the culture's growth and under different culture conditions. Lastly, as until now only cryptophycin-1 was identified in the examined strain, it was investigated which analogues might be present.

The thesis was in the frame of "Solar Energy to Biomass – Optimization of light energy conversion in plants and microalgae - SE2B" (se2b.eu), and funded by European Union's Horizon 2020 research and innovation programme under the Marie Skłodowska-Curie grant agreement No. 675006. The 15 involved projects aimed at the optimizing the yield of valuable biological components through studying the parameter of light energy. The academic consortium and the involved trainings and workshops provided scientific support for the general better outcome.

That manuscript is split into three chapters:

**Chapter 1** introduces the producing microorganism and the compound of interest. In relation to the microorganism, it is presented its physiology -in relation to the differences among the three cell differentiations-, and the general phytochemical profile of *Nostoc* sp. Then, regarding cryptophycin, it is examined its mechanism of action, its structure-activity-relationship, and the involved gene cluster.

**Chapter 2** first reviews the various parameters influencing the culture of the strain. Then, it describes the material and techniques that were applied in the culture treatment, and the chemical-analysis methods which we developed for cryptophycin's quantification. At last, it is the core of the chapter where the experiments of the culture conditions and the obtained outcome are presented. Following the conditions' development, the scale-up adaptation was tested in scale-up photobioreactor facilities.

**Chapter 3** examines the phytochemical profile of *Nostoc* sp. ATCC 53789 through the aspect of molecular networks, visualizing the data from UHPLC-ESI-Q-TOF-HRMS<sup>2</sup> analysis. The examined samples came from photobioreactor-cultures, so at a first step are presented the developed techniques for extraction and purification for high-scale volume. Lastly, UHPLC-HRMS<sup>2</sup> data were interpreted and we made assumptions and hypotheses for phytochemical composition and analogues presence based on the obtained networks.



## Chapter 1

Cyanobacterial physiology,  
Cyanotoxin of interest- cryptophycin



# 1 Chapter 1 - Cyanobacterial physiology, Cyanotoxin of interest- cryptophycin

The first chapter is divided into two parts. The first part is about cyanobacterial physiology and metabolites (1.1-1.3), while the second part focuses specifically on the metabolite of interest - cryptophycin (Cry) (1.4-1.7).

So, in the first part, we examine cyanobacterial compounds which can be useful in people lives from nutritional to cosmeceutical applications, though sometimes they can be harmful -and then are called cyanotoxins. Then, we study the physiology of the cell, the three different cell types in *Nostoc* sp. and their related metabolic processes. Lastly, the general phytochemical profile of *Nostoc* species is presented. In the second part, we focus on cryptophycin. Beginning from the historic development, we present the natural Cry-analogues, their mechanism of action and lastly the implicated genes on their expression process.

## 1.1 Cyanobacterial treat and threats

### 1.1.1 Applications of Cyanobacterial products in people's lives (biofuels, agriculture, nutrition, food supplements, cosmeceuticals)

Cyanobacteria, or as they called "green-blue-algae", are gram-negative prokaryotic microorganisms. Specifically, they belong in the kingdom of Prokaryota, division of Eubacteria, class Cyanobacteria. They consist of a broad group as they include approximately 150 genera and 2000 species (Hitzfeld B.C. *et al.* 2000). Due to the significant number of genera, noticeable variations are observed in their habitats, from hot-springs to frozen lakes, as well as in their dimensions from few  $\mu\text{m}$  up to visible to the naked eye. They are adaptable also to environmental changes, and under some conditions, due to their fast growth, they are considered as invasive species (Paerl H.W and Paul V.J. 2012). It is one of the most ancient groups as it dates back more than 3.5 billion years. They serve a valuable role in the global ecosystem as they capture carbon dioxide and supply oxygen through photosynthesis and also supply nitrogen through nitrogen fixation process (Percival S.L. and Williams D.W.2014). That heterogeneity among the genera provides the chance for a range of applications of the cyanobacterial products in many aspects of people's lives (Zahra Z. *et al.* 2020). These applications vary from nutrition, biofuels, and biofertilizers to pharmaceuticals and cosmeceuticals.

Cyanobacteria produce a large number of secondary metabolites, including toxins, with a wide range of biological activities. Their therapeutic effects are predominant in the field of antibiotics, antiviral and antifungal compounds, and antitumor drugs (Vijayakumar S. and Menakha M. 2015, Singh R.K. *et*

*al.* 2011). Noscomin from *Nostoc commune* was reported with antibacterial activity against *B. cereus* and *E. coli* (Jaki B. *et al.* 1999). A family of about 80 indole alkaloids (hapaloindole type alkaloids) has been identified only from four genera of *Stigonematales* (*Fischerella*, *Hapalosiphon*, *Westiella*, *Westiellopsis*). They exhibit antimicrobial activity and antialgal activity and are also toxic to insects (Walton K. and Berry J.P. 2016).

Several cyanobacteria exhibit antiviral properties. Acidic polysaccharides such as spirulan from *Spirulina* sp. (Patterson P. *et al.* 1993) or nostoflan from *Nostoc flagelliforme* (Kaneykio K. *et al.* 2005) are potent virus inhibitors against several enveloped viruses as human immunodeficiency viruses (HIV) and herpes simplex (HSV). Cyanovirin N from *Nostoc ellipsosporum* is a protein which activity is mediated through high-affinity interactions with the viral surface envelope glycoproteins (Botos I. *et al.* 2003). Scytovirin is a 95 amino acid polypeptide containing five intra chain disulphide bonds extracted from *Scytonema varium*. It binds to the envelope glycoprotein of HIV and inactivates the virus in low nanomolar concentrations (Singh R.K. *et al.* 2011). Lastly, anticancer agents have been developed based on cyanobacterial products. Some well-known compounds are curacin A from *Lyngbya majuscula* and dolastatin 10 which is originally isolated from *Dolabella auricularia*, and actually is a cyanobacterial metabolite, obtained from *Symploca* sp. (Singh R.K. *et al.* 2011).

Furthermore, several primary metabolites with complex sugar, proteins, amino acids, phycocyanin, chlorophyll, beta-carotene, essential fatty acids could be useful as food supplements. The well-known “spirulina” obtained from cyanobacteria of the following genus: *Arthrospira maxima* and *A. platensis* culture, and holds the most significant share of the market. *Spirulina* has a surprisingly high percentage of proteins (65-70% of dry weight), vitamins, and minerals. Moreover, it contains significant portions of  $\gamma$ -linolenic acid (GLA), phycocyanin,  $\beta$ -carotene, and polysaccharides. Based on that composition *Spirulina* is consumed widely worldwide as a food supplement and cosmeceutical for its antioxidant and anti-inflammatory activity as well as for its ability to prevent hypercholesterolemia (Hongsthong A. and Bunnag B. 2009). It should be highlighted the use of cyanobacteria in nutritional habits and the food supplements market. Several species of genus *Nostoc* have been used from ancient years as the primary source of nutrition. For example, *Nostoc fragelliforme* is a common ingredient of Chinese cuisine, mainly in the northern and northwest parts of China. Due to its appearance, it is called “Fa-cai” (hair-like vegetable) and its annual yield can reach up to 0.5 tons (Qiu B. *et al.* 2002).

The ongoing overconsumption of fossil fuels in combination with the climatic change crisis lead to the need for alternative fuels’ development. In that way, cyanobacteria are proposed as an alternative source due to their high lipidic content (Barbosa M.J and Wijffels R.H. 2017, Nozzi N.E *et al.* 2013). That idea has been developed in the last 5 decades with pioneering projects, such as the Aquatic Species Program, starting in U.S.A already in 1978 (Sheehan J. *et al.* 1998). Nowadays, the



value of biodiesel is that low that the cost price should be lower than 0.26 € per kg dry biomass. However, based on the current facilities, the cost price is approximately 0.68 € per kg of dry biomass. As can be easily understood, the biodiesel market is not profitable under the current conditions. One of the reasons that restrict the market is the required space for the facilities. Remarkably, in the case that Europe wanted to replace fossil fuel with biodiesel, an area similar to Portugal would be required just for the reactors (Wijffels R.H. *et al.* 2010). A second reason is the yield of lipid production. Several studies focus on the amelioration of lipid production per cell to decrease the production cost. In these studies, it has been shown that under stress conditions, such as nitrogen starvation, the lipid content is elevated (Wilhelm C. and Jakob T. 2011). A combination of new facilities, which would occupy less space, with the development of strains that produce higher lipid content, is needed to make biodiesel profitable and cyanobacteria an alternative source of biofuel. Cyanobacteria have also been used by humans indirectly to support his activities in both agriculture and animal farming. In the first case, cyanobacteria contribute to soil's water-holding capacity while at the same time improve its physicochemical characteristics by enriching its mineral nutrient profile. Nitrogenfixation is a key-process at this step as it supplies the crops with the needed amount of nitrates, and it increases land's fertility (Singh J.S. *et al.* 2016). Regarding the second case, it has a significant contribution to fisheries. The cyanobacterial blooms with high growth rates are the first-choice food for fish and shrimps. Significantly, cyanobacteria can be genetically modified also to give specific proteins in higher concentrations to the consumer fish (Gressel J. 2013).

### 1.1.2 Cyanotoxins

However, besides the profit that several cyanobacterial products could serve, there are other products which could be harmful to human, animals, and the environment. These products are secondary metabolites of cyanobacteria and are known as cyanotoxins. Cyanobacterial toxins or cyanotoxins are hazardous secondary metabolites produced by cyanobacteria. Cyanotoxins are considered the most prevalent natural toxins in the environment. Some environmental factors could enhance bloom formations, like eutrophication, the resulting high concentrations in waters represent health and ecological risks for animals and humans (Bláha L. *et al.* 2009). Four groups of cyanotoxins are commonly observed and are responsible for toxicity, in particular microcystins and nodularin for hepatotoxicity, and anatoxin and saxitoxin for neurotoxicity, while their presence must be determined in drinking water (Yen H.K. *et al.* 2011).

These toxins may have a harmful impact on the health of people and animals. The variety of the symptoms depends on; the type of toxin, the strain of the producer as well as the concentration that

the victim is exposed to. The main ways of infections are the oral route, dermal exposure, and inhalation. The oral route infection can be direct, when contaminated water is consumed, or indirect when food (as fish and vegetables), that was exposed to cyanotoxins, is eaten. The indirect way causes the phenomenon of bioaccumulation to secondary consumers (as a human) in the food chain with multiple impacts on them. Lastly, dermal exposure and inhalation are another potential threat, when the victim swims in contaminated waters or lives near toxic blooms.

Regarding the symptoms, these may appear rapidly in few days as damage mostly in the liver, kidney, and colon. However, long-term symptoms may also be revealed as tumors and cancer when the patient is exposed chronically to doses of the toxin (Zanchett G. and Oliveira-Filho E.C. 2013). It is reported that chronic exposure to even small quantities of 50 pg of microcystin per mL of drinking water is sufficient to multiple the risk of collateral cancer by 7.9-fold (Hernández J.M. *et al.* 2009). Ferrão-Filho A.S. and Kozlowsky-Suzuki B. 2011 state the categorization of cyanotoxins based on two methods. In the first case, the cyanotoxins are grouped based on the effect they cause on the victim and in that way, they can be characterized as neurotoxins, hepatotoxins, and dermatotoxins (table 1.1). In the second method, the toxins are identified based on their main chemical structure as *e.g.* cyclic peptides, alkaloids, and lipopolysaccharides (LPS) (Zanchett G. and Oliveira-Filho E.C. 2013). The chemical structures of cyanotoxins are very different. Hepatotoxins are cyclic peptides that are composed of five (nodularin - NOD) or seven (microcystins - MCs) amino acid. Nodularin NOD is produced by *Nodularia spumigena* while microcystins, are produced by several cyanobacteria strains. NOD is a group of 7 compounds, while on the other hand, there is a significant amount of MC types, about 70 different MCs have been identified with the most common variation on their L-aminoacids combination (Van Apeldoorn M.E. *et al.* 2007).

The microcystins are the most common hepatotoxins in nature. They are often a health threat for humans as for instance they can easily contaminate water deposits. So, extended studies have been done to understand the growth factors which affect the producer microorganism. These studies can be used for the indirect examination of the relative compound, cryptophycin, and its producer cyanobacterium, *Nostoc* sp. Regarding MC's structure-activity-relationship (SAR), the  $\gamma$ -D-glutamate group and the ADDA side-chain play critical roles in the mode of action of microcystins binding and inhibiting protein phosphatases (PP1 and PP2A) in mammalian cells and acting as an inhibitor of this group of enzymes (MacKintosh C. *et al.* 1990, Campos A. and Vasconcelos V. 2010).

Cylindrospermopsin (CYN) is considered hepatotoxin even if it differs from the above by its structure and its mechanism of action. It is an alkaloid containing a tricyclic guanidine combined with hydroxymethyl uracyl. It is a potent inhibitor of protein synthesis that subsequently leads to metabolic disturbances. Cylindrospermopsin poisoning may also include damage to the stomach, small intestine, lungs, adrenal glands, heart, thymus and spleen, and various hemorrhages (Duy T.N.

*et al.* 2000, Ohtani I. *et al.* 1992, Kehr J.C. *et al.* 2011).

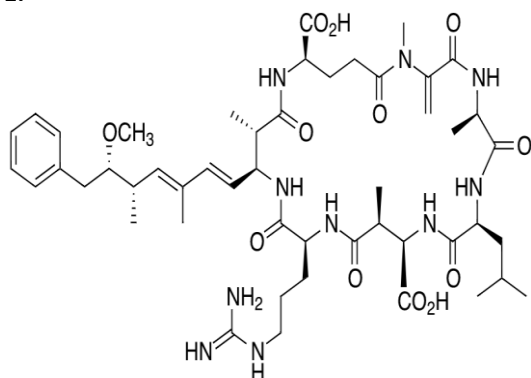
The most potent group is that of neurotoxins. They affect mainly respiratory muscles by attacking the neuromuscular system. In that way, death in rats-experiments has been observed in a few minutes (Mankiewicz J. *et al.* 2003). A representative of this type is the group of the saxitoxins (STXs) which were firstly isolated from a marine species of dinoflagellates, which are produced by algae and cyanobacteria. Structurally, they are complex alkaloids, with an unusual, for bacteria, non-terpene alkaloid pathway.

They are selective, reversible, voltage-gated sodium channel blocker of neurons, preventing the flow of sodium through the membrane, and the propagation of the action potential, leading to paralysis (Falconer I.R.*et al.* 2008). The ingestion by human of a sufficient amount of saxitoxins by consumption of contaminated shellfish leads to paralytic shellfish poisoning (PSP). The shellfish is able to concentrate toxins by filtration of water with dinoflagellates or cyanobacteria.

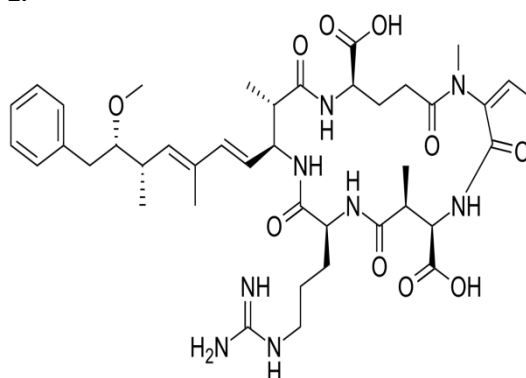
Lastly, the dermatotoxins have been isolated, they are bioproducts of benthic cyanobacteria, and include compounds as aplysiatoxins and lyngbiatoxins. They usually cause dermatitis to human when the victim baths in contaminated waters (Solter P.F. and Beasley V.R. 2013).

**Hepatotoxins**

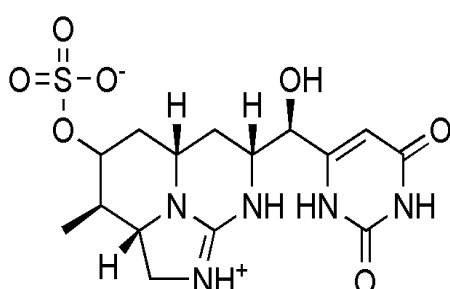
1.



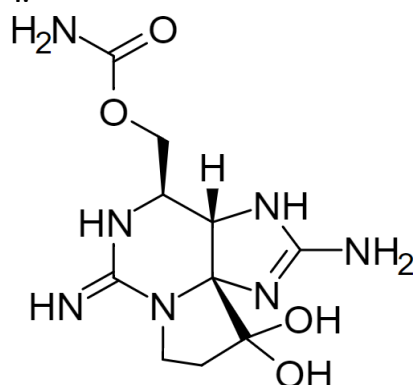
2.



3.

**Neurotoxin**

4.

**Dermatotoxin**

5.

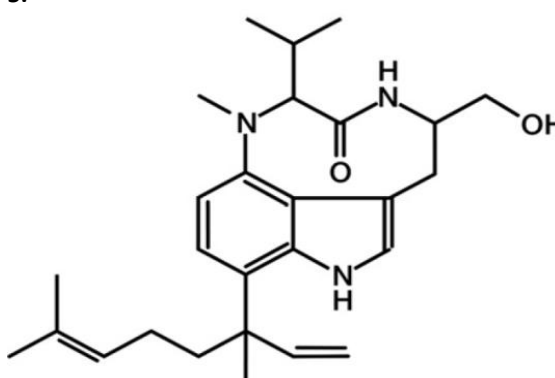


Table 1.1 Cyanotoxins can be grouped into three main categories based on their effect on the victim as hepatotoxins, neurotoxins and dermatotoxins. Representative examples of the hepatotoxins are the cyclic peptides microcystin L-R (fig.1) and nodularin (fig.2) as well as the alkaloid cylindrospermopsin (fig.3). A characteristic of neurotoxin is saxitoxin (fig.4) and an example of dermatotoxins is lyngbiatoxin (fig.5) (Adapted from Duy T.N. et al. 2000, and Solter P.F. and Beasley V.R. 2013).

The main hypothesis for the reason of cyanotoxin's production is the contribution to chemical defense. It is well established that cyanobacteria produce these compounds in order to protect themselves from their predators, like zooplankton, and also to defend the possible nutrient limitations of their inhabitant. That hypothesis though, is doubted as many zooplankton species develop resistance or tolerance to these toxins (Hansson L.A *et al.* 2007). Specifically, it has been noticed that species of zooplankton that invest in pro-longed life cycles are less sensitive in cyanotoxins than the species with shorter life-cycles and early-reproduction phase, as the first group

is less based on food limitations and cyanobacteria, respectively (Ferrão-Filho A.S *et al.* 2000).

Some classes of cyanopeptides are common to several cyanobacterial genera (*e.g.* microcystins, anabaenopeptins, cyanopeptolins), others are only found in species belonging to the genus *Nostoc* (*e.g.* nostocyclopeptides, cryptophycins, nostopeptolides). Recently, a review on bioactive peptides produced by cyanobacteria of the genus *Nostoc* was published, which remarks that *Nostoc* sp. is a high producer of metabolites belonging to nonribosomal peptides (NRPs) or polyketides (PKs) (Fidor A. *et al.* 2019).

We decided to focus on one particular cyanotoxin: cryptophycin. Firstly, we are going to look at the physiology of cyanobacteria. Through the study; a) of the variety of the cell-types, b) the metabolic processes, and then specifically c) of the phytochemical profile and of genome *Nostoc* sp., it will be clarified the reason and the way of cryptophycin's production.

## 1.2 Physiology of cyanobacteria

### 1.2.1 Cyanobacterial cells

#### Simultaneous process of nitrogen fixation and oxygenic photosynthesis

Cyanobacteria base their nutrient sources on two main processes, oxygenic photosynthesis and nitrogen fixation. These two processes cannot take place at the same time in one cell since the oxygen produced by photosynthesis inactivates the nitrogenase needed for nitrogen fixation. So, cyanobacteria have developed two ways to separate these two processes. They could happen in the same cell but at different periods of the day, or they happen at the same time but in different cell types. An example of the first case is the unicellular *Cyanothece* sp. ATCC 51142 which performs photosynthesis in the day and nitrogen fixation at the night (Toepel J. *et al.* 2008). On the other hand, an example of the second way is *Nostoc* sp. where the two processes can be conducted simultaneously in two different cell types: vegetative cells and heterocysts.

#### Cyanobacterial cells' physiology

The cyanobacterial cell shares plenty of characteristics with gram-negative bacteria but also has few characteristics of gram-positive bacteria. For instance, the peptidoglycan layer is a feature of gram-negative though its extent cross-linking in cyanobacteria resembles to gram-positive (Hoiczuk E. and Hansel A. 2000). In order to study the cyanobacterial cell, it could be divided in two main domains, the cytoplasm and the cell wall.

The cell wall is a three-layer-package. From the inner to the outer, there is; a) cytoplasmic membrane, b) a peptidoglycan layer, c) the outer membrane. One difference between the gram-negative bacteria and cyanobacteria is that the cyanobacterial peptidoglycan layer is thicker (Allen M.M. 1984). Another difference is that in filamentous cyanobacteria the outer membrane is a

continuous formation that covers the total of the filament (Hoiczky E. and Hansel A. 2000).

In the cytoplasm, it can be found membranous sacs, called thylakoids, involved in the photosynthetic process. There are contained the pigment-protein complexes involved in the photochemical reactions, and the photosynthetic electron transport chain. These thylakoids could be grouped in parallel around the cells in groups of 2-5 units, or they can be expanded randomly in the cytoplasm. The phycobilisomes, the major light harvesting complex of cyanobacteria, are disk-shaped formations with a diameter up to 40 nm, which are attached to the outer part of the thylakoids. They are formed by phycobiliproteins covalently attaching blue and red pigments, the bilins (Stanier R.Y. and Cohen-Bazire G. 1977). Other cell's structures are present in cyanobacteria cells: polyphosphate granules, glycogen granules ("a-granules"), cyanophycin granules ("structured granules"), and carboxysomes ("polyhedral bodies"). The glycogen granules (31-65 nm), composed of branched polyglucosyl units and serve as carbohydrate reserves, are placed between the thylakoids. Cyanophycin or multi-L-arginyl-poly (L-aspartic acid) is the cellular deposit of nitrates. It consists of two amino acids polyaspartic acid and erginyl, in a ratio 1:1. The last structure, the carboxysome, has a major role in CO<sub>2</sub> fixation as it is packed with the responsible molecules for this process, the ribulose diphosphate carboxylase and serves to concentrate the CO<sub>2</sub> (Vermaas W.F 2001).

### Oxygenic Photosynthesis

The contribution of cyanobacteria to the biosphere is undeniable, as about 3 million years ago, the ancestors of cyanobacteria were the first to conduct oxygenic photosynthesis. That fact is characterized as biological Big Bang and sets the base for the development of the whole biosphere (Shevela D. *et al.* 2013). Nowadays, through oxygenic photosynthesis, they participate in the Oxygen cycle and additionally, they perform a major role in the Nitrogen cycle since a large number of cyanobacteria strains has the ability to fix Nitrogen (Waterbury J.B *et al.* 1979). In addition, cyanobacteria belong to the minority of species which can combine photosynthesis and respiration at the same moment, at the same place.

As far as the photosynthetic process is concerned, cyanobacteria have a high resemblance with algae and higher plants. Since they have many similarities and only few differences, cyanobacteria have been usually used as a model for the study of algae and plant photosynthesis. Likewise to the eukaryotic photosynthetic organisms, they do oxygenic photosynthesis using two photosystems, photosystem II (PSII) and photosystem I (PSI). These complexes bind photosynthetic pigments that could be categorized into three main groups; a) chlorophyll, b) carotenoids, b) phycobilins. The absence of phycobilins in higher plants is the first of the differences between them and cyanobacteria.

The second difference -as it was mentioned above- is that photosynthesis and respiration in

cyanobacteria occur at the same place, at the thylakoid membrane, while in plants photosynthesis occurs in chloroplasts and respiration in mitochondria (Blankenship R.E. 2002).

### Photosynthetic electron flow

The Photosynthetic process can be split into two categories; the “light reactions” and the “dark reactions”. In the “dark reactions”, ATP's energy and the reducing power of NADPH lead to the fixation of CO<sub>2</sub> into sugars through the Calvin-Benson cycle. On the other hand, the “light reactions” produce the required reducing power and ATP through a series of reactions. These light reactions occur in the thylakoid and involve PSII, PSI and cytochrome b6f, which contain chlorophyll-a and carotenoids with several cofactors related to electron transfer. It should be mentioned here that in contrast to the higher plants and algae where the quantity of PSI and PSII is equal, in the case of cyanobacteria the ratio of PSII / PSI is smaller and may vary from 0.3 to 0.7 (Melis A. 1989).

PSII is a dimer of 700 kD. Each monomer consists of 19 protein subunits and contains 36 chlorophyll a, and 7 carotenoid molecules. Two polypeptides PsbA (D1) and PsbD (D2) have a significant role in PSII photochemical charge separation and water splitting. Each of them consists of five transmembrane  $\alpha$ -helices (TMHs). The heterodimer binds a number of functional chromophores and cofactors. Specifically, it binds 6 Chl a molecules, 2 Pheophytin a (Pheo) molecules, 2 quinones, 2 or more  $\beta$ -Cars (Gabdulkhakov A.G. and Dontsova M.V. 2013).

In the PSII, upon excitation Reaction Center II chlorophyll a, P680, by absorbing energy equal to a photon of 680 nm, the energy is enough to induce charge separation. The excited Chl a donates an electron the Pheo creating a radical pair that is rapidly stabilized by electron transfer to the two quinones, QA and QB. Chlorophyll cation will regain an electron from the Mn cluster. Attached to the heterodimer D1-D2 there is an inorganic cluster, Mn<sub>4</sub>CaO<sub>5</sub>, known as OEC (or water oxidizing complex) and three surrounding proteins; PsbO, PsbV, PsbU. Positive charges are accumulated in the Mn cluster and after 4 charge separations H<sub>2</sub>O is split into molecular Oxygen, O<sub>2</sub>, and protons (H<sup>+</sup>) (Zhang L. *et al.* 1994, Shevela D. *et al.* 2013). After a second charge separation, the double reduced QB, takes two protons and leave the PSII. The electrons will be transferred to the PSI *via* the cytochrome b6f complex (Cyt b6f) and plastocyanin. In contrast to higher plants where PSI can be found only as monomer, in cyanobacteria it mainly exists as a trimer. Each monomer of this trimer is composed of 12 protein complexes, with an approximate molecular weight of 80 kDa. Charge separation occurs in the heterodimer formed by the subunits PsaA and PsaB. In these subunits, there are attached a pair of P700-chlorophylls, two phylloquinones molecules, and four more chlorophylls, A and A<sub>0</sub>. In contrast to PSII, in PSI there are Fe-S clusters, in the core (F<sub>x</sub>) and on the PsaC protein (F<sub>A</sub> and F<sub>B</sub>), which help on the primary electron transfer (Grotjohann I. and Fromme P. 2005). The excitation of the PSI complex has as final outcome the reduction of Ferredoxin, a soluble protein. In

order to do that, the initial PSI excitation leads to P700 oxidation and chlorophyll's  $A_0$  reduction. Then, there is an electron transfer through the phylloquinone  $A_1$  to the Fe-S clusters of the core  $F_x$  and then of the PsaC protein ( $F_A$  and  $F_B$ ). That leads to the mentioned Ferredoxin's reduction and then to the production of NADPH (Shevela D. *et al.* 2013).

Some cyanobacteria strains have developed differentiated cell types, other than vegetative cells in which photosynthesis occurs, to serve a variety of several processes such as nitrogen fixation and propagation of new inhabitants. Depending on the need that should be covered, cyanobacteria can transform a vegetative cell into other specialized cells, which are the heterocysts the akinetes, and hormogonia.

### 1.2.2 Heterocysts

#### Heterocysts' physiology

Several differences can be noticed between the vegetative cells and the heterocysts. The heterocysts are usually larger and rounder, with thicker cell envelope. That happens since two more layers are present: there are two heterocyst-specific glycolipids (HGLs) and one polysaccharide layer (HEP) (Nicolaisen K. *et al.* 2009). There is a general intracellular reorganization as the thylakoid membranes are organized spatially in "honeycomb" shape and the poles are narrowed and form the "heterocyst neck". In that heterocyst neck, on the side that interacts with the following vegetative cell, phycocyanin is concentrated (Fay P. 1992).

Moreover, heterocysts have almost lost their phycobilisomes and PSII. A consequence of the absence of PSII and Rubisco's repression is the inability to conduct oxygenic photosynthesis and fix  $CO_2$ . That lack of reductants and carbon in the heterocysts is covered by the vegetative cells which supply heterocysts with sucrose. Heterocysts from their side provide glutamine and a dipeptide (baspartyl-arginine) to the vegetative cells. That transport from heterocysts to vegetatives and vice versa takes place through a continuous periplasm and *via* the septal junctions (Flores E. *et al.* 2006, Mullineaux C.W. *et al.* 2008). Lastly, in heterocysts is observed a rise in respiratory rate to lower the oxygen levels. The differentiation of a vegetative into heterocyst is regulated by the level of combined nitrogen molecules on the surrounding of the cell. In the case of low Nitrogen levels, the process of the transformation of a vegetative cell into a heterocyst takes approximately 20 hours at 30 °C (Thiel T. and Pratte B. 2001, Ehira S. *et al.* 2003).

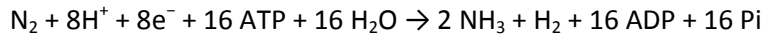
#### Nitrogen fixation process

As mentioned above the nitrogen fixation is an ATP-dependent process that takes place in the heterocysts, under nitrogen starvation conditions, and it is conducted by an enzyme called nitrogenase.

This process is responsible for the reduction of diazote  $N_2$  into ammonium, which would be



assimilated by the microorganism. The process is summarized in the following equation. The equation reveals the high amount of energy needed in terms of ATP and reducing power.



The high-energy-cost process is catalyzed by nitrogenases present almost exclusively in heterocysts. The nitrogenase consists of two components: dinitrogenase (Mo-Fe protein) and dinitrogenase reductase (Fe protein).

The molybdenum dinitrogenase can be found rarely as a variant of vanadium dinitrogenase (V-Fe protein). That dinitrogenase is a heterotetramer ( $\alpha_2\beta_2$ ) composed respectively of two heterodimers  $\alpha\beta$ . On each heterodimer, on subunit  $\alpha$  there is a Fe-Mo cofactor, while on the interface of  $\alpha$  and  $\beta$  subunits there is a P cluster, which consists of two pairs of two complex metalloclusters. The second component of nitrogenase, which is the dinitrogenase reductase (Fe protein), is an  $\alpha_2$  homodimer. Dinitrogenase reductase is reduced by flavodoxins or ferredoxins, and then with dinitrogenase they hydrolyze two molecules of ATP to ADP, so one  $\text{e}^-$  is transferred to dinitrogenase. These obtained electrons are stored and transferred by dinitrogenase to Mo-Fe cofactor.

The responsible gene clusters are organized in operons. The amount of the responsible genes could vary from one strain to another. However, the minimum amount of *nif* (nitrogen fixation) genes is 6; *nifH*, *nifD*, *nifK*, *nifE*, *nifN*, *nifB*. The *nifH-K* encodes Mo-Fe protein while *nifE-B* encodes the Fe protein (Kumar K. *et al.* 2010, Herrero A. *et al.* 2019).

### 1.2.3 Akinetes

Akinetes could resemble bacterial endospores as both are resistant to tough culture conditions. They serve the role of microorganism's survive in an unfavorable environment and its re-germination when the conditions would be better. So, the process of transformations of a vegetative into akinete and *vice versa*, have specific timing to achieve its goal. The cell differentiation from vegetative to akinete happens between the logarithmic and stationary phase when the microorganism faces energy limitation. Then, the akinete germinates when it is diluted in fresh medium with optimum light and temperature conditions (Sutherland J.M. *et al.* 1979). Their placement is most often in the terminal position of the filament, but they are also frequently developed close to heterocysts. At the moment that akinete is in the right conditions to propagate the new culture, rapid divisions lead firstly on short filaments. From these filaments, the later culture will occur. Regarding their metabolic processes, the  $\text{CO}_2$  fixation is decreased, and the respiration rate is slightly increased. They lose their functional PSI, and Chl content significantly decreases (Kaplan-Levy R.N. *et al.* 2010). That can be macroscopically observed, as compared to the greenish vegetatives the akinetes have a brownish color. Lastly, there is an accumulation of glycogen and phycocyanin(PC) (PC amounts are up to eightfold higher than in vegetative cells) to store the required components (Sutherland J.M. *et al.*

1979).

Two major differences occur when a vegetative cell is transformed into an akinete. The first and most obvious is a clear enlargement in size, and sometimes a differentiation is also observed in shape. The cell is increased more in length than in width. The second difference is happening on the cell wall. At that point, a multilayer thick envelope is developed on the outer side of the existed cell-wall. That envelope is composed mainly of glucose-rich carbohydrates and amino compounds (Lambein F. *and* Wolk C.P. 1973).

#### 1.2.4 Hormogonia

Regarding the propagation of *Nostoc* sp. and the creation of new colonies, mainly the four strategies are followed. The primary mechanism is through the germination of akinetes, which is the cell-type addressed to go through tough periods for an extended period and propagate new inhabitants. Fragmentations of filaments could be developed into new colonies, or large colonies can develop branches that will be fragmented in the same way. Lastly, hormogonia is a common way of forming a new colony (Borowitzka M.A. 2018).

Hormogonia are short motile filaments which consist of few cells. These cells are smaller than the vegetative cells and may contain gas vesicles (Liaimer A. *et al.* 2011). The formation of hormogonia is the result of a combination of environmental changes that signalizes a stress state. That stress could be caused by limitation of nitrates level and nutriment, changing of light quality, or dilution of the culture in fresh medium (Campbell E.L. *et al.* 2007). Under these stress conditions, a multiple cell division takes place which is followed by fragmentation of the existed filaments, usually in the junction of heterocyst-vegetative cell. The occurred short filament moves through the culture approximately for the following 48-72 h. During this period the cells of the hormogonia are in non-growth condition and they have lack of protein and chlorophyll content. Then, the filament is able to differentiate into heterocysts cells at the both ends (Meeks J.C *et al.* 2002).

#### 1.2.5 Taxonomy of the producing strain

Following the physiology of the phylum of Cyanobacteria it is useful to introduce the taxonomy of the producing strain in order to understand more about its features and characteristics.

|         |               |
|---------|---------------|
| Kingdom | Bacteria      |
| Phylum  | Cyanobacteria |
| Order   | Nostocales    |
| Family  | Nostocaceae   |
| Genus   | Nostoc        |

Table 1.2: Taxonomy of *Nostoc* sp.

*Nostoc* sp. ATCC 53789 belongs to the genus *Nostoc*, in the family of *Nostocaceae* under the order of *Nostocales* and phylum of *Cyanobacteria*. *Cyanobacteria* is a phylum of almost 150 genera and 2000 species (Krumbein W.E 1979, Woese C.R. *et al.* 1990). *Nostoc* is a genus of nitrogen-fixing cyanobacteria, which is described by high diversity in several characteristics such as; its inhabitant, size, shape, and color. To begin with, its inhabitant could range from terrestrial to aquatic environments while often it can also be in symbiotic consortia as with liverworts, ferns, or even in endosymbiotic states as in the case of *Geosiphon pyriformis* (Schüßler A. 2012). The size varies also, colonies of *Nostoc pruniforme* could reach a diameter up to 25 cm while *Nostoc commune* can form spheres up to 3 cm in diameter. Macroscopically the color of the *Nostoc* colony could vary depending on the species from dark-green to red-brown (Mollenhauer D. *et al.* 1999).

### 1.3 Phytochemical Profile of cyanobacteria

Especially for the project's strain, apart from its genome which was recently published (April 2020) and will be presented in chapter 1.7, very few studies have been done. So, the following comments and assumptions on phytochemistry will be based on the hypothesized similarities of the strain with other relevant nitrogen-fixing cyanobacteria.

The cyanobacterial biochemical profile could be split into three main groups of primary metabolites; lipids, carbohydrates and proteins. Specifically, a summary of 12 *Nostoc* strains sums up that the protein ratio to dry weight ranges from 37 % to 52 %, carbohydrate ratio from 15 to 30%, and lipid from 8 % to 13 % respectively (Vargas M.A. *et al.* 1998).

#### 1.3.1 Proteins

Proteins are the third major biochemical group based on the dry weight range. Proteins content is affected by culture conditions, such as the medium's composition. Specifically, the content of proteins is higher when *Nostoc* strain is cultivated in the presence of  $\text{NO}_3^-$  or  $\text{NH}_4^+$ . Moreover, their cell quota is modified during the cell cycle with the optimal period to be the exponential phase. Phycobiliproteins are the biggest group of proteins with up to 50 % of the total amount. Another significant amount of proteins is detected in the peptidoglycans cell walls. In this way, it is remarked the diversity of the proteins as well as their role in a variety of cellular mechanisms. Their contribution ranges from the oxygenic photosynthesis process to the nitrogen fixation process, while one of their main uses is the Nitrogen storage. Regarding proteins' composition, the C/N ratio is 4/5 (Vargas M.A *et al.* 1998, Andersen R.A 2013).

### 1.3.2 Carbohydrates & Polysaccharides

The carbohydrates in the cyanobacterial cells are starch-like formation. Laminarins are polysaccharides of glucose with a  $\beta$ -1,3-linked glucan backbone with  $\beta$ -D-1,6 linked side chains. These formations vary in size from the smaller, such as chrysolaminarin with 30 glucose residues, found in photosynthetic heterokonts, to significantly bigger formations, which can be seen even in a light microscope (Andersen R.A 2013). Cyanobacteria form an extracellular capsule of mono- and polysaccharides (EPS). That capsule, in some cases has the ability to partially protect the microorganism from the UV-radiation. Specifically, the EPS of *Nostoc flagelliforme* may have an activity against colon cancer based on rats-tests (Takenaka H. *et al.* 2015). These EPS may reduce the amount of the cancer cell or their malignant alteration.

Nitrates' level has a quantitative effect on EPS but not a qualitative effect on their composition. The composition of the polysaccharides may differ from the one *Nostoc* species to the other. Moreover, it could differ even on the same species depending on the culture conditions. However, there are some main components that can be detected in most cases, such as; mannose, galactose, glucose, xylose, and glucuronic acid (Huang Z. *et al.* 1998).

### 1.3.3 Lipids

The lipids in the cyanobacterial cell can be mainly found in two formations. They are detected; a) in the bilayer structure of biomembranes, b) in the photosynthetic membranes combined with proteins.

In cyanobacteria, the higher ratio of lipids -up to 80%- is in the form of triacylglycerols. The second biggest group is polar lipids, while neutral lipids (as sterol esters, waxes, and free sterols) exist in minor quantities. Lastly, it is observed an absence of phosphatidylcholine, phosphatidylethanolamine, phosphatidylserine, and diphosphatidylglycerol.

Regarding the polar lipids, these are distinguished into four main groups; monogalactosyl diacylglycerols, digalactosyl diacylglycerols, sulfoquinovosyl diacylglycerols, and phosphatidylglycerol. Fatty acids in cyanobacteria exist in three forms. Mainly they exist as n-saturated while rarely in the form of hydroxy acid and dioic acids (Dembitsky V.M. and Rezanka T. 2005).

Regarding the saturated fatty acids, they can be as monounsaturated, di-, tri- or oligounsaturated. However, their composition is closely related to the culture's temperature. For instance, studies at *Anabaena variabilis* have shown that when temperature elevates from 22 °C to 38 °C the microorganism produces higher amounts of 18:3 and lower ones of 18:1 and 18:2 (Sato N. and

Murata N. 1981). That range of temperature has an effect not only on fatty acids but on other lipid classes also. High biomass growth rate does not correspond directly to higher lipid production. For instance, *Nostoc carneum* MBDU 709 and *Nostoc commune* MBDU 707 which had higher growth rates comparing to other *Nostoc* species had inversely lower lipid production. It was assumed that the values of growth rate and lipid production have an inverse correlation. That is explained by the required equilibrium of ATP and NADPH. That ratio should be at 3:2 for an effective CO<sub>2</sub> fixation. In that way, when NADPH is invested in lipid production there is a CO<sub>2</sub> fixation decrease, and so the growth rate is also diminished (Anahas A.M.P. *et al.* 2018).

Lastly, regarding the further industrial exploitation of fatty acids, there should be mentioned the case of linoleic and  $\alpha$ - and  $\gamma$ - linolenic acid. These components are usually used in cosmetics, medication, and nutritional supplements.

#### 1.3.4 Other compounds

Besides the three main mentioned groups of compounds, there are other groups in smaller quantities, such as hydrocarbons and polypeptides. A characteristic example of hydrocarbons is oxalic acid soluble substance (OOSS), which is detected in high levels in *Nostoc commune*. OOSS is responsible for the decrease of LDL-cholesterol when dietary fibers of that species were addressed nutritionally to rats (Hori K. *et al.* 1992).

#### Depsiptides

In the group of depsipeptides (also named peptolides) we detect the two components most studied in the strain of interest; cryptophycins and nostocyclopeptides (Golakoti T. *et al.* 2001). Molecules of nostocyclopeptides group (Ncp-M1) (fig.1.1) were later isolated also from another strain of *Nostoc* sp., the strain XSPORK 13A (Jokela J. *et al.* 2010). In relation to Cry, most of the 25 natural produced Cry analogues, have been isolated from *Nostoc* sp. GSV 224. However, these two strains, apart from the group of cryptophycins, have many differences in the rest of their metabolites. For instance, nostopeptolides are only in GSV 224, while nostocyclopeptides are expressed only by ATCC 53789, and in that way they are a unique characteristic of the strain (Chaganty S. *et al.* 2004). There are three analogues of nostocyclopeptides; A1, A2, A3, which are expressed in a ratio of 10:1:1. Despite their unique presence in *Nostoc* sp. ATCC 53789, these compounds have shown no significant biological activity until today. Specifically, they showed no toxicity against LoVo and KB cell lines, neither antifungal nor antibacterial activity. Lastly, they had no inhibition against protease activity (Golakoti T. *et al.* 2000, 2001).

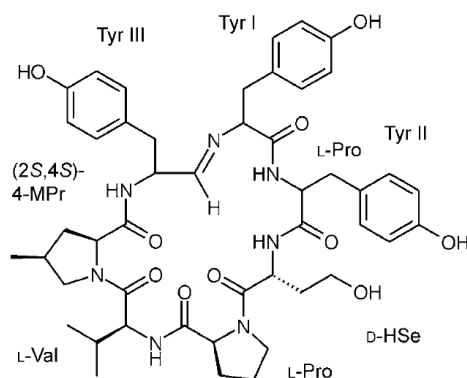


Figure 1.1: Nostocyclopeptide M1 is a representative example of Nostocyclopeptides, depsipeptides found in *Nostoc* sp. Pro for proline, Tyr for tyrosine, Val for valine, MPr for methylproline, HSe for homoserine (Adapted from Jokela J. *et al.* 2010).

## 1.4 Historical development & Natural occurring analogues

Cryptophycin, a 16-membered cyclic depsipeptide was isolated from three different terrestrial strains of cyanobacteria and from a marine sponge, *Dysidea arenaria* in the form of arenastanin A. The three cyanobacteria strains are the *Nostoc* sp. MB 5357, *Nostoc* sp. GSV 224 and *Nostoc* sp. ASN\_M.

### 1.4.1 Detection on *Nostoc* sp. MB5357, focus on antifungal activity

The article of Schwartz R.E *et al.* 1990 and later the patent of Hirsch F.H *et al.* 1990, both from *Merck Laboratories* and *Ocean Genetics*, firstly described Cry-1 and the producer microorganism. *Nostoc* sp. MB 5357 is known now under the code ATCC 53789 (American Type Culture Collection - ATCC). The strain was firstly collected from a lichen on Arron island in Scotland. Specifically, 3 sq.mm from the thallus of the mentioned lichen were incubated with 2.5 mL of BG-13 at 25 °C for 3-4 weeks. From the obtained culture, the desired strain was isolated and then stored in BG-13 medium.

Though, regarding its biological activity, only its antifungal activity was firstly described. That activity was detected against filamentous fungi and yeast of *Cryptococcus* sp. The activity against *Cryptococcus* sp. was that significant that the newly discovered compound was named “cryptophycin” according to the species name of the fungi. Apart from that species, antifungal activity was also detected against the *Aspergillus* species (as *Aspergillus niger* and *Aspergillus flavus*), *Alternaria solani*, *Penicillium* species, *Cochliobolus miyabeanus*, *Phoma* species, *Botrytis allii*, *Ceratocystis ulmi* and *Fusarium oxysporum*.

The first study of total Cry production in relation to growth (fig.1.2), reveals that the highest metabolite’s levels are achieved at the late exponential phase and are correlated with a depletion of phosphate in the medium (Schwartz R. E. *et al.* 1990, Hirsch C.F. *et al.* 1990). This strain is the only commercially available Cry producing strain, and it is provided by the American Type Culture Collection with the code ATCC 53789, from the respective abbreviation.

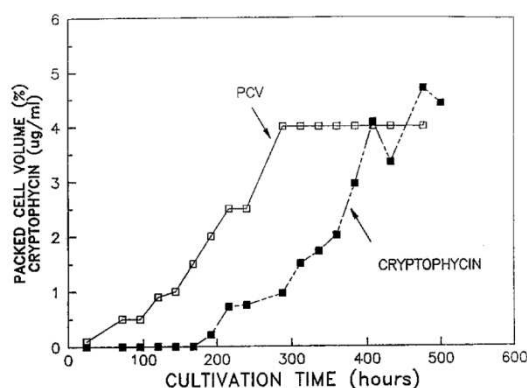


Figure 1.2: Time Culture's growth, in Packed cell volume (PCV), and Cry production ( $\mu\text{g}/\text{mL}$ ) in a fermentor (Schwartz R.E. *et al.* 1990).

#### 1.4.2 Detection on *Nostoc* sp. GSV 224, focus on cytotoxic activity

Later, Cry was isolated from one more strain, *Nostoc* sp. GSV 224 (Golakoti T. *et al.* 1994). That strain was initially isolated from a terrestrial sample in India by an Indian botanist Gopalasmudram Sitaraman Venkataraman, director of the *Department of biotechnology- Centre for Blue-Green Algae* at Madurai Kamaraj University and so it had the related abbreviation GSV. From that strain, 7 Cry analogues were isolated and characterized; Cry-1,-2,-3,-4,-5 methyl ester,-6 methyl ester and -7 and they run for the first time cytotoxic assays (on KB and LoVo cell lines) (Golakoti T. *et al.* 1994). Then, for further research, it was provided by Professor Wolk C.P., MSU-DOE Plant Research Laboratory, Michigan State University, but it was not commercially available.

#### Arenastatin A

In the same year arenastatin A was isolated and evaluated (Kobayashi M. *et al.* 1994). That was isolated from the Okinawan sponge *Dysidea arenaria*. Noticeably it has a similar  $\text{IC}_{50}$  -5  $\mu\text{g}/\text{ml}$ - value on KB cell line as Cry-1 and -2. It was later shown that arenastatin A was identical with Cry-24, this compound was due to a cyanobacterial symbiont (Robert A.B *et al.* 2018).

#### 1.4.3 Detection on *Nostoc* sp. ASN\_M

Lastly, Nowruzi B. *et al.* 2012 examined the suspicious deaths of dogs and mice in the surroundings of paddy fields in Iran. The team sampled soil from the paddy fields and cultivated it in petri-dishes with BG110. The cultivated heterocystous cyanobacterium strain was characterized as *Nostoc* sp. ASN\_M. Among the compounds isolated from the strain, three classes of peptidic compounds were identified: anabaenopeptins, cryptophycins, and nostocyclopeptides. At that point, it was claimed that the toxicity and deaths of the surrounding fauna were due to the cyanotoxins but not much further research has been done on that species (Nowruzi B. *et al.* 2012).

Consequently, the project focused on the strain *Nostoc* sp. ATCC 53789, which is the only commercially available, and as the project aimed in a potential further industrial application of the obtained outcome and so it was needed a commercially available strain.

#### 1.4.4 Naturally occurring analogues

Cryptophycins is a wide group of peptolides, naturally produced by cyanobacteria of the genus *Nostoc* sp. There are several naturally produced analogues and numerous synthetic ones. Among all these analogues, Cry-1 is the analogue that was first isolated and studied. Cry-1 is also the major representative regarding the ratio in the wild-type producer microorganism. For these reasons, we select that analogue as a case-study and representative example of the cryptophycins' group.

Cry-1 has a molecular formula of  $C_{35}H_{43}ClN_2O_8$  and the IUPAC name:

(3*S*,6*R*,10*R*,13*E*,16*S*)-10-[(3-chloro-4-methoxyphenyl)methyl]-6-methyl-3-(2-methylpropyl)-16-[(1*S*)-1-[(2*R*,3*R*)-3-phenyloxiran-2-yl]ethyl]-1,4-dioxo-8,11-diazacyclohexadec-13-ene-2,5,9,12-tetrone.

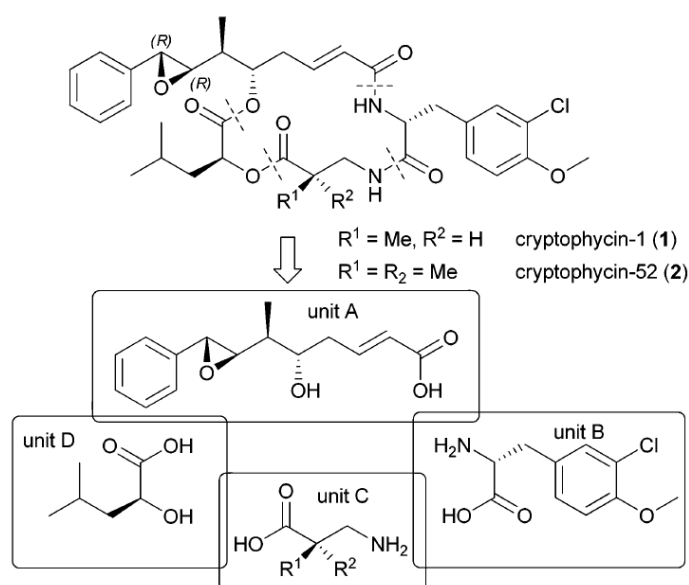


Figure 1.3: Two of the most representative analogues of Cry. Cry-1 is a representative of naturally occurring analogues and it was the first analogue detected, while Cry-52 is representative of the synthetic analogues and was the most prominent synthetic analogue and investigated up to Clinical Phase II. Cryptophycin is composed of 4 units in cyclic sequence A, B, C, D. Unit A includes a phenyl-octenoic acid, Unit B 3-chloro-*O*-methyl-D-tyrosine, Unit C methyl  $\beta$ -alanine, and unit D L-leucic-acid (Adapted from Weiss C. *et al.* 2013).

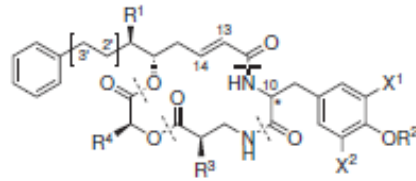
Cry-1 is a circular depsipeptide with molecular weight of 655.2 g/mol and molar mass of 655.2 Da. It is composed of four subunits. Unit A includes a phenyl-octenoic acid, with an epoxide group which plays an essential role in the molecule's potent activity. Unit B with 3-chloro-*O*-methyl-D-tyrosine, unit C with methyl  $\beta$ -alanine, and unit D with L-leucic-acid. These units are linked in a cyclic ABCD sequence (fig 1.3).

As mentioned, Cry can be produced by three strains of *Nostoc* sp. However, it was mostly studied at *Nostoc* sp. GSV 224 due to a higher Cry production of this specific strain compared to the other two.



The chemical study of a large culture of *Nostoc* sp. GSV 224 allowed to identify 28 natural Cry analogues. The first isolated Cry analogues were; Cry -2, -3, -4, -5, -6, -7 while among these analogues only Cry-2 showed high potency, similar to the activity of Cry-1 (Golakoti T. *et al.* 1994). However, Cry-5, -6, -7 were not originally Cry analogues but methanol artifacts which were produced during the isolation process (Golakoti T. *et al.* 1995). Then, 18 more analogues were characterized, and exhibited modifications only in one Unit A-D, while Cry-24 was the only one with modification in two Units (B and C) (Golakoti T. *et al.* 1995). Most of the analogues had modifications in Unit B, and there were only two analogues (Cry-21 and -29) with modifications in Unit C (Golakoti T. *et al.* 1995).

Regarding the relative concentrations, Cry-1 is the major analogue in *Nostoc* sp. GSV 224 with a concentration of 220 mg in 40 g of dry biomass. It is followed by Cry-21 with 14 mg, Cry-2 with 6 mg, Cry-16 with 3.0 mg and Cry-23 with 1.2 mg in 40 g of dry biomass, respectively. The rest of the analogues were occupied in minor quantities, less than 1 mg (table 1.3) (Golakoti T. *et al.* 1995). The following year, three new modified analogues on Unit B were isolated (Subbaraju G.V. *et al.* 1996). Cry-46 has a S configuration at C-2 of Unit B, so it is an analogue of Cry-3. Cry-175 is the O-methyl analogue of Cry-45 and Cry-176 is the O-desmethyl analogue of Cry-21. Lastly, there are three more analogues (Chaganty S. *et al.* 2004). Cry-38 which is a stereoisomer of Cry-1 as the epoxide in Unit A is *S,S* instead of *R,R*. However, the molecule was proven to be potent only under the specific stereochemistry (*R,R*), so the analogue Cry-38 is inactive. Cry-326 is analogue of Cry-21 with two o-chlorines to the methoxy group in Unit B. The addition of the extra chlorine also leads to reduced toxicity. Cry-327 is a geometric isomer of Cry-1, as the *cis*- $\Delta^2$ -double bond in unit A is *trans* in the case of the analog, a difference that decreases its potency dramatically.



| Fragment:        | A                              |                |                                  | B               |                |                |                | C              | D              |
|------------------|--------------------------------|----------------|----------------------------------|-----------------|----------------|----------------|----------------|----------------|----------------|
|                  | C <sup>2</sup> -C <sup>3</sup> | R <sup>1</sup> | C <sup>13</sup> =C <sup>14</sup> | C <sup>10</sup> | R <sup>2</sup> | X <sup>1</sup> | X <sup>2</sup> | R <sup>3</sup> | R <sup>4</sup> |
| Cryptophycin-1   | $\beta$ -Epoxyd                | Me             | <i>trans</i>                     | ( <i>R</i> )    | Me             | Cl             | H              | Me             | <i>i</i> -Bu   |
| Cryptophycin-2   | $\beta$ -Epoxyd                | Me             | <i>trans</i>                     | ( <i>R</i> )    | Me             | H              | H              | Me             | <i>i</i> -Bu   |
| Cryptophycin-3   | CH=CH                          | Me             | <i>trans</i>                     | ( <i>R</i> )    | Me             | Cl             | H              | Me             | <i>i</i> -Bu   |
| Cryptophycin-4   | CH=CH                          | Me             | <i>trans</i>                     | ( <i>R</i> )    | Me             | H              | H              | Me             | <i>i</i> -Bu   |
| Cryptophycin-16  | $\beta$ -Epoxyd                | Me             | <i>trans</i>                     | ( <i>R</i> )    | H              | Cl             | H              | Me             | <i>i</i> -Bu   |
| Cryptophycin-17  | CH=CH                          | Me             | <i>trans</i>                     | ( <i>R</i> )    | H              | Cl             | H              | Me             | <i>i</i> -Bu   |
| Cryptophycin-18  | CH=CH                          | Me             | <i>trans</i>                     | ( <i>R</i> )    | Me             | Cl             | H              | Me             | <i>s</i> -Bu   |
| Cryptophycin-19  | CH=CH                          | Me             | <i>trans</i>                     | ( <i>R</i> )    | Me             | Cl             | H              | Me             | <i>i</i> -Pr   |
| Cryptophycin-21  | $\beta$ -Epoxyd                | Me             | <i>trans</i>                     | ( <i>R</i> )    | Me             | Cl             | H              | H              | <i>i</i> -Bu   |
| Cryptophycin-23  | $\beta$ -Epoxyd                | Me             | <i>trans</i>                     | ( <i>R</i> )    | H              | Cl             | Cl             | Me             | <i>i</i> -Bu   |
| Cryptophycin-24  | $\beta$ -Epoxyd                | Me             | <i>trans</i>                     | ( <i>R</i> )    | Me             | H              | H              | H              | <i>i</i> -Bu   |
| Cryptophycin-28  | $\beta$ -Epoxyd                | H              | <i>trans</i>                     | ( <i>R</i> )    | Me             | Cl             | H              | Me             | <i>i</i> -Bu   |
| Cryptophycin-29  | CH=CH                          | Me             | <i>trans</i>                     | ( <i>R</i> )    | Me             | Cl             | H              | H              | <i>i</i> -Bu   |
| Cryptophycin-31  | $\beta$ -Epoxyd                | Me             | <i>trans</i>                     | ( <i>R</i> )    | Me             | Cl             | Cl             | Me             | <i>i</i> -Bu   |
| Cryptophycin-38  | $\alpha$ -Epoxyd               | Me             | <i>trans</i>                     | ( <i>R</i> )    | Me             | Cl             | H              | Me             | <i>i</i> -Bu   |
| Cryptophycin-40  | CH=CH                          | H              | <i>trans</i>                     | ( <i>R</i> )    | Me             | Cl             | H              | Me             | <i>i</i> -Bu   |
| Cryptophycin-43  | CH=CH                          | Me             | <i>trans</i>                     | ( <i>R</i> )    | H              | H              | H              | Me             | <i>i</i> -Bu   |
| Cryptophycin-45  | CH=CH                          | Me             | <i>trans</i>                     | ( <i>R</i> )    | H              | Cl             | Cl             | Me             | <i>i</i> -Bu   |
| Cryptophycin-46  | CH=CH                          | Me             | <i>trans</i>                     | ( <i>S</i> )    | Me             | Cl             | H              | Me             | <i>i</i> -Bu   |
| Cryptophycin-49  | CH=CH                          | Me             | <i>trans</i>                     | ( <i>R</i> )    | Me             | Cl             | H              | Me             | <i>n</i> -Pr   |
| Cryptophycin-50  | $\beta$ -Epoxyd                | Me             | <i>trans</i>                     | ( <i>R</i> )    | Me             | Cl             | H              | Me             | <i>n</i> -Pr   |
| Cryptophycin-54  | $\beta$ -Epoxyd                | Me             | <i>trans</i>                     | ( <i>R</i> )    | Me             | Cl             | H              | Me             | <i>s</i> -Bu   |
| Cryptophycin-175 | CH=CH                          | Me             | <i>trans</i>                     | ( <i>R</i> )    | Me             | Cl             | Cl             | Me             | <i>i</i> -Bu   |
| Cryptophycin-176 | $\beta$ -Epoxyd                | Me             | <i>trans</i>                     | ( <i>R</i> )    | H              | Cl             | H              | H              | <i>i</i> -Bu   |
| Cryptophycin-326 | $\beta$ -Epoxyd                | Me             | <i>trans</i>                     | ( <i>R</i> )    | Me             | Cl             | Cl             | H              | <i>i</i> -Bu   |
| Cryptophycin-327 | $\beta$ -Epoxyd                | Me             | <i>cis</i>                       | ( <i>R</i> )    | Me             | Cl             | H              | Me             | <i>i</i> -Bu   |

Table 1.3: Structures of natural occurring Cry analogues in relation to the Units A, B, C, D. Cry-1, -21, -2 and -3 and the four major analogues in *Nostoc* sp. GSV224 with a concentration of 220, 14, 6 and 3 (mg/220mg) (Adapted from Nahrwold M. 2009 and Golakoti T. *et al.* 1995).

Among the identified natural occurring Cry-analogues Cry-1 showed the highest potency (table 1.4). Only few other analogues, had noticeable toxic activity. Specifically, Cry-21 which is highly potent, presented biological activity close to the one of Cry-1 (Golakoti T. *et al.* 1995).

| Cryptophycin | KB IC <sub>50</sub> (nM) | LoVoIC <sub>50</sub> (nM) | SKOV3 IC <sub>50</sub> (nM) |
|--------------|--------------------------|---------------------------|-----------------------------|
| 1            | 0.0092                   | 0.01                      | 0.02                        |
| 2            | 0.073                    | 0.11                      | 0.057                       |
| 3            | 3.13                     | 1.88                      | 4.36                        |
| 4            | 16.5                     | 21.5                      | 34.5                        |
| 5            | 10.9                     | 8.75                      | 10.8                        |
| 8            | 0.019                    | 0.0091                    | 0.022                       |
| 15           | 4.17                     | 5.21                      | 17.2                        |
| 16           | 0.359                    | 0.273                     | 0.606                       |
| 17           | 7.53                     | 9.46                      | 17.7                        |
| 18           | 48.6                     | 20.4                      | 36.6                        |
| 19           | 11.7                     | 11.2                      | 65.1                        |
| 21           | 0.017                    | 0.019                     | 0.05                        |
| 23           | 3.12                     | 0.59                      | 2.52                        |
| 24           | 0.198                    | 0.157                     | 0.499                       |
| 25           | 0.027                    | 0.027                     | 0.101                       |
| 26           | 35.1                     | 18.3                      | 142                         |
| 28           | 2.88                     | 1.11                      | 9.76                        |
| 29           | 3.69                     | 1.04                      | 5.9                         |
| 30           | 18.3                     | 10.8                      | 31.6                        |
| 31           | 2.62                     | 0.218                     | 1.23                        |
| 40           | 0.61                     | 0.625                     | 2.63                        |
| 43           | 1.22                     | 1.36                      | 1.88                        |
| 45           | 3.5                      | 3.6                       | 2.48                        |
| 49           | 2.24                     | 3.04                      | 1.82                        |
| 50           | 0.047                    | 0.094                     | 0.607                       |
| 54           | 1.22                     | 3.36                      | 3.33                        |

Table 1.4: Toxicity of Cry analogues in KB (human nasopharyngeal carcinoma), LoVo (human colorectal adenocarcinoma), and SKOV3 (human ovarian carcinoma) (Adapted from Golakoti T. *et al.*1995).

## 1.5 Cryptophycin's mechanism of action

Microtubules are involved in the regulation of numerous cellular processes and the mitotic spindle. So, microtubules are the target of a large group of successful natural product anticancer drugs. Microtubules are highly dynamic assemblies of the heterodimeric protein tubulin, while they are polymerized and depolymerized in cells. These drugs either inhibit microtubule polymerization at high drug concentrations, like: the *Vinca* alkaloids, cryptophycins, halichondrins, estramustine, and colchicine. Either one stimulates microtubule polymerization and stabilizes microtubules at high concentrations: taxol, taxotere, eleutherobins, epothilones, laulimalide, sarcodictyins, and discodermolide. At lower concentrations, these drugs suppress the dynamics of microtubules without appreciably changing the mass of microtubules in the cell. These two groups of compounds bind to diverse sites on tubulin and at different positions within the microtubule. Binding to tubulin occurs on different sites depending on the nature of the compounds: *Vinca*, taxoide, colchicine domain. These two groups have a common mechanism by suppression of microtubule dynamics, blocking mitosis, and inducing cell death by apoptosis (Panda D. *et al.* 1997, Jordan M.A. *et al.* 2002).

### 1.5.1 Affinity of cryptophycin for *Vinca* domain

*Vinca* alkaloids such as vinblastine and vincristine and its semi-synthetic analogue vinorelbine inhibit polymerization and induced microtubule depolymerization *in vitro*: they are microtubule - destabilizing agents. On the contrary, taxoids are inducers of the polymerization of the tubulin into microtubules. Cry was found to be a potent microtubule disruptor. Incubation of L 1210 leukemia cells with Cry resulted in dose-dependent inhibition of cell proliferation. In parallel, the percentage of cells in mitosis is increased. Pre-treatment of cells with taxol prevented microtubule depolymerization in response to either vinblastine or Cry because the pre-treatment has strongly stabilized the microtubules. While a rapid reverse action is observed after removing vinblastine, cells treated by Cry remained microtubule depleted for at least 24 h after removal. At last, combinational treatments with vinblastine and Cry resulted in additive cytotoxicity (Smith C.D. *et al.* 1994). The high affinity of Cry with *Vinca* domain was proven *via* [<sup>3</sup>H]vinblastine assay. [<sup>3</sup>H]vinblastine assay is based on liquid scintillation counting and tests the ability of a compound to bind with the *Vinca* domain of tubulin. Thus, if the compound interacts with that domain, it inhibits the [<sup>3</sup>H]vinblastine from binding with the microtubule protein (MTP). The positive result of Cry on [<sup>3</sup>H]vinblastine assay and the fail on other assays as [<sup>3</sup>H]colchicine, indicates Cry's selectivity with the *Vinca* domain(fig.1.4) (Panda D. *et al.* 1997, Kerskiek K. *et al.* 1995). That is also verified through fluorescence assay. That assay is based on the increase of fluorescence (measured at 432 nm) in the case of the colchicine-tubulin binding, and on the decrease of that fluorescence when another component takes colchicine's place on the bond with tubulin. While a ratiopodophyllotoxin(control)/tubulin of 2.5 was sufficient to decrease the fluorescent, a respective ratio of 5 for Cry was not enough to alter the fluorescence's intensity, so Cry does not interact with colchicine binding place (fig.1.4) (Kerskiek K. *et al.* 1995).

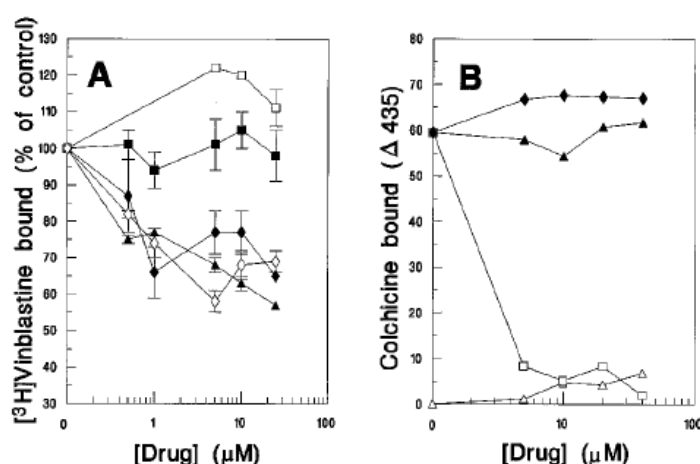


Figure 1.4: Cryptophycin was efficient in inhibiting the binding of [<sup>3</sup>H]vinblastine to MTP (panel A), though it did not reduce the binding of [<sup>3</sup>H]colchicine to MTP (panel B), demonstrating the Cry selectivity with the *Vinca* domain. cryptophycin (▲), colchicine (■), vinblastine (◆), rhizoxin (◇), podophyllotoxin (◻) (Smith C.D. and Zhang X. 1996).

Cry-tubulin interaction finally leads to the formation of aggregates, which are observed as ring-shaped under Electron microscopy (fig.1.6) (Kerskiek K. *et al.*1995, Smith C.D. and Zhang X. 1996).

Lastly, it was found that even if Cry seems to interact with *Vinca* position, it probably doesn't attach exactly, but it overlaps that position, as it has few structural similarities with *Vinca* alkaloids. This hypothesis is partially verified from the above microscopic observation, because while Cry leads on ring-shaped aggregates, vinblastine forms spiral ones (Kerskiek K. *et al.* 1995).

During a physiological operation, microtubules could experience three different phases; a shortening phase, a growth phase, or a pause phase. In both shortening or growth, the respective addition or diminution of tubulins units takes place at the ending part of the microtubules. All these three phases could be generally described with the term of microtubule's dynamics. All these dynamics are affected by the presence of Cry. The inhibition of the shortening phase could be described as "rescue mechanism" while the inhibition of the growing phase as "catastrophe mechanism". A dimer of tubulin-GDP (Guanosine 5'-diphosphate)forms the unstable core of microtubules while another dimer of tubulin-GTP (Guanosine-5'-triphosphate) forms a cap on microtubules' end. The binding of the cap with the microtubules' core signalizes the end of the growth phase of the core, and stops the polymerization of tubulin to microtubules. Cry-1 interacts with that cap, and in this way enforces the rescue or catastrophe. When microtubule loses its cap, the process of depolymerization of the unstable core begins. If Cry-1 contributes to regain the cap at that point, it leads to rescue. On the other hand, when Cry-1 contributes to the loss of that cap, it leads to depolymerization back into tubulins units (Smith C.D. *et al.* 1994, Smith C.D. and Zhang X. 1996, Panda D. *et al.* 1997).

### 1.5.2 Cryptophycin's activity comparing to known anticancer drugs

Cry's most significant advantage, in contrast with the *Vinca* alkaloids, is that it appears to be a poor substrate for the drug-efflux pump P-glycoprotein. Natural anticancer drugs like *Vinca* alkaloids are good substrates for P-glycoprotein, leading to resistance to treatment by removing the active substance from the cell before it acts (Smith C.D. *et al.* 1994). This property is listed as its major point in the development of a novel active pharmaceutical compound. That is verified through studies on the resistance factor (ratio of "sensitive cell line IC<sub>50</sub>" to "cancer cell line IC<sub>50</sub>") of ovarian and breast cancer to vinblastine, colchicine, taxol, and Cry. That difference of resistance factor between Cry and the mentioned anticancer agents may be due to their relevance to P-glycoprotein. A second advantage is the high binding ability of Cry to tubulin. Indeed, Cry has multiple higher binding ability to tubulin comparing to colchicine and vinblastine, according to microtubule protein (MTP) assay (fig.1.5). It shows 4-fold better binding activity comparing to colchicine and 2-fold comparing to vinblastine. Specifically, a Cry:tubulin ratio of 0.1 is sufficient to halve the *in vitro* polymerization of

bovine brain microtubules, while Cry-concentrations below 5  $\mu\text{M}$  have no significant effect (Smith C.D. and Zhang X. 1996).

| Cell line         | IC <sub>50</sub> (nm) |            |           |              |
|-------------------|-----------------------|------------|-----------|--------------|
|                   | Vinblastine           | Colchicine | Taxol     | Cryptophycin |
| SKOV3             | 0.65±0.25             | 9.0±3.0    | 1±0.4     | 0.007±0.02   |
| SKVLB1            | 4200±1700             | 8000±2400  | 8000±2000 | 0.60±0.19    |
| Resistance factor | 6400                  | 890        | 8000      | 85           |
| MCF-7             | 3.0±0.8               | 8.8±3.0    | 2.5±0.2   | 0.016±0.002  |
| MCF-7/ADR         | 183±14                | 930±280    | 4300±270  | 0.017±0.004  |
| Resistance factor | 61                    | 106        | 1720      | 1.1          |

Table 1.5: Toxicity of cryptophycin on human ovarian carcinoma cells (SKOV3), breast carcinoma (MCF-7) and their resistance cell lines, in comparison to the respective toxicity of vinblastine, colchicine and taxol. Resistance factor is the ratio of SKVLB1-IC<sub>50</sub>/SKOV3- IC<sub>50</sub> and for MCF-7 respectively (Adapted from Smith C.D. *et al.* 1994).

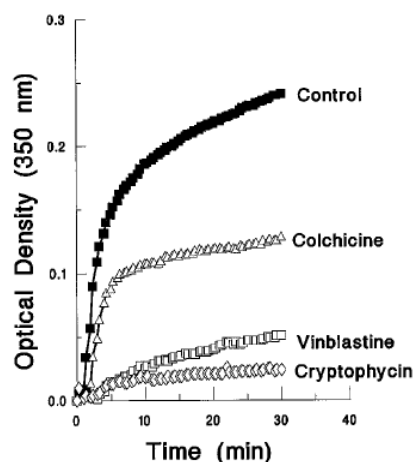


Figure 1.5: Cry inhibits MTP polymerization (measured at 350 nm) faster and for longer period comparing to Vinblastine and Colchicine. Control in EtOH, 5  $\mu\text{M}$  of each compound added 15 min before the addition of GTP, T at 37 °C (Smith C.D. and Zhang X. 1996).

The last important specificity of the action is the high level of irreversibility of Cry-binding (Smith C.D. *et al.* 1994, 1996). For instance, studies compared the reversibility of vinblastine and Cry-1 in A-10 cell line. The two compounds resulted in total tubulins' depolymerization, and then the cells were incubated in drug-free medium. The first new microtubules re-formed on vinblastine-treated cells after 1 h while on Cry treated, these were not observed even after 24 h. Similar assays in SKOV-3 cells as well as direct Cry-MTP treatments, concluded on the same outcome (Smith C.D. *et al.* 1994, Smith C.D. and Zhang X. 1996).

### 1.5.3 Mechanism of action at the molecular level

The high irreversibility of Cry-tubulin bond is due to the presence of a reactive epoxide ring, implying that Cry forms a covalent bond with nucleophilic attack of the epoxide on tubulin's aminoacid side-chain (Smith C.D. *et al.* 1994). However, it is proven that the tight binding is entropy-driven and noncovalent (Panda D. *et al.* 1997, 2000). Several assays conclude on that assumption as for example that radiolabeled Cry-52 could be released from the radiolabeled tubulin after denaturation of the dimer through boiling or urea treatment (Panda D. *et al.* 2000).

A sum of Cry-tubulin dimers forms a ring formation. That ring is noticeably smaller comparing to a ring made of Guanosine diphosphate(GDP)-tubulin dimers. The decrease in the ring's size is due to the big intradimer angle of Cry and tubulin. On the other hand, in the case of GDP-tubulin dimer, the

relative link is insignificant, so the ring is bigger. Consequently, in the case of Cry induced rings, smaller size leads to unstable microtubules (fig.1.6) (Watts N.R. *et al.* 2002, Nogales E. *et al.* 2003).

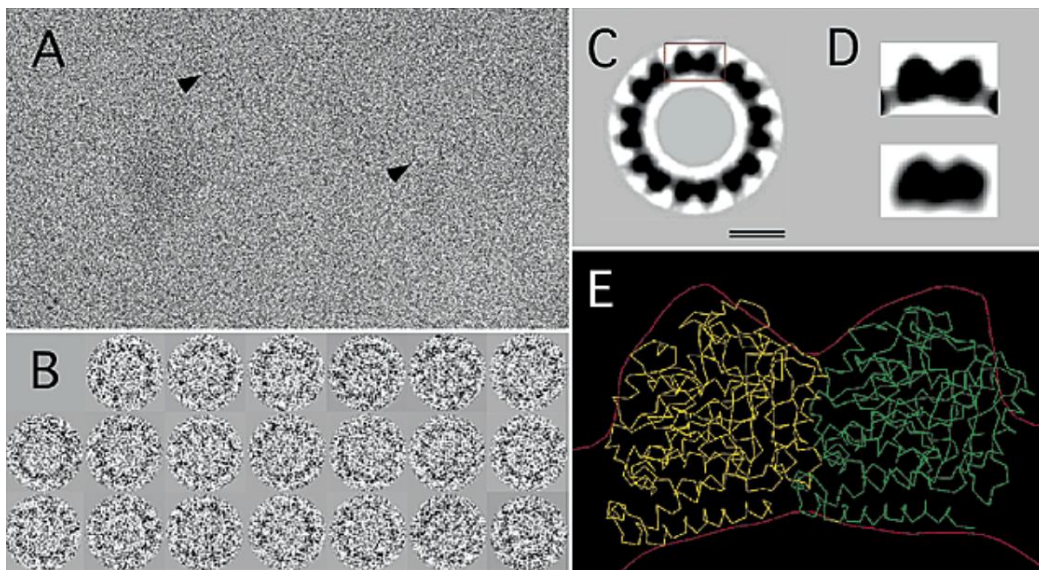


Figure 1.6: Cry-tubulin ring formations. A) Field of particles in a film of vitreous buffer on a thin continuous carbon film. (B) Two-fold focus on the formations of panel A (C) 8-fold focus on the formation of panel A (bar is 10 nm long). (D) Comparison of the projection of a curved dimer (upper), compared with a similar projection of a straight dimer (lower) (E) Fitting of the  $\alpha$ - and  $\beta$ -tubulin subunits into the projected cryo-EM envelope of the ring (Watts N.R. *et al.* 2002).

Cryptophycin's related mechanism of action is similar to that of dolastatin 10 and phomopsin A. Firstly, the binding site of these three compounds was characterized as "Vinca domain" (Bai R. *et al.* 1996). Though, despite their structural and binding similarities, Cry-1 is much more potent than dolastatin 10, for instance it is 15-fold more potent on L1210 cell line (Bai R. *et al.* 1996). The dominance of Cry is also proved, as Cry inhibits competitively the binding of dolastatin-10 with tubulin (at the same time, it inhibits uncompetitive the binding of vinblastine with  $\beta$ -tubulin) (Mitra A. and Sept D. 2004). Cryptophycin's binding pocket in  $\beta$ -tubulin neighbors with the GTP site. So, when Cry is attached to tubulin, it interacts with GTP and leads to inhibit nucleotide exchange and the hydrolysis of GTP (fig.1.7) (Mitra A. and Sept D. 2004).

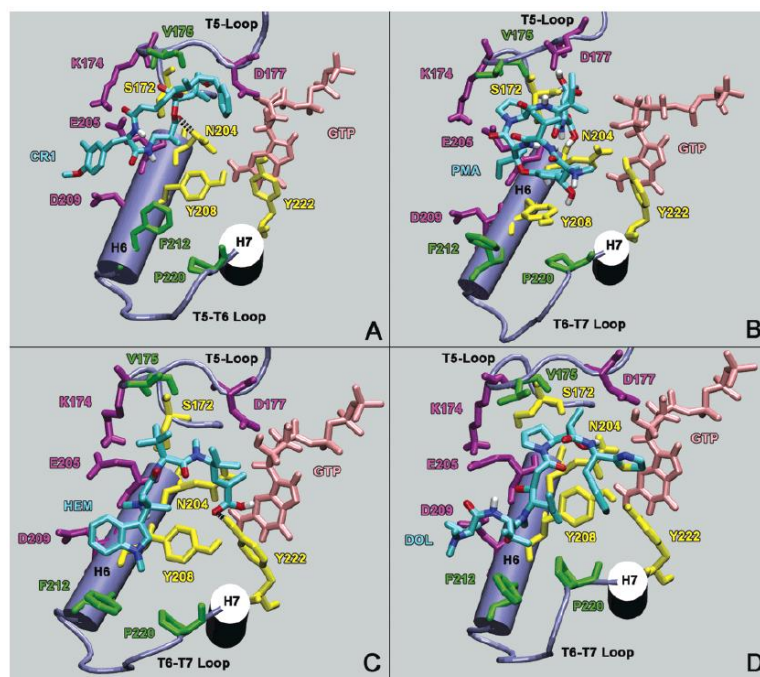


Figure 1.7: Comparative depiction of the bound to bovine  $\beta$ -tubulin of (A) cryptophycin 1, (B) phomopsin A, (C) hemiasterlin, and (D) dolastatin 10. The binding pocket is formed by hydrophobic residues (green), polar uncharged residues (yellow), and polar charged residues (magenta), all within 3 Å of the ligand. GTP is colored pink, Hydrogen bonds are depicted as black springs, and only polar hydrogens are shown (Mitra A. and Sept D. 2004).

Cry-1 and Cry-52 have a similar binding orientation. Cry contain modified Tyrosine (Unit B), Valine (Unit C), and Leucine (Unit D) residues. These residues bind on  $\beta$ -tubulin in an opposite orientation, in comparison to the one of dolastatin 10. The cryptophycin's binding orientation leads the phenyl ring (Unit A) to block the access to the *Vinca* and exchangeable nucleotide sites (Mitra A. and Sept D. 2004). A similar function is served in dolastatin 10 by the diaminopimelic acid moiety. Finally, the cryptophycin's C20 carbonyl group of Unit C forms hydrogen bond with the  $\delta$ -amino group of Asparagine 204 (Mitra A. and Sept D. 2004).

## 1.6 Structure activity relationship of cryptophycin-analogues

### 1.6.1 Structure activity relationship of natural occurring analogues

The epoxide oxygen can also be transformed in hydroxy group when Cry-1 is opened by HCl to chlorohydrin (Cry-8), while the two compounds, Cry-1 and Cry-8 have similar potency (Golakoti T. *et al.* 1994). However, in the case of methanolysis (Cry-9) there is no activity (Golakoti T. *et al.* 1994, Biondi N. *et al.* 2004). No activity is also observed on analogues Cry-3 and -4, where there is a total removal of the hydroxy group and the epoxide respectively, from unit A. All the above highlight the significant role of oxygen on Unit A in the form of hydroxy group or epoxide.

Other important characteristics for the SAR are the leucic acid and the ester bond between Units C



and D. Concerning the leucic acid, in case of its absence, the analogues Cry-6, -7, -10, -12 have noticeable weaker activity while regarding the absence of the ester bond Cry-5 is also inactive (Golakoti T. *et al.* 1994).

On the other hand, chloro substituent on the O-methyltyrosine, as well as its absolute configuration, is not majorly implicated in the SAR. So, Cry-1, where the substituent is present, and Cry-2, where it is absent, have similar potency against KB (cervical adenocarcinoma) and LoVo (Human colon adenocarcinoma) cell lines (Golakoti T. *et al.* 1995).

### 1.6.2 Structure activity relationship of synthetic analogues

Apart from the variety of naturally occurred analogues numerous synthetic ones, which were composed in the way of developing novel cytotoxic agents were obtained. These compounds are analogues of Cry-1 which were modified in one or more Units A, B, C or D.

#### Analogues with Unit A modifications

The epoxide of Unit A, as well as its  $\beta$ -stereochemistry, is crucial for the biological activity. Specifically, when the epoxide is replaced with other groups such as enones, ynones, allylic and propargylic electrophiles, it is shown that none of these analogues have any biological activity. The same happens when the epoxide is totally removed to give the respective thiirane and aziridine analogues (De Muys J.M. *et al.* 1996). Moreover, comparison between  $\alpha$ -epoxide and  $\beta$ -epoxide analogues shows  $\beta$ -stereochemistry is important for the activity (Moore R.E. *et al.* 1996). Comparison among bromo-, iodo- and chloro-hydrin analogs reveals that the last one is significantly active. That analogue though is also a naturally occurred one (Moore R.E. *et al.* 1996, Golakoti T. *et al.* 1994). The better activity of chlorohydrin, in comparison to the other halohydrins, might be due to its better uptake by the cancer cell line (Eggen M. and Georg G.I. 2002).

In Unit A another major component which is the phenyl group, its substitutes and their respective -ortho, -meta, -para position. Indeed, for instance if the phenyl group is replaced with methyl group the activity is decreased by 4-fold, while the replacement with thiophene also leads to inactive analogue (Moore R.E *et al.* 1996).

Assuming the importance of phenyl group, the research interest is focused on phenyl's substitutes. The ones with the best activity were 3-methyl, 3,4-dimethyl, as well as the analogues which contain amino-groups and especially the piperazine analogs. The potency of these analogues might be due to their increased solubility (Patel V.F. *et al.* 1999). Moreover, in para substitution analogues with methyl group or halogens as -Cl and -F the activity augments (Moore R.E. *et al.* 1996). On the other

hand, the analogues with carboxyl group in -para substitution increase the respective IC<sub>50</sub> value (Al-awar R. S *et al.* 2003).

### Analogues with Unit B modifications

Unit B consists of a methoxy in an aromatic group, which is a chlorinated derivative of D-tyrosine. In that way, analogues' synthesis focuses on modifying one of the three compounds of Unit B; the linker between the molecule and the phenol, the phenolic group, and the substitutes. Firstly, regarding the linker, its prolongation, or extinction, leads to a dramatic decrease of the activity (Patel V.F. *et al.* 1999). Secondly, concerning the phenolic nucleus, its replacement with cyclohexyl, naphthyl, or isopropyl gives inactive analogues (Patel V.F. *et al.* 1999). Lastly, regarding the substitutes on phenyl a replacement of methoxy group with dimethylamine is half-active analogue while removing all the substitutes leads to 5-fold less activity. All the other substitutes-modifications is a lot more inactive, indicating the sensitivity in that area.

Docking results have shown that the phenyl's epoxy substitution does not implicate in tubulin interaction (Mitra A. and Sept D. 2004). However, if the epoxy group is replaced by an azide, triethylene glycol chain terminated with an alcohol, or hydroxyethyl group, the obtained analogues are inactive in the first case while the two other substitutes lead to decreased activity (Mitra A. and Sept D. 2004).

### Analogues with Unit C modifications

Unit C contains two main elements, C2 with the methyl group and the C3 which can be substituted. Remove that methyl from C2 and a simultaneous to add in C3 methyl or phenyl reduce the activity in half and 4-fold, respectively (Varie D.L. *et al.* 1999). The addition of two ethyl or propyl groups in geminal-disubstitution on C2 has no significant activity. The addition though, of two methyl groups leads to the most active analogue which is the Cry-52, twelve times more active than Cry-1 in human colon carcinoma cells. Moreover, cyclic analogues in C2, such as cyclopropyl and cyclohexyl had IC<sub>50</sub> values similar to the one of Cry-1 (Eggen M. and Georg G.I. 2002).

On the other hand, C1 is essential both for stability and activity and so it should not be replaced in the analogues (Varie D.L. *et al.* 1999).

### 1.6.3 Case of Cryptophycin-52

LY355703 or Cry-52 is a synthetic Cry derivative that was developed and patented by Eli Lilly Company in the early 2000s and was chosen for clinical trials.

### Clinical Phase I

Cry-52 is 40-400 fold more active comparing to known anticancer drugs as paclitaxel (Sessa C. *et al.* 2002). It is even active against Multidrug-Resistant (MDR) cell lines. The irreversible effect of Cry gives the advantage of prolonged effect of Cry-52 even 24 h after the compound's removal, in contrast to paclitaxel's short-time action.

Two strategies were examined; the first one was a *IV* single dose every three weeks, and the second was with three *IV* doses (one per week with progressively lowering concentrations) and one week break. However, the second strategy leads progressively, in the third week, to low concentrations with insignificant effect. So, only the first strategy was forwarded to clinical phase II. The main dose limiting toxicity (DLTs) were peripheral neuropathy and myalgia, which are common DLTs for *Vinca* alkaloids and taxanes also. Other DLT is severe pain on tumor site, which was explained by possible tumor ischemia. Because of these DLTs the maximum tolerated dose (MTD) was identified at 2.2 mg/m<sup>2</sup>, so the dose for the clinical Phase II was proposed at 1.48 mg/m<sup>2</sup> (Sessa C. *et al.* 2002, Stevenson J.P. *et al.* 2002).

### Clinical Phase II

As mentioned, the strategy of *IV* single dose Cry-52 was examined in clinical phase II. Cry-52 was tested against non-small cell lung cancer (NSCLC) where it has shown a significant impact. Specifically, it was tested in patients with stage IIIB or stage IV, who have been treated before with other anticancer drugs like cisplatin. Firstly, it appeared severe toxicity and pain. So, the dose was decreased by 20 %, which made milder the side-effects. However, that treatment was not successful as in one survey 12 out of 14 patients died due to side-effects (Groth G. *et al.* 2001), and in a second survey, only 5 out of 26 patients managed to receive a full course of six cycles (Edelman M.J. *et al.* 2003). Recapitulative, Cry-52 could be used more as a cytostatic than a cytotoxic agent.

As patients with non-small cell lung cancer (NSCLC) did not respond to Cry-52 treatment, three years later, in 2006, it was tested in Clinical Phase II against ovarian cancer. Then, the same therapeutic protocol (1.5 mg/m<sup>2</sup> on days 1 and 8 every 21 days) was applied to 26 patients who were pre-treated with cisplatin. The outcome of that study was not successful but it was a lot more prominent than in NSCLC. Specifically, there was a percentage of 12.5 % regarding the response rate, while the stabilization rate was 29 %. At the same time, the side effects were milder. The study stopped at the first group of 24 patients, and did not continue on the second group of 25 according to the "early stopping rule" (d' Agostino G *et al.* 2006). So, even if the study was not complete, the outcome was better than in NSCLC and provided the perspective for further research.

### Analogues with Unit D modifications

Unit D is composed of an L-leucic-acid and the main part of the modification, where the synthesis of analogues was focused, is the ester bond between Unit D and Unit C. Analogues were synthesized focusing on the ester-bond's hydrolyzation. In the way of ester modifications, amide, keto, and ether Cry analogues were also composed. Among these analogues, the amides showed the highest *in vitro* potency while the ether-analogue the lowest. That implicates that the carbonyl in the ester bond may participate in an intramolecular hydrogen bond or participate in the mechanism of action (Norman B.H. *et al.* 1998, Eggen M. and Georg G.I. 2002).

Following these results, amide analogues of arenastatin A (Cry-24) were also constructed. Triamide analog-II of arenastatin A was potent with significant low *in vitro* IC<sub>50</sub> value, though *in vivo* it had almost no toxicity. It was proposed that the hydrolysis of the ester bond leads to analogues that cannot be easily metabolized, so they lose their *in vivo* activity. This hypothesis was verified in mice experiments (Murakami M. *et al.* 2000).

## 1.7 Gene cluster

In bacteria, several genes that are related to the same function are structured in an operon. An operon is a unit of DNA containing multiple genes under the control of a single promoter. Before the start of the first gene of the operon, there are three places; the promoter and two binding sites for regulatory proteins, which control the expression of the gene cluster. These are the operator and the activator. The promoter is the part where the RNA polymerase binds in order to start the transcription of the gene. The operator is the binding site for the protein, which contributes to the decrease of the gene-cluster expression. On the other hand, the activator with its bonded substrate is the part of the DNA which leads to the protein overexpression.

### 1.7.1 Cryptophycin's gene cluster

The main survey on that field has been contacted by Magarvey N.A. *et al.* 2006. In their work, the gene cluster of Cry (*crp*), which consists of 40,304 bp, was described and analyzed for the first time by stable-isotope labeling experiments (fig.1.8). *Nostoc* sp. ATCC 53789 and *Nostoc* sp. GSV 224 have >99,9% similarities in the operon of Cry. Specifically, *crp* encodes a collinear set of enzymes, starting by three modular polyketide synthetases (PKSs). For the first PKS, doubts are expressed because even if the gene cluster is known, the main issue is the real starter of PKS in unit A (Méjean A. and Ploux O. 2013). Then there are genes for two non-ribosomal peptide synthetase modules and a series of genes for the tailoring enzymes, CrpE CrpF CrpG CrpH, which are responsible for the catalyzation of functional group modifications. CrpE is responsible for epoxidation while CrpH for chlorination

(Ehrenreich I.M. *et al.* 2005, Magarvey N.A. *et al.* 2006). The DNA sequences after *crpH* are completely different. In this way, it can be proved that the *crpH* was the terminal gene of the operon (Magarvey N.A. *et al.* 2006).

A particularly significant characteristic is that Cry bio-synthetic system is flexible and able to generate 25 related natural products that include alterations in subunit structures: units A, B, C, D, depsipeptide ring size (14 vs 16), and variations in tailoring reactions. Using the flexibility of the unit C pathway enzymes, Magarvey N.A. *et al.* 2006 by direct supplementation of gem-dimethyl-alanine to *Nostoc* cultures led to Cry-52. That gave the proof that a precursor-directed biosynthesis to access analogues previously only obtained by total synthesis (Magarvey N.A. *et al.* 2006).

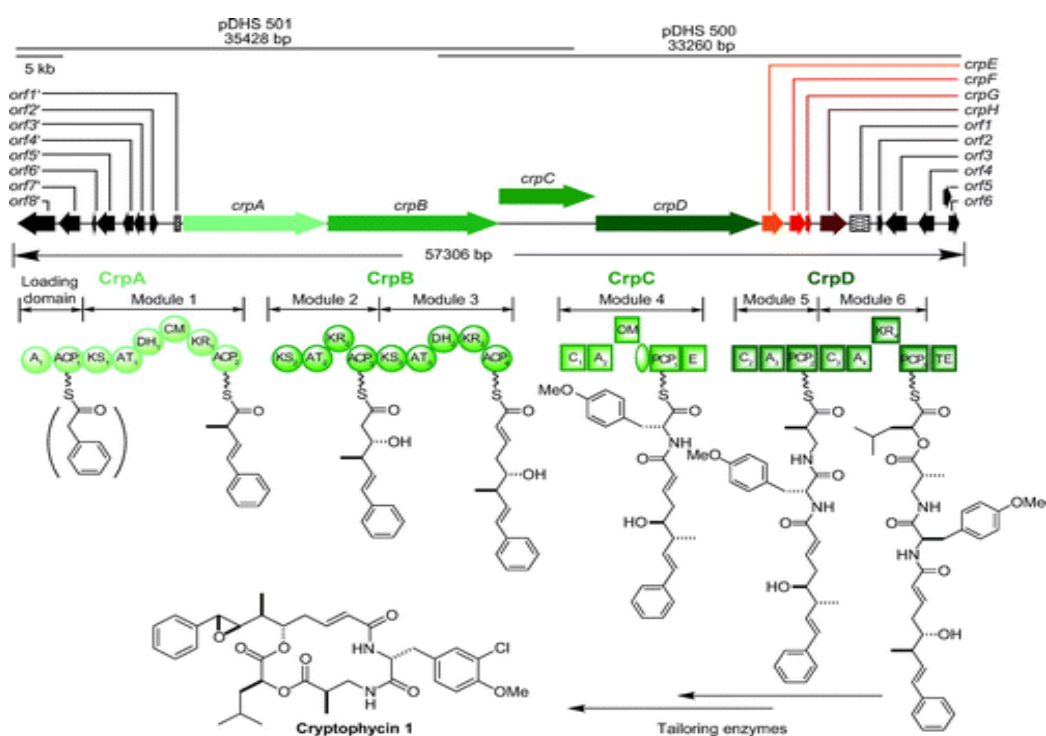


Figure 1.8: The Cry (*crp* for this figure) gene cluster and the deduced PKS/NRPS assembly line. Block arrows indicate opening-reading-frames. Green color genes are responsible for products with function as NRPSs or PKSs. Orange, red color genes are responsible for tailoring enzymes or enzymes involved in precursor biosynthesis, while black genes are out of the *crp* gene. Circle domains are found within the proposed *crp* PKS assembly line while square within the NRPS. Abbreviations (AT, acyltransferase domain; KS, ketosynthase domain; CM, C-methyltransferase domain; DH, dehydratase domain; KR, ketoreductase domain; ACP, acyl carrier protein; A, adenylation domain; C, condensation domain; PCP, peptidyl carrier protein; OM, proposed O-methyltransferase domain; E, epimerase; TE, thioesterase domain) (Magarvey N.A. *et al.* 2006).

### 1.7.2 Genome sequence of *Nostoc* sp. ATCC 53789

In addition to the work of Magarvey N.A. *et al.* 2006, Tippelt A. *et al.* 2020 completely sequenced the genome of *Nostoc* sp. strain ATCC 53789. The genome is composed of 8,653,729 bp, and includes 1 circular chromosome, 10 circular plasmids, and 2 linear plasmids. Especially, there are identified 7,408 genes, 7,300 protein-coding sequences, 88 tRNAs, 12 rRNAs, and 8 non-coding RNAs (ncRNAs).

Regarding the gene cluster of Cry, it is noted that it takes place at the plasmid pNsp\_c. In addition, the authors point out that the strain is able to bio-synthesize anabaenopeptin (Tippelt A. *et al.* 2020).

## Conclusion - Chapter 1

Cyanobacteria is a wide group of microorganisms, which respectively produces diverse compounds. These compounds can be used in several aspects of people's lives, such as nutritional uses, biofuels, and even as biofertilizers. Though, some of these secondary metabolites are a threat to humans due to their neurotoxic, hepatotoxic, or dermatotoxic effect. The study of these compounds could lead to novel anticancer agents, so we focus on a cyanotoxin with high potential Cry. To study the compound, we firstly study the producer microorganism. It is a filamentous cyanobacterium with three main cell-types; vegetatives, heterocysts and akinetes. Oxygenic photosynthesis, which is the main source of energy, takes place in vegetatives. Nitrogen fixation process happens in heterocysts and lastly akinetes are responsible to propagate new inhabitants. Regarding the phytochemical profile, the microorganism contains proteins, carbohydrates, lipids, and polypeptides such as nostocyclopeptides and cryptophycins.

There are 25 naturally occurred analogues of Cry, while Cry-1 is the most potent and in abundance. Until today it has been identified in three species of *Nostoc*, though the rest of the analogues have been studied only at one strain *Nostoc* sp. GSV 224. However, the project is focused on *Nostoc* sp. ATCC 53789 as it is the only commercially available. Cry has high affinity to Vincaposition and disrupts microtubule's dynamics leading to apoptosis. Indeed, Cry has significantly lower  $IC_{50}$  value on ovarian and breast cancer cell lines, in comparison to known anticancer drugs as taxol. One of the most significant groups for that activity is the epoxide in Cry's Unit A. Studying the SAR, Cry-52 analogue was synthesized with modification in Unit C. That analogue examined until clinical phase II but failed due to high toxicity issues.

As it has been extensively presented the nature of the microorganism as well as the nature of Cry, we can now further study the expression of Cry from *Nostoc* sp.





## Chapter 2

### Optimizing culture conditions for cryptophycin's overproduction



## 2 Chapter 2 - Optimizing culture conditions for cryptophycin overproduction

As presented in Chapter 1, Cry has shown a great anticancer activity with high potential (Panda D. *et al.* 1997, Smith C.D. and Zhang X. 1996). However, its chemical synthesis has more than 30 steps. In addition, it faces stereoselectivity issues, and it has moderate yield (3.5 %), which is unprofitable for industrial-scale production (Moore R.E. *et al.* 1996). So, the need to develop alternative ways of production seems necessary. The optimization of culture parameters is examined for Cry overproduction. Specifically, in Chapter 2 we examine a range of abiotic culture parameters in relation to: light (photoperiod, intensity, wavelength), pH, temperature, medium composition. Moreover, as potential industrial exploitation would need high quantities, a range of culture volume and vessels is examined to test the effect on the total yield. So, Chapter 2 is split into three parts. Firstly, it is presented a review of the examined parameters and the related vessels, and how these affect cyanobacterial physiology and phytochemical profile (2.1-2.2). Then, in the second part, there are described the techniques that we developed and applied in relation to the culture (2.3) and in relation to the chemical-analysis where we quantified Cry production (2.4). At last, it is the main part (2.5) where the experiments and their results are analyzed. That experimental part was conducted in the lab of Dr.Diana Kirilovsky(CNRS, Institut de biologie Intégrative de la cellule- CEA) where we had access to the culture facilities such as multi-cultivator MC 1000 (PSI- Photon System Instruments) and "Brunswick Innova 4340 Refrigerated Incubator Shaker", while the development of quantification method and sample analysis took place at the lab of PNAS (Produits Naturels Analyse et Synthèse, Université de Paris, CiTCoM, UMR CNRS 8038).

### 2.1 Review on the culture parameters

The environmental culture conditions often affect the growth and physiology of the strain as well as its cyanotoxin production. Thus, tuning culture conditions is an indirect way to modify the strain's growth and phytochemical profile. A wide variety of abiotic and biotic factors have been examined for their effect on cyanobacteria. In some cases, cyanobacteria propagate water depots with unpleasant odor and taste, or even they form water blooms with a harmful effect on humans' health. In these cases, culture conditions have been studied on the way to eliminate their growth and toxins' production. On the other hand, in cases where the microorganisms and their metabolites have nutritional, pharmaceutical, or other beneficial use, the research has focused on the maximization of their growth and metabolites' yield. As a result, we use these bibliographic sources to detect case-studies for Cry and to cover the lack of research for the parameter's effect on the specific

compound. The main culture parameters are the culture's pH, Temperature, medium composition and the parameter of light. Specifically, the main metabolic process of cyanobacteria is oxygenic photosynthesis. So, it can be understood that a modification of the light parameter could have a significant impact on cyanobacterial growth rate and physiology. The main light conditions are light photoperiod, intensity, and wavelength.

### 2.1.1 Light photoperiod

Since the growth of photosynthetic organisms depends on light, light periods are essential for cyanobacterial growth. In nature, all organisms are exposed to periods of light and darkness, which vary with seasons and latitudes. In laboratory experiments, it has been demonstrated that the rate of cyanobacteria cell growth increases when the length of the light period increases until it reaches its maximum, which varies from 16:8 Light:Dark (L:D) to 22:2 depending on the strain (Jacob-Lope E. *et al.* 2009, Zevenboom W. and Mur L.R. 1984). From that maximum until constant light, the growth rate faces a decrease. As an example, in medium light intensities, cyanobacterium *Microcystis aeruginosa* has a 30 % lower growth rate under constant light in comparison to the growth rate at 16:8 (L:D) (Zevenboom W. and Mur L.R. 1984). This may be attributed to two reasons. Firstly, constant light differs a lot from any natural conditions that the microorganism has been isolated from and has firstly developed its growth rate (Jacob-Lopes E. *et al.* 2009). Secondly, it is implied that a light period of 16 to 22 hours can store sufficient energy to maintain the cell growth for a non-light period of up to 8 hours. In general, the growth rate can be described as a function of photoperiod based on the Monod equation:

$\mu_{L/D} = \mu_{max} * [L / (K_L + L)]$ , where  $\mu_{L/D}$  is the growth rate at a specific photoperiod,  $\mu_{max}$  is the maximum growth rate,  $K_L$  is the needed light period to achieve  $\mu_{max}/2$ ,  $L$  is the length of light period (Post A.F. *et al.* 1986, Tang E. and Vincent W. 2000). Exceptionally in some studies, a photoperiod of 12:12 (L:D) differs from the linear correlation between light period and growth rate. For example, in a photoperiod 12:12 (L:D) cyanobacterium *Aphanothece microscopica Nægeli* has a growth rate of 37% higher than in 14:10 and 20 % than in 16:8 (L:D). This indicates that some species show a preference for the photoperiod of their natural habitat from which they were initially isolated (Jacob-Lopes E. *et al.* 2009). Another photoperiodic phenomenon, with an effect on growth rate, is the periodic light-fluctuations which occur in nature by weather-conditions, as for example in an outdoor pond with cloudy sky. Experiments in reactors have shown that when the intensity fluctuates, the growth rate is decreased in comparison to the same photoperiod without fluctuations. This decrease is smaller if the fluctuation is progressive and the period cycle length of each repetitive fluctuating-cycle is longer (Nicklisch A. *et al.* 1998, da Fontoura Prates *et al.* 2018, Tang E. and Vincent W. 2000).

Photoperiod also affects the cell's biochemical composition. Light photoperiod and intensity are in inverse proportion regarding the productivity of *Nostoc* sp. That means that lower light intensities need more extended light portions, and vice versa for the higher light intensities (Johnson E.M. *et al.* 2014). A characteristic influence of photoperiod is depicted on pigment's degradation when the light portion is increased. Specifically, total phycobiliprotein content is increased by 23 % when *Nostoc* sp. culture is moved from 24:0 to 16:8 (L:D). The phycobilin proteins are photosensitive components, so constant light in high light intensities causes a reduction of the concentration of chromophore proteins per cell (Johnson E.M. *et al.* 2014, da Fontoura Prates *et al.* 2018).

Regarding the production of cyanobacterial toxins, studies in cyanotoxins, such as geosmin in the cyanobacterium *Phormidium* sp., have shown that their production increases as the light portion of photoperiod increases as well (Ludwig F. *et al.* 2007). In general, alternation on photoperiod seems to have a more significant impact on cyanobacteria, than on diatoms, and lastly for *Chlorophyceae* (Shatwell T. *et al.* 2012, Foy R.H. and Gibson C.E. 1993). For instance, a change from constant light to a photoperiod of 12:12 (L:D) causes a decrease of 35-40 % on cyanobacteria (*Planktothrix agardhii*), 20-25 % for Chlorophyceae (*Scenedesmus armatus*), and 15-20 % for diatoms (*Stephanodiscus minutulus*) (Nicklisch A. *et al.* 1998).

### 2.1.2 Light wavelength

Studies in *Nostoc* sp. and *Synechococcus* sp. strains have shown a positive effect on growth under red light and a negative one under blue. Specifically, growth rates under red light are approximately 25% higher and under blue light 25 % lower than under white light. These proportions slightly vary depending on the cyanobacterial strain (Dai Y.J. *et al.* 2013, Choi C.Y. *et al.* 2013, Kim N.N. *et al.* 2014). Indeed, red light provides higher photosynthetic capacity in comparison to blue light. Red light is absorbed by chlorophyll and phycobiliproteins. Thus, red light is absorbed by both photosystems, PSI and PSII. In contrast, blue light is absorbed only by chlorophyll. Since the chlorophyll antenna of PSI is largely bigger than that of PSII (100 Chl versus 35 Chl), blue light is mostly absorbed by the PSI, creating an imbalance in the electron transport chain. This is unfavorable for cyanobacteria growth (Luimstra V.M. *et al.* 2018). In order to overcome this phenomenon and increase the photosynthetic activity of PSII, cyanobacteria upregulate the expression of PSII related genes like *psbA* and *psbD* (encoding D1 and D2 proteins of PSII reaction center) and *psbB* (encoding CP47, one of the chl-antenna of PSII). Also, genes encoding phycobiliproteins are upregulated like allophycocyanin. For example, in *Nostoc flagelliforme* allophycocyanin reaches its highest content per cell, under red light, with a 5 % increase comparing to white light (Lönneperge A. *et al.* 1985, Dai Y.J. *et al.* 2013).

Strain's metabolomic profile is also affected by the wavelength of the growth light. For example, in *N.*

*flagelliforme* the level of polysaccharides is increased by 10 % under red light and decreased by 35 % under blue light comparing to white light. Red light has a positive effect also on chlorophyll- $\alpha$  content; under red light, the cells have 40 % higher chlorophyll- $\alpha$  content, than in white light. Red light also increases the levels of carotenoids compared to those present in white light. Carotenoids mainly take part in the prevention of chlorophyll's photooxidation and in the antioxidant response (Kim N.N. *et al.* 2014, Chen M. *et al.* 2012).

Regarding the effect on cyanotoxin's production, it should be noted that red light has a positive effect on microcystin's (MC) expression, while blue light has no effect in comparison to white light. Specifically, red light of low intensities has equivalent results to white light of higher intensities, regarding the production of MC's transcripts *mcyB* and *mcyD*. On the other hand, blue light does not affect transcripts' levels (Kaebernick M. *et al.* 2000).

### 2.1.3 Light intensity

The relationship between light intensity and cyanotoxins' production can be studied through the case of MC, which has been extensively examined. The relationship between MC production per cell and light intensity is generally characterized as a wide downward-opening parabola (Rapala J. *et al.* 1997). From low-light to medium-light intensity, there is an increase of MC per cell production. Then, at medium-light intensities the production per cell reaches its maximum. These light intensities vary from 25 to 70  $\mu\text{mol photons m}^{-2} \text{s}^{-1}$  depending on the strain and experimental parameters such as the culture vessel. When light intensity increases beyond 70  $\mu\text{mol photons m}^{-2} \text{s}^{-1}$ , the cyanotoxin per cell production decreases. In some studies, the decrease rate is low (Watanabe M.F. and Oishi S. 1985, Song L. *et al.* 1998, Kaebernick M. *et al.* 2000) while in others, it is larger. For instance, at light intensities which are double the size of the intensity at which the maximum per cell production has been achieved, the per-cell production can be decreased by 3-fold of the maximum value (Sivonen K. 1990, van der Westhuizen A.J. and Eloff J.N. 1985). This explains why, in outdoor ponds, the highest amount of MC is detected at depths of 1 m, where the light intensity is medium-low and ranges from 20 to 80  $\mu\text{mol photons m}^{-2} \text{s}^{-1}$ , and not at the water surface, where the light intensity is in average 400  $\mu\text{mol photons m}^{-2} \text{s}^{-1}$ .

MC-producing-strains often have two distinguished genotypes; the MC-producers and the non-producers. In some strains, as in *Planktothrix rubescens*, the ratio between the MC-producers and the non-producers is fixed while in other cases, as in *Planktothrix agardhii*, the ratio of these two genotypes may vary depending on environmental conditions (Briand J.F. *et al.* 2005, Tonk L. *et al.* 2005). It has been shown that when a MC producer strain is under stress condition, *e.g.* with either too low or too high light intensity, as well as in competition with other strain, the MC-producer

genotype is in a higher percentage than the non-producer-genotype. Under such stress-conditions, the benefits of MC overpass its production's high energy cost and so the MC-producer genotype is favored. On the contrary, in optimal conditions when the microorganism's survival is not threatened and there is no need for MC production, the non-producer genotype is favored (Briand J.F. *et al.* 2005).

In cyanobacterial heterocystous strains, light intensity has a similar effect to growth as per cell metabolite production. Studies at *Nostoc* sp. strains, as *N. calcicola*, *N. sphaeroides*, *N. strain 152* *Anabaena* sp. strains *A. NIER*, *A. chusori* and *Microcystis aeruginosa*, have shown that strains reached their maximum growth rate at medium light intensities. Then, the growth rate decreases as the light intensity elevates, and then it faces a significant drop at high light intensities (Kurmayer R. 2011, Johnson E.M. *et al.* 2014, Khajepour F. *et al.* 2015, Ma R. *et al.* 2015, Oh H.S. *et al.* 2017, Chmelík D. *et al.* 2019, Zheng T. *et al.* 2020). High light intensity conditions in microorganism's culture lead to an increase of dangerous species of oxygen (ROS) at the level of PSII (Johnson E.M. *et al.* 2014). This increase leads to the damage of photosystems and cell death because transcriptional and translational machines are damaged. Since PSII is the first damaged during photoinhibition, the efficiency of PSII decreases. In order to protect themselves from photoinhibition cyanobacterial cells evolved different photoprotection mechanisms and adaptations. One of these adaptations includes the decrease of transcription of phycobiliprotein genes (Johnson E.M. *et al.* 2014, Zheng T. *et al.* 2020). The inhibition of PSII leads to the decline of cell growth (Johnson E.M. *et al.* 2014, Zheng T. *et al.* 2020). Under high light intensity conditions, there are also changes in the cell's physiology. Specifically, there is an increase of concentration of necridic cells of *Tolypothrix* sp. when the strain is cultivated under high light intensity comparing low light intensity (Zapomělová E. *et al.* 2008).

Necridic are called the cells that follow a "suicidal" pathway (apoptosis) lose some cellular components and then shrink (Garcia-Pichel F. 2009). High light intensity has an impact also on the filaments' morphology. In *Nostoc muscorum*, the cells are grouped in circular formations under non-light conditions while as the light intensity is increased to medium-intensity, longer filaments are developed (Lazaroff N. and Vishniac W. 1961). The productivity of H<sub>2</sub> increased with light intensity in *Anabaena* sp. PCC 7120 (Masukawa H. *et al.* 2017). Differentiations were observed in the phytochemical profile also: carbohydrates and carotenoids increased while chlorophyll a decreased per cell by increasing light intensity (Khajepour F. *et al.* 2015). *Nostoc* sp. prefers medium light intensities for the phycobiliprotein production (Ma R. *et al.* 2015, Johnson E.M. *et al.* 2014). In most cyanobacterial strains, low light conditions have a positive effect on levels of fatty acids (FA). Also, in some cases of microalgae (such as in the case of coccoid alga *Pinguicoccus pyrenoidosus*) maximum FA content is observed at medium light intensities (Sang M. *et al.* 2012).

#### 2.1.4 Medium's composition

Natural Seawater (NW) is generally acceptable for marine algal and cyanobacteria cultures. For long-term cultivation, the addition of nutrients and trace elements is necessary, otherwise the collapse of the culture is a matter of time. Additionally, the uncertainty and the unstable quality of NW, which is affected by a range of factors such as the season and the place of collection, leads to the need of Artificial Seawater (AW) (Harrison P.J. and Berges J.A. 2005, Grobbelaar J.U. 2013). AW is also a more convenient solution for mainland laboratories where the natural source is not always available. For these reasons, since the late 1800s, researchers have tried to replace NW and produce an AW of equivalent composition (Allen E.J. and Nelson E.W. 1910). One of the first successful and well-known efforts is the "Erdshreiber medium" (Schreiber E. 1927), followed by more complex recipes (Levring T. *et al.* 1946), and even in the development of commercially available recipes like the Instant Ocean (King J.M and Spotte S.H. 1974).

Aiming to understand the medium's composition, the term of "Redfield ratio" should be introduced. "Redfield ratio" or "Redfield stoichiometry" is the atomic ratio of carbon, nitrogen, and phosphorus found in phytoplankton and throughout the deep oceans. This empirically developed stoichiometric ratio was set initially as 106:16:1 (C:N:P), later to be revised to 117:14:1. Phosphorus Vs Nitrate trend, measured in  $\mu\text{mol}\cdot\text{kg}^{-1}$ , follows a ratio of 16:1 C:N:P. This ratio was firstly described in 1934 by the American oceanographer Alfred C. Redfield. It provides an ideal image of algae's environment, so it is consequently considered as a useful tool in calculating elements' stoichiometry on algae's medium. When the ratio is used for the medium's composition, the proportions can be modified depending on the microorganism addressed. For instance, for diatoms' culture, the ratio is expressed as 16:16:1 (N:Si:P) (Ingall E. and Jahnke R. 1997, Geider R. *et al.* 2002, Klausmeier C.A. *et al.* 2004). Nitrate and Phosphate source are usually added in the form of  $\text{NaNO}_3$  and  $\text{NaHPO}_4\cdot\text{H}_2\text{O}$ . An alternative source of N is ammonium, which can be added as  $\text{NH}_4\text{Cl}$ , and rarely urea which is decomposed easily when heated. Nitrate is the most appropriate source of N as it provides better growth than urea, while ammonium has even a lethal effect on the microorganism (Hemlata Fatma T. 2009).

Culture's performance is mostly based on medium's composition and nutrients' levels. Phosphates have been shown to have a positive influence on the growth rate of *Anabaena* sp., which reaches its maximum at 0.5  $\text{PO}_4^-$  mg/L, and then from 0.5  $\text{PO}_4^-$  mg/L to 5.5 mg/L no further increase in growth rate is observed (Sivonen K. *et al.* 1990, Rapala J. *et al.* 1997, BI Y.H and Hu Z.Y. 2004, Beversdorf L. *et al.* 2017). Concerning the effect of nitrates level on growth, that depends on the ability of the strain to fix nitrogen. Heterocystous cyanobacteria are not noticeably affected under N-stress, if they have already developed heterocysts, as they can serve the nitrogen fixation process through these



differentiated cells. On the contrary, non-nitrogen fixing cyanobacteria face a noticeable decrease under nitrogen limitation. Studies on heterocystous *Anabaena* sp. and non-nitrogen-fixing *Oscillatoria agardhii* verify the effect of nitrogen (Rapala J. *et al.* 1997). Regarding other micronutrients of medium's composition, it was noticed that a  $\text{Ca}^{2+}$  decrease causes a proportional drop on culture's growth while lacking of  $\text{K}^+$  has neither negative nor a positive effect (BI Y.H and Hu Z.Y. 2004).

On the other hand, components heavy metals should be avoided in medium's composition. Heavy metals such as chromium, cadmium, lead, nickel, copper, and zinc, provoke a noticeable decrease in growth and phycobiliproteins' content and in the end have a lethal effect on the culture. For instance, even a concentration of 160  $\mu\text{g Cu/L}$  is sufficient to inhibit the growth of *M. aeruginosa* and to terminate microcystin's production (Tsai K. 2015).

Medium's components have a direct effect on the cell's biochemical composition, such as the lipid profile and the light harvesting pigments: carotenoids, chlorophyll- $\alpha$ , and phycobiliproteins. The level of carotenoids is proportional to the nitrates' concentration, while the opposite happens for chlorophyll  $\alpha$  content. As a result, the carotenoid/chlorophyll ratio, which is a stress indicator, is higher in nitrogen-omitted culture (Paliwal C. *et al.* 2015). Phycobiliproteins can be characterized as nitrogen storage components. In this way, they are degraded under N-stress conditions to supply the cell with the needed compounds (Johnson E.M. *et al.* 2014). Phycocyanin's content faces a proportional drop, which leads to a phenomenon described as "nitrogen chlorosis". Macroscopically "nitrogen chlorosis" causes a change of culture's color from blue-green to brownish (Allen M.M. and Smith A.J. 1969). However, in some cases, as in *Anabaena* NCCU-9, nitrate-free medium leads to an increase of total phycobiliprotein content (Hemlata Fatma T. 2009). The inorganic carbon of Sodium Carbonate is in reverse proportion to phycobiliproteins content. The highest phycoblioproteins content is observed at low level of  $\text{Na}_2\text{CO}_3$ , while in  $\text{Na}_2\text{CO}_3$  concentration double than the optimal one, the phycobiliproteins content has been shown to be halved (Johnson E.M. *et al.* 2014).

Mediums' composition also has a direct effect on the cell's lipid profile. Phosphate limitation cause accumulation of triglycerides (TGA). At the same time, it is lowering the level of polyunsaturated fatty acids (PUFAs) as eicosapentaenoic acid (EPA). On the contrary, under phosphate abundance there are high levels of valuable PUFAs, such as  $\omega$ -3 and low levels of TGA. Nitrogen starvation has similar effects on TGA as phosphate-stress (Paliwal C. *et al.* 2017).

Lastly, cyanotoxins' content and cyanobacterial metabolites are also controlled by the presence and the levels of different nutrients. The effect of nitrates on cyanotoxins' production is related to the ability of the cyanobacterium to fix nitrogen. In non-nitrogen fixing strains, such as *Oscillatoria agardhii*, nitrogen limitation significantly decreases toxin's production (Sivonen K. *et al.* 1990, Orr P.T. and Jones G.J. 1998). On the other hand, in heterocystous cyanobacteria, as *Anabaena* sp., nitrates

limitation can be balanced by nitrogen fixation process. Consequently, in these species N-stress does not have a significant effect on the total toxin's production, though sometimes it slightly affects the portions of toxin's analogues (Rapala J. *et al.* 1997, Oh H.S. *et al.* 2017). It should be noted, that the strain is not affected when it is already adapted in low levels of N, and has developed heterocysts. Regarding the effect of phosphorus on cyanotoxins' production, there is a positive linear relationship between the increase of phosphorus on medium's composition and toxins production, as for example, MC production by *Anabaena* sp. (Rapala J. *et al.* 1997, Sivonen K. *et al.* 1990). This effect is approximately the same on heterocystous and non-heterocystous strains (Rapala J. *et al.* 1997, Sivonen K. *et al.* 1990). This is why P-limitation has a more severe impact on heterocystous strains than N-starvation. A similar pattern on nutrients' effect is observed in other cyanobacterial metabolites, such as geosmin and 2-methylisoborneol; their unpleasant taste and odor in running waters lead to studies for their diminution by *Anabaena* sp., where P-limitation has been a proposed solution (Orr P.T. and Jones G.J. 1998).

#### 2.1.5 The effect of pH

Culture's pH affects nutrient solubility, byproduct formation, cell membrane morphology, enzyme activity, and oxidative-reductive reactions (Bajaj I.B. *et al.* 2009). As a result, the value of pH significantly influences microorganisms' physiology and growth.

Regarding the growth, the majority of cyanobacteria prefer basic environments, while acidic environments have a lethal effect on the microorganism (Guckert J.B. and Cooksey K.E. 1990, Qian F. *et al.* 2014). More precisely, for chlorophyta, microalgal, and cyanobacterial strains the optimal growth is observed between pH 7.7 and 9. In neutral environment and at pH higher than 9, the strain exhibits 25 % lower growth comparing to pH 9 (Guckert J.B. and Cooksey K.E. 1990, Ray S. *et al.* 2001, Sang M. *et al.* 2012). On the other hand in acidic environment, even a few hours at pH 4-5,5 cause cell lysis in cyanobacterial strains (Qian F. *et al.* 2014). pH also affects microorganism's biochemical composition. The per-cell contents of EPSs and poly- $\beta$ -hydroxybutyrate (PHB) increase as the pH elevates from neutral to basic and reaches the maximum at pH 8-9, based on studies on *Nostoc* sp. (Tiwari O.N. *et al.* 2015, Sharma L. and Mallick N. 2005). EPSs are responsible for the extracellular sheath or mucilaginous film that surrounds the cyanobacterial cell (Desikachary T.V. 1959). These polysaccharides can be used in a variety of biotechnological applications such as the removal of heavy metals from aqueous solutions (Pereira S. *et al.* 2011). PHB is a compound that can be used as a biomaterial alternative to common plastic (Sharma L. and Mallick N.2005).

The lipid profile of the microorganism is also affected under pH alternation. The formation of FA is a natural process that takes place in cyanobacteria and microalgae in order to contribute to several

intracellular processes such as the construction of membrane lipids. FA can be categorized as TGAs and membrane lipids, which are the glycolipids (GLFA) and polar lipids (PLFA). Each group behaves differently in relation to pH. The proportion of TGFA increases in basic environments while the opposite happens for the portion of the membrane lipids (both GLFA and PLFA), while the sum of total FA decreases in basic pH, based on studies on microalgal strain *Chlorella* CHLOR1 (Guckert J.B and Cooksey K.E. 1990). Studies have shown that neutral culture-environments are optimal for the production of augmented nutritional value PUFAs, such as EPA by microalgae, as *Pinguicoccus pyrenoidosus* (Sang M. *et al.* 2012).

The majority of cyanotoxins face a high increase of per cell production when the pH is elevated from 8 to 9. This impact can be by 75 % in the case of *Microcystis viridis* and MC (Song L. *et al.* 1998) or by 4-fold in the case of *Oscillatoria laetevirens* and its toxin (Ray S. and Bagchi S.N. 2001). Beyond this point, the increase of pH does not significantly affect the intracellular cyanotoxin production until pH reaches 11 (Song *et al.* 1998, Ray S. and Bagchi S.N. 2001, Beversdorf L.J *et al.* 2017). In contrast, a variation is observed in neutral pH where some cyanotoxin's are expressed more than others (Song L. *et al.* 1998, Ray S. and Bagchi S.N. 2001). In acidic environments (pH 3-5), an important extracellular concentration of toxin is noticed. That extracellular uptake is caused by the lethal effect that the acidic environments have on the microorganism. This effect leads to cell lysis, so all the intracellular quantity of toxin is instantly released on the culture's medium (Qian F. *et al.* 2014). Environmental pH also indirectly affects the toxicity by modifying its bioaccumulation on consuming organisms. This happens as the potential bioavailability of toxins increases when a higher percentage of the toxin is in un-ionized form (Jungkon K. *et al.* 2014).

The pH effect is pronounced when then strain is in co-culture. Studies have shown that when cyanobacterial species (*Cylindrospermopsis raciborskii* and *Microcystis aeruginosa*) were in a co-culture-state with two Chlorophyta species (*Chlamydomonas asymmetrica* and *Scenedesmus obtusiusculus*) the production of cyanotoxins (cylindrospermopsin and MC) is increased as the pH increases from 7 to 9. On the contrary, when the cyanobacterial strains were cultivated in monoculture, no difference was observed in cyanotoxin's concentration as a result of the pH changes (Dzhambazov B. *et al.* 2018).

### 2.1.6 The effect of temperature

Cyanobacteria have managed to impressively adapt their metabolic processes and phytochemical components in a wide range of temperatures, from frozen lakes to hot springs. Some species can survive in Antarctic environments with temperatures as low as 0 °C, such as *Oscillatoria* sp. (Singh S.M. and Elster J.2007), while other thermotolerant strains as *Synechococcus* sp. that grow in hot

springs with temperatures up to 60 °C (Miller S.R. and Castenholz R.W. 2000). So, the optimal growth temperature varies. However, high temperature causes in most of cyanobacteria species an increase in ROS,  $O_2^-$ ,  $^1O_2$ ,  $\cdot OH$ , and  $H_2O_2$ . This leads to a chain reaction of photosystems' damaging and phycobiliproteins decrease as described in the case of photoinhibition (Zheng T. *et al.* 2020). Another reason that high temperatures decrease cyanobacterial growth might be the decrease of  $O_2$  solubilization in the culture media, which would then be a leading cause of stress (Hemlata Fatma T. 2009). As mentioned, there is high heterogeneity in optimal growth temperature. In relation to the genus of interest, studies at strains of *Nostoc* sp., have shown that the growth rate elevates as temperature increases. These strains reach their maximum growth rate at a range of 26-35 °C, depending on the strain. Temperatures higher than 35 °C have a lethal effect on these strains, as even a few hours at 40 °C are sufficient to cause cell death. The same happens for strains of *Microcystis aeruginosa*, and coccoid alga *Pinguicoccus pyrenoidosus* (Sang M. *et al.* 2012, Kakimoto M. *et al.* 2014, Cirés S. *et al.* 2017, Chmelík D. *et al.* 2019, Zheng T. *et al.* 2020). In other strains, the optimum temperature for growth is lower. In *Anabaena* sp. strains, the percentage of both necridic cells and heterocysts was augmented by increasing the temperature from 10 °C to 25 °C; the maximum of heterocysts' concentration was observed at 22 °C while necridic cells have a linear relation to temperature (Zapomělová E. *et al.* 2008).

Regarding the changes that take place in the cell due to temperature, there is an effect on fatty acids' (FA) composition. For example, on *Pinguicoccus pyrenoidosus*, the percentage of saturated fatty acids (SFA) on total FAs is increasing by raising the temperature from 20 °C to 28 °C. In contrast, the portion of monosaturated fatty acids (MUFA) remains stable while PUFAs, such as EPA and  $\omega$ -3, decreased as temperature increased (Sang M. *et al.* 2012, Paliwal C. *et al.* 2017). Long-chain PUFAs such as EPA contribute mostly to the cell membrane fluidity. In low-temperature-stress, membrane fluidity is threatened. This is a possible explanation for the elevation of PUFAs at low temperatures as a metabolomic response to reinforce cell-membrane (Paliwal C. *et al.* 2017). It is further noted that the toxin production per cell is higher within the range of 20-25 °C than at higher temperatures (van der Westhuizen A.J. and Eloff J.N. 1985, Sivonen K. *et al.* 1990, Kurmayer R. *et al.* 2011). A proposed explanation of the reduced cyanotoxin's production at higher temperatures is the expression of toxin's different analogs. These analogs, which occur at temperatures high as 30-35 °C, often have either reduced toxicity or no activity at all (Rapala J. *et al.* 1997, Dziallas C. and Grossart H.-P. 2011). For instance, with *Microcystis aeruginosa*, when the temperature increases from 20°C to 32°C, the production of MC analogs, MC-YR, increases significantly while the portion of analog MC-LR remains at the same level (Song L. *et al.* 1998, Dziallas C. and Grossart H.-P. 2011). However, MC-YR is on average 2-fold less toxic than the -LR, so the per cell toxicity of *M.aeruginosa* is approximately up to 4-fold higher at 20 °C comparing to 35 °C (van der Westhuizen A.J. and Eloff J.N. 1985). However,

*M.aeruginosa* grows faster at 30 °C than at 20 °C, so in some cases the total concentration of the toxin in the culture at 30 °C is higher than at 20 °C, even if the per-cell production is maximal at 20 °C (van der Westhuizen A.J. 1985). This happens as the difference in per cell production cannot outweigh the higher growth rates at elevated temperatures (Sivonen K. *et al.* 1990, Kurmayer R. *et al.* 2011, Dziallas C. and Grossart H.-P. 2011). Lastly, temperature also affects the way that the grazers of the local ecosystem interact with the cyanotoxins. In addition to the increased total toxin concentration, there is a parallel shift of the feeding habits of grazers such as *Moina macrocopa*, species of daphnids *Daphnia*, and their chemical metabolism. Consequently, these organisms become in total more vulnerable with temperature changes (Jungkon K. *et al.* 2014).

### Applied culture conditions for cryptophycin's production

As it was noted from early 90's the importance and the potential that Cry had for the development of a novel anticancer agent, lead several studies to focus on its examination. As a result, a variety of conditions applied for the production of the compound from the two producer strains. Firstly, Schwartz R.E. *et al.* 1990 managed to isolate and identify the molecule of Cry from ATCC 53789. Their project was related generally to algal pharmaceuticals. They cultivated with the same method a variety of strains that were further examined, so their method was not focused on cryptophycin's production, which until then was unknown. The method includes an initial cultivation of the strain with BG-13 medium, at a 24-well plate with 5-10 mg of soil. The plate was incubated at 25 °C under 5 % CO<sub>2</sub> and kept under a cool-white light of 5,000 lux with a photoperiod 24:0 (Light:Dark). After the growth of a sufficient amount of culture, that inoculum was transferred at BG-12 agar medium and then also with BG-12 medium at 500 mL flasks. The conditions were the same with the 24-well plates with the addition of a magnetic stirring bar at 100-200 rpm. BG-12 and BG-13 are identical media with the difference that BG-12 is buffered with N-2-hydroxyethylpiperazine-N'-2-ethanesulfonic acid (HEPES) while BG-13 is not buffered and contains extra NaHCO<sub>3</sub>. The same study is described in the patent of Hirsch C.F. *et al.* 1990. It is mentioned that during the first two weeks of fermentation most of the compound stays inside the cells, while after the two weeks period there may be cell-lyse and quantities of the compounds are found in the medium also.

A second study was conducted by Golakoti T. *et al.* 1994, where they examine both strains of ATCC 53789 and GSV 224 for the presence of Cry analogues. They cultivate both strains in 20 L carboys. The culture was maintained at 24 ± 1 °C under aeration of 5 L/min with 0.5 % CO<sub>2</sub> and an illumination of 200 μmol photons m<sup>-2</sup> s<sup>-1</sup> cool-white light. The medium was BG11 buffered with MOPS at pH 7. A project from the University of Hawaii, 10/2004 to 09/2006, focused on the effect of medium, time of life-cycle, and axenic conditions in cryptophycin's production. Regarding the relation of total production with life-cycle, it is demonstrated that both growth and total intracellular production

have similar patterns, reaching a maximum plateau at day 30 with 0.246 g/L under the specific conditions. However, the per cell production faces a significant drop since the one third of life-cycle on day 10. That fact implies that the toxin-production helps the microorganism to defeat the competence of other microorganisms on nutrient limitation when it is mostly needed, in other words until the late exponential phase (Back S. and Liang J. 2004, Liang J. 2006).

Focusing on the medium's composition it was shown that BG11 was better for optimal metabolite production, followed by A3M7 and lastly modified BG11. Surprisingly, A3M7 medium has lower nitrates' level than 'modified BG11' but leads to higher cryptophycin's levels in comparison to 'modified BG11'. That fact indicates that the nitrates level is not the most crucial factor in medium's composition. Comparing the two main producer-strains they end-up that GSV 224 produces at least double quantities of Cry than ATCC 53789 when the two strains are cultivated under the same conditions. However, unfortunately GSV 224 strain is not available for industrial exploitation. Lastly, it was shown that axenic and non-axenic conditions had a similar result regarding the metabolite, so it is proposed that the high-cost axenic culture is not financially profitable. However, the type of contaminants and the non-axenic conditions are not defined and so a generalization about the preference on non-axenic would be non-coherent.

Biondi N. *et al.* 2004 examined the isolation of Cry starting as well from ATCC 53789 strain. In their study, they use 1- and 10-liter glass tubes bubbled with an air-CO<sub>2</sub> mixture (98:2 v/v) as in related studies, and illuminated under a constant light of 200 μmol photons m<sup>-2</sup> s<sup>-1</sup>. The temperature was regulated at 25-28 °C, and the medium was BG11o.

## 2.2 Review on photobioreactors and photoacclimation

The need for higher production of metabolites promotes the use of photobioreactors. In these facilities, the selected optimal conditions can be applied in order to maximize the obtained biomass, as well as the required metabolite. Several types of photobioreactors have been developed which are adapted in the provided space and conditions. However, in all the types of reactors the light is always a complicated parameter. As the culture-volume is elevated, the light should be adapted to respond to that complexity. The study of the light in reactors through the terms of photoacclimation helps in understanding the function and construction of the photobioreactors.

### 2.2.1 Introduction to photoacclimation

Photoacclimation is the response that is developed by the microorganism in the change on the environmental light parameters. The term should not be confused with photoadaptation. On the one hand, photoadaptation is the process of responding to light conditions by changing the genotype

through several generations. On the other hand, photoacclimation is the process of cell modifications for responding to light changes. However, these modifications take place at the same cell generation and have no impact on cell's genotype (Falkowski P.G *et al.* 1991).

These phenotype changes include mostly a decrease of photosynthetic pigments' concentration, or changes in pigment's complement, on the electron transfer components or finally, in Calvin cycle enzymes. When there are low-light conditions, photosynthesis is proportional to the amount of chlorophyll a, while when there are light-saturated conditions the phenomenon is proportional to the content of cellular carbon (Sukenik A. *et al.* 1987).

Photoacclimation should be considered as terminated when a balanced growth has been achieved. For instance, for cells that follow a L:D cycle, that process has finished when the cell composition remains the same after 24h (MacIntyre H.L *et al.* 2002). It should be noted that in several cases, the acclimation cannot be achieved through severe light changes, and that may cause photoinhibition. For example, the cyanobacterium *Synechococcus* is able to go through light changes only through intermediate irradiances (Kana T.M. and Glibert P.M. 1987). To sum up, the acclimation rate may differ among the taxa of cyanobacteria. Though, it follows a similar pattern of phenotypic changes. The expression-rate of these changes is important. That rate, in comparison to the maximum rate of light absorption, draws a slight point for each taxon. That point slightly separates the phase of photoacclimation from the phase of photoinhibition, and the phase that the light is beneficial from the phase that it causes the opposite results.

The study of microorganism's photoacclimation provides a tool for understanding; a) the effect of culture's density on microorganism's growth rate and b) the light utilization efficiency.

### The effect of photoacclimation in photobioreactors

As it was described above, photoacclimation is depicted as the phenotypic changes in order to respond to the variable light conditions. More specifically, in cyanobacteria, *Synechocystis* sp. PCC 6803 has been used as a case study. There, we observe an increase in cell wall thickness, while a remarkable fact is the increase of photosynthetic pigments' concentration (Straka L. and Rittmann B.E. 2018). That happens as lower light availability leads the cell to increase pigments' concentration in order to make the best profit of the limited light conditions.

Photoacclimation is a result of the microorganism's constant movement between places with different light intensities. That difference in light intensity is caused in two cases; a) in high-density cultures b) in photobioreactors with low liquid circulation. In the first case, an amount of cells creates a border that absorbs and reflects most of the light, and in that way, it creates shadowed areas. In the second case, the low circulation does not mix well the cells, and as a result there are cells that stay more near the photobioreactor's wall and the light beam, and others that stay more on the

inner layers.

The level of photoacclimation can be calculated averagely by the ratio of optical density at 680 nm to the optical density at 750 nm. It is known that the photosynthetic pigment Chl *a* absorbs at 680 nm while above 700 nm is the area where the pigments do not absorb, so only the turbidity is recorded. Based on that, it is concluded that the ratio of Optical Densities (ODs) on these wavelengths ( $OD_{680}/OD_{750}$ ) depicts the quantity of Chl *a* in relation to the total cell quantity. That ratio reveals the light utilization efficiency. According to the above data, it can be understood that in low cell concentrations, light efficiency would be maximum. In low concentrations, the cells are well positioned in the liquid, and the light is spread naturally with few shadowed areas. So, most of the amount of light is absorbed by the cells. Indeed, in studies at *Synechocystis* sp. PCC 6803 the most efficient was in low cell-density while later is plateau (fig.2.1) (Straka L. and Rittmann B.E. 2018).

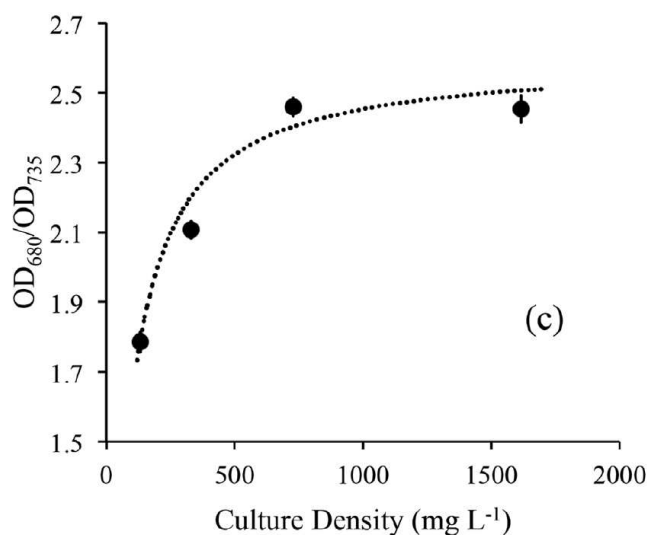


Figure 2.1: Photoacclimation development, measured as ratio of  $OD_{680}/OD_{735}$ , during the growth of *Synechocystis* sp. PCC 6803 culture. The quotient of Chl *a* absorption to turbidity indicates the light utilization efficiency (Adapted from Straka L. and Rittmann B.E. 2018)

## 2.2.2 Photobioreactors

The need to produce secondary metabolites in large quantities leads to the development of scale-up facilities. The scale-up could be done outdoors in ponds or indoors in fermentors and photobioreactors (PBRs). Fermentors and photobioreactors are both closed vessels for the indoor scale-up level. In PBRs the main source of energy is light, which is provided by external light sources. In the case of cultivation of photosynthetic microorganisms, like cyanobacteria, PBR is the optimal choice for a scale-up approach. However, as mentioned above, one of the main issues that photobioreactors' design faces is the low-liquid-circulation, which leads to photoacclimation. To solve this issue, several agitation techniques have been developed. Indoor vertical photobioreactors are divided into two categories based on their agitation system; a) the bubble column PBRs, and b) the airlift PBRs.



The bubble column photobioreactor (fig.2.2) contains an air sparger on the bottom, which is connected to the air pump, and it provides agitation through bubbling. The number and the type of spargers can be varied, so the airflow, the size, and the speed of the bubbles can be regulated. These parameters have an essential role in mass transfer. So, these are responsible for the creation or not of shadowed areas, and for the homogenization of the culture. Moreover, heavy agitation may cause fragmentations to filaments, so it should regulated to achieve the maximum homogenization and at the same time the minimum fragmentations (Gupta P.L. *et al.* 2015, Granata T. 2017).

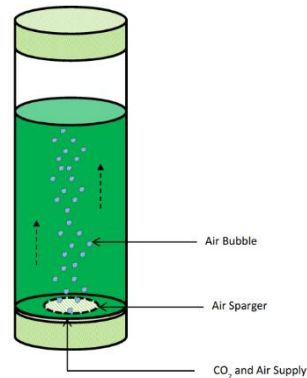


Figure 2.2: Instrumentation of bubble column photobioreactor. The sparger in the bottom regulates the size of the bubble and the air flow, parameters essential for the homogenization of the culture and the state of the filaments (Adapted from Gupta P.L. *et al.* 2015)

The second category is based on the same principle of agitation by air bubbles, though it is slightly modified. In contrast to the bubble-column-photobioreactor where the flow is linear in one zone, in airlift photobioreactor, the flow is circular in two zones. The one zone is the flow which is going upstream, and the second one the flow which is going downstream. That could be achieved either with an external loop or with a centric tube that separates the two zones and leads the airflow to the top. In that way, the culture constantly passes from shadowed to light zones, and it faces a "flash effect" (fig.2.3) (Gupta P.L. *et al.* 2015).

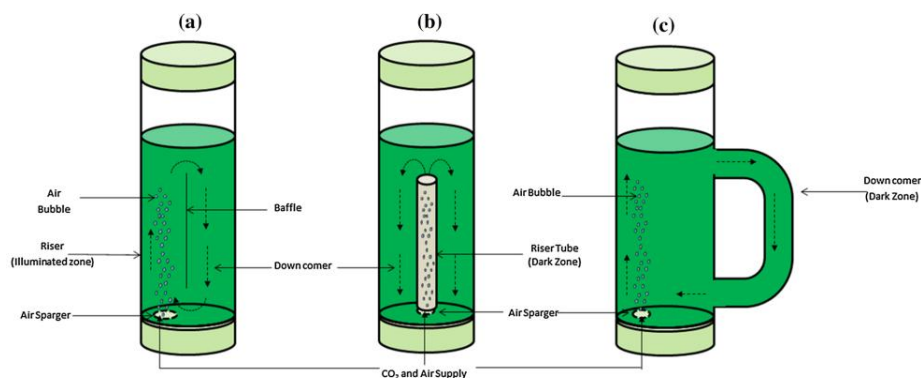


Figure 2.3: Instrumentation of airlift photobioreactor with ; a) internal loop, b) internal loop concentric, c) external loop. These loops create separate light and dark zones, and the culture face flash effect while passing from the one zone to the other (Gupta P.L. *et al.* 2015)

## 2.3 Personal work: involved techniques and methods in cyanobacterial culture

As mentioned above, in relation to the optimization of culture conditions, the physicochemical parameters which were examined were the light parameters (intensity, photoperiod, wavelength), temperature, pH, and medium composition. In order to analyze the experimental process and the obtained outcome, the involved techniques should be firstly reported. These techniques could be split into two categories; a) cyanobacterial culture methods b) Cry quantification process. *Nostoc* sp. ATCC® 53789™ was purchased by ATCC® (American Type Culture Collection) and was maintained in BG-11 medium (Rippka R. *et al.* 1979). Conservation and growth of the culture request a range of techniques such as a) familiarizing with the experimental equipment, b) working under sterile conditions, c) growth observations.

### 2.3.1 Working under sterile conditions

To protect the strain, as well as the environment, and ourselves, safety protocols are followed to ensure sterile conditions and minimize the threat of potential contamination.

All manipulations and culture-treatment took place in a horizontal-laminar-flow cabinet (ADS Laminaire). The cabinet was under UV radiation overnight. UV radiation has the ability to form covalent bonds between adjacent thymine in DNA. As a consequence, it causes mutations and has lethal effect on microorganisms. Further than the UV radiation, the workplace was cleaned with EtOH/H<sub>2</sub>O 70 % spray 30 min prior to the use. The cleaning process with EtOH/H<sub>2</sub>O was repeated right after. Moreover, every material that was inserted in the cabinet was sprayed with EtOH/H<sub>2</sub>O solution, as well as the user. During the treatment, in the middle of the cabinet it was placed a Bunsen burner which produced a single open gas flame and provided an extra level of sterility in a diameter of 15 cm around the flame. After the treatment, all the used materials were left overnight in an appropriate closed basket with sodium hypochlorite (bleach). Cultures were disposed in the same way by decontaminating overnight with bleach. All the materials which were in contact with the culture, as well the medium, were autoclaved before the use and kept in closed shelves. An autoclave apparatus is composed of a heavy-walled closed chamber. The sterilizing ability of autoclave is based on steam with high-temperature and high-pressure. The duration and temperature are parameters that change depending on the material that should be sterilized. In the project's case, 1 h at 120 °C provides the needed sterility for the materials and the liquids. Lastly, every second month a sterility test was conducted on the working and storing surfaces to verify the sterility of the workplace (fig.2.4). In that test, a petri-dish of agar with Trypticase-Soja medium is exposed on three spots for 1 h. These spots are firstly the area of manipulation, which is the laminar flow, secondly the areas of cultures' conservation, which is the incubator, and lastly on the lab's

bench. Then, the petri-dishes are incubated for 72 h at 30 °C. If more than two colonies are observed, then the conditions in the examined area should not be considered as sterile.

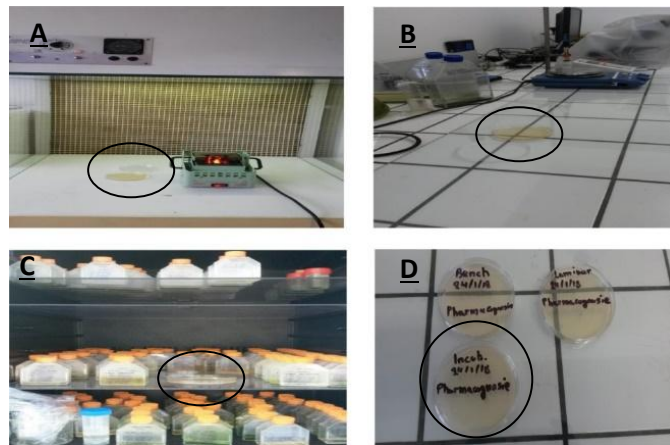


Figure 2.4: Petri-dishes of agar with Trypticase-Soja (in red circle) are exposed to laminar flow (A), bench (B, D), and incubator (C).

### Culture containers

Depending on the use and the amount of culture, the appropriate container with the respective top was used (fig.2.5). For stock cultures and small-scale inoculums, T-flasks (Thermo Fisher Scientific) were used. A stock culture was always stored in triplicate, in T75 flasks at 20 °C. From these flasks, T225 flasks were inoculated in order to prepare higher volume inoculums for the experimental process. For transferring culture samples in other labs or institutes, self-standing plastic tubes with screw caps were used. Lastly, for the experimental process, 500 mL Erlenmeyer flasks were chosen. It is known that among different species, there is a variety of preferences as far as their container is concerned (Kawachi M. and Noël M.-H. 2005). Regarding the caps, the T-flasks were always with the plastic cap with plastic filter directly from the manufacturer. On Erlenmeyer flasks, cotton top with gaze was adjusted.

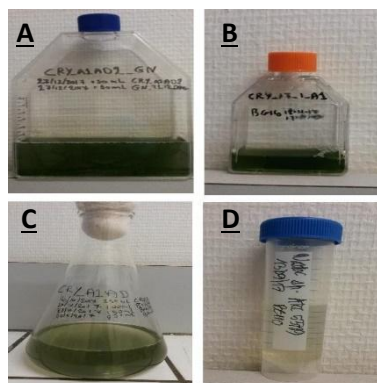


Figure 2.5: The culture containers differ in size, shape and the top. Cell-culture on T225 (A) and T75 (B) plastic flasks with filter cup. Plastic self-standing tube with a screw top (D) 500 mL Erlenmeyer flask with cotton-gaze top.

### 2.3.2 Growth observations

There are several tools to study the development of cyanobacteria's culture. The three main ways are; a) the hemocytometer, b) the Optical Density (OD) c) Dry Biomass Calculation (DBC).

#### Hemocytometer

Hemocytometer is a microscope slide with designed chambers of specific dimensions, which help the researcher to count the number of cells per chamber. Then using statistical tools, the user is able to calculate the total concentration of cells. Hemocytometer is a useful tool in monocellular cultures where the cells can be distributed homogeneously. However, in filamentous strains, such as *Nostoc* sp., that technique seems not applicable.

#### Optical Density (OD)

Optical density is the most common indirect way of calculating the biomass of microorganisms in a suspension. Cellular formations of the microorganism, like photosynthetic pigments, can absorb the light at specific wavelengths. However, above a value of approximately 700 nm the wavelength cannot be absorbed by any of these formations. As a consequence, when the sample is exposed in the spectrometer to radiation with a wavelength higher than 700 nm, the light beam passes through the suspension without being absorbed. On the other hand, that amount of light is scattered while passing through the sample, and at the end only a part of that beam reaches the detector. This is an indirect way of calculating the culture's concentration. However, it should be highlighted that the decrease of light intensity that reaches the detector is due to the scattering that occurs by the obstacles in the cuvette. These obstacles could be anything like leaving cells, dead cells, fragments, or even contaminants. In that way, the OD above 700 nm does not strictly depict the living cell-density. It depicts the turbidity that occurs by all the floating formations on the culture. This is the reason why OD should be accompanied by microscopic observation to verify that the majority of the "floating formations" are living cells.

As mentioned above, there is a fundamental difference between the wavelengths below and above 700 nm. In the first case, the light beam is partially absorbed and then reaches the detector. In the second case, the light beam is scattered while heating the floating portions and then reaches the detector. As can be understood, in the first case the beam continues linearly after the cuvette, so the measurement would be the same no matter the type of the meter. On the other hand, in the case of the scattered radiation there is a series of factors; a) the distance between the cuvette and the detector, b) the characteristics of the detector's lenses (size and focal length), c) the detector's size and sensitivity.

As a result of the above statement, OD from different UV meters (or from the same after significant amount of time) cannot be compared. It has been shown that even the same sample can give different values on different instruments (Ependorf 2015). When growth curves of the same sample are drawn in different spectrometers, the difference between the two curves augments proportionally to the growth (Ependorf 2015). The ratio of the OD value of the instrument A with the OD value of instrument B is called "conversion factor". As the difference between the two curves is not stable, the same happens with the conversion factor as well. In the end, this factor is the mean of all the conversion factors that are depicted throughout the growth period, and that mean depicts an overall image about the relation of different instruments. This factor can be useful when the researcher changes labs or when the lab's spectrophotometer has been changed (Matlock B. 2019).

### Dry Biomass Calculation (DBC)

Lastly, an alternative way for growth's measurement is DBC. A nylon-filter 0.2  $\mu\text{m}$  pore (Supelco, Nylon 66, 58060-U, 0.20  $\mu\text{m}$ ) was heated at 105  $^{\circ}\text{C}$  for 2 h and weighed. Then, 10 mL of sample were filtered, and 10 mL more of  $\text{H}_2\text{O}$  were added right-after to wash away the remaining salts. Lastly, the filter was heated again at 105  $^{\circ}\text{C}$  for 4 h and weighted. The dry biomass was calculated as the mean of three samples. Considering that the hemocytometer is not accurately applicable for filamentous cyanobacteria and the OD differs among different spectrometers, DBC is mentioned as the most appropriate technique for the project.

Though, DBC is time-consuming in comparison to OD. So, a calibration curve was established to correspond the OD into mg of dry biomass (fig.2.6). Based on that curve, OD was used for everyday measurements, and then the results were expressed in dry weight through the formula:  $y=5.6848*x$ , where  $y$  is the mg of dry biomass in 10 mL of medium and  $x$  is the optical density measured at 860 nm.

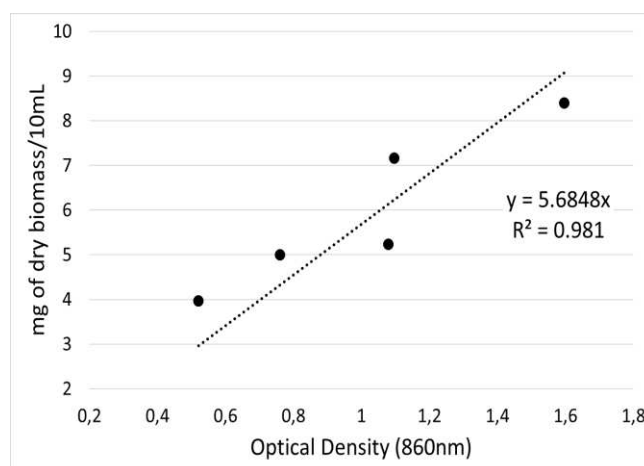


Figure 2.6: Optical density to dry biomass

## pH measurements

As mentioned above, the main source of energy for *Nostoc* sp. is oxygenic photosynthesis. This process is based on consumption of CO<sub>2</sub> by the microorganism. The impact of that process is depicted on the change of pH value when the medium does not contain a pH-buffer. In other words, as the photosynthetic process takes place in the microorganism, a proportional increase in pH value is observed, and vice-versa, low photosynthetic process, or cell-death, would be depicted as decrease or stabilization of the pH value. Consequently, the pH observation functions as an indirect depiction of our cell-growth.

### 2.3.3 Microscopic observations

The culture was examined through microscopic observations with an optical microscope (Motic) at 10x, 40x, and 100x (fig.2.7, 2.8, 2.9). The observations at 10x depict a general image of the culture. A focus at 40x enables the observation to verify the absence of contaminants and the possible fragmentations. Finally, at 100x, the user can have a better look at the physiology of the filaments and on the different cell types.

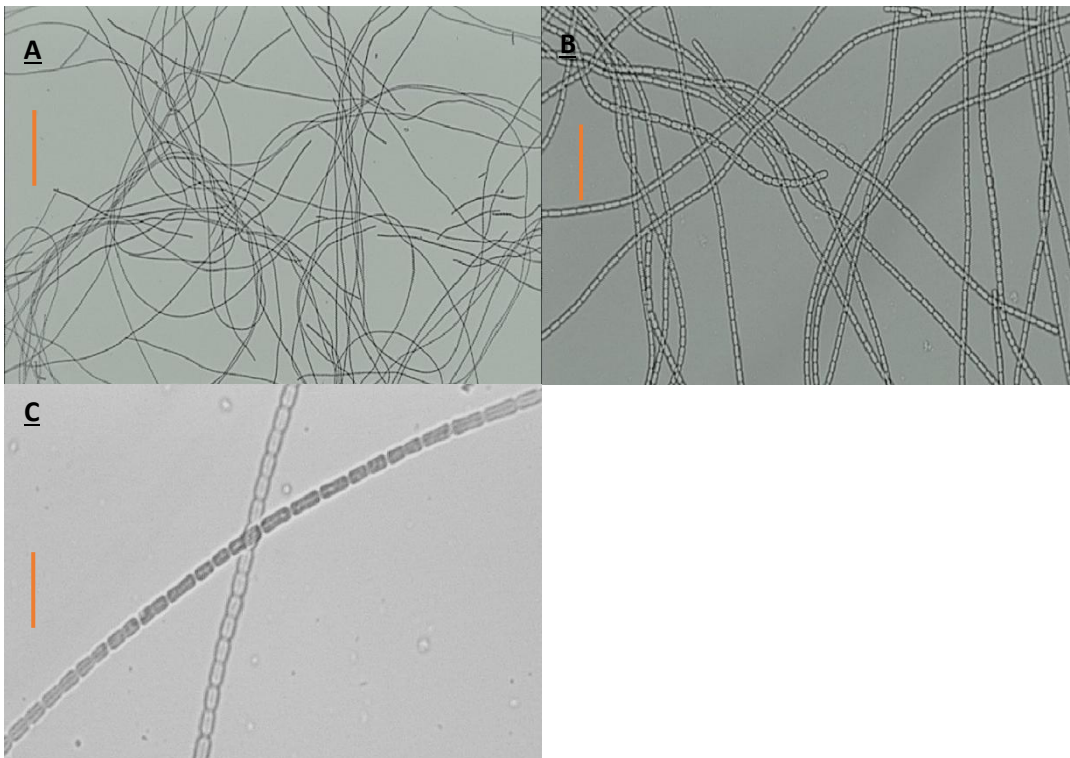


Figure 2.7: Filaments with vegetative cells at 10x (A), 40x (B), 100x (C) magnification. The bar is 1590  $\mu\text{m}$  (A), 397.5  $\mu\text{m}$  (B) and 159  $\mu\text{m}$  (C). (observations by Polyzois A.)

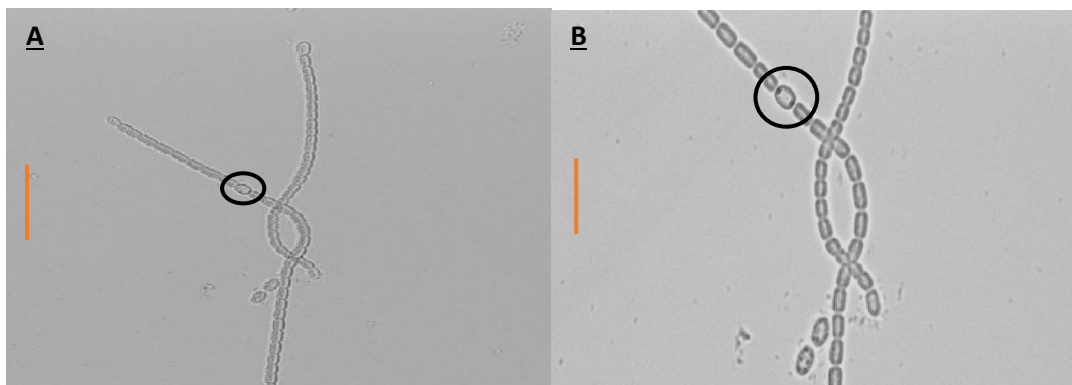


Figure 2.8: Filaments with heterocysts (in circle) at 40x (A) and 100x (B) magnification. The bar is 397.5  $\mu\text{m}$  (A) and 159  $\mu\text{m}$  (B) (observations by Polyzois A.).

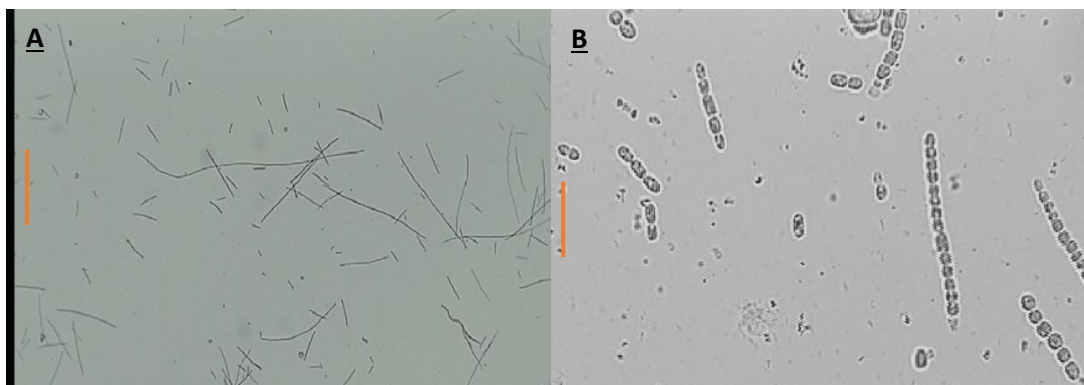


Figure 2.9: Observation at 10x (A), and 100x (B). On image A, culture of long filaments with vegetatives, and short filaments which are hormogonia. On image B focus on hormogonia. The bar is 1590  $\mu\text{m}$  (A) and 159  $\mu\text{m}$  (B) (observations by Polyzois A.).

## 2.4 Personal work: involved techniques in cryptophycin's quantification method

### 2.4.1 Development of extraction and quantification method of cryptophycin from small volumes

#### Cryptophycin extraction from small volumes

The experimental process demands to work on biological and technical triplicates in order to ensure the repeatability of the obtained results. In that amount of repetitions, it is not applicable to work on a high scale for all the experiments. The most efficient experimental setting was to cultivate the strain in an Erlenmeyer flask of 500 mL with a working volume of 300 mL. Consequently, we had to develop a method to quantify the metabolite from a small level of culture, that level was 20 mL. 20 mL sample was taken every sampling-day under sterile conditions, and the intracellular metabolite's quantity was measured. The quantification was calculated as described below.

The sample was centrifuged at 2,000 Rounds Per Minute (rpm) for 25 min ("BR4i – Jouan" centrifuge). Then the upper face, which is composed only by culture's medium, was discharged. The lower face, which contains medium and cells, was recentrifuged at 10,000 rpm for 10 min ("1-14 – Sigma" centrifuge). Again, the upper phase was discharged. In the tube with the lower phase, it was added 0.5 g of beads (1.4-1.0 mm diameter) and 500  $\mu\text{L}$  of MeCN, and the tube was applied in in

"PRECELLYS® 24 Tissue homogenizer" (Bertin instruments, CNIM group, Paris, France).

PRECELLYS® 24 is a grinder-homogenizer which adapt tubes of 2 mL, and apply them on a figure-8-multi-directional motion. In order to enforce the grinding process of the cells beads were be added in the tubes. Based on protocols of *Nostoc Punctiforme* ATCC 29133 (bertin-instruments.com), we developed a lysis method for the culture. Specifically, the tube was placed in "PRECELLYS® 24 Tissue homogenizer" for 3 rounds of 20 sec with 5 sec stop at 5,000 rounds-per-minute (rpm). Then the tube was centrifuged at 10,000 xg for 1 min ("1-14 – Sigma" centrifuge).

### Cryptophycin quantification from small volumes

The final upper phase was subjected to HPLC analysis. The HPLC quantification process, as well as the above extraction process, took place at the lab of PNAS(Produits Naturels Analyse et Synthèse, Université de Paris, CiTCoM, UMR CNRS 8038).

The HPLC was Dionex Ultimate, pump Ultimate 3000 coupled with a DAD detector Ultimate 3000 which was set on cryptophycin's  $\lambda_{\max}$  (235 nm). The autosampler was Ultimate 3000 with an injection volume of 20  $\mu$ L, and the software which was used was "Chromeleon". The column was Zorbax Eclipse Plus-C18, 4.6 x 150 mm i.d., 5  $\mu$ m and also a precolumn Zorbax Eclipse Plus-C18, 4.6 x 12.5 mm i.d., 5  $\mu$ m was used. We applied a gradient mode with H<sub>2</sub>O and MeCN (table 2.1), in a flow rate of 1 mL/min.

| Time (min.) | MeCN % V/V | H <sub>2</sub> O % V/V |
|-------------|------------|------------------------|
| 0           | 50         | 50                     |
| 60          | 70         | 30                     |
| 65          | 100        | 0                      |
| 75          | 100        | 0                      |
| 80          | 50         | 50                     |
| 90          | 50         | 50                     |

Table 2.1: Gradient mode H<sub>2</sub>O/MeCN



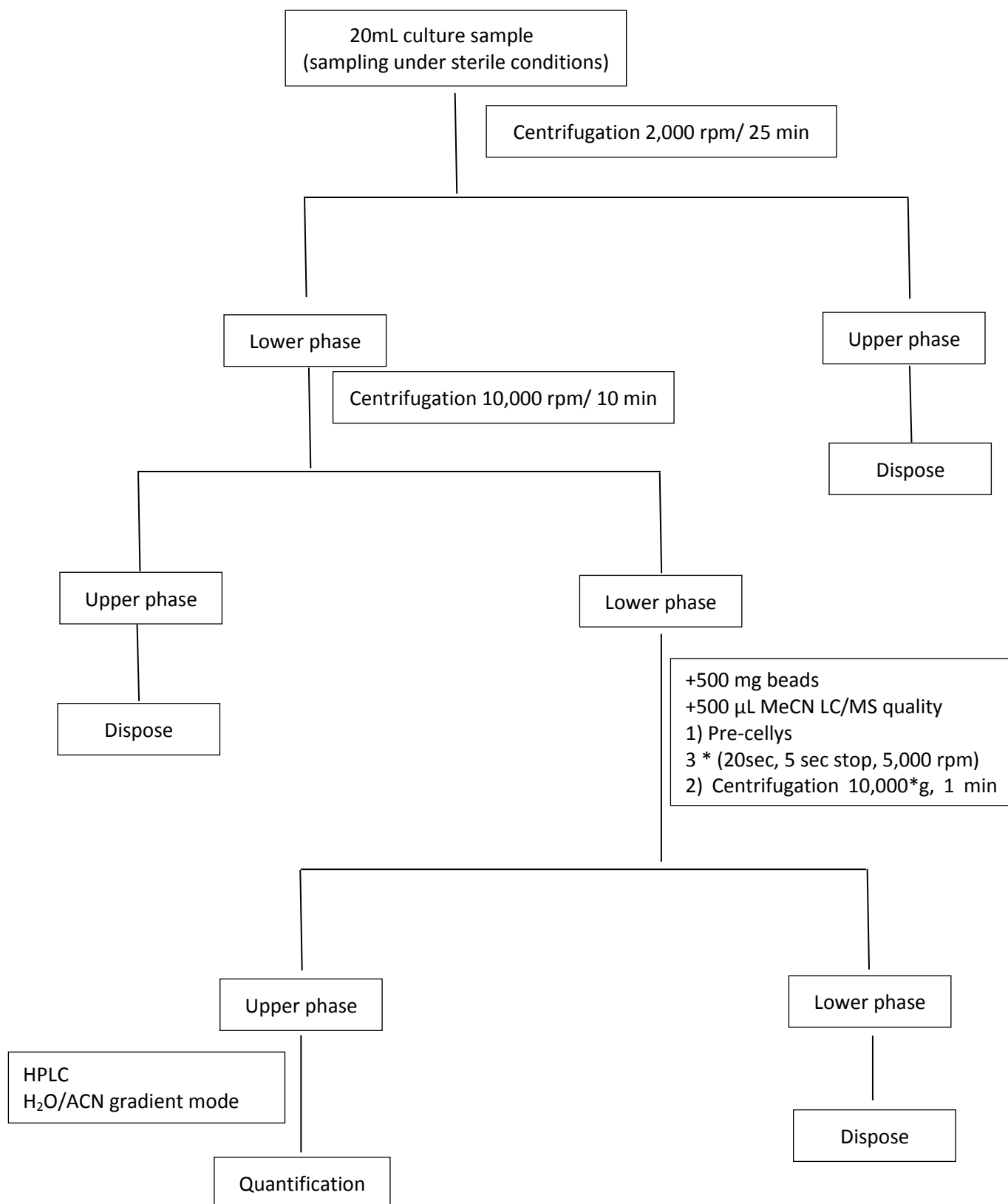


Figure 2.10: Extraction and quantification process from small volumes of culture.

Following the analysis, "Chromeleon" software depicts the chromatogram and calculate the AreaUnder the Curve (AUC). Based on a calibration curve that we set (fig.2.11), we managed to translate that AUC value into concentration of Cry. The concentration was calculated and expressed

in “ $\mu\text{g}/\text{in sample of } 20 \text{ mL}$ ” as that was the sampling amount for our tests. A range of 9 known concentrations of Cry-standard, provided by Dr. Thai Q.D. (Pronovalg), sets the curve and corresponds the AUC-235 nm to the quantity of Cry on  $\mu\text{g}$ . Lastly, regarding the experiments, the values were presented as means  $\pm$  standard deviation of the technical and biological replicates. The related graphs of productivity and growth were drawn using Microsoft Excel software.

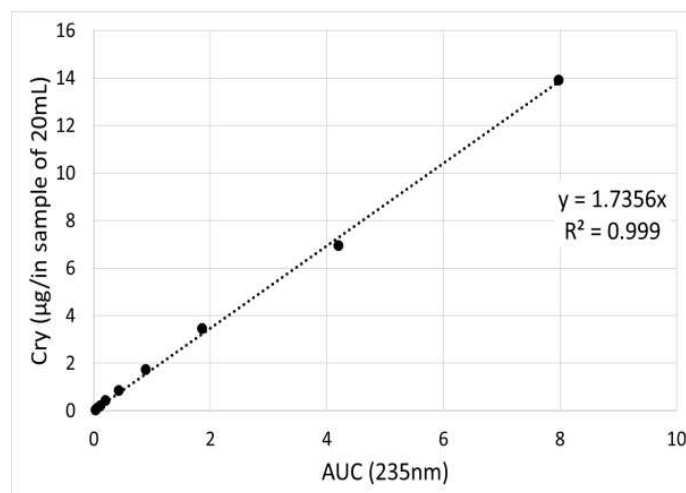


Figure 2.11: The calibration curve which was set to translate AUC value into “ $\mu\text{g}/\text{in sample of } 20 \text{ mL}$ ”.

## 2.5 Overproduction of cryptophycin through optimizing the culture conditions of *Nostoc* sp. ATCC 53789

### Observation before culture’s inoculation

The techniques mentioned above, which were on growth of cyanobacterial culture and quantification of its metabolites, are used for the examination of culture conditions. These conditions are the light parameters (intensity, photoperiod, wavelength), temperature, pH, and medium composition.

An experiment consists of biological and technical replicates, which are inoculated from the "mother-culture" with the appropriate dilution of fresh medium. Before the inoculation of one experiment - and its replicates- several things should be checked on the mother culture.

Firstly, a microscopic observation takes place to ensure the state of the strain. The culture should be with filaments without fragmentations (fig.2.7). Secondly, we have to ensure the absence of contamination. That is verified through microscopic observation at 40x and 100x. Lastly, we have to check the level of Cry, as described above. All the sets of biological and technical replicates of one experiment should have the same initial Cry value, as they are inoculated from the same mother culture with the same dilution. However, the initial Cry value among different biological replicates of one experiment might slightly fade when the mother culture is cultivated for an extended period of time. That may happen due to the strain's age, history, or physiological shear stress (Schatz D. *et al.*

2007). For the same reason, the initial Cry value of two experiments that have been conducted in different periods may also slightly vary. That should be taken into consideration in order to compare equally the results of different experiments.

### Cryptophycin measurements and growth observation on sampling day

Following the above developed methods on every experiment we draw three curves. Firstly, we observed the culture's growth based on the developed dry biomass calculation method, which was expressed in mg of dry biomass in 10 mL of culture.

Then, with the method of calculation of metabolite's concentration in small quantities, we managed to calculate the actual Cry quantity in a 20 mL sample. That is mentioned as "Cry quantity per culture", and even if it depicts the Cry quantity only 20 mL, it could give proportionally an overall image about the total culture's Cry quantity and permitted to compare total amount between different experiments.

Lastly, the quotient of Cry in 10 mL to the calculated dry biomass of 10 mL, depicts the  $\mu\text{g}$  of Cry per mg of dry biomass. So, it provides an approach for the Cry production per cell.

#### 2.5.1 Light intensity experiment

##### Experimental session

The strain was cultivated in a multi-cultivator MC 1000 (PSI- Photon System Instruments) using tubes of 5 cm diameter. Each tube had an initial culture volume of 90 mL. The agitation was provided through air bubble column. The provided air was filtered by sterile-cotton-filter. The temperature was stable at  $25 \pm 1$  °C through water bath control. As the total working volume of each tube was sufficient only for 3 samplings, the culture started with an initial concentration of 4.0 mg of dry biomass/10 mL. That initial concentration was chosen to examine, with these 3 samples, the late exponential phase where we expect to detect Cry. So, each tube was inoculated directly from a "mother-culture" at 4.0 mg of dry biomass/10 mL. The experiment was conducted in three biological and technical replicates.

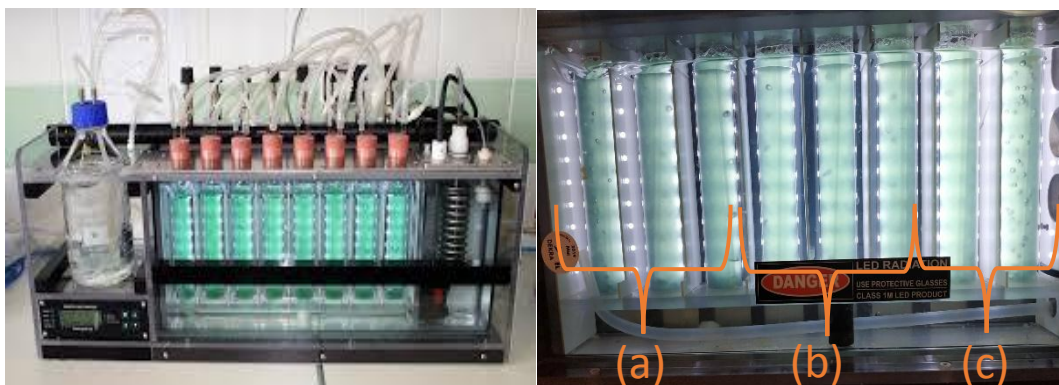
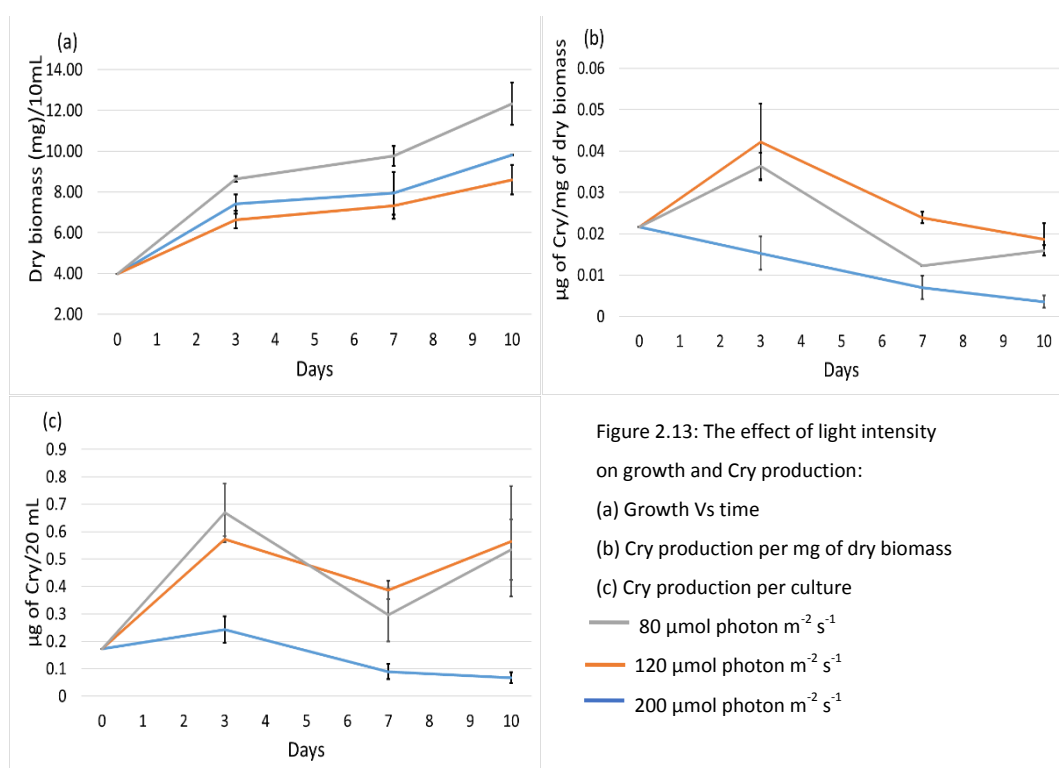


Figure 2.12: Light intensity experiment instrumentation of MC1000 multi-incubator. a) 80 b) 120 c) 200  $\mu\text{mol photon m}^{-2} \text{s}^{-1}$

## Results and discussion



The effect of light intensity was studied at 80  $\mu\text{mol photon m}^{-2} \text{s}^{-1}$ , 120  $\mu\text{mol photon m}^{-2} \text{s}^{-1}$  and 200  $\mu\text{mol photon m}^{-2} \text{s}^{-1}$  of white light. Light intensity has different effect on the culture when that is cultivated on different containers since the quantity of light that cells will absorb depend on the radius of the vessel and the culture volume and concentration. Under our experimental conditions the light intensities used corresponded to medium, high and very high intensities. Regarding the culture's growth, in the lowest light intensity the dry biomass doubled after three days and triplicated in 10 days (fig.2.13a). Under higher light intensities, the cells grew slower and so, the biomass doubled only after 8 days of growth (fig.2.13a). These results suggested that these higher light intensities stressed the cells. This was in accordance with microscopic observations. I observed

fragmentations and shorter filaments in the light stressed cultures grown at 120 and 200  $\mu\text{mol photon m}^{-2} \text{s}^{-1}$ . The number of fragments increased with the light intensity. The culture grown at medium light intensity, which is the lowest among the examined intensities, had the highest growth rate. At the same time, the very high light intensities led to cell death by photoinhibition.

The Cry production per dry biomass was also affected by light intensity. At point 0, the production of Cry is that present in the inoculum of very concentrated cells. Indeed, the experiment began by the dilution of a concentrated *Nostoc* sp. culture. Then, during the three first days of the experiment in which the cells were in logarithmic phase of growth, the production of Cry increased under 80 and 120  $\mu\text{mol photon m}^{-2} \text{s}^{-1}$  white light. Then, at days 7 and 10 when the culture was again concentrated (and the growth was slower than in the first three days) the Cry production decreased arriving to a level even slightly lower than in point 0. Under 200  $\mu\text{mol photon m}^{-2} \text{s}^{-1}$ , the Cry production per dry biomass decreased from the first day and continued to decrease during the 10 days of experiment. Thus, we can see that although 120  $\mu\text{mol photon m}^{-2} \text{s}^{-1}$  was already negative for cell growth, it did not decrease Cry production per biomass. Moreover, it seemed to have a slight positive effect (fig.2.13b). In contrast, 200  $\mu\text{mol photon m}^{-2} \text{s}^{-1}$  negatively affected both growth and Cry production. As a consequence, in the graph of "Cry production per 20 mL culture", it was observed that the Cry concentration in the culture increased during the first three days under 80 and 120  $\mu\text{mol photon m}^{-2} \text{s}^{-1}$  light intensity and then decreased. Under 200  $\mu\text{mol photon m}^{-2} \text{s}^{-1}$  the Cry concentration was maintained during the first three days due to cell growth and then decreased. Consequently, we conclude that the Cry production is affected only in very high light intensities. Under our experimental conditions, light intensities going from 80 to 120  $\mu\text{mol photon m}^{-2} \text{s}^{-1}$  are the more convenient for Cry production. More generally, light stress is not good to increase Cry production. The outcome of metabolite's production agreed with the bibliographic data (Khajepour F. *et al.* 2015, Ma R. *et al.* 2015, Kurmayer R. *et al.* 2011, Johnson E.M. *et al.* 2014, Chmelík D. *et al.* 2019, Zheng T. *et al.* 2020, Oh H.S. *et al.* 2017) which proposes that medium-low light intensities would be optimal. To sum up all the three graphs on light intensity, we can say that in accordance with the bibliographic data *Nostoc* sp. prefers medium light intensities for growth and Cry production.

## 2.5.2 Photoperiod experiment

### Experimental session

The strain was cultivated in an Erlenmeyer flask of 500 mL with a working-volume of 300 mL. An inoculum (187.5 mL) at 4.0 mg of dry biomass/10 mL, was diluted with fresh BG11 medium and adjusted at a final concentration of 2.5 mg of dry biomass/10 mL giving a final volume of 300 mL. The culture was cultivated in a "Brunswick Innova 4340 Refrigerated Incubator Shaker" under constant aeration with a cotton top and under agitation of 80 rpm. The temperature was regulated at  $25 \pm 1$  °C through air ventilation. The light was provided at an intensity of  $45 \mu\text{mol photon m}^{-2} \text{s}^{-1}$  and 50 mbar of  $\text{CO}_2$  were provided constantly in the incubator chamber. The experiment was conducted in three biological repetitions, starting in different periods from three different inoculums at 4.0 mg of dry biomass/10 mL and diluted at the same starting concentration of 2.5 mg of dry biomass/10 mL. Each biological replicate was composed by three Erlenmeyer-cultures which were the three technical replicates.

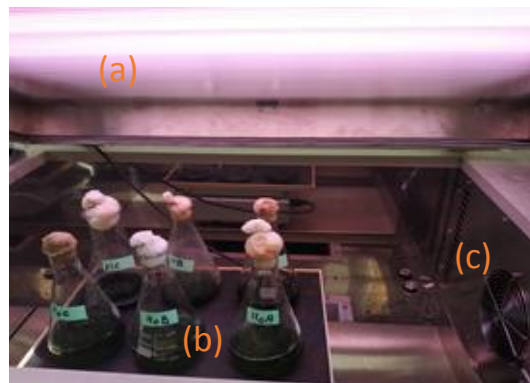


Figure 2.14: Photoperiod experiment instrumentation on Brunswick Innova 4340. a) Light panel b) agitation table c) temperature regulation through air climatization

## Results and discussion

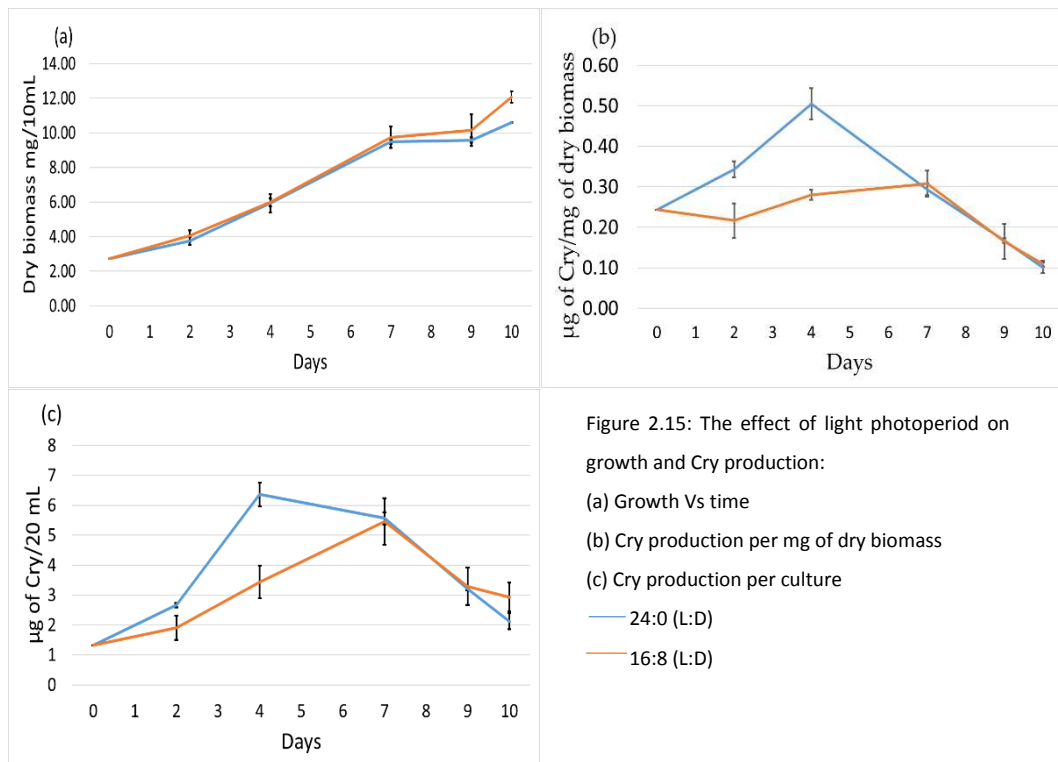


Figure 2.15: The effect of light photoperiod on growth and Cry production:

(a) Growth Vs time

(b) Cry production per mg of dry biomass

(c) Cry production per culture

— 24:0 (L:D)

— 16:8 (L:D)

We compared continuous light (24:0) to a photoperiod of 16 hours light and 8 hours dark (16:8). The growth rate was similar in both conditions (fig. 2.15a), even if growth of cells on incubator with agitation table, was completely different than in the bioreactor used in the light intensity experiment (compared figures 2.13). This result (fig. 2.15) suggested that a light period of 16 hours was sufficient to store enough energy to maintain cell growth for a non-light period up to 8 hours. A second explanation is that *Nostoc* sp. as other cyanobacterial strains show a preference on the photoperiod of their natural habitat from which they were initially isolated (Jacob-Lopes E. *et al.* 2009). The strain has been initially isolated from Arron island, Scotland where the natural photoperiod resembles to the 16:8 (L:D) photoperiod. In contrast, the dark period had a very negative effect on Cry production. Under continuous light, the Cry production per dry biomass increased until the fourth day (the production doubled) and then decreased with increasing cell concentration. When the photoperiod 16:8 was used, the production of Cry remained low like at point 0 and then when the cells were concentrated the production decreased. As a consequence, the concentration of Cry in the culture increased faster under continuous light. We concluded that continuous light is favorable to Cry production. That observation indicates two hypotheses for the cyanotoxin's production. Firstly, the production might be photo-dependent and so light is a necessary factor for the process. Secondly, under non-light conditions the microorganism provides limited energy that must be used for survival and not for secondary metabolite's production.

### 2.5.3 Wavelength experiment

#### Experimental session

The culture conditions were identical to the ones of the photoperiod experiment. In order to evaluate the effect of specific wavelength of light, color films (Eurolite, Toronto, Canada) were placed along the external surface of each flask. The transmittance curves of the filters were drawn in a UV-Vis spectrophotometer (Beckman, DU 640). Based on the curves the emission peak of red filter was 590-700 nm and for the blue filter was 410-490 nm.

#### Results and discussion

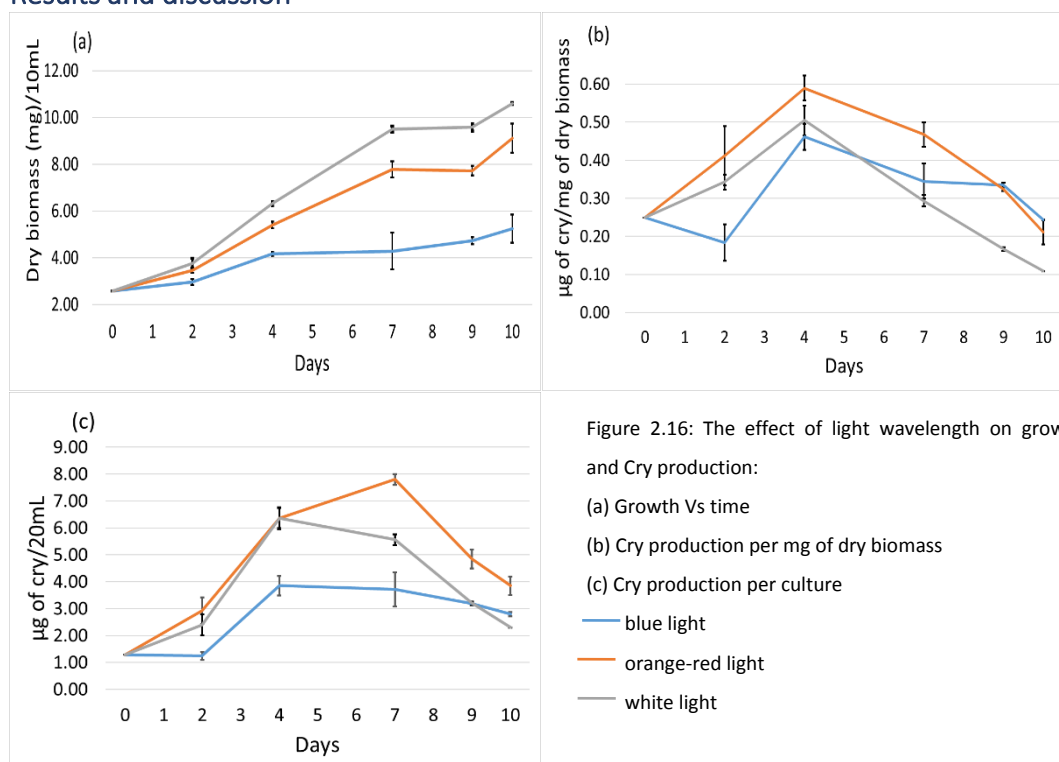


Figure 2.16: The effect of light wavelength on growth and Cry production:

(a) Growth Vs time

(b) Cry production per mg of dry biomass

(c) Cry production per culture

— blue light  
— orange-red light  
— white light

Figure 2.16 presents the effect of light-wavelength on growth and Cry production under orange-red, blue and white light. A lack period was observed during the first two days and then the growth was faster (fig.2.16a). The biomass triplicated under orange light and duplicated under blue light after 10 days of growth. As it was previously observed in other laboratories, cell growth was largely slower under blue light than under orange-red light. In comparison to orange-red light, blue light did not improve the per cell Cry production. Specifically, blue light faced a drop during the first two days and then a slight increase to its maximum on the fourth day. On the contrary, orange-red light has a constant increase until the fourth day (fig. 2.16b). So, after 4 days of growth, the production of Cry triplicated under orange-red light and only doubled under blue light. Finally, like in the rest of experiments when the cells became more concentrated, the Cry production per cell decreased (fig. 2.16b). When the culture's Cry concentration was followed, it was observed under orange-red light



an increase of Cry concentration during 7 days due to the combination of a higher cell concentration and a higher production of Cry per cell. Then the total Cry concentration decreased due to the lower Cry production per cell (fig.2.16c). Under blue light, the concentration of Cry increased between days 2 and 4 principally due to the better production of Cry per cell. The slow growth of cells under blue light is related to the fact that blue light is mostly absorbed only by PSI leading to an imbalance of photosystem activities and a lower photosynthetic efficiency. Blue light affects also the production of Cry, most probably related to a low photosynthetic efficiency decreasing the power for metabolite's synthesis.

#### 2.5.4 pH experiment

##### Experimental session

As mentioned above, oxygenic photosynthesis, which is the conversion of CO<sub>2</sub> and water to sugars through the aid of light-energy, is the main metabolic process in cyanobacteria (Vermaas W.F 2001, Blankenship R.E. 2002). The consumption of CO<sub>2</sub>, automatically leads to an increase in pH value. In order to examine the effect of pH on the culture, we tried to stabilize the pH value and stop its occurred increase. The pH values that we wanted to examine based on bibliographic research (Guckert J.B. and Cooksey K.E. 1990, Ray S. and Bagchi S.N. 2001, Sang M. *et al.* 2012) and lab's experience were pH 7.5 and pH 8.0. There are two ways of stabilizing the pH; a) through constant CO<sub>2</sub> injection, b) *via* the addition of pH buffers in culture's medium. In small scale cultures, as the Erlenmeyer flasks, which were used in experimental instrumentation, the addition of a buffer is the most common technique. We tested different chemical buffers in a range of concentrations to find the one which would not be toxic for the strain, and at the same time would be able to maintain the pH at the desired value. The tested buffers were Tris-HCl and Glycine-glycine at concentrations of 5 mM and 10 mM. We assumed that higher concentrations of these buffers could have a lethal effect on the culture (fig. 2.17). The experiment showed that Tris at 10mM had the best combination of low toxicity with relatively good control of the pH, among the compared tests. However, this concentration of Tris-HCL could not completely stabilize the pH, it only slowed down its increase. Thus, the buffer maintained the two experiments in separate pH-zones (fig. 2.18d). The culture conditions (temperature, light intensity, agitation, CO<sub>2</sub>, culture vessel, and culture volume) were identical to the ones of the photoperiod experiment. The only difference was the addition of Tris 10 mM and the initial pH value at 7.5 in one case and 8.0 in the other.



Tris 5 mM pH 8,5      Tris 10 mM pH 8,5      Glycylglycine 10 mM pH 8,5      Glycylglycine 5 mM pH 8,5      Tris 5 mM pH 7,5      Tris 10 mM pH 8,5      Tris 5 mM pH 8,5      Glycylglycine 10 mM pH 7,5

Figure 2.17: Macroscopic observation of cultures after 7 days inoculation with Tris and Glycylglycine buffers

## Results and discussion

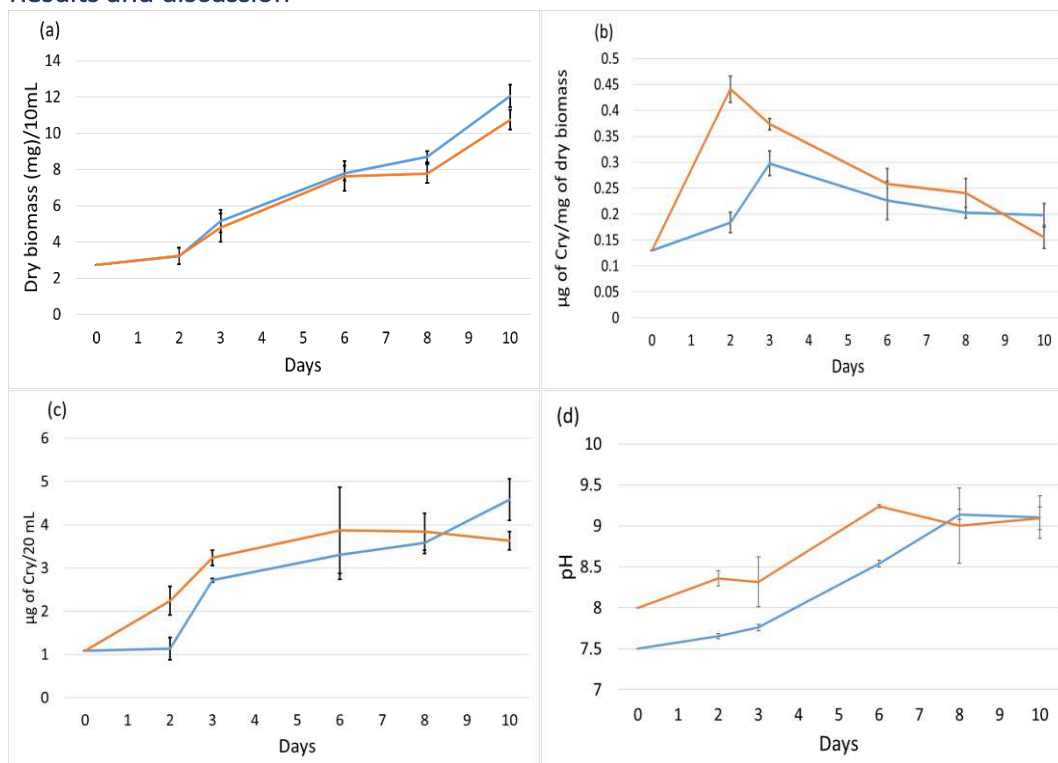


Figure 2.18: The effect of pH on growth and Cry production:

- (a) Growth Vs time      — pH 7.5
- (b) Cry production per mg of dry biomass      — pH 8.0
- (c) Cry production per culture
- (d) evolution of pH

The constant pH rise did not permit to extract a clear outcome for the effect of pH. During the first 6 days one culture was always at a pH lower ("lower pH" culture) than the other culture ("higher pH" culture) (fig. 2.18d). Although the difference in pH the growth rate was similar in both cultures (fig. 2.18a). The Cry production per cell was higher in the "higher pH" culture. The "lower pH" reached its maximum per cell production on the third day, when the pH value was 7.76. The "high pH" reached its maximum per cell production on the second day when its pH was 8.36, while its maximum was 1.5

fold higher than the maximum of "low pH".

So, due to pH variations, we can only generally make a first hypothesis that pH higher than 8.3 is favorable for both growth and Cry production.

From this experiment, we can only hypothesize that the synthesis of Cry is favored at pH 8-8.5 while the cells are less happy under lower pHs. Further studies with better pH control are needed to verify our general observation and examine further the effect of pH. The buffers seem that are not able to regulate the pH, so the following studies could be done with precise pH auto-regulation through CO<sub>2</sub> injections, as described in the photobioreactor's experiment below. Based on the current experiment and the bibliographic data, the proposed pH range which should be examined, is pH 8.5-9.0.

### 2.5.5 Medium's composition experiment

#### Experimental session

In order to test the effect of nitrates starvation stress and the implication of heterocysts in the Cry expression process, two different culture media were compared. The difference between the two culture media was the presence or absence of nitrate as N source. In one culture NaNO<sub>3</sub> was replaced with NaCl, with a proportional amount of Na (Table 2.2). The rest of culture conditions (Temperature, light intensity, agitation, CO<sub>2</sub>, culture vessel, and working volume) were identical to those of the photoperiod experiment

| Stock solution |  |                      |
|----------------|--|----------------------|
| No             | Stock solution                                       | Quantities (g)/0.2 L |
| 1              | K <sub>2</sub> HPO <sub>4</sub> ·3H <sub>2</sub> O   | 0.8                  |
| 2              | MgSO <sub>4</sub> ·7H <sub>2</sub> O                 | 1.5                  |
| 3              | CaCl <sub>2</sub> ·2H <sub>2</sub> O                 | 0.72                 |
| 4              | Citric Acid, H <sub>2</sub> O                        | 0.12                 |
|                | (NH <sub>4</sub> ) <sub>5</sub> [Fe <sup>2+</sup> ]  | 0.12                 |
| 5              | EDTA (K <sub>2</sub> , Mg)                           | 0.02                 |
| 6              | Na <sub>2</sub> CO <sub>3</sub>                      | 0.8                  |
| 7              | Solution metal trace:                                | Quantities (g)/0.2 L |
|                | H <sub>3</sub> BO <sub>3</sub>                       | 0.572                |
|                | MnCl <sub>2</sub> ·4H <sub>2</sub> O                 | 0.362                |
|                | ZnSO <sub>4</sub> ·7H <sub>2</sub> O                 | 0.044                |
|                | Na <sub>2</sub> Moo <sub>4</sub> ·2H <sub>2</sub> O  | 0.078                |
|                | CuSO <sub>4</sub> ·5H <sub>2</sub> O                 | 0.016                |
|                | CO(NO <sub>3</sub> ) <sub>2</sub> ·6H <sub>2</sub> O | 0.010                |

| Medium composition                   |                     |
|--------------------------------------|---------------------|
| No                                   | Stock solution mL/L |
| NaCl 1.03 g/L (for BG11o)            |                     |
| NaNO <sub>3</sub> 1.5 g/L (for BG11) |                     |
| 1                                    | 10                  |
| 2                                    | 10                  |
| 3                                    | 10                  |
| 4                                    | 10                  |
| 5                                    | 10                  |
| 6                                    | 10                  |
| 7                                    | 1                   |

Table 2.2: BG11 & BG11o composition

## Results and discussion

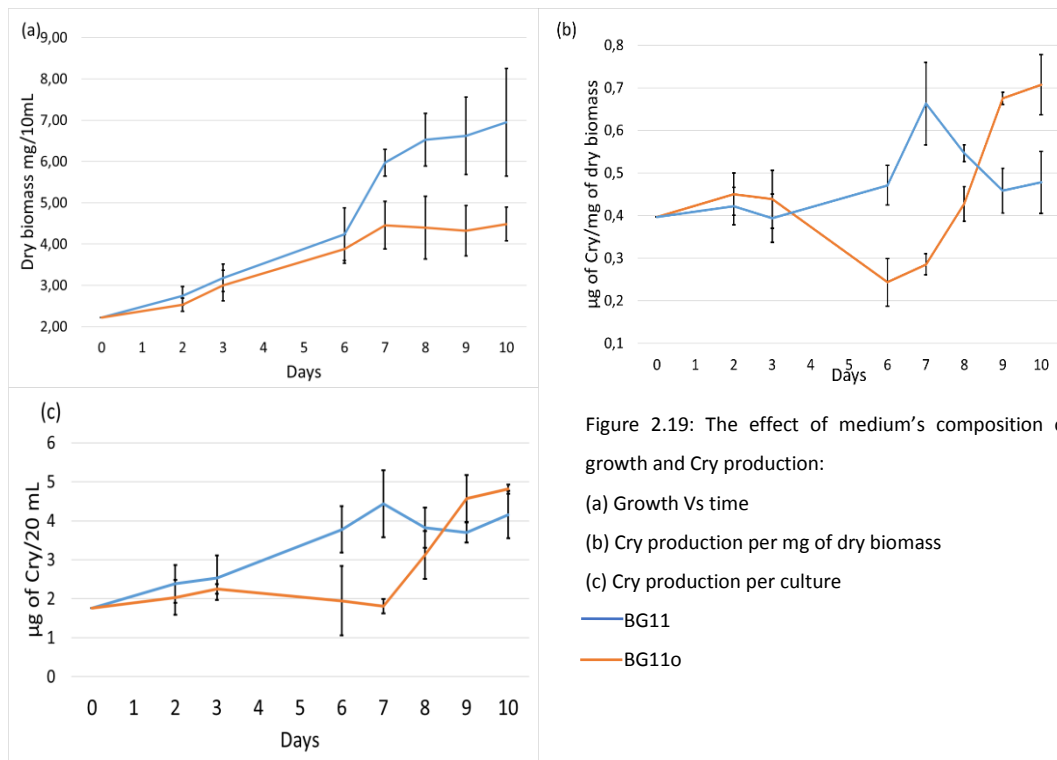


Figure 2.19: The effect of medium's composition on growth and Cry production:

(a) Growth Vs time

(b) Cry production per mg of dry biomass

(c) Cry production per culture

— BG11

— BG11o

In the absence of combined nitrogen, the formation of heterocysts, in which nitrogen is converted to ammonia by the nitrogenase, is induced.

In the experiment, the inoculum of both sets came from a mother-culture grown in BG11 medium. This medium contains nitrate, and so the *Nostoc* sp. filaments consisted only of vegetative cells. In the Nitrate-lacking BG11o-culture metabolic processes were induced and heterocysts were formed. The first apparition of heterocysts was detected, under microscopic observation, on the third day. Until that point, the cell probably degraded the N-suppliers to cover its essential needs to survive. The production of secondary metabolites is not considered as a primary need. So, the Cry per cell production remained stable for the first two days, at the same level that in the inoculum. Following the appearance of the first few heterocysts, from the third to the sixth day, on BG11o-culture, the Cry per cell production dropped, as; a) not sufficient amount of heterocysts had been developed yet, and b) the decomposed nitrogen-storages supplied only primary needs or have been already consumed. From day 6, where sufficient amount of heterocysts had been developed, the per cell production of BG11o culture increased significantly, and its rate slightly dropped only on day 9. On the other hand, the Cry per cell production in the BG11-culture slowly augmented until it reached its maximum on day 7 in a density of approximately 6 mg of dry biomass/10 mL.

Concerning the growth, both cultures followed similar patterns until the sixth day. From that point, BG11 culture continued its growth while the culture in BG11o stopped to grow at day 7. That plateau

is significantly in lower cell density comparing the BG11 culture.

The combinational effect of growth and "Cry per cell production" is depicted on the total Cry production graph. In nitrate-lacking medium the culture remains almost on the same level until the seventh day. Then, due to the high production of Cry per dry biomass (per cell), the concentration of Cry rapidly increased reaching a level even higher than the nitrate containing culture. BG11 culture produces Cry proportionally to its growth rate and reaches its maximum on the seventh day, which corresponds to the late exponential phase.

## 2.5.6 Temperature experiment

### Experimental session

In this experiment in which I wanted to study the effect of temperature on cell growth and Cry production, culture conditions (light intensity, agitation, CO<sub>2</sub>, culture vessel and culture volume) were identical to those of the photoperiod experiment. The only difference was that the temperature was at 25, 30 and 35 °C.

### Results and discussion

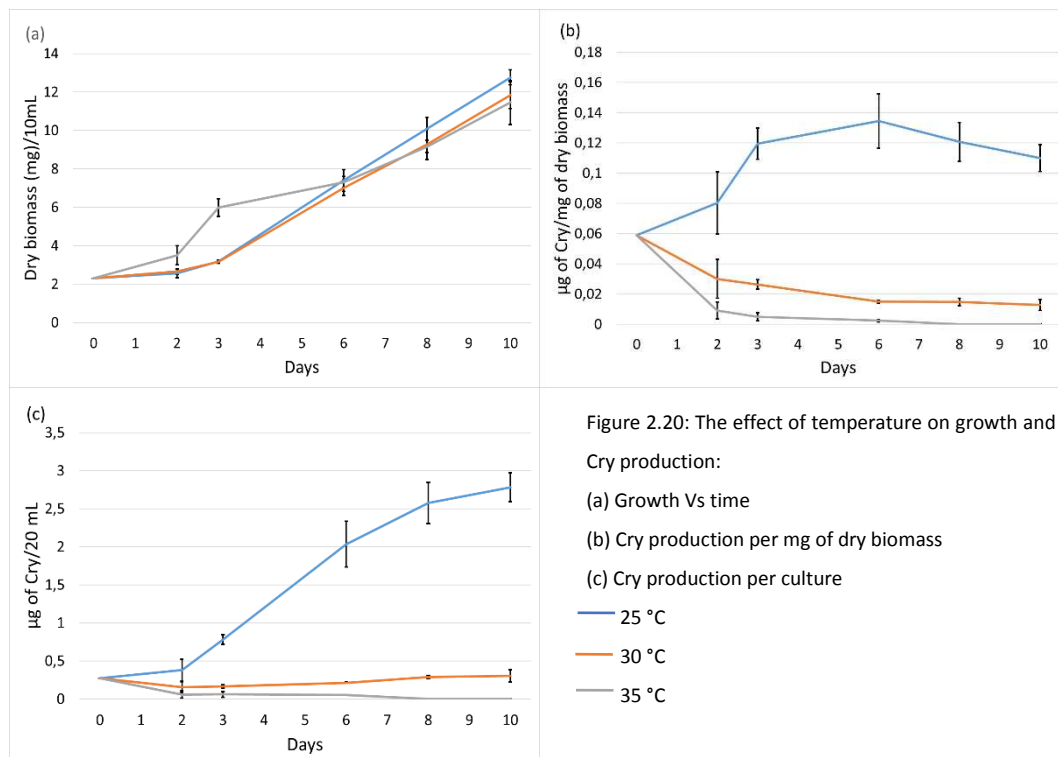


Figure 2.20: The effect of temperature on growth and

Cry production:

(a) Growth Vs time

(b) Cry production per mg of dry biomass

(c) Cry production per culture

— 25 °C

— 30 °C

— 35 °C

The growth rates at 25 and 30 °C were similar. The culture at 35 °C had an early higher growth rate until the third day, when it slowed down and became lower than that at 25 and 30 °C.

The significant outcome of this experiment was the observation of the effect of the temperature on the Cry per cell production. The metabolite's per cell production under ambient temperature (25 °C) slightly increased during the first two days, then it steeply augmented until the third day and it reached the maximum at the sixth day. Remarkably, temperatures higher than 25 °C had a severe impact on cell's metabolomic profile: the cells largely decreased Cry production from the beginning and after 3 days at 35 °C they almost stopped producing the toxin. The culture's Cry concentration followed similar pattern. At 25 °C, the concentration remained stable during the first two days, and then was doubled from day 3 to day 4. The concentration of Cry in the culture continued to increase during the 10 days of the experiment although the rate of increase was slightly lower in the last two days. In contrast, at 30 and 35 °C, the concentration did not increase. At 30 °C the toxin's level slightly declined during the first 6 days, and slightly increased to the initial low level. At 35 °C rapidly the Cry concentration rapidly decreased and from the third day there was almost no toxin in the culture. The above outcome indicated that the metabolite production is heavily affected by temperature, as was previously mentioned for other cyanotoxins such as MC (Kurmayer R. *et al.* 2011, van der Westhuizen A.J. and Eloff J.N. 1985, Sivonen K. *et al.* 1990).

### 2.5.7 Combined set of optimal conditions

#### Experimental session

Following the outcome of the above experiments, we have formed the optimal conditions on light intensity, light wavelength, light photoperiod, pH, medium composition, and temperature. These conditions were examined separately, and so it would be useful to precise the overall outcome of this "optimum set" on growth and toxin's production. At the same time, it was tested the potential synergic effect that optimal parameter could have on each other.

The instrumentation was identical to the photoperiod experiment. The strain was cultivated in Erlenmeyer flasks of 500 mL with a total working volume of 300 mL. The initial concentration of the culture was 2.5 mg of dry biomass/10 mL, and was inoculated by diluting a culture of 4.0 mg of dry biomass/10 mL in fresh medium. The culture conditions were the optimal for Cry production, as developed on the above experiments. Specifically, temperature was  $25 \pm 1$  °C, the wavelength was selected through orange-red filter, the photoperiod was set at 24:0 (L:D), and BG11 was chosen as culture medium. The light intensity was set at  $45 \mu\text{mol photon m}^{-2} \text{ s}^{-1}$ , which in the current instrumentation of "Brunswick Innova 4340 Refrigerated Incubator Shaker" corresponds approximately at medium light intensity, where we have shown that the strain performs better. Lastly, for the pH we aim to maintain for an extended period the culture at the optimum range of pH 8.5-9.0. So, we chose pH 7.5, as we expected fast growth and pH elevations due to optimal

conditions.

A second group of conditions, which would be set as "blank", was needed to compare and validate the results. In this way, we set as "blank" the experiment that was conducted at pH 7.5.

## Results and discussion

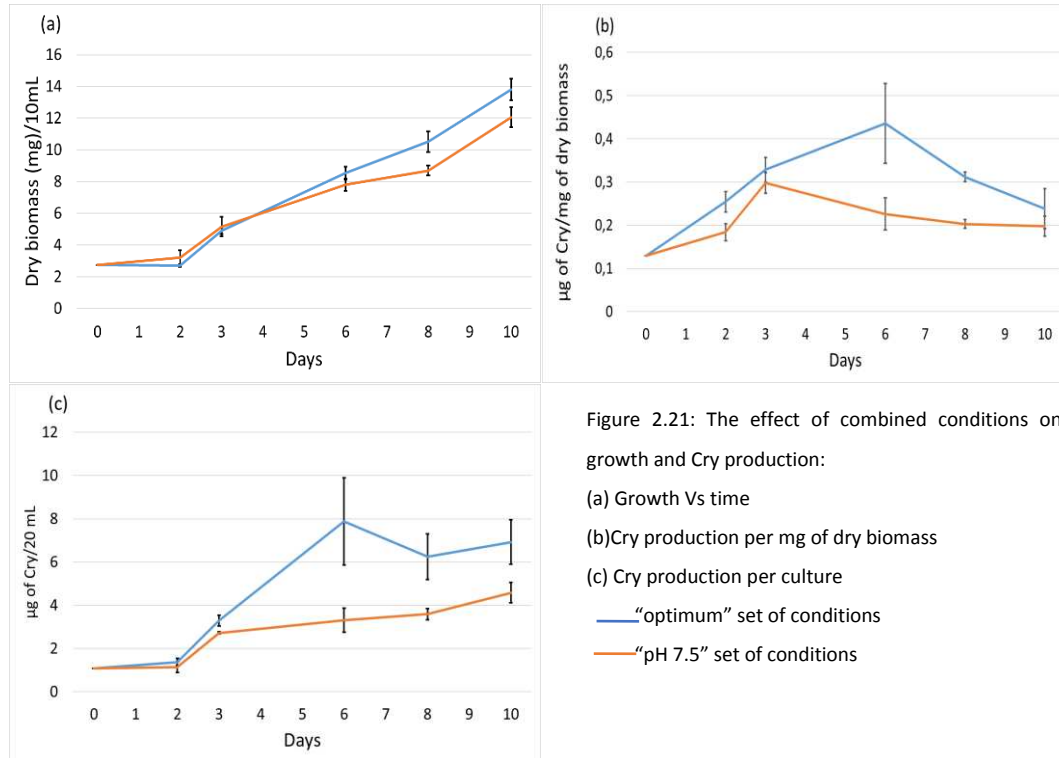


Figure 2.21: The effect of combined conditions on growth and Cry production:

(a) Growth Vs time

(b) Cry production per mg of dry biomass

(c) Cry production per culture

— "optimum" set of conditions

— "pH 7.5" set of conditions

The two sets do not significantly differ regarding their growth during the first six days, and they have approximately similar growth rates until that point. However, later the optimum set had slightly better performance and ended up to 13.7 mg of dry biomass/10 mL while the pH 7.5 set at 12.0 mg of dry biomass/10 mL.

Concerning the Cry production, the peak of "optimum set" is almost 30 % higher than the peak of "pH 7.5" set. The "optimum set" reached that maximum on day 6 with a density of 8.5 mg of dry biomass/10 mL while the "pH 7.5" reached its maximum on the third day with a density of 5.15 mg of dry biomass/10 mL.

These combined conditions based on all the above results (5 experiments in Erlenmeyer flasks and 1 in the Multicultivator). When we compare the "combined conditions" with each experiment that compose them, in Erlenmeyer flask, we observe that the "combined conditions" have a synergic effect as the strain performs better. As we mentioned above the performance of the strain may slightly vary from one experiment to another due to the strain's age, history, or physiological shear stress (Schatz D. *et al.* 2007), so we could not conduct precise comparison. However, we can

conclude in general that the growth and total Cry production was higher under the "combined conditions". Specifically, the growth on the 10<sup>th</sup> day at optimal production was 13.8 mg of dry biomass/10 mL while second was the experiment at 25 °C with 12.8 and the rest were lower. Then, the maximum of total Cry production was under "combined conditions" with 7.87 µg of cry/20 mL, followed by 7.80 at the experiment of orange-red light. Recapitulating the examined parameters on flasks culture, it can be noted that in all the experiments the maximum per cell Cry production takes place at a range of 5.15-8.0 mg of dry biomass/10 mL. The value of that maximum varies due to strain's physiological state and the experimental parameters. However, there is repeatability on the phase that this maximum happens. The mentioned range 5.15-8.0 mg of dry biomass/10 mL corresponds to the medium to late exponential phase, in the case that the strain is cultivated in a 500 mL Erlenmeyer flask. When the culture vessel changes, the maximum density changes also as well as the log exponential and stationary phase due to parameters as the distance between the light source and the culture and the vessel's diameter. However, based on the above experiments, no matter the size and type of the vessel, the maximum Cry per cell should be expected on medium-late exponential phase, even if the actual growth value would not be the same. That comes in accordance with the bibliographic data of cyanotoxins' production, which mention that for instance MC production is optimal between exponential and stationary phase, while in stationary phase its concentration is 6 fold less comparing to the exponential phase (Watanabe M.F *et al.* 1983, Watanabe M.F. and Oishi S. 1985).

### 2.5.8 Cryptophycin production on scale-up conditions

It was mentioned above the significance of Cry and its potential contribution on developing novel anticancer drugs. So, it is clear that higher production of the metabolite is needed. That chapter examines if the set of optimal conditions, which was developed, could be applied on higher scale and how the up-scale would affect the metabolite's yield.

#### Photobioreactor's experimental instrumentation and treatment

The scale-up could be done outdoors in facilities such as slopping platforms, raceway ponds, or indoors in fermenters and photobioreactors (Ación F.G. *et al.* 2017, Rahimpour M.R. *et al.* 2017). The photobioreactor (PBR) which was used is a made in-house 15 L airlift PBR with 12 L working volume, and it was made of plexiglass (polymethyl methacrylate) with a wall thickness of 5 mm.





Figure 2.22: A 15 L photobioreactor with cylindrical main chamber.

Sterilization is one of the most critical issues that the PBRs face. The size of the PBR, and the material which are used, such as acrylic, make inapplicable the steam-sterilization. For this reason, sanitization is preferred instead of sterilization. The sanitization process includes cleaning with bleach, neutralization with sulfuric acid, continuing with peracetic acid, and a final washing with sterile-water. LED tape provides white light, which is measured on the surface of the PBR at  $145 \mu\text{mol photon m}^{-2} \text{s}^{-1}$ , while an electronic timer can regulate the light photoperiod. The highest percentage of the light energy is converted into heat, which causes a constant rise in temperature. To control that increase and stabilize the temperature at the desired level a temperature controller method was used. A metal jacket with water circulation was placed on the bottom of the PBR. The jacket is made of metal to provide easily heat exchange. Moreover, it is placed on the bottom, aiming not to block on the light beam. The temperature is monitored through a sterile-thermometer. When the temperature exceeds the pre-set limit, the water-circulation starts automatically.



Figure 2.23: A metal jacket with water circulation system lays on the bottom of the photobioreactor.

The pH is regulated *via* an automatic system. A sterile-pH meter records the pH level and when it overpasses the limit it activates the CO<sub>2</sub> system. A CO<sub>2</sub> tank is connected with the PBR and provides CO<sub>2</sub>, filtered through 0.2  $\mu\text{m}$  pore filter, when it is activated. Then the injected CO<sub>2</sub> drops the pH level and then the injection stops automatically. Lastly, air, filtered through 0.2  $\mu\text{m}$  filters, passes through a sparger and provides the needed airlift agitation. The sparger is placed to minimize the size of the air-bubbles, and to maximize the surface area of the culture with them. On PBR's top, there are two

outlets with filters, which aid the exhausting of the disengaged bubbles from the CO<sub>2</sub> and the agitation air bubble. It is noted in previous researches that different types of agitation and different culture containers can affect strain's growth and biochemical composition (Kumar K. and Das D. 2012, Johnson E.M. *et al.* 2014, Kumar K. *et al.* 2014). Specifically, the airlift PBR provides better homogenization of the culture than the table-agitation in the case of Erlenmeyer flask. Additionally, the LED tape covers most of PBR's surface, so the "dark" areas inside the PBR are minimized. The combination of airlift agitation with the minimized "dark" areas leads to the optimal light utilization per cyanobacterial cell and almost doubles the maximum Optical Density that the culture can reach (Kumar K. and Das D. 2012, Johnson E.M. *et al.* 2014, Kumar K. *et al.* 2014, Kuan D. *et al.* 2015). However, even if the shaded-areas are few in the PBR, the light intensity from the reactor's surface to its center significantly fades. That fading of light intensity increases during the culture's growth, as the culture is denser and there are more barriers -cells- in the path of the light. Consequently, the cell moves rapidly from high light intensities of PBR's surface to low light intensities of PBR's center, and faces a flash-effect. In project's case, that effect is low due to the central airlift, but still affects the cells. That effect can be increased, if the user wants, through the ad of specific internal tubes, which clearly separates the light and dark zones. Experiments with *Synechococcus elongatus* revealed that culture in PBR performs almost the half growth rate comparing flask culture on the same conditions (temperature, medium, photoperiod, light intensity) (Kuan D. *et al.* 2015). That may happen firstly due to the mentioned flash-effect that the cells face while passing from PBR's surface to the center. Secondly, another reason is the shear stress, which is caused majorly by sparging airlift agitation in PBRs and not in the vertical table-agitation in the flasks (van Alphen P. *et al.* 2018). Lastly, the pH control through CO<sub>2</sub> injection is not easy to be exactly regulated, so usually higher amounts of CO<sub>2</sub> lead to pH drop out of the optimal pH-zone (Kuan D. *et al.* 2015).

### Experimental session

The optimization of culture conditions would lead to metabolite's overproduction. In a step forward, the pharmaceutical industry would take profit from these conditions to develop further the potential anticancer component. That would demand the cultivation of the strain in industrial-scale conditions, such as high-scale photobioreactors. However, the project's experiments until now, have been conducted in lab-scale vessels and tubes. So as a final step, the strain was tested in larger scale conditions to note the effect of scale-up conditions in growth and metabolite's production. The strain in the PBR was cultivated with a working volume of 12 L with BG11 medium under  $25 \pm 1$  °C and pH 7.5-8. The light intensity was set at  $145 \mu\text{mol photon m}^{-2} \text{ s}^{-1}$  (medium light intensity), and the photoperiod was 16:8 (L:D). The experiment was conducted in one PRB-run with 4 technical replicates on every sampling day. The same culture conditions were adapted in the flask culture

experiment also. The culture conditions were the same as in the experiment of photoperiod on 16:8 (L:D). Both cultures commenced at a density of 2.5 mg of dry biomass/10mL, which was inoculated from a mother-culture of 4.0 mg of dry biomass/10 mL. Concerning the flask experiment, each biological replicate was composed of three Erlenmeyer-cultures, which were the three technical replicates.

## Results and discussion

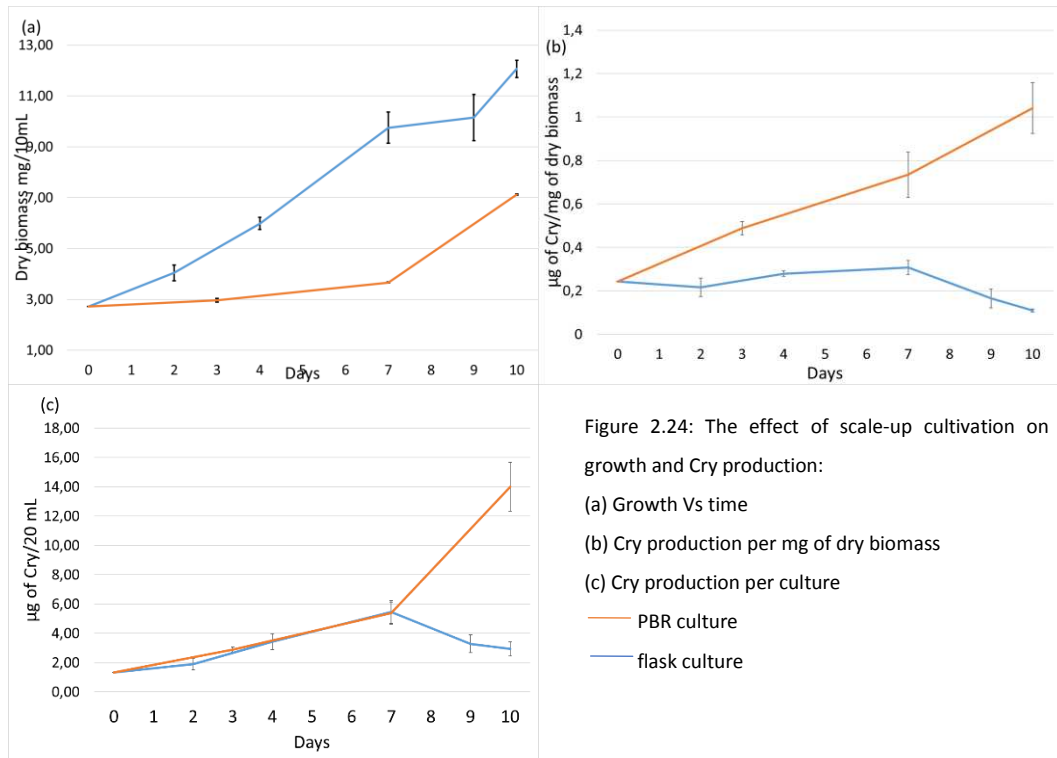


Figure 2.24: The effect of scale-up cultivation on growth and Cry production:

(a) Growth Vs time

(b) Cry production per mg of dry biomass

(c) Cry production per culture

— PBR culture

— flask culture

Based on the experimental outcome it seems that the scale-up adaptation affects the culture significantly. Firstly, there is a major difference in growth rates. The PBR culture went through a lag phase until the seventh day. The log phase was followed by an exponential phase, which almost doubled the cyanobacterial density from day 7 to day 10. On the other hand, the flask-culture had an earlier rise with a growth rate of approximately 20 % per day until the seventh day. Then, the rate decreased for the two following days to augment again until the end of the experiment. That decrease in growth rate reveals that the culture is in late exponential phase at 12 mg of dry biomass/10 mL.

The growth data agrees with the bibliographic research, which proposes that scale-up facilities lead to lowering the growth rate. As mentioned above that may happen firstly due to the light flash-effect that face the cells face, secondly because of the shear stress caused by heavy agitation (van Alphen P. *et al.* 2018) and lastly due to non-exact CO<sub>2</sub> injection that often drops the pH out of its optimal

zone (Kuan D. *et al.* 2015). In low densities, the cells might be exposed more in the phenomenon of shear stress and photoinhibition. They have not yet formed aggregates, so the filaments are more fragile in the heavy agitation, while the shading from the one cell to the other is few and they are more easily photoinhibited. That explains the slow growth rate on PBR in the range of 3-4 mg of dry biomass/10 mL, which appears as lag phase.

The most important difference is noted in the per cell production. The per cell production of the PBR-culture increases constantly, and approximately it was increased by 4-fold in a ten-day-period. On the contrary, the flask-culture has not great variations on its per cell production. For instance, its highest per cell productions, which is noted on the seventh day, is greater than its initial values only by 1.3 fold. A consequence of that vast difference between the two culture's per cell production, is the fact that when the PBR is on its exponential phase it produces almost 5 time more Cry in total than the flask culture.

The PBR-culture has better light utilization than the flask culture, as the airlift agitation and the distribution of light sources minimize the "dark" areas in the vessel (Kumar K. and Das D. 2012, Johnson E.M. *et al.* 2014, Kumar K. *et al.* 2014, Kuan D. *et al.* 2015). That utility optimization with the CO<sub>2</sub> providing lead the PBR culture to a higher metabolic rate, which is depicted on the higher Cry per cell production. As the PBR-culture has a greater maximum density and Cry per cell production, is evident that the PBR produces can produce significantly higher amounts of secondary metabolites per unit. However, the strain's growth rate is lower, so the production takes longer.

An optimization of PBR's parameter is needed to increase the growth rate. That optimization should firstly focus on the sparger and on the air-flow which cause fragmentations and shear stress. Secondly, it should focus on the CO<sub>2</sub> injection system; a) volume and flow of injection, b) speed of accuracy of pH-meter. The optimization of pH-system would reduce the pH range and would keep the culture in the optimum pH value.

## Conclusion – Chapter 2

As described in Chapter 1, Cry has a great potential for the development of novel anticancer agents. However, its chemical synthesis is unprofitable for high-scale production due to its moderate yield. So, we focus on modifying the culture parameters of *Nostoc* sp. ATCC 53789 to lead to a natural overproduction directly from the wildtype. These parameters were light (photoperiod, intensity, wavelength), pH, temperature and medium composition. In light photoperiod, photoperiods 24:0 and 16:8 (Light:Dark) were tested, in wavelength, orange-red light, and blue were compared with white. Medium, high and very high light intensity experiments were performed in order to test the effect of light stress. Temperatures of 25, 30 and 35 °C were examined and pH of 7.5 and 8.0. Lastly, it was tested the nitrates omission from the culture medium to examine the implication of heterocysts. For a 10-day period, growth was measured and metabolite concentration was calculated through HPLC. Then, growth and toxin's total and per cell productivity curves were drawn.

Regarding the parameter of light, the microorganism prefers medium light intensities and red-orange for both growth and metabolite expression, Remarkably, photoperiod has an opposite effect on the two curves. Regarding growth, the optimal period was 16:8 however, the inverse occurred for Cry production. Different temperatures did not affect the growth, though Cry production was significantly inhibited in  $T > 30$  °C. Lastly, a pH zone 8.5-9.0 seem to have optimal outcome and nitrates are needed for strains optimal performance.

Then, as every parameter was examined separately, we wanted to test if there was a synergic effect among the examined conditions. Indeed, we concluded that the strain performed better under the “combined set” of conditions than the rest of the experiments where we modified only one condition per time. Lastly, as the obtained results would address to industrial applications, we compared lab-scale culture (in Erlenmeyer flasks) to high-scale one (in 15 L PBR). There, it was noted a decrease on growth rate probably due to the shear stress that the bubble column provokes. However, there is significant rise on Cry production which provides the potential for further industrial exploitation.

As we developed the optimal conditions for the production of Cry-1 by *Nostoc* sp. ATCC 53789, then we wanted to explore the rest of strain's phytochemical profile, and most importantly the potential Cry-analogues.



## Chapter 3

Examination of strain's phytochemical profile  
through molecular networks study





### 3 Chapter 3 - Examination of strain's phytochemical profile through molecular networks study

Following the optimization of culture conditions, we aim to study a) the phytochemical profile of *Nostoc* sp. ATCC 53789, b) how the optimization of culture conditions affects that profile, c) how that profile changes during the growth of the culture. To do that, we had to develop extraction and purification techniques for high-scale volume. The development and the execution of these methods took place at the lab of PNAS (Produits Naturels Analyse et Synthèse, Université de Paris, CiTCoM, UMR CNRS 8038). Then, these crude extracts and fractions were studied through the “molecular networks” aspect to obtain an overview of their profile. The analysis of these crude extracts was in collaboration with Institut de Chimie Organique et Analytique (ICOA UMR 7311 CNRS Université d'Orléans), and Dr. Cyril Colas.

#### 3.1 Review of applied cryptophycin's isolation-purification processes

Based on the physicochemical characteristics of the compound, which were mentioned above, several extraction and purification methods have been developed and applied in order to isolate Cry-1 and its analogs. These methods start from the treatment of the culture until the identification of the pure compound. The process from the culture of *Nostoc* sp. until the pure compound of Cry-1 has been studied mainly in 7 studies. The main parts included in the process are; a) the centrifugation of the initial culture, b) the treatment of the obtained biomass for the isolation of the intracellular metabolite's quantities, c) the extraction of the medium for the isolation of the extracellular metabolite's quantities, d) the isolation and final purification of the compound.

##### Centrifuging the culture

The culture sample is centrifuged at 10,000 rpm at 10 °C for 10 min (Back S. and Liang J. 2005). The upper phase is then filtered on “Whatman 55” filter and “Calbiochem miracloth” filter (Back S. and Liang J. 2005, Schwartz R.E *et al.* 1990). This cell-pellet is connected with the cell pellet obtained from the centrifugation. The sum of them is lyophilized for 48 h at 0.1 mbar (Back S. and Liang J. 2005). The biomass can also be stored frozen before lyophilization (Biondi N. *et al.* 2004).

##### Extracting the biomass

The lyophilized biomass is extracted with a mixture of acetonitrile (MeCN):methylene chloride (DCM) for 48 h. The ratio of MeCN:DCM varies from 4:1 (Back S. and Liang J. 2005, Chaganty S. *et al.* 2004) to 5:1 (Golakoti T. *et al.* 1995, Subbaraju G. *Vet al.* 1997). The ratio of lyophilized-biomass to solvent-

system is approximately 2 L of 5:1 MeCN:DCM per 50 g of dry biomass (Golakoti T. *et al.* 1995). Moreover, methanol (MeOH) or MeOH/H<sub>2</sub>O solutions can be used for the extraction of the biomass. However, the presence of methanol produced artifacts of cryptophycin due to methanolysis effect (Golakoti T. *et al.* 1994, Biondi N. *et al.* 2004). At last, the extract is filtered with a layer of "Carbiochem miracloth" and "Whatman 55" filter (Back S. and Liang J. 2005).

### Extracting the upper phase

The suspension can be extracted by liquid-liquid extraction using DCM as organic phase. Specifically, 1 L of upper phase is added in a separatory flask with 150 mL of DCM. The flask is shaken thoroughly, and it is left for 24 h to ensure sufficient separation. Then, the organic phase is isolated and filtered through packed cotton. To eliminate any dissolved water 3-6 g of anhydrous magnesium sulfate are added, the sum is left for several hours and then is filtered through packed cotton. Finally, the solution is concentrated *in vacuo* (Back S. and Liang J. 2005).

### Isolation and purification of cryptophycin

Several different techniques have been developed in order to isolate our compound from the previous extract. Some of them are medium pressure liquid chromatography, or flash column chromatography with H<sub>2</sub>O/MeOH system. The second one is not recommended due to the Cry artifacts, as it was mentioned above (Golakoti T. *et al.* 1995, Subbaraju G.V. *et al.* 1997, Chaganty S. *et al.* 2004). Specifically, Golakoti T. *et al.* 1995 mention that the extract, 1 g which comes from 50 g of biomass, is applied at an ODS-silica column (55 g, 7x5 cm) and the mobile phase used is 1:3 MeCN/H<sub>2</sub>O (0.8 L): fraction 1, 1:1 MeCN/H<sub>2</sub>O (0.8 L) fraction 2, 65:35 MeCN/H<sub>2</sub>O (1.0 L) fraction 3, MeOH (0.8 L) fraction 4, and DCM (0.5 L) fraction 5. The fraction 3 contains Cry-1 but need further purification.

The crude fraction 3 is further separated by reversed phase HPLC (Econosil C18, 10 µm, 25 cm x 22 mm, UV detection at 254 nm, 65:35 MeCN/H<sub>2</sub>O, flow rate 6mL/min) in order to isolate the compound of interest, Cry-1. The desired compound is expected to have ret.time 53 min (Golakoti T. *et al.* 1995). The obtained quantity of Cry-1 was 220 mg, starting from 50 g of *Nostoc* sp. GSV 224 dry biomass.

| Article                             | Methods / Comments   |
|-------------------------------------|--|
| (Schwartz R.E. <i>et al.</i> 1990)  | Centrifugation at 4,000 for 10 min.  |
| (Golakoti T. <i>et al.</i> 1995)    | <ul style="list-style-type: none"> <li>• 50 g of lyophilized biomass are extracted with 2 L of 5:1 MeCN:DCM 48 h.</li> <li>• Flash chromatography with 1:3 MeCN:H<sub>2</sub>O (0.8 L), 1:1 MeCN:H<sub>2</sub>O (0.8 L), 65:35 MeCN:H<sub>2</sub>O (1 L), MeOH (0.8 L), DCM (0.5 L).</li> <li>• The fraction of 65:35 continued with further HPLC 65:35 MeCN:H<sub>2</sub>O.</li> </ul>  |
| (Subbaraju G.V. <i>et al.</i> 1997) | <ul style="list-style-type: none"> <li>• The biomass is extracted with 5:1 MeCN:DCM.</li> </ul>  |
| (Chaganty S. <i>et al.</i> 2004)    | <ul style="list-style-type: none"> <li>• The lyophilized biomass is extracted with 4:1 MeCN:DCM</li> <li>• The concentrated extract is fractioned by reversed-phase column chromatography with increasing percentages of H<sub>2</sub>O:MeCN.</li> <li>• On the fraction of 35% H<sub>2</sub>O/MeCN all the Cry-analogues have been eluted</li> <li>• That fraction is further analyzed by reversed phase HPLC. Fraction at 1.16 ret.time was further fractionated and led to 3 analogues.</li> <li>• These subfractions are further examined by normal phase and reverse phase HPLC which lead to two analogues.</li> </ul>                                 |
| (Biondi N. <i>et al.</i> 2004)      | <ul style="list-style-type: none"> <li>• The biomass is extracted with 50 mL MeOH/g of biomass.</li> <li>• MeOH may cause artifacts because of the effect of methanolysis.</li> </ul>  |
| (Back S. and Liang J. 2005)         | <ul style="list-style-type: none"> <li>• Centrifugation at 10,000 rpm at 10 °C for 10 min.</li> <li>• The suspension is filtered with layer of "Carbiochem miracloth" &amp; "Whatman 55".</li> <li>• The cell pellet and the removed cells are collected, frozen, lyophilized 48h.</li> <li>• 10:1.5 culture-medium:DCM → the organic phase is filtered with paper filter (the aqueous phase is discharged) → 3-6 g anhydrous MgSO<sub>4</sub>, then concentration</li> <li>• The lyophilized biomass is extracted with 4:1 MeCN:DCM, stirred for 48 h.</li> <li>• The extract is filtered with layer of "Carbiochem miracloth" and "Whatman 55".</li> </ul> |

Table 3.1: Review of cryptophycin's isolation procedures

## 3.2 Personal work on cryptophycin isolation-purification process

### 3.2.1 Occupation of dry biomass

The current part of the project focuses on the study of culture's biomass. We focused on the biomass and not on the medium for two reasons. Firstly, in general cyanotoxins' extracellular portion is minor comparing to intracellular during the exponential phase. The extracellular portion is significantly increased only after the cell-death during the lysis face where all the intracellular component is released in the culture's medium (Park H.D. *et al.* 2001, Qian F. *et al.* 2014). Secondly, the project aims at the industrial scale-up, so the treatment of high-volume liquid, coming from the culture's medium, is a lot more complicated and expensive than the treatment of dry biomass' solid phase. For these two reasons, it will be studied the biomass and not the culture's medium.

The first step is the occupation of the culture from the PBR and the separation of the medium from biomass. The growth of the culture in the reactor is checked every second day *via* OD and DBC, as described in Chapter 2. Based on these measurements, at the growth's desired point, an amount of culture is taken out of the reactor for harvesting. Simultaneously, a new fresh medium is added

under sterile conditions in the remaining culture on PBR to continue the cultivation. The obtained amount of culture is placed in a 6 L decantation-flask and is left overnight for gravitational separation of the biomass from the medium. The wet biomass is centrifuged at 2,000 rpm for 15 min for further separation from the medium. The last step includes the lyophilization of that amount to obtain the final dry biomass. That biomass is then powdered with mortar and pestle, and the final powder's weight is calculated.

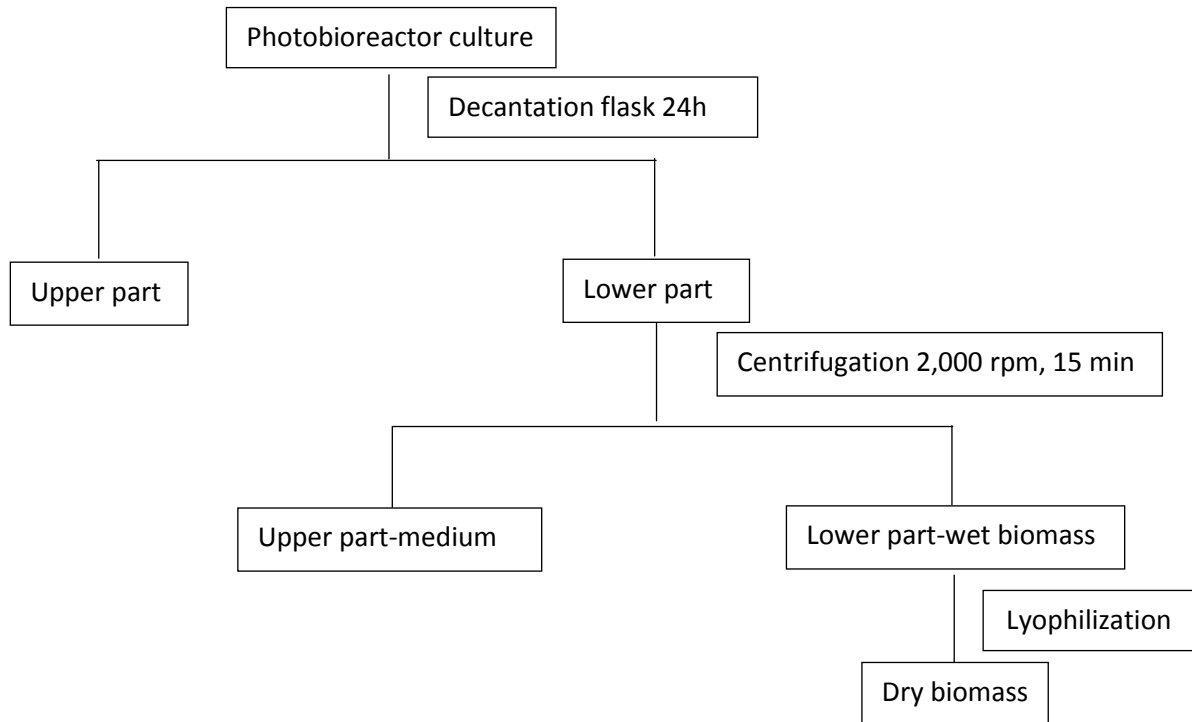


Figure 3.1: Schematic representation of the dry biomass occupation process, beginning from a high-scale culture in PBR.



Figure 3.2: (1) The culture of *Nostoc* sp. ATCC 53789 is collected from the PBR (2) then it is added in a decantation flask for the first separation of the medium from the biomass (3) the medium after the decantation flask is disposed (4) and the wet biomass after the decantation flask is collected (5) that dry biomass is lyophilized to obtain dry biomass (6) and at last that dry biomass is pulverized with mortar and pestle

In contrary to the method which was developed in Chapter 2, in this case biomass should be dried before the extraction process, mainly for two reasons. Firstly, large quantities of wet-biomass store high volumes of the medium, which makes inefficient the breaking of the cells in contrast to the previous method where the biomass came from a 20 mL-sample. Secondly, high-quantities of biomass may require to be extracted in a following step of the project and not the same day. The only way for long-term storage is biomass dehydration. That drying is conducted through lyophilization. Lyophilization, or freeze-drying or cryodesiccation, is called the dehydration process of a solid material by sublimation. Firstly, the mixture of cells and medium should be in freeze

condition. That was achieved by freezing instantly with liquid N<sub>2</sub>. Then the pressure is increased at 0.1 mbar, and the sample is left in the lyophilization for 48 h (Pansare S.K. and Patel S.M 2019). Following the separation of biomass from the initial suspension, and its drying, the next step is the extraction to obtain the crude extract. The dry-pulverized biomass can be stored at ambient temperature in a closed shelf until the extraction process.

### 3.2.2 Extraction method development

For the extraction method development, four different solvent-systems of different polarities were compared according to the literature. a) MeCN:DCM 4:1 (Back S. and Liang J. 2005, Chaganty S. *et al.* 2004), b) MeCN:DCM 5:1 (Golakoti T. *et al.* 1995 and Subbaraju G.V. *et al.* 1997), and c) MeOH 100 % (Biondi N. *et al.* 2004, Golakoti T. *et al.* 1994) were tested based on the bibliographic data, while d) DCM 100 % was tested based on a protocol developed by Phycosource (E. Duran, Thai D.Q., not published data). Comparing the above solvent-systems concerning their ability to extract Cry, we test four samples of 1 g of dry biomass. The powdered biomass was added with 50 mL of solvent in ultrasound for 1 h. The temperature of the water was checked not to overpass 30°C as secondary metabolites are often heat-sensitive. Then, a filtration through paper-filter was done, and the filter was washed with 10 mL more of the respective solvent. The extract was finally concentrated *in vacuo*. That extract was dissolved in 3 mL of MeCN (LC-MS quality), filtered, and subjected to HPLC-quantification, as described in Chapter 2.4. The weight of the methanolic extract was significantly higher, possibly because of the polarity which extracted other polar compounds. A repetition of the methanolic extraction verified the initial results.

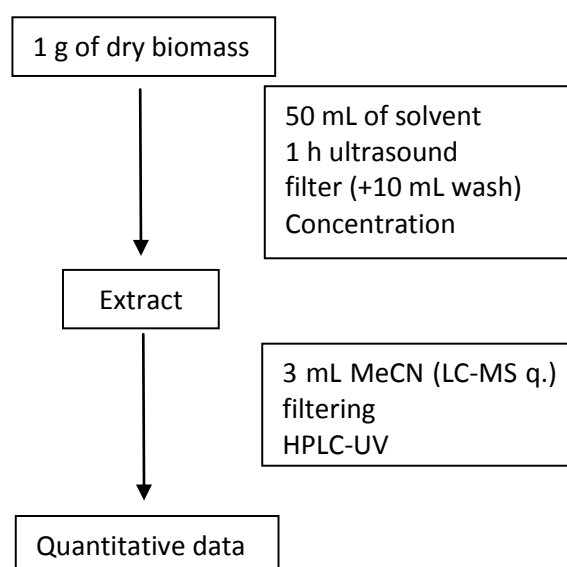


Figure 3.3: Comparison of extraction solvent systems *via* HPLC quantification

| Solvent      | W <sub>extract</sub> (mg) | Ret.time | AUC <sub>(234 nm)</sub> |
|--------------|---------------------------|----------|-------------------------|
| DCM          | 34.1                      | 22.81    | 79.524                  |
| MeCN:DCM 4:1 | 30.8                      | 22.79    | 102.299                 |
| MeCN:DCM 5:1 | 26.1                      | 22.79    | 84.6070                 |
| MeOH a       | 188.8                     | 22.79    | 5.665                   |
| MeOH b       | 173.8                     |          |                         |

Table 3.2: Comparison of extraction solvent systems

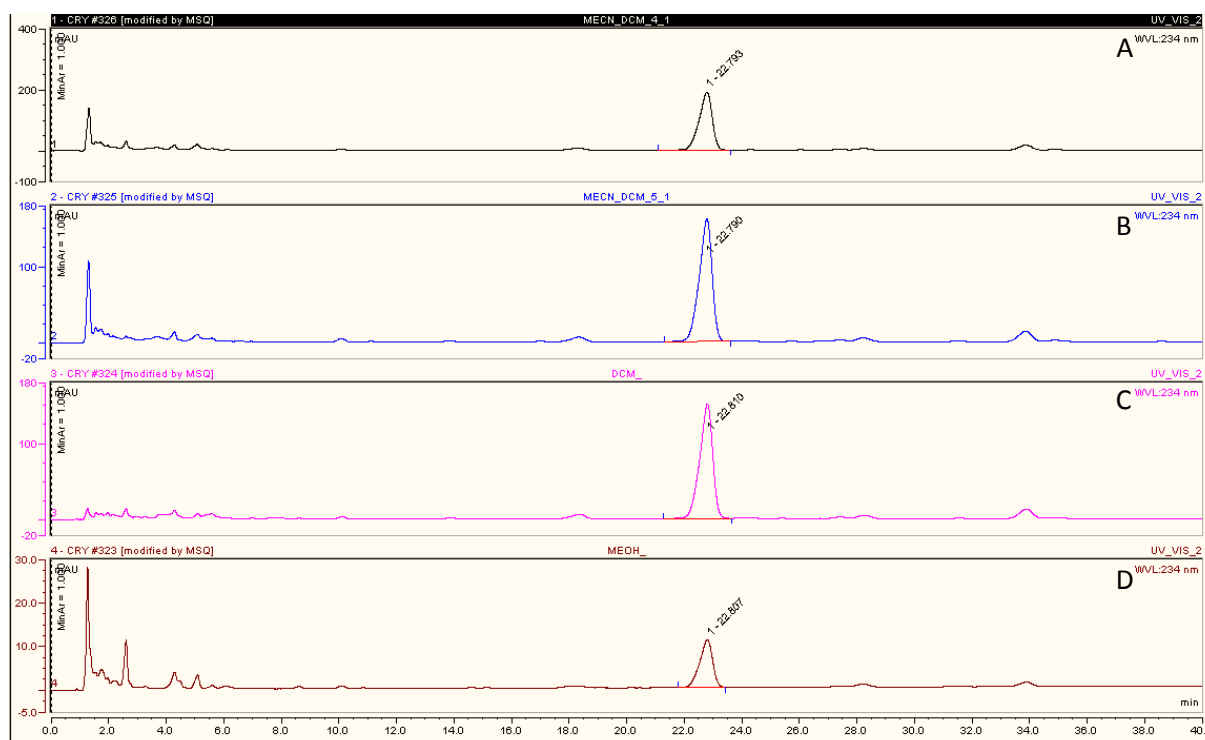


Figure 3.4: Comparative HPLC-chromatograms of different solvent systems for the extraction of Cry-1 (ret.time 22.80 ± 0.01 min).

A) MeCN:DCM 4:1, B) MeCN:DCM 5:1, C) DCM, D) MeOH (Gradient phase MeCN:H<sub>2</sub>O, conditions chapter 2.4, table 2.1).

From these obtained data, we conclude that the optimal solvent system is MeCN:DCM 4:1. Four crude extracts were analyzed, which come from different conditions on the PBR.

| Code      | DBC (mg/10mL) | OD   | Medium      | T(°C) | pH      | Light intensity (μmol photons m <sup>-2</sup> s <sup>-1</sup> ) | Photoperiod (L:D) | Color-light |
|-----------|---------------|------|-------------|-------|---------|---|-------------------|-------------|
| A_MIX     | 6.54          | 1.15 | BG11& BG11o | 24-28 | 7.4-7.9 | 250   | 24:0              | White       |
| B_BG11    | 5.68          | 1.0  | BG11        | 24-28 | 7.4-7.9 | 250   | 16:8              | White       |
| C_OPT_1.3 | 7.67          | 1.35 | BG11        | 25-26 | 7.4-7.9 | 250   | 24:0              | Orange-red  |
| C_OPT_0.2 | 1.14          | 0.2  | BG11        | 25-26 | 7.4-7.9 | 250   | 24:0              | Orange-red  |

Table 3.3: List of examined cultures

These four sums of biomass were extracted with the solvent system, as was chosen above. Regarding the amount of solvent per gram of dry biomass Back S. and Liang J. 2005 and Biondi N. *et al.* 2004 used 50 mL/g while Golakoti T. *et al.* 1995 used 40 mL/g. In our case for each code, 40 mL/g of dry biomass were added in an Erlenmeyer flask with the biomass. The flask was put in an ultrasound bath for 2 h, and the water of the bath is checked and changed when needed in order not to overpass 30 °C. Then, it was filtered through paper-filter "Cloup\_papier filter, standard plisse, ref:43986405" and the filter was washed with 10 mL of the system of solvents. The remaining of the filter was put back in the Erlenmeyer, again with an amount of MeCN:DCM 4:1 40 mL/g of dry biomass, and the process was repeated for 2 more hours. Then, it was filtered through the same type paper filter, and the total extract was concentrated *in vacuo*.

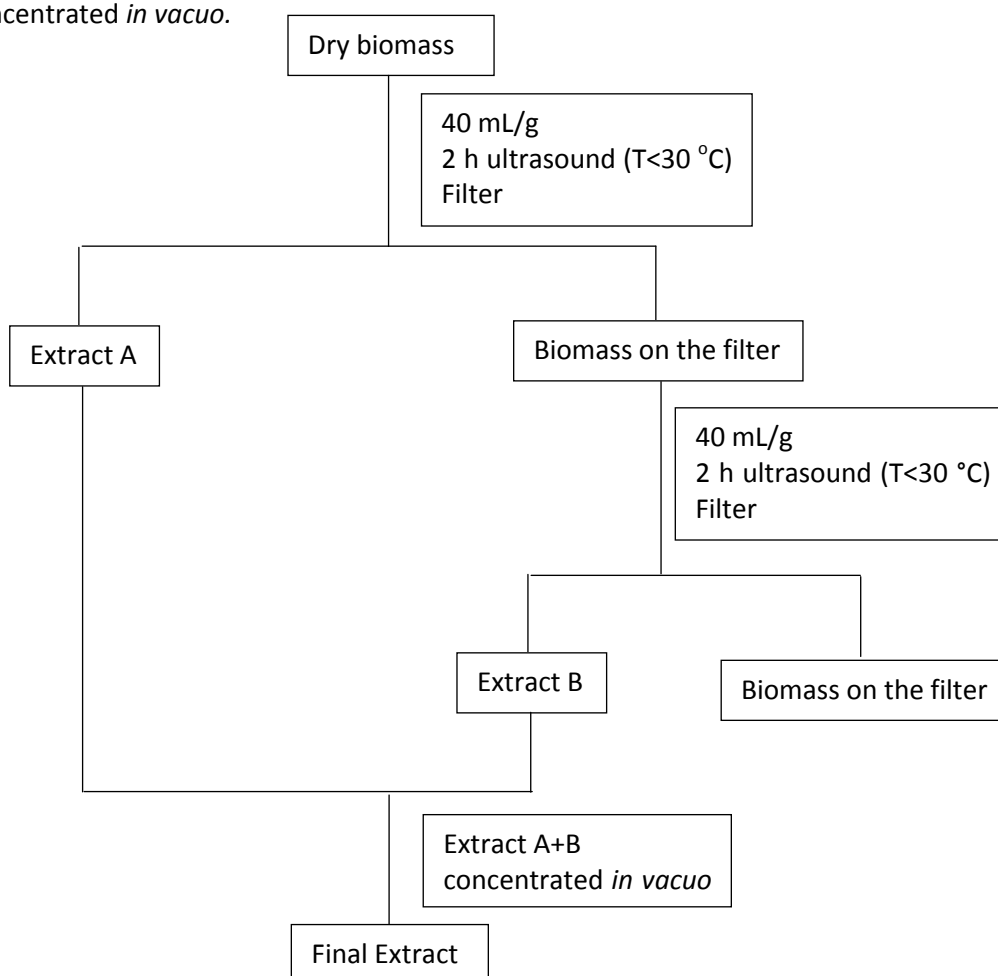


Figure 3.5: Extraction process from high-scale volumes

Following the above extraction process, proportionally in 1 L of medium the extracts were as followed.

| Examined culture | Dry biomass (g) | Extract (mg) | Yield % |
|------------------|-----------------|--------------|---------|
| A_MIX            | 0.681           | 31.1         | 4.56    |
| B_BG11           | 0.517           | 31.1         | 6.00    |
| C_OPT_1.3        | 0.583           | 35.3         | 6.04    |
| C_OPT_0.2        | 0.093           | 8.8          | 9.46    |

Table 3.4: List of examined extracts and respective yields



### 3.2.3 Development of two purification methods for the study of cryptophycin and strain's phytochemical profile

Aiming to study Cry and strain's phytochemical profile, we developed and applied two chromatographic techniques.

The first method focuses on Cry-1 purification and consists of two steps. On each step we apply an OPC for the gradual purification of the crude extract until we get the fractions enriched with Cry-1. The second method focuses on the sample preparation for UHPLC-ESI-Q-TOF-HRMS<sup>2</sup> analysis and molecular networking. So, we aimed at fractionating the crude extract directly on four major groups, based on their polarity. As a result, the second method consists of a single step, a flash column chromatography. The development of these two purification methods took place at the lab of PNAS (Produits Naturels Analyse et Synthèse, Université de Paris, CiTCoM, UMR CNRS 8038).

#### Purification of cryptophycin through two step Open Column Chromatography

The biomass "A\_MIX" was the first occupied high-volume sum of biomasses from the photobioreactor, so was used for the development of the Cry-purification method (fig. 3.6) and for the first study of *Nostoc* sp. ATCC 53789 phytochemical profile.

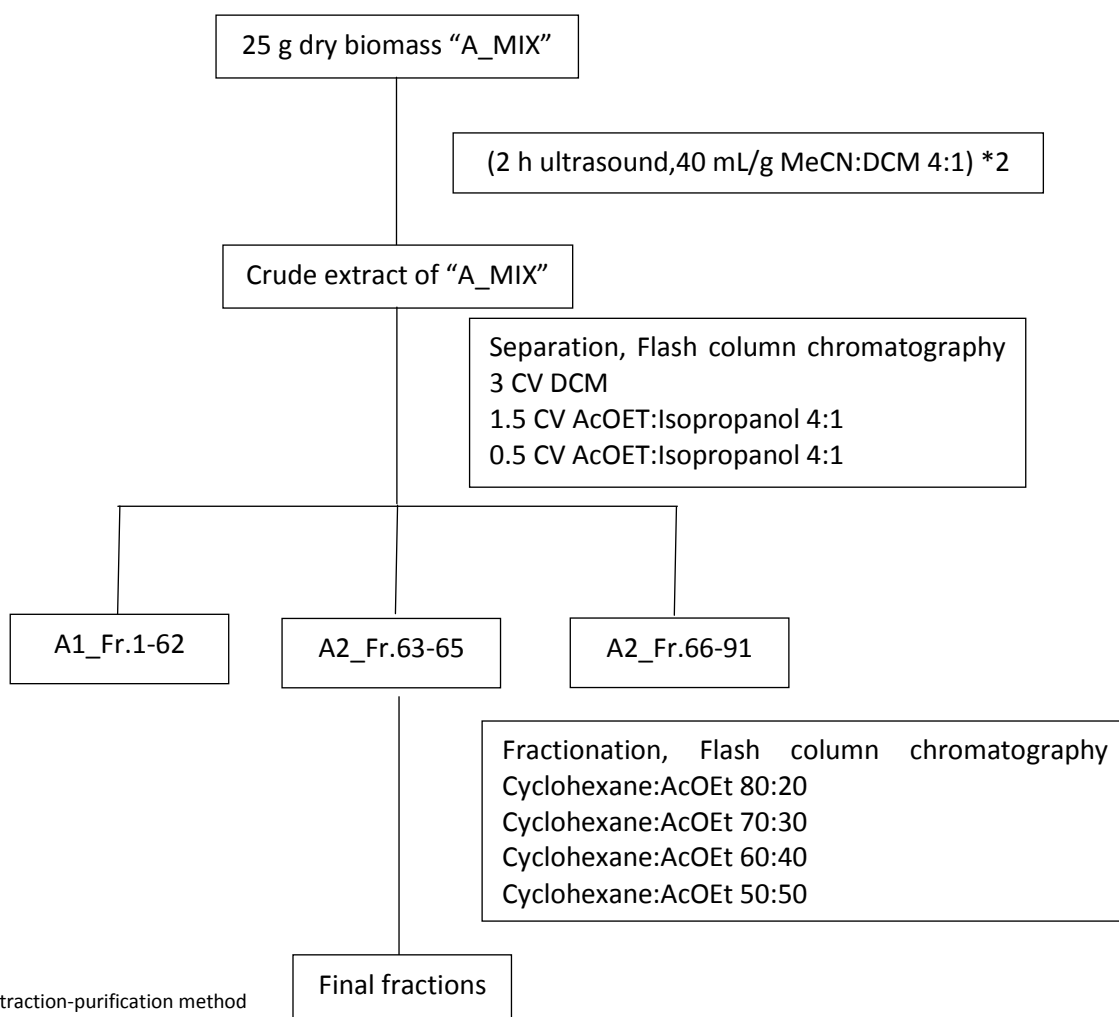


Figure 3.6: Extraction-purification method

25 g of "A\_MIX" dry biomass, which come from approximately 36.7 L of culture, were subjected to the extraction process as described above and led to 1.14 g of crude extract. The extract was diluted in 35 mL of DCM and was submitted as liquid-depot to flash-column-chromatography at a column of 2.5 cm. For the stationary phase 32.7 g of silica with 15-40  $\mu$ m diameter was used.

Based on the method of Back S. and Liang J. 2005, firstly 3 column-volumes (CVs) of DCM were added. Then, the polarity is significantly increased by changing the mobile phase to AcOEt:Isopropanol 4:1. The aim of that abrupt change is to shortly group the crude extract into three parts, and later the group which contains the compound of interest will be subjected in further purification. The second group is composed of 1.5 CV of the solvent system AcOEt:Isopropanol 4:1. Then, when no more Cry was detected at the TLCs, 0.5 CV of the same system was passed to verify that all the Cry was occupied on the second group. The aim of the current chromatography was to hold the metabolite of interest, Cry, so after its occupation on the second group, there was no interest to increase more the polarity and occupy other compounds.

One CV was averagely 27 mL. On each fraction, we collect 3-5 mL, and the process of collection is described below.

| Fractions | Solvents/Comments                             |
|-----------|---|
| 1-4       | The forehead of the extract enters the silica |
| 5-50      | 3 column volumes of DCM                       |
| 51-73     | 1.5 column volume of AcOEt:Isopropanol 4:1    |
| 74-79     | 0.5 column volume of AcOEt:Isopropanol 4:1    |
| 80-90     | 1 column volume of AcOEt:Isopropanol 4:1      |

Table 3.5: List of "MIX\_A" fractionation

Following the severe polarity change between the two different solvents at tube 61 we observe the forehead of the extract to exclude concentrated. The collection process is followed by TLC Normal Phase and liquid phase; Cyclohexane:Ethylacetate (AcOEt) 30:70, and based on these the fractions are connected in three groups.

| Grouped fractions | Weight (mg) |
|-------------------|-------------|
| A1_Fr.1-62        | 96.0        |
| A2_Fr.63-65       | 342.4       |
| A3_Fr.66-91       | 360.5       |

Table 3.6: List of grouped fractions

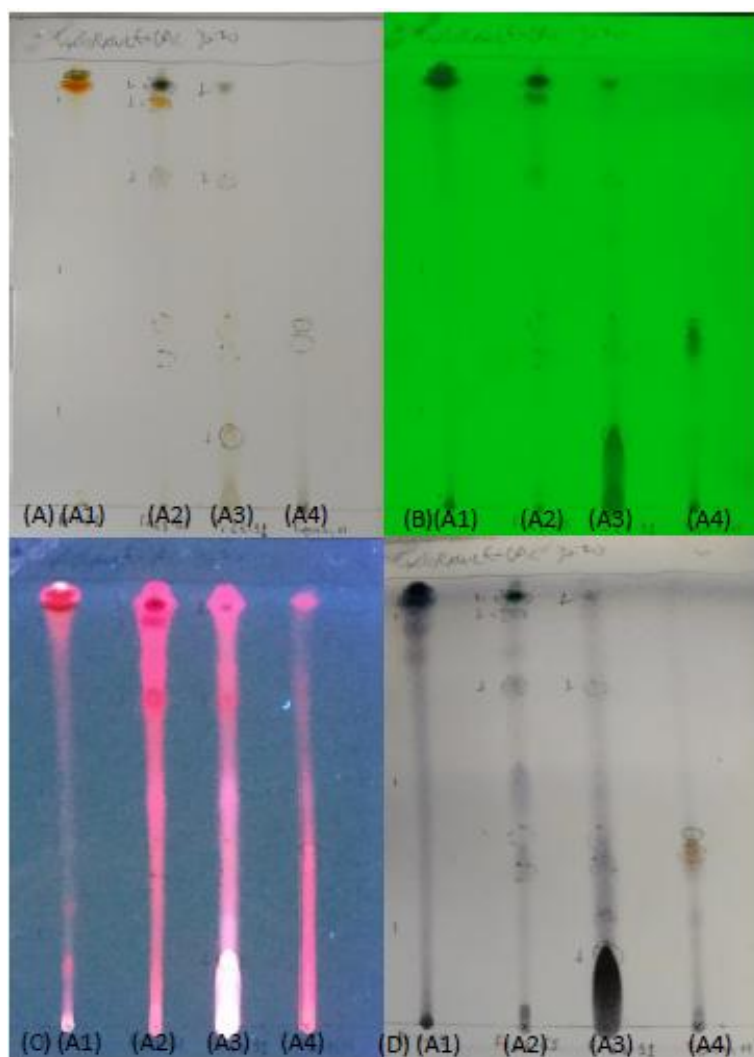


Figure 3.7: (A) Visible light, (B) UV radiation (C) Blacklight (D) SV (A1)Fr.1-62, (A2)Fr.63-65 (A3)Fr.66-91, (A4) Standard

The second group, “A2\_Fr.63\_65”, which contains the majority of the compound of interest is forwarded to further fractionation through flash column chromatography. 295.3 mg from the group “A2\_Fr.63\_65” were added with a funnel as dry-loading at the top of the stationary phase. 11.0 g of silica, 15-40  $\mu\text{m}$  diameter, were used as stationary phases. Though, this time as the sample was in smaller quantity, a thinner glass column (2.0 cm diameter) was used. The gradient mode consisted of Cyclohexane:AcOEt (table 3.7).

| Quantity (mL) | Cyclohexane (%) | AcOEt(%) |
|---------------|-----------------|----------|
| 100           | 80              | 20       |
| 100           | 70              | 30       |
| 100           | 60              | 40       |
| 500           | 50              | 50       |

Table 3.7: Gradient mode solvent system

The collection process is followed by TLC Normal Phase and liquid phase; Cyclohexane:AcOEt 30:70  
According to the observed TLCs we group the fractions into 8 groups (table 3.8).

| Group              | Weight (mg) |
|--------------------|-------------|
| A2_1_FR.1-18       | 2.6         |
| A2_2_FR.19-30      | 34.4        |
| A2_3_FR.31-87      | 94.0        |
| A2_4_FR.88-99      | 12.5        |
| A2_5_FR_FR.100-139 | 14.8        |
| A2_6_FR.140-175    | 16.0        |
| A2_7_FR.176-217    | 7.3         |
| A2_8_FR.Washing    | 80.6        |

Table 3.8: Fractionation of A2\_FR.63-65

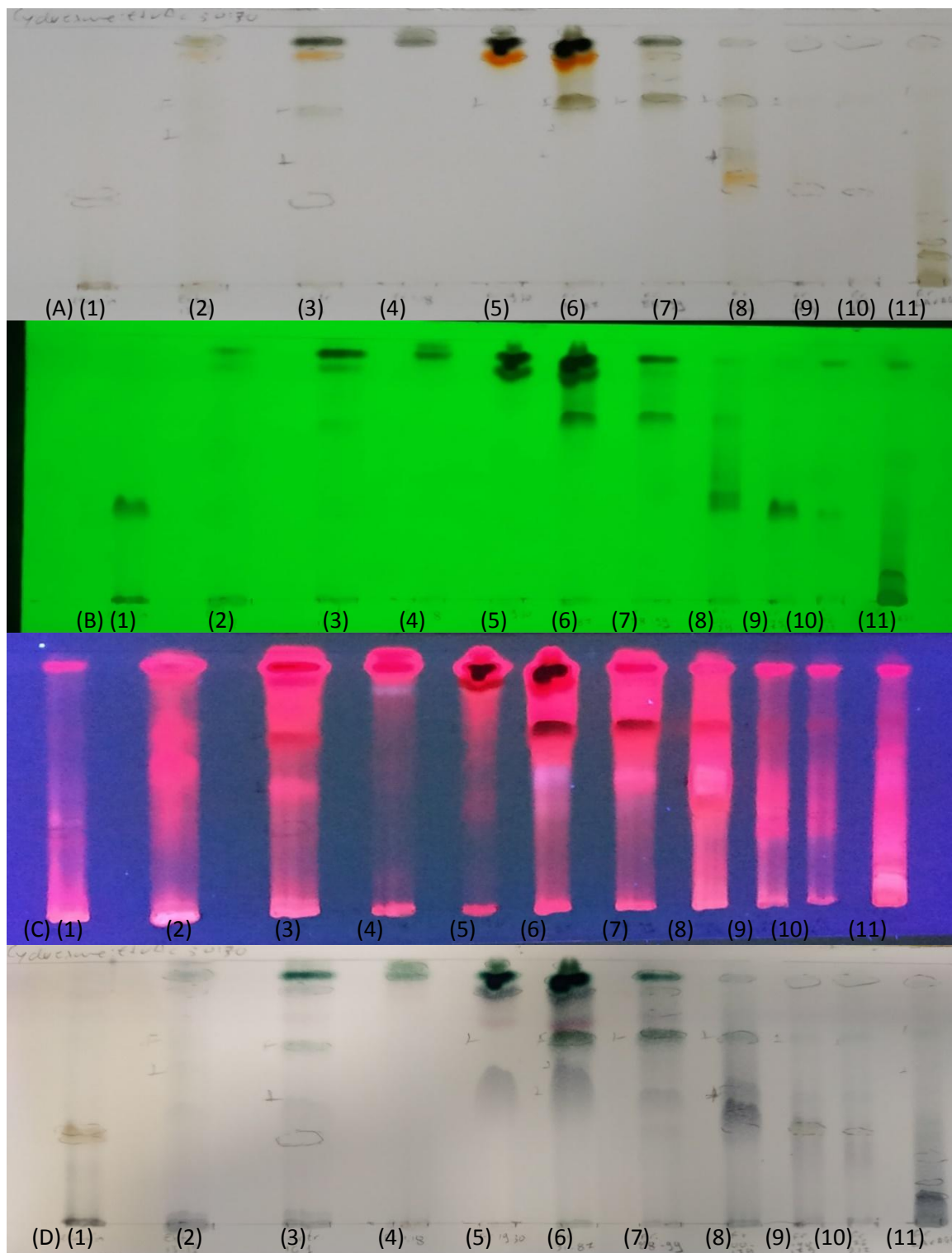


Figure 3.8: (A) Visible light, (B) UV radiation, (C) Blacklight, (D) SV

(1)Standard (2)A\_MIX (3) A2\_FR.62-65 (4) FR.1-18 (5)FR.19-30 (6)FR.31-87 (7)FR.88-99 (8)FR.100-139 (9)FR.140-175 (10)FR.176-217 (11)FR.Washing.

Based on the above observations, comparing to the Cry-1 standard (spot1, fig.3.8), we assume that the majority of Cry is contained in FR.140-175 and FR.176-217 (spots 9 and 10, fig.3.8).

At last, we verify the presence of Cry-1 in FR.140-175 and FR.176-217 through HPLC, with comparison to Cry-1 standard. We unite these fractions in one group "FR.140-217" with a final weight of 23.3 mg.

We compare the "FR.140-217" to Cry-1 standard, at HPLC with detection at 235 nm in gradient mode MeCN/H<sub>2</sub>O and conditions as described in HPLC quantification in Chapter 2.4 (table 2.1 p.80). The chromatogram of "FR.140-217" has its major peak almost at same ret.time to Cry-standard at 22.85 min, and same absorption spectrum.

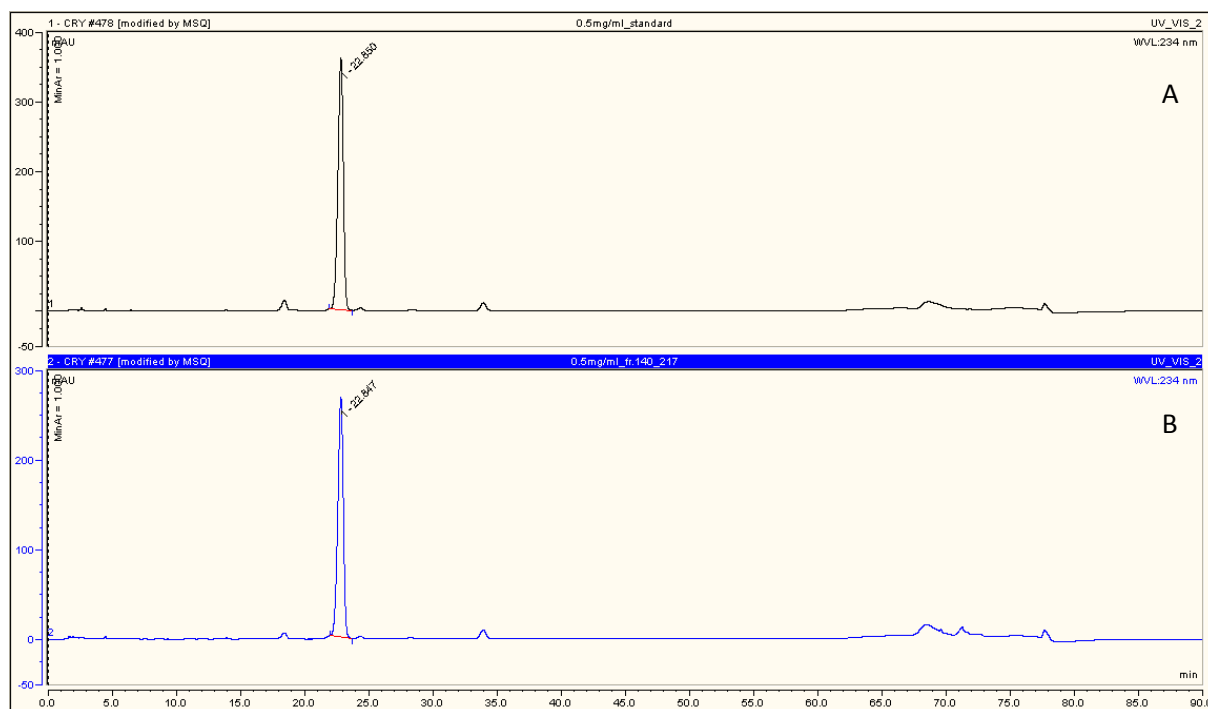


Figure 3.9: Comparative chromatogram of Cry-1 standard (Panel A) to FR.140-217 (Panel B). Both samples were at concentrations of 0.5 mg/mL.

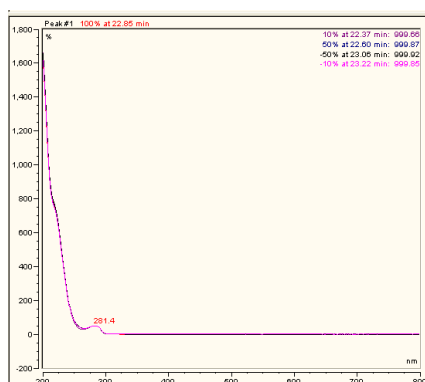


Figure 3.10 Absorption spectrum of peak at ret.time 22.85 min

In relation to semi-quantification data, few quantity Cry-1 should also be contained in FR."100-139" (comparing spot 1 and spot 8, fig.3.8). So, for "MIX\_A", considering that we started from 25 g of dry biomass, which comes from 36.7 L of culture, the obtained Cry-1 from FR.100-217 corresponds approximately to 0.83 mg of Cry-1/L of culture.

### Single step method through Flash-Column Chromatography

In order to study the phytochemical profile of *Nostoc* sp. ATCC 53789 the strain was examined in nominal, no-stress conditions. So, the "B\_BG11" biomass was examined, which was cultured under photoperiod 16:8 (L:D), averagely 25 °C, pH 7.4-7.9, and white light of 250  $\mu\text{mol photons m}^{-2} \text{s}^{-1}$ . 26.6 L of that sum resulted in 13.4 g of dry biomass. That dry biomass after extraction, applying the developed process, lead to 0.8 g of crude extract. That extract formed dry loading and subjected at flash-column-chromatography at "Isolera one" (Biotage). The fractionation was handled by auto-collector based on UV-spectrometer, which detected the eluted compounds. The UV-spectrometer was regulated to scan at 235 nm and 245 nm, which are the wavelength where Cry is detected. The gradient mode (table 3.9) was based on the method which was developed for the fractionation of A2\_Fr\_63\_65. The flow rate was stable at 25 mL/min.

| Volume | Cyclohexane (%) | Ethyl acetate (%) |
|--------|-----------------|-------------------|
| 75     | 90-80           | 10-20             |
| 100    | 80              | 20                |
| 100    | 70              | 30                |
| 200    | 60              | 40                |
| 475    | 50              | 50                |
| 665    | 0               | 100               |

Table 3.9: Gradient mode solvent system

The elution process was followed both by UV-spectrometer and TLC. Based on these, the obtained fractions are grouped into four groups.

| Group           | Weight (mg) |
|-----------------|-------------|
| A3_1_FR.1-8     | 204.8       |
| A3_2_FR.9-34    | 114.0       |
| A3_3_FR.35-80   | 172.8       |
| A3_4_FR.Washing | 242.2       |

Table 3.10: Grouped fractions of B\_BG11

The groups were examined on TLC normal phase in three polarity solvent-systems (fig.3.11).

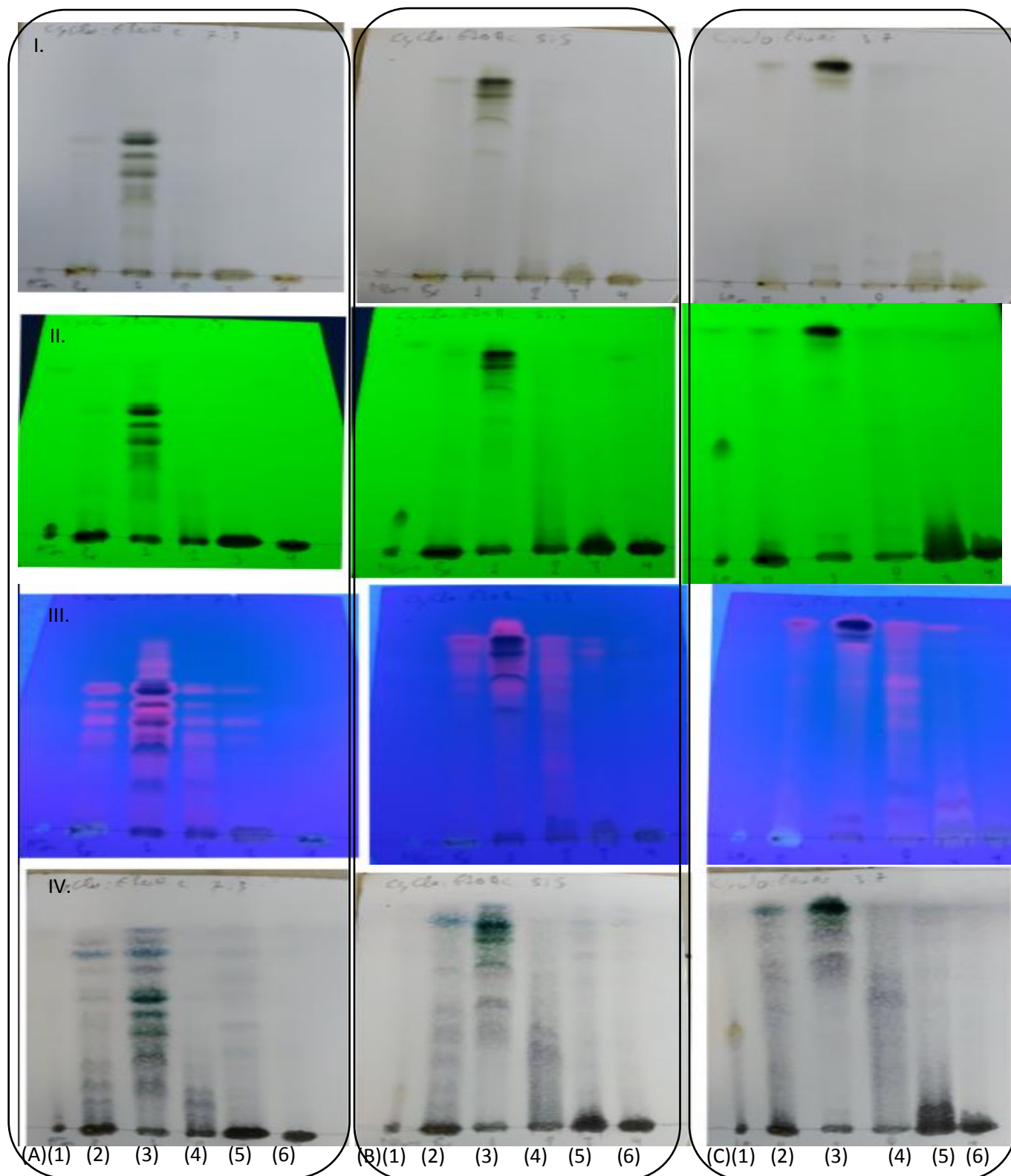


Figure 3.11: (I.) Visible light, (II.) UV radiation, (III.) Blacklight, (IV.) SV.

(A) Cyclohexane:AcOEt7:3, (B) Cyclohexane:AcOEt5:5, (C) Cyclohexane:AcOEt3:7.

(1) Cry Standard, (2) Crude extract "B\_BG11", (3) Fr.1-8, (4) Fr.9-34, (5) Fr.35-80, (6) Fr.Washing



Following the above fractionations, the grouped fractions were subjected to further study of their phytochemical profile. That was done through LC-MS/MS technique and interpretation of the obtained results in molecular networks.

### 3.3 Personal work: Phytochemical investigation through UHPLC-ESI-Q-TOF-HRMS<sup>2</sup> analysis and molecular networking

#### 3.3.1 Introduction in molecular networking bioinformatic approach

LC-MS/MS analysis generates a large amount of data, which could be a significant source of information. However, in order to extract that information, the vast data pool should be organized in a coherent way. Molecular networking constitutes an innovative bioinformatic approach initially developed in 2014 by the Peter Dorestein's team from the University of California *San Diego* (UCSD). Free-available tools are proposed on the Global Natural Products Social Molecular Networking (GNPS; <http://gnps.ucsd.edu>) environment platform that enables an optimal visualization of the recorded LC-MS/MS data (Yang J.Y. *et al.* 2013).

MS<sup>2</sup> data could be analyzed by means of an alignment algorithm (*e.g.* MS-Cluster<sup>®</sup>) and generation of consensus spectra. Finally, MS/MS spectra are gathered according to their similarity, that corresponds to structural similarities between related molecules and thus similar fragmentation patterns, and visualized as nodes connected together into a cluster. The similarity between spectra is expressed as a *cosine score* parameter. In case that a node has no proximity with another one, it does not connect with any other node, it remains free in the organization, and it is called *selfloop*. Classical GNPS work-flow is not able to distinguish between isomeric and isobaric molecules that could appear as a same node despite different retention times in the chromatogram. To address the issue, a new work-flow has been developed by P. Dorestein's, that is also available on the GNPS platform: the Feature Based Molecular Networking (FBMN). In this case, the treatment and alignment of MS/MS data is performed by processing software such as MZmine or MS-DIAL and the resulting data exported and clustered with the FBMN tool (Nothias L.F. *et al.* 2020). Another improvement of this tool is the possibility to extract "feature parameters" from chromatograms such as the "area under curve" (AUC) of the peaks in the Ion-Extract Chromatogram (IEC or XIC). As a consequence, the size of nodes in the molecular network could be annotated with the AUC of the peak of the corresponding parent ion, allowing a semi-quantitative estimation that cannot be done with the classical GNPS work-flow.

In order to construct and analyze the corresponding networks using the FBMN work-flow, we have to go through 4 steps; a) MZmine treatment (preprocessing), b) online construction of GNPS network, c)

network analysis through Cytoscape<sup>®</sup> visualization software, d) nodes annotation.

As described above, in the first step LC-MS and MS/MS data are recorded. These obtained chromatograms should be treated through mathematic transformations to be in a GNPS-exploitable format. The most common software for that treatment is MZmine. The process is split into several steps. Firstly, we set the noise level for MS1 and MS2 levels. Then the obtained data built a list of MS peaks through "chromatogram builder" session (Pluskal T. *et al.* 2010, Myers O.D. *et al.* 2017), and then these peaks are addressed to three respective retention time through "chromatogram deconvolution". The potential isotopes are grouped to form one unit through isotopes grouper. In case that we analyze more than one sample, the chromatograms should be compared to identify the common peaks. That is done through "alignment" and "filtering", while "gap filing" finally units the occurred gaps from slightly different retention time or peak formation.

At a second step, these data are transformed into ".mgf" and ".csv" files and are imported on online treatment for the network construction, through the "Feature Networking" portal (Pluskal T. *et al.* 2010, Wang M. *et al.* 2016, Nothias L.F. *et al.* 2020). In this online session, we can modify several parameters as the minimum value of cosine score or the minimum amount of required fragment ions for a node formation.

Following that online process, we can arrange the network spatially and depict the related information. One of the most appropriate software is Cytoscape. In this case, we can depict several values by modifying the thickness of the connecting-lines, the size of the nodes, or even split the nodes with chart-pies.

Last step is the nodes annotation and characterization. In that annotation, a starting point is required. That starter, which is called "seed" spectra, is a standard or purified compound, and based on this "seed" a cluster could be characterized. For the further annotation of the obtained fragments, a source of natural products' MS/MS data was needed. It has been developed already a similar library for the genomic and metabolomic analysis, UniProt KnowledgeBase (UniProtKB), which served as a model. It is hosted online at California San Diego (UCSD) Center for Computational Mass Spectrometry (CCMS; <http://proteomics.ucsd.edu/>). GNPS is an interactive platform where a researcher can submit spectra-data, while the following researcher who will use them can re-evaluate them in a ranking up to 4 to establish a higher quality on the system. GNPS is a global collaborative project, which is continuously expanding with the contribution of researchers worldwide. It consists of an open-access online vast library of MS/MS NP data, which enables the automatic approximate annotation of any unknown NP MS/MS spectrum. In 2016 it included more than 6.5 thousand MS/MS spectra or 4.2 thousand compounds (Johnson S.R and Lange B.M.2015, Wang M. *et al.* 2016, Olivon F. *et al.* 2017).

### 3.3.2 UHPLC-ESI-Q-TOF-HRMS<sup>2</sup> method development

In our project, a ESI-Q-TOF-HRMS<sup>2</sup> mass spectrometer was selected, thus a combination of a quadrupole with a time-of-flight analyzer. The first analyzer (Q) creates an electrostatic field, which allows ions to move due to the change of electrode charge. That change leads to a separation of the ions in relation to their mass. Then the ions are moved in the collision cell, and are subjected to collision induced dissociation (CID).

The analysis and the data collection were conducted in collaboration with Institut de Chimie Organique et Analytique (ICOA UMR 7311 CNRS Université d'Orléans), and Dr. Cyril Colas. The settings used for our MS/MS study will be described briefly herein. Specifically, Ultimate 3000 RSLC (Dionex, Germany) was coupled with a maXis UHR-Q-ToF (Bruker, Germany). Regarding the MS/MS settings, the mode was ESI positive-AutoMS/MS. Data collection was performed in a data-dependent analysis (DDA) mode in a mass window from  $m/z$  150 to 1200. Only three precursor ions were selected among the most intense ions and forwarded in the CID where an average collision energy of 30 eV was applied. The voltage at the capillary was 4500 V. The pressure at the gas nebulizer was at 2 bars, the flow at dry gas was 9 L/min at 200 °C. Concerning the detection settings, the mass range was 50-1650  $m/z$ , the acquisition frequency was 2 Hz (MS and MS/MS).

Based on the relevant parameters mentioned at 3.3.1, we developed a reversed-phase UHPLC method suitable for MS/MS studies of crude extracts of *Nostoc* strain or rich fractions thereof. Due to the cyclic structure of Cry and their relatively high average molecular mass, a large pore (*e.g.* 200 Å) core-shell column specifically designed for the reversed phase separation of biomolecules was selected for the project (Aeris WidePore XB-C18 2.1 x 150 mm; 3.6 µm - Phenomenex®). The mobile phase was remained the same with a solvent system of H<sub>2</sub>O/ACN in gradient mode (table 3.11), and buffer of formic acid (FA) was maintained in minimum quantities. That happens as few amounts of acid facilitates protonation and ion formation. Flow rate and column temperature were set at 40 °C and 500 µL/min respectively. The solvent system was H<sub>2</sub>O/ACN, in gradient mode.

| Time (min.) | (ACN + 0.08% FA) % V/V | (H <sub>2</sub> O + 0.1% FA) % V/V |
|-------------|------------------------|------------------------------------|
| 0           | 30                     | 70                                 |
| 1           | 30                     | 70                                 |
| 11.4        | 90                     | 10                                 |
| 12.0        | 100                    | 0                                  |
| 18.0        | 100                    | 0                                  |
| 18.5        | 30                     | 70                                 |
| 20.5        | 30                     | 70                                 |

Table 3.11: Gradient mode solvent system

Following the developed method, we first examined crude extracts A\_MIX, B\_BG11 and the fractions A3\_1, A3\_2, A3\_3, A3\_4 to study the phytochemical profile of *Nostoc* sp. ATCC 53789, the crude extract C\_OPT\_1.3 to compare the effect of different culture conditions and the crude extract C\_OPT\_0.2 to compare the effect of different growth phases. Moreover, we injected standards of Cry-1,-2 and -3 provided by Dr. Thai Q.D (Phycosource).

### 3.3.3 Parametrization of the softwares involved in the molecular networking

In order to get the optimal molecular network, the above parameters of MZmine as well as of GNPS, had to be optimized. The goal of that optimization was; a) a minimum amount of selfloops on the final graph, b) the obtaining of the maximum amount of clusters, c) the clustering of standards with the obtained compounds from the extracts, d) the correspondence of one node per compound and not the false over-depiction.

For instance, in MZmine software one complicated parameter was the fact that due to concentrated standards, the standard's peaks had a "tail", which could be considered as a second compound under wrong parameters. To solve that issue, the parameters of "min ratio of peak top/edge" and "search minimum in RT range (min)" in the section of "Chromatographic deconvolution" were essential. These parameters are responsible for signaling for the shape of the peak.

Regarding the GNPS modifications, an essential parameter was the "Minimum Matched Fragments Ions" which allowed the construction of the network to include more nodes, so enabled the better of the clusters. Based on that development, we formed the applied parameters.

|  |                                       |  |                                     |   |                    |          |
|--|---------------------------------------|--|-------------------------------------|---|--------------------|----------|
| MZmine                                       | Raw data method><br>Feature detection | >mass detection                                      | Set filters                         |   | MS1                | MS2      |
|  |                                       |  |                                     | Scan number                               |                    |          |
|  |                                       |  |                                     | Base Filtering Integer                    |                    |          |
|  |                                       |  |                                     | Retention time                            |                    |          |
|  |                                       |  |                                     | MS level                                  | 1                  | 2        |
|  |                                       |  |                                     | Scan definition                           |                    |          |
|  |                                       |  |                                     | Polarity                                  | ANY                | ANY      |
|  |                                       |  | Spectrum type                       | ANY                                       | ANY                |          |
|  |                                       |  | Mass detector                       | Mass detector                             | CENTROID           | CENTROID |
|  |                                       | Noise level  |                                     | 100                                       | 50                 |          |
|  |                                       | >ADAP Chromatogram Builder                           | Set filter                          | Scan number                               |                    |          |
|  |                                       |  |                                     | Base Filtering Integer                    |                    |          |
|  |                                       |  |                                     | Retention time                            |                    |          |
|  |                                       |  |                                     | MS level                                  | 1                  |          |
|  |                                       |  |                                     | Scan definition                           |                    |          |
|  |                                       |  |                                     | Polarity                                  |                    |          |
|  |                                       |  | Spectrum type                       |   |                    |          |
|  |                                       |  | Min group size in # of scans        | 3   |                    |          |
|  | Group intensity threshold             |  | 100                                 |   |                    |          |
|  | Min highest intensity                 | 3000   |                                     |   |                    |          |
|  | m/z tolerance                         | 0.01 m/z or 20 ppm                                   |                                     |   |                    |          |
|  | >Feature list methods                 | >Feature detection><br>Chromatographic deconvolution | Algorithm><br>Local minimum search  | Chromatographic threshold                 |                    | 1.0      |
|  |                                       |  |                                     | Search minimum in RT range (min)          |                    | 0.10     |
|  |                                       |  |                                     | Minimum relative height                   |                    | 1.0      |
|  |                                       |  |                                     | Minimum absolute height                   |                    | 200      |
|  |                                       |  |                                     | Min ratio of peak top/edge                |                    | 2        |
|  |                                       |  | Peak duration range (min)           |   | 0.01 – 3.00        |          |
|  |                                       | m/z range for MS2 scan pairing (Da)                  |                                     | <input checked="" type="checkbox"/> 0.025 |                    |          |
|  |                                       | RT range for mS2 scan pairing (min)                  |                                     | <input checked="" type="checkbox"/> 0.15  |                    |          |
|  |                                       | >Isotopes><br>Isotopic peak grouper                  | m/z tolerance                       |   | 0.01 m/z or 20 ppm |          |
|  |                                       |  | Retention time tolerance            |   | 0.1                |          |
|  |                                       |  | Maximum charge                      |   | 2                  |          |
|  |                                       | Representative isotope                               |                                     | Most intense                              |                    |          |
|  |                                       | >Alignment><br>RANSAC Aligner                        | m/z tolerance                       |   | 0.01 m/z or 20 ppm |          |
|  |                                       |  | RT tolerance                        |   | 0.2                |          |
|  |                                       |  | RT tolerance after correction       |   | 0.05               |          |
|  |                                       |  | RANSAC iterations                   |   | 0                  |          |
|  |                                       |  | Minimum number of points            |   | 20                 |          |
|  |                                       | Threshold value                                      |                                     | 1   |                    |          |
| >Filtering> Feature list row filter          | Keep only peaks with MS2 scan (GNPS)  |  | <input checked="" type="checkbox"/> |   |                    |          |
|  | Reset the peak number ID              |  | <input checked="" type="checkbox"/> |   |                    |          |
| >Gap Filing>Same RT and m/z range gap filter |                                       | m/z tolerance  | 0.01 m/z , 20 ppm                   |   |                    |          |
| GNPS   | Basic options                         | Precursor Ion Mass Tolerance                         |                                     | 0.05                                      |                    |          |
|  |                                       | Fragment Ion Mass Tolerance                          |                                     | 0.05                                      |                    |          |
|  | Advanced Network Options              | Min Pairs Cos  |                                     | 0.6                                       |                    |          |
|  |                                       | Minimum Matched Fragments Ions                       |                                     | 3   |                    |          |
|  |                                       | Maximum shift between precursors                     |                                     | 500                                       |                    |          |
|  |                                       | Network TopK   |                                     | 15  |                    |          |
| Maximum Connected Component Size             |                                       | 500  |                                     |   |                    |          |

Table 3.12: MZmine and GNPS settings

As mentioned above, the goals of these methods were to examine; the phytochemical profile and specifically focusing the Cry-analogues, as well as how that phytochemical profile changes under different culture conditions, and under different growth phases.

3.3.4 Results on cryptophycin's analogues in *Nostoc* sp. ATCC 53789

Cry-1 was firstly discovered in *Nostoc* sp. ATCC 53789 (Schwartz R.E. *et al.* 1990, Hirsch C.F. *et al.* 1990) though later all the rest of analogues were studied at *Nostoc* sp. GSV 224 due to the higher yields that the second strain offers. Until today, 28 Cry analogues have been characterized in *Nostoc* sp. GSV 224 (table 3.13).

| No. | Analogue | Molecular weight | Molecular Formula   |                                      |
|-----|----------|------------------|---|--------------------------------------|
| 1   | Cry-1    | 654.2708         | C <sub>35</sub> H <sub>43</sub> ClN <sub>2</sub> O <sub>8</sub>               | Golakoti T.<br><i>et al.</i> 1994    |
| 2   | Cry-2    | 620.3098         | C <sub>35</sub> H <sub>44</sub> N <sub>2</sub> O <sub>8</sub>                 |                                      |
| 3   | Cry-3    | 638.2759         | C <sub>35</sub> H <sub>43</sub> ClN <sub>2</sub> O <sub>7</sub>               |                                      |
| 4   | Cry-4    | 604.3149         | C <sub>35</sub> H <sub>44</sub> N <sub>2</sub> O <sub>7</sub>                 |                                      |
| 5   | Cry-30   | 656.2864         | C <sub>35</sub> H <sub>45</sub> ClN <sub>2</sub> O <sub>8</sub>               | Golakoti T.<br><i>et al.</i> 1995    |
| 6   | Cry-26   | 656.2864         | C <sub>35</sub> H <sub>45</sub> ClN <sub>2</sub> O <sub>8</sub>               |                                      |
| 7   | Cry-23   | 674.2162         | C <sub>34</sub> H <sub>40</sub> Cl <sub>2</sub> N <sub>2</sub> O <sub>8</sub> |                                      |
| 8   | Cry-31   | 688.2318         | C <sub>35</sub> H <sub>42</sub> Cl <sub>2</sub> N <sub>2</sub> O <sub>8</sub> |                                      |
| 9   | Cry-17   | 624.2602         | C <sub>34</sub> H <sub>41</sub> ClN <sub>2</sub> O <sub>7</sub>               |                                      |
| 10  | Cry-43   | 590.2992         | C <sub>34</sub> H <sub>42</sub> N <sub>2</sub> O <sub>7</sub>                 |                                      |
| 11  | Cry-45   | 658.2213         | C <sub>34</sub> H <sub>40</sub> Cl <sub>2</sub> N <sub>2</sub> O <sub>7</sub> |                                      |
| 12  | Cry-21   | 640.2551         | C <sub>34</sub> H <sub>41</sub> ClN <sub>2</sub> O <sub>8</sub>               |                                      |
| 13  | Cry-29   | 624.2602         | C <sub>34</sub> H <sub>41</sub> ClN <sub>2</sub> O <sub>7</sub>               |                                      |
| 14  | Cry-24   | 606.2941         | C <sub>34</sub> H <sub>42</sub> N <sub>2</sub> O <sub>8</sub>                 |                                      |
| 15  | Cry-18   | 638.2759         | C <sub>35</sub> H <sub>43</sub> ClN <sub>2</sub> O <sub>7</sub>               |                                      |
| 16  | Cry-50   | 640.2551         | C <sub>34</sub> H <sub>41</sub> ClN <sub>2</sub> O <sub>8</sub>               |                                      |
| 17  | Cry-49   | 624.2602         | C <sub>34</sub> H <sub>41</sub> ClN <sub>2</sub> O <sub>7</sub>               |                                      |
| 18  | Cry-19   | 624.2602         | C <sub>34</sub> H <sub>41</sub> ClN <sub>2</sub> O <sub>7</sub>               |                                      |
| 19  | Cry-54   | 654.2708         | C <sub>35</sub> H <sub>43</sub> ClN <sub>2</sub> O <sub>8</sub>               |                                      |
| 20  | Cry-28   | 624.2602         | C <sub>34</sub> H <sub>41</sub> ClN <sub>2</sub> O <sub>7</sub>               |                                      |
| 21  | Cry-40   | 640.2551         | C <sub>34</sub> H <sub>41</sub> ClN <sub>2</sub> O <sub>8</sub>               |                                      |
| 22  | Cry-16   | 640.2551         | C <sub>34</sub> H <sub>41</sub> ClN <sub>2</sub> O <sub>8</sub>               |                                      |
| 23  | Cry-46   | 638.2759         | C <sub>35</sub> H <sub>43</sub> ClN <sub>2</sub> O <sub>7</sub>               | Subbaraju G.V.<br><i>et al.</i> 1997 |
| 24  | Cry-175  | 672.2369         | C <sub>35</sub> H <sub>42</sub> Cl <sub>2</sub> N <sub>2</sub> O <sub>7</sub> |                                      |
| 25  | Cry-176  | 626.2395         | C <sub>33</sub> H <sub>39</sub> ClN <sub>2</sub> O <sub>8</sub>               |                                      |
| 26  | Cry-327  | 654.2708         | C <sub>35</sub> H <sub>43</sub> ClN <sub>2</sub> O <sub>8</sub>               | Chaganty S.<br><i>et al.</i> 2004    |
| 27  | Cry-38   | 654.2708         | C <sub>35</sub> H <sub>43</sub> ClN <sub>2</sub> O <sub>8</sub>               |                                      |
| 28  | Cry-326  | 674.2162         | C <sub>34</sub> H <sub>40</sub> Cl <sub>2</sub> N <sub>2</sub> O <sub>8</sub> |                                      |

Table 3.13: Review of Cry-analogues, detected in *Nostoc* sp. GSV 224 (adapted from Golakoti T. *et al.* 1994, Golakoti T. *et al.* 1995, Subbaraju G.V. *et al.* 1997, Chaganty S. *et al.* 2004)

So, as the *Nostoc* sp. ATCC 53789 is the only commercially available cryptophycin's producer we wanted to examine its phytochemical profile, and mostly to examine if it produces other analogues of Cry than Cry-1. A first view on the potential Cry-analogues that could exist in the strain could be

done through the aspect of molecular networks. The first step, is to study the way of fractionation of the Cry-1, to know which fragments we should expect and their respective molecular mass. The fragmentation, which would result to free carboxylic acid, could occur mainly by two possible ways, by a direct opening (c/z in scheme), or by another two-step process (b/y in scheme). The first way is a direct cleavage, while the second is followed by OH transfer (fig.3.12) (Golakoti T. *et al.* 1994, Niedermeyer T.H. and Strohm M. 2012). From that fragmentations, main observed ions are the C-D units with water adduct with 218  $m/z$  (depending the substrates of the analogues in these units), and the B-C-D units at 412  $m/z$ , which varies also depending the analogue's substrates. Other ions that are observed in examination of Cry-1 are: 195, 218, 227, 246, 262, 384, 392, 412, 427, 438, 542, 627, 658  $m/z$ . These values are for fragments of Cry-1 so, actual values of analogues may vary due to their different substrates (Golakoti T. *et al.* 1994, Nowruzi B. *et al.* 2012, Niedermeyer T.H. *et al.* 2012). The injected standards Cry-1, -2, -3 are used as "seeds" to annotate the first nodes, and to identify the expected retention time. These nodes helped us to annotate the Cry cluster. At that point, we managed to make hypothesis for the identity of their neighbor nodes (table 3.14, fig.3.13). In this process, we were based on the parent mass of the nodes, their fragments as well as their cosine score in relation to the nodes of standards.

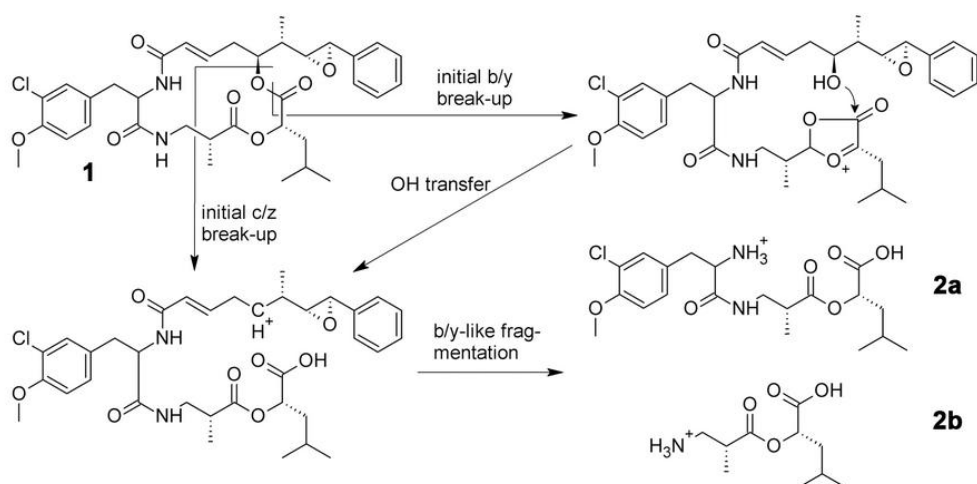


Figure 3.12: Proposed fragmentation pathway by direct opening (c/z) and a two-step process of opening and -OH transfer (b/y) (Niedermeyer T.H. *et al.* 2012).

| Compound              | Ret. Time (min) | [M+H] <sup>+</sup> (m/z) | Fragments   | $\Delta$ theoretical mass (ppm) | Molecular Formula   |
|-----------------------|-----------------|--------------------------|---|---------------------------------|---|
| Cluster A             |                 |                          |   |                                 |   |
| Cry-19, -28, 29       | 9.276           | 625.2659                 | 609.30; 565.24; <b>538.25</b>   | -2.56                           | C <sub>34</sub> H <sub>41</sub> ClN <sub>2</sub> O <sub>7</sub> |
| Cry-176               | 7.942           | 627.246                  | 609.23; 567.22; <b>540.25</b>   | -1.28                           | C <sub>33</sub> H <sub>39</sub> ClN <sub>2</sub> O <sub>8</sub> |
| Cluster B             |                 |                          |   |                                 |   |
| Cry-4                 | 7.268           | 605.3231                 | 577.32; 360.19; <b>218.14</b>   | 1.65                            | C <sub>35</sub> H <sub>44</sub> N <sub>2</sub> O <sub>7</sub>   |
| Cry-24                | 5.964           | 607.3021                 | 597.31; 350.19; <b>218.14</b>   | 1.15                            | C <sub>34</sub> H <sub>42</sub> N <sub>2</sub> O <sub>8</sub>   |
| Cry-2                 | 6.318           | 621.3181                 | 593.26; 360.17; 350.20; <b>227.11</b>                                 | 1.77                            | C <sub>35</sub> H <sub>44</sub> N <sub>2</sub> O <sub>8</sub>   |
| Cry-3                 | 8.346           | 639.2821                 | 395.16; <b>219.14</b> ; <b>212.12</b> ; <b>169.10</b>                 | -1.72                           | C <sub>35</sub> H <sub>43</sub> ClN <sub>2</sub> O <sub>7</sub> |
| Cry-50, -40, -16, -21 | 5.874           | 641.2616                 | 613.27; <b>396.16</b> ; <b>227.10</b> ; <b>219.14</b>                 | -1.25                           | C <sub>34</sub> H <sub>41</sub> ClN <sub>2</sub> O <sub>8</sub> |
| Cry-50, -40, -16, -21 | 6.305           | 641.2621                 | 613.27  | -0.78                           | C <sub>34</sub> H <sub>41</sub> ClN <sub>2</sub> O <sub>8</sub> |
| Cry-1, -54, -327, -38 | 6.821           | 655.2777                 | <b>218.10</b> ; <b>227.11</b> ; 254.08; <b>384.16</b> ; <b>412.15</b> | -0.61                           | C <sub>35</sub> H <sub>43</sub> ClN <sub>2</sub> O <sub>8</sub> |
| Cry-26, -30           | 7.167           | 657.2907                 | <b>395.16</b> ; <b>186.05</b> ; <b>414.16</b> ; <b>219.14</b>         | -4.56                           | C <sub>35</sub> H <sub>45</sub> ClN <sub>2</sub> O <sub>8</sub> |

Table 3.14: Hypothesis of detected compounds (fragments in red in accordance with the proposed fragmentation pathway).



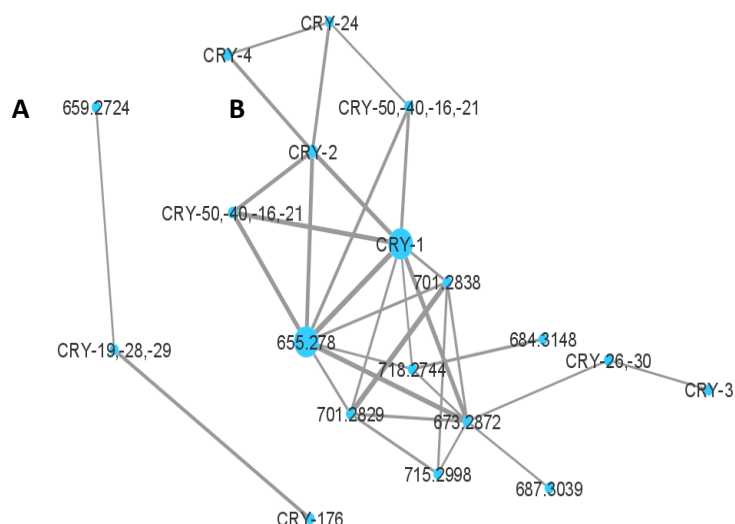


Figure 3.13: Cry cluster A and B, the size of the nodes is in relation to the concentration in MIX\_A

Based on the above table we try to annotate the potential Cry-analogues and clusters (fig. 3.15 clusters A and B), and make the hypothesis that in *Nostoc* sp. ATCC 53789 there are nine more Cry-analogues than Cry-1. These are Cry-2, -3, -4, -24, -176. Moreover, there is one of Cry-26, -39, 2 of Cry-50, -40, -16, -21, and 1 of Cry-19, -28, 29. The area of the peak of the Cry-analogues in the crude extract MIX\_A implies the analogues' proportions (table 3.15). These proportions are relevant with the concentrations of the analogues in the *Nostoc* sp. GSV 224.

| N <sub>o</sub> | Cry analogues       | % in the total amount of analogues, ATCC 53789 | % in the total amount of analogues, GSV 224 (Golakoti T. <i>et al.</i> 1995) |
|----------------|---------------------|--|--|
| 1              | Cry-1               | 79.74  | 85.04  |
| 2              | Cry-2               | 8.37   | 2.32   |
| 3              | Cry-4               | 3.81   | 0.58   |
| 4              | Cry -21/-16/-50/-40 | 3.36   | 5.41/1.16/0.18/0.12  |
| 5              | Cry-30/-26          | 2.53   | 1.17/0.19  |
| 6              | Cry -21/-16/-50/-40 | 1.61   | 5.41/1.16/0.18/0.12  |
| 7              | Cry-3               | 0.26   | 1.16   |
| 8              | Cry-24              | 0.16   | 0.31   |
| 9              | Cry-29/-28/-19      | 0.16   | 0.77/0.19/0.12   |
| 10             | Cry-176             | 0.001  |  |

Table 3.15: Cry-analogues' proportions in the two producer strains

The analogues Cry -21,-16,-50,-40 are stereoisomer, so they have the same molecular mass and their identification cannot be done only by the mass data. The same happens for analogues Cry-30, -26 and analogues Cry-29,-28,-19. However, their expected proportions, considering their already known percentages in *Nostoc* sp. GSV 224, (table 3.15) implies which of the analogues is present. So, we assume that in N<sub>o</sub> 4 should be Cry-21, in N<sub>o</sub> 5 Cry-30 and in N<sub>o</sub> 9 Cry-28.

Regarding the variations of Cry-analogues we compared their proportions in different growth phases and different culture conditions. As expected, in log phase we detected almost no Cry production, as Cry is secondary metabolite and is expected later in the growth curve (fig.3.15). In comparison of different conditions, we noted that in combined -optimal- conditions there was higher production of the major analogues, as Cry-1, -2, -4 (fig.3.14). It should be remarked that the network provides only a first semi-quantification representation with low level of accuracy, so further research is needed for the exact comparison of the different conditions. However, based on these clusters and the expected ret.times we can build a future isolation method. That future isolation is needed also for the verification of our hypothesis on the clusters. Specifically, further verification is required in cluster A with Cry-28, -176 where OPT\_1.3 is in unexpectable low quantities.

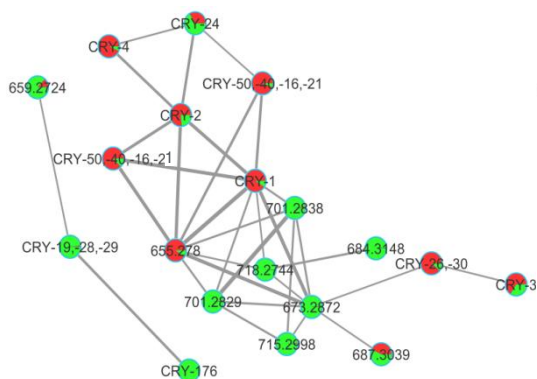


Figure 3.14: comparison of Cry content optimal conditions OPT\_1.3 (red) to non-optimal, B\_BG11 (green).

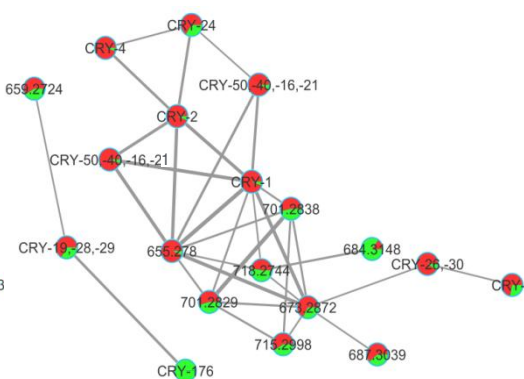


Figure 3.15: Comparison of Cry content in late exponential phase, OPT\_1.3 (red), to log phase, OPT\_0.2.

### 3.3.5 Results General phytochemical profile of *Nostoc* csp. ATCC 53789

The annotation of the Cry-clusters was based on the “seeds” standards. Though, we managed to annotate more nodes than these indicated by the standards, based on GNPS hits and bibliographic research.

We remark the nostocyclopeptides firstly based on the m/z of the ions, and at a second step by their retention time. Specifically, they were eluted from 1.06 to 1.86 which comes in accordance with the fact that they are polar compounds (fig.3.16 selfloops E, F, G).

Moreover, the online library hits on GNPS site are also a tool that contributed to the annotation. So, we got a hit of “bronze class” to pheophorbide A, with cosine value 0.93. Pheophorbide A (PPBa) is a breakdown product of chlorophyll. Specifically, PPBa is a product of the dephytylation and demetallation of chlorophyll a. These catabolic processes are due to the effect of chlorophyllase and Mg-dechelatase and take place in higher plants, algae, and cyanobacteria (Das A. *et al.* 2018, Saide A. *et al.* 2020). In that way, we annotate the cluster of PPBa (fig.3.16 cluster C).

The PPBa cluster is connected with a multi-complex of clusters (fig.3.16, complex of clusters D). This

broad complex probably contains less polar compounds such as chlorophylls and lipids. We come up with this hypothesis for several reasons. Firstly, the complex H is connected with the PPBa cluster with multiple edges, which reveals its proximity with the chlorophyll's compounds. Then, based on the retention time of the nodes 12.00 to 17.30 min, we assume that they should be less polar compounds that were eluted with the "washing phase" of the UHPLC method (fig.3.17). The method was developed mostly focused on Cry examination, so less polar compounds were eluted in the latest part of the chromatography. The polarity of the compounds is also verified by the comparison of the fractions of the extract B\_BG11. These compounds are mostly present in fractions 1 and 2, where less polar compounds should be expected (fig.3.19). Lastly, another reason which justifies the general characterization of that complex is the comparison of the crude extracts of log phase and late exponential (fig.3.18). Here, we observed high ratio of these nodes in the log phase, which means that the compounds are mostly primary metabolites.

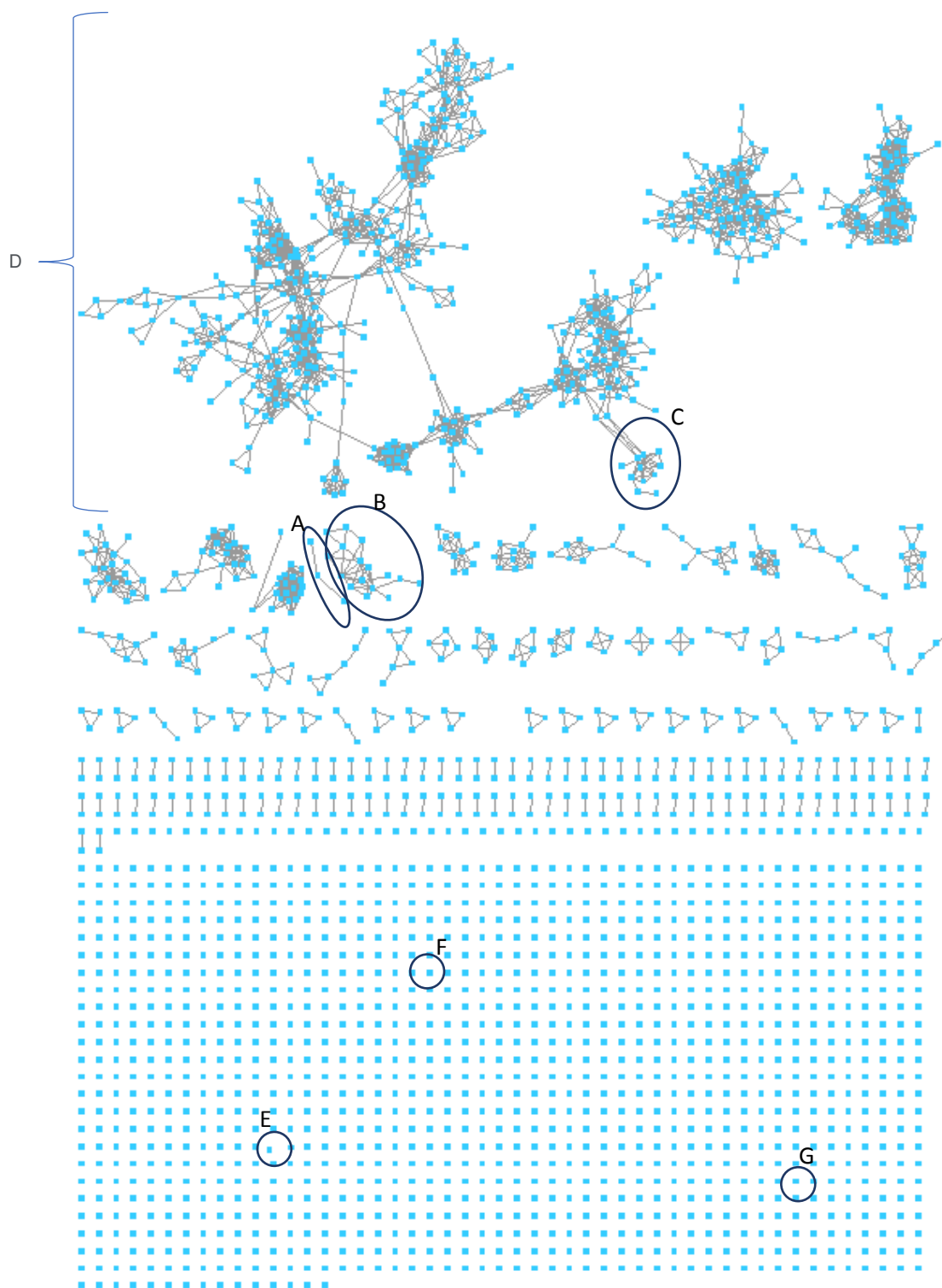


Figure 3.16: Total molecular network of the examined samples. A,B, Cry clusters, C PPBa cluster, D multi-complex of clusters of polar compounds, E, F, Gnostocyclopeptides,

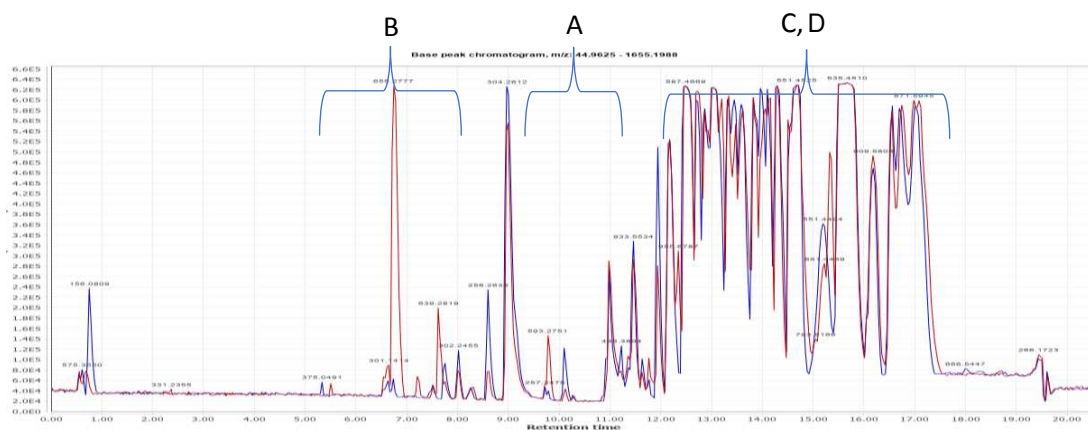


Figure 3.17 Comparative chromatogram of OPT\_1.2 (red) and OPT\_0.2 (blue). A,B, Cry clusters, C PPBa cluster, D multi-complex of clusters of polar compounds

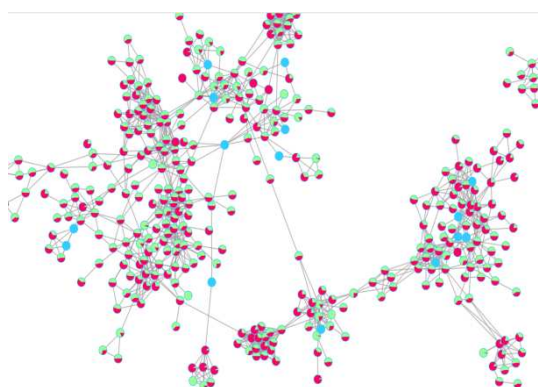


Figure 3.18 Focus on the part of cluster-complex H. comparison of OPT\_0.2 (green) and OPT\_1.2(red)

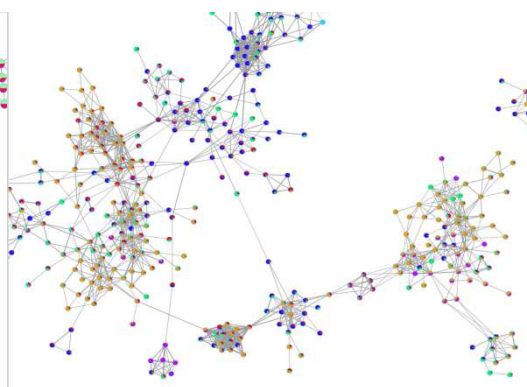


Figure 3.19 Focus on the part of cluster-complex H. comparison of; B\_BG11(red), A3\_1 (blue), A3\_2(green) A3\_3(orange), A3\_4(purple)

## Conclusion – Chapter 3

The third chapter focuses, through the aspect of molecular networks, on the examination of the phytochemical profile of *Nostoc* sp. ATCC 53789, as well as on how that profile is affected by different culture conditions, and microorganism's different growth phase. Firstly, it was developed a protocol for the occupation of dry biomass from high-scale cultures. Then it was established an extraction and purification method for the obtained biomass. The crude extracts and fractions were subjected to ESI-Q-TOF-HRMS<sup>2</sup>. The results were interpreted through molecular networks, and the relative parameters of all the involved softwares were set accordingly.

Regarding the general phytochemical profile, we identified Pheophorbide A (PPBa), through GNPS-library-hit, which is a break-down product of chlorophyll. In that way, we annotated the general complex of primary metabolites' clusters. We verified that complex, as it was overexpressed in log-phase culture. Then, we verified the presence of nostocyclopeptides in the culture, which are cyclic heptapeptides expressed by *Nostoc* sp. ATCC 53789 (Golakoti T. *et al.* 2001).

In relation to the Cry-analogues, until now they were studied only at *Nostoc* sp. GSV 224. For the first time, we manage to make a hypothesis about the presence of 9 more Cry-analogues than Cry-1 in *Nostoc* sp. ATCC 53789, and to precise their respective proportions. We note, through the network's aspect, that the analogues are mostly expressed in the late exponential phase, as they are secondary metabolites. Moreover, under the combined optimal culture conditions that we developed, the major analogues seem to be overexpressed. Now, that we have made an initial hypothesis about the presence and physicochemical properties of specific analogues, a more targeted isolation and purification method would enable their characterization and precise quantification.

## General conclusion and future perspectives

Cryptophycin is a cyanotoxin with potent anticancer activity, produced by cyanobacterium *Nostoc* sp. Its potent anticancer activity indicates the compound as a prominent novel anticancer drug candidate. Though, until now its low total synthesis yield is the main obstacle for further research and industrial exploitation. The aim of the study is to lead to cryptophycin overproduction by optimizing the abiotic culture parameters of *Nostoc* sp. ATCC 53789. At the same time, we investigate the phytochemical profile of the strain and the presence of Cry analogues, as very few studies have been conducted on this specific strain.

Firstly, examining the light parameters, we showed that high light intensities lead to cell death, while a medium light intensity is suitable for growth and metabolite production. Then, comparing different wavelengths, orange-red light was proven to be optimal for Cry production among the compared color lights. That may happen as orange-red light can be absorbed by both photosystems PSI & PSII. It has significantly higher photosynthetic activity than the blue spectrum, which is mostly absorbed only by PSI. Concerning the light photoperiod, we remark that even if 16:8 (L:D) and constant light have similar effect on growth patterns, the continuous light produces noticeably higher amount of metabolite. That indicates that Cry production might be a photo-dependent process, and also that under non-light conditions the microorganism provides the limited produced energy to fulfill its priorities of survival and not to the secondary metabolite's production.

Apart from the light conditions, we examined nitrates levels in medium's composition to investigate the implication of heterocysts on Cry expression process. It was shown that under nitrogen omission, the transformation of vegetatives to heterocysts and cell's primary needs consumed the few nitrogen-storages, so the Cry level in the culture was significantly lower. The optimal pH range is indicated as 8.5-9.0, while Cry production was significantly inhibited in  $T > 30$  °C. It was also demonstrated that the combination of the developed conditions had a positive synergic effect. Lastly, we compared flask cultures to scale-up conditions (culture in 15 L PBR) and the Cry concentration had an important rise in PBR, even if the growth rate was slower due to severe shear stress.

In addition to the obtained optimal conditions, which would maximize Cry production, another significant outcome was the developed methods for quantification of the metabolites from small volumes of cultures. As we examined biological samples, the quantification method should be: a) fast (we should have the quantitative data the same day with the sampling), b) accurate (the sample volume was small due to the flask-culture and metabolite's concentration significantly low), c) repetitive (each test consists of three biological and technical replicates, which acquire repeatability). These developed extraction-quantification techniques could be applied in a range of biological

samples examination, with the appropriate adaptation of the HPLC method.

At a second step, phytochemical profile of the strain was investigated, as only nostocyclopeptides and cryptophycin-1 have been identified on the strain to this date. The strain was cultivated in PBR, and the related extraction purification isolation methods were developed based on open column and flash chromatography. The obtained extracts were subjected to UHPLC-ESI-Q-TOF-HRMS<sup>2</sup> analysis. The results were treated through MZmine and GNPS software, and depicted in molecular networks. About the general molecular fingerprint, we identified break-down products of chlorophyll and verified the presence of nostocyclopeptides. Especially, interesting was the finding in Cry analogues, where we managed to identify and precise the relative portions of 9 analogues non-detected before in that strain. From the molecular networks approach as well as from the culture-conditions-experiments, it was shown that the Cry concentration faces its maximum from medium to late exponential phase.

Several perspectives could be examined based on the obtained results and the developed methods. As mentioned above, the combination of the developed conditions provided the maximum yield of Cry, while the scale-up culture increased, even more, the production. These results set the ground for the industrial exploitation of the compound. So, biotechnological industries could apply these conditions for the overproduction and the development of the pharmaceutical agent. The light optimization studies provided useful outcomes for the PBR design. Based on the data, that suggests long tubes with small diameter, novel photobioreactor's design can be developed and compared with the already existed designs in the market. Then, a customized PBR model could be built based on our remarks, and produce the maximum yield of Cry.

In our studies, a broad range of culture conditions were studied, though no biotic stress was tested. In this way, the co-culture of *Nostoc* sp. with other microorganisms could be examined to investigate if Cry could be used as a defense mechanism and produced in higher concentrations. Using the approach of molecular networks, we indicated the presence of 9 Cry analogues in the Cry cluster. Though, in the same cluster, there are 8 more unidentified nodes. Based on the obtained networks and the related chromatogram, a separation method can be developed and applied in preparative mode. Then, it will be possible to study the 9 analogues and most importantly to examine the 8 unidentified compounds, their relation to Cry and their biological properties.

Moreover, biological activity data could be included in the present network to indicate the potential active compounds. Specifically, Cry-1 has demonstrated low IC<sub>50</sub> values on KB, LoVo and SKOV3 cell lines. Assays, like the mentioned, could help with the annotation of potentially cytotoxic compounds, and contribute to the further targeted analysis.

The molecular networks could be improved to depict the general strain's profile. The current UHPLC method was developed focusing on the study of Cry cluster. As a result, the less polar compounds



were eluted last, with a significantly low level of separation. Consequently, their detection and identification were not applicable. So, only generic assumptions could be made for the less polar components of the extract, and further examination can be done in that part. The MZmine and GNPS parametrization could be also developed more to decrease the amount of selfloops and ameliorate the clusters depiction. In combination with a modified UHPLC gradient mode, these developments would provide a network focused on the non-examined less polar compounds.

## Annexes – Instrumentation of used equipment and techniques

### High Performance Liquid Chromatography

High Performance Liquid Chromatography (HPLC) is a chromatographic technique with a range of applications and especially on natural products (Sarker S.D. and Nahar L. 2015). The principle behind Column Chromatography technique is the gravitational force or works under low pressure. Higher pressure cannot be applied as the resulting backpressure damages the stationary phase and the separation process. The need for higher quality of separation of complex phytochemical profiles leads to the development and use of HPLC. HPLC consists of 6 units (fig.4.1). 1) Solvents (mobile phase) 2) High pressure pump 3) Injector 4) Column (Stationary Phase) 5) Detector 6) Data recording.

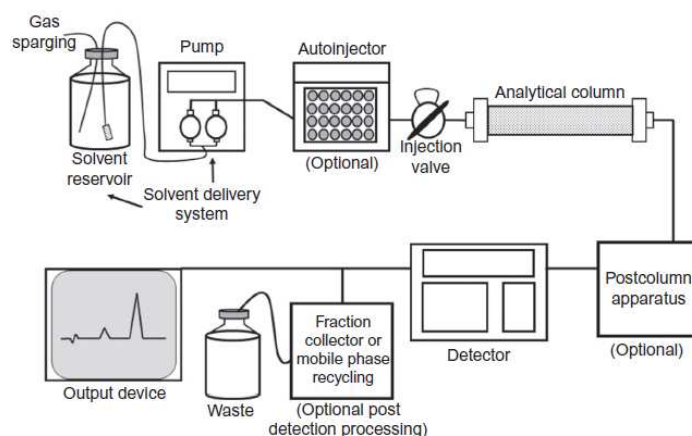


Figure 0.1 : HPLC system illustration (LaCourse M.E. and LaCourse W.R 2017)

### Mobile phase reservoir

The Mobile Phase of the chromatography consists of the solvents. Their proportions can be stable in the case of isocratic chromatography. On the other hand, in the case of gradient chromatography the proportions can be changed. That change of percentages can be done in an automatic way through the appropriate software. The solvents should be filtered prior to the use through nylon filters of 0.1 to 0.2  $\mu\text{m}$  pore size. That filtering retains particles and impurities that would block the stationary phase. Lastly, the water that would be used should have significantly low levels of chemicals such as Chloride and Sodium, and resistivity greater than 18 megaohms ( $\text{m}\Omega$ ) (LaCourse M.E. and LaCourse W.R. 2017).

### High pressure pump

The pump in HPLC can cause a pressure up to 400 bars. In our case, the pressure changes during the gradient, and it reaches a maximum of 100 bars.

## Injector

The injector is responsible for inserting the sample into the column compartment and it can be automatic or manual. In the manual injector, which is known as "Rheodyne injector", the sample is manually injected by the user through a glass or plastic syringe, while in the other case, the process is automated. The automatic injector was the one used in the project, and that mainly permits the automatic launching of multiple sequences without the required presence of the user (Malviya R. *et al.* 2010).

## Column

The column is the main core of the HPLC. It is composed of small polymer or spherical silica components. Their diameter varies from 3 to 10  $\mu\text{m}$ . In the case of the project's column is silica components of 5  $\mu\text{m}$  diameter. Attached to the surface of the silica is the bonded face. This bonded phase in the case of reversed-phase chromatography is usually C8, C18 (octadecyl-silica ODS) or phenyl. Longer chains provide a wider surface of contact with the mobile phase and so more interaction between the mobile phase and the elutes. In our case octyldecylsilane C18 is used.

A pre-column or guard-column can be attached prior to the main column. Its main utility is to protect the column from plugging and contamination by impurities of the mobile phase or the sample. In the project's case, the used precolumn has the same characteristics as the main column, but it is shorter in length. So, it is a C18 column with 5  $\mu\text{m}$  Silica diameter. In order to ensure the good condition of the column, a quality control test was performed once very semester. The test included firstly the injection of Uracil, which is an unretained component, to detect the  $t_0$  and  $V_0$ . Then, Phenol and Toluene were injected under specific concentrations to compare with the initial characteristic of the manufacturer (Campíns-Falcó P. *et al.* 2019).

## Detector

There is a range of detectors which vary depending on the nature of the examined compound. In the case of chromophores' presence, UV is the most common type of detector. UV detector can be Diode-Array Detection (DAD), which scans a range of wavelengths at the same time, or it can be UV-Visible "simple" which can simultaneously scan only few specific wavelengths (Dong M.W. 2005). The project focuses on the quantification of a specific compound and not on the analysis of the total phytochemical mixture. So, a UV-Vis "simple" detector which focuses on cryptophycin's  $\lambda_{\text{max}}$  (235 nm) is the detector that was used.

## Column Chromatography

Chromatography is a principle technique in the field of natural products. It contributes majorly on isolation and purification of natural extracts. A wide range of chromatographic techniques has been developed, so the researcher can choose the one which adapts on its needs depending; the nature of the compounds, the volume of the extract as well as the goal at he aims (*e.g.* preparative or analytical techniques).

From that wide range of chromatographic techniques, one of the first developed and most used is the Open Column Chromatography (OPC). In OPC stationary phase is packed into a glass column. The eluent flows, forced by gravitational forces or pump pressure, and in that way transfers the dissolved sample through the stationary phase.

There are a few appropriate materials for the stationary phase. These materials differ on their physicochemical characteristics as; the specific surface area, pore diameter distribution, pore-volume, packing density, and average diameter of the particles. The features of each material will address it for different chromatographic methods. Commonly used stationary phases are Silica gel, alumina, charcoal, diatomaceous earth (Celite), and others. In the project's case, Silica gel of 15-40  $\mu\text{m}$  diameter was used. The stationary phase is often packed between a layer of glass-wool on the bottom and sand on the top. Glass wool is placed to avoid silica leaking out of the column. The sand ensures that the forehead of the stationary phase will remain straight and unaffected from the liquid's turbulence during the ad of eluents (Palamareva M.D. *et al.* 2005).

The sample is placed between the silica and the sand, on top of the stationary phase. That can be done in two ways; as liquid or dry loading. In the case of liquid loading, the extract is dissolved in a minimum quantity of non-polar solvent-system. Often, the extract is not soluble in non-polar systems, and dry-loading is the optimal alternative. In dry-loading technique, the extract is dissolved in a solution and then absorbed in silica by evaporating the solvent. Then, the silica with the attached extract is finely added as a powder at the top of the stationary phase (Hayes W. and Rannard S. 2004).

About the system of solvents, the composition of the system can remain stable, which is called "isocratic", or change during the chromatographic process, which is called "gradient". In the case of gradient mode where the composition of the mobile phase is not stable, the change is done by increasing the system's polarity, from non-polar systems to more polar ones.

Air pressure can be adapted on the top of the column to contribute to better performance. That pressure can be an essential parameter that affects the proper elution of the compounds. Low pressure can lead to band widening through diffusion while high pressure can cause long tails on the descending compound's band. The ad of air pressure is the significant difference between OPC and flash-column chromatography (Regenstein J.M. and Regenstein C.E. 1984).

There are several methods of observing the eluted compounds and following the chromatographic process, such as; adapted UV-spectrometer and thin-layer chromatography (TLC). The most common technique, which is the one that we used at OPC, is the TLC.

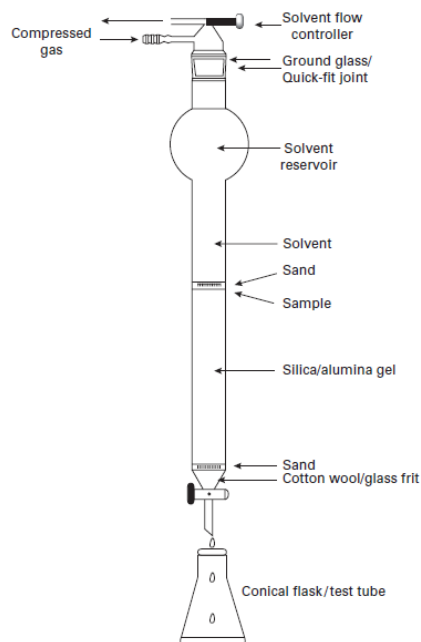


Figure 0.2 : OPC instrumentation (Hayes W. and Rannard S. 2004)

Automated instrumentations have been developed, which combine the flash-chromatography system with automated UV-detection of the eluted components. “Isolera one” (Biotage) is one of these automated systems which was used in the project. In this case, the main chromatographic column is a plastic cartridge with packed silica gel, which replaces the glass column of OPC. Before the main column, there is a second smaller plastic cartridge, which is used as pre-column for the dry loading. At the bottom of that second cartridge, there is a polyethylene (PE) frit of 20  $\mu\text{m}$  diameter, which serves the role of glass-wool at OPC. Dry-loading is then placed above that frit, and lastly, the top of the cartridge is filled with a small quantity of sand as done in the OPC (LaCourse W.R. 2002).

### Thin-layer Chromatography

TLC is one of the most common chromatographic techniques. Its use is well spread on laboratory practice due to the fact that it can be purchased ready-for-use at low cost. The stationary phase consists of a surface which is coated by the adsorbent. The surface can be a sheet of glass, plastic, or more often aluminum foil. The adsorbent can be aluminum oxide, cellulose, and in most cases silica gel. The most common combination is aluminum foil with silica gel. In this case, the silica particles have a diameter of 10 to 12  $\mu\text{m}$ , and the layer has 6 nm pore size, which leads to a thickness of 0.25 mm. That provides 1,000-2,000 theoretical plates per 5 cm of migration. The physicochemical

characteristics of silica may also vary to adapt to different conditions. For instance, smaller particles of silica are addressed in High Performance Thin Layer Chromatography (HPTLC), which gives quantitative results with good separation and accuracy. Another option as  $C_{18}$  is used for reversed-phase chromatography (Lewis S.W. and Lenehan C.E. 2013).

The mobile phase is a system of solvents which are chosen considering the stationary phase and the nature of the examined compounds. TLC is a unique case of chromatography. Only isocratic mode can be applied in TLC in contrast to other techniques where the composition of the mobile phase can be continuously changed.

The sample is placed in a liquid state in spots at the baseline of the TLC approximately 1 cm above the lower end of the sheet. The plate is put in a closed vessel with an amount of mobile phase. The air in the vessel has been prior homogenized with eluent's vapor. Then, the spots are moving axially *via* capillary action and the plate is taken out of the vessel when the forehead of the eluent is approximately 1 cm close to the upper top.

The visualization of the spots can be done in several ways depending on the nature of the examined compounds. The first observation can be done simply under visible light to detect compounds with chromophores which absorb in the visible spectrum. Then, ultraviolet radiation (254 nm) and blacklight (366 nm) can be applied on the plate to reveal the related spots. The plate can also be pulverized with chemicals that are addressed in specific chemical groups. For instance, *Dragendorff* reagent is used to detect alkaloids, and Vanillin-sulfuric acid reagent (VS) is used for terpenoids and phenols (Waksmundzka-Hajnos M. *et al.* 2015).

### Mass spectrometry (MS)

Mass spectrometry (MS) is a characterization technique for compounds, that analyzes ions formed in a source on the basis of their mass-to-charge ratio ( $m/z$ ).  $m/z$  is the quotient of the division of an ion mass expressed in unified atomic mass unit (amu) by its number of charges, so it is always positive and dimensionless. There is a range of equipment related to MS, which mostly differ on; a) the method of ionization and b) the mass analyzer technology. In the 19<sup>th</sup> century, pioneers on the MS development and instrumentation were Thompson J.J. and Aston F.W., who first established the MS idea and managed to separate ion beams by magnetic fields and record them on photographic plates. Significant contributions by Dempster A.J., Mattauch J. & Herzog R., and Johnson W. & Nier A. lead to the first accurate mass determination by late 1950s (Johnson W. and Nier A. 1957).

The MS instrumentation is split into three main compartments; the ion source (desorption/ionization step), the mass analyzer, and the ion detector. The ionization process depends on the physicochemical properties of the compound, such as molecular weight, polarity, proton affinity and

thermo-sensitivity. The main methods are electronic impact (EI), chemical ionization (CI), fast atom bombardment (FAB), matrix-assisted laser desorption ionization (MALDI), electrospray ionization (ESI), atmospheric pressure chemical ionization (APCI), and atmospheric pressure photoionization (APPI). EI and CI are suitable for low molecular weight, volatile, non-polar and non-heat-sensitive compounds. EI and CI are thus optimal for Gas Chromatography-Mass Spectrometry (GC-MS) (Kaklamanos G. *et al.* 2020). On the other hand, ESI, APCI, and APPI are of a broader scope and mostly used in combination with liquid chromatography (LC-MS).

ESI was chosen for our project. In ESI process, the solvent (*e.g.* MeCN in our case) that contains analyte(s) is pumped through a capillary at a low flow rate. At the end of the capillary, a high voltage is applied (*e.g.* 4.5 kV) resulting in ion formation into a fine spray of charge droplets. Dispersal of the highly charged droplets was followed by solvent evaporation and ion ejection (fig.4.3). The most common observed ions in ESI positive mode are the protonated  $[M+H]^+$  or sodiated  $[M+Na]^+$  pseudo-molecular ions (Pitt J.J. 2009).

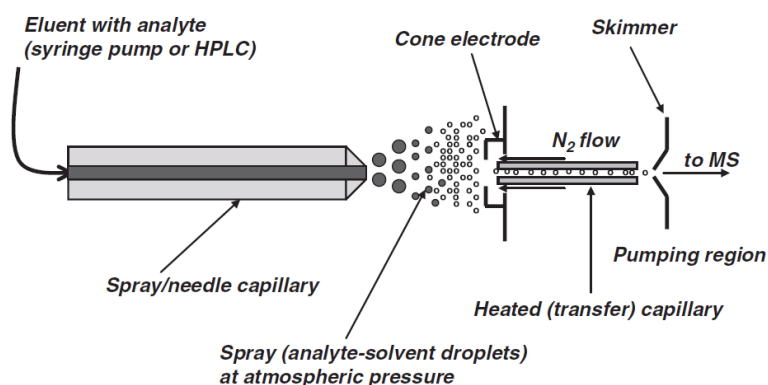


Figure 0.3: Instrumentation of electrospray ionization (ESI) source. (Somogyi Á. 2008)

Following ionization, the second important compartment is the mass analyzer. The principal role of the mass analyzer is the separation of ions according to their  $m/z$  ratio. The most common analyzers are Fourier transform ion cyclotron resonance (FT-ICR), orbitrap, ion traps (ITs), time-of-flight (TOF) analyzers and quadrupoles (Qs). Orbitrap and FT-ICR provide high accuracy measurements. Orbitrap set the ions in a circular motion using magnetic fields which then leads on separation based on their  $m/z$  ratio. TOF is based on the concept that ions of different weight take different time to cover the distance from the capillary to the detector. So, the period that it takes for the ion to cover the distance is measured and the value could be related to its  $m/z$  ratio. TOF analyzers accurate-mass determination.

Lastly, Qs have a limited mass range, low mass accuracy and resolution. However, they can be easily coupled with chromatographic instrumentations and so they are broadly use (Sparkman O.D. *et al.*

2011).

In order to enhance instrument performance, different analyzers can be coupled and form tandem mass spectrometers (MS/MS). That coupling depends on the required resolution, sensitivity, and acquisition speed. A large range of coupled analyzers has been developed mostly in combination with a Quadrupole or a Linear Ion Trap mass analyzer. To summarize, QqQ triple-stage quadrupole (TSQ) has the highest sensitivity, Q-orbitrap has the highest resolution and Q-TOF provides the most top acquisition speed (Hartonen K. *et al.* 2011).

Collisions transfer energy to the ions leading to unimolecular reactions and the respective fragments. In the next step, ions are sorted with a time-of-flight (TOF) equipped with a single-stage ion mirror which provides correction to ion time spread. The time necessary to cover the specific distance is recorded through a time-to-digital converter (TDC), and the mass of respectively, both the precursor and fragment ions is calculated (MS1 and MS2) (Chernushevich I.V. *et al.* 2001). As above, mass spectrometer affords useful structural information and could advantageously be coupled with chromatographic systems for the analysis of complex mixtures, offering complimentary performances to classical detectors such as Diode Array Detector (DAD).

The first coupling with MS took place with gas-chromatography in the 1950s and was commercially available in the 1970s. Liquid chromatography was later coupled with MS. It was the contribution of Fenn J.B. thanks to the development of ESI sources (Fenn J.B. *et al.* 1989), which led the base for the broad development of LC-MS. Until the middle of the 90s the instrumentation has been efficiently developed and reached better analytical performances, the cost has been lowered, allowing a broader range of applications. To achieve optimal conditions of separation HPLC can be replaced in the LC-MS system with Ultra High Performance Liquid Chromatography (UHPLC) that works at pressures up to 1,200 bars. In HPLC conditions, silicaparticles ranged in a size of 3-5  $\mu\text{m}$ , while in UHPLC that size is less than 2  $\mu\text{m}$ , resulting in narrower chromatogram peaks, significant higher resolution with shorter analysis times (Schäfer M. 2019).

Several key parameters should be considered and optimized in the LC method development, which would enable the optimal analysis with MS and MS/MS detections. Firstly, the flow rate has a direct effect on the outcome. ESI source can handle a flow of 1 mL/min, but lower flows 0.2-0.5 mL/min lead to better sensitivity (in our case the flow was set at 0.5 mL/min). However, such flow rates generally correspond to optimal flow rates for UHPLC column packed with small size fully porous particles with internal diameters ranging from 1.0 to 2.1 mm, as well as for HPLC columns packed with partially porous material (core-shell) that constitute a valuable alternative.

Another parameter is the pore diameter that impacts interactions between analyte and interactive surface of the solid phase and needs to be taken into account particularly when analyzing large molecules. However, a compromise should be made in setting this parameter since larger are the



---

pore sizes, lesser is the specific surface area (Lloyd L. *et al.* 2011). The last parameter which affects the obtained peak integration is the scanning speed. That value should be at least 10 scans per chromatographic peak (Schäfer M. 2019).

## Bibliographic References

### A

1. Acién F.G., Molina E., Reis A., Torzillo G., Zittelli G.C., Sepúlveda C., Masojídek J., Photobioreactors for the production of microalgae. In *Microalgae-based biofuels and bioproducts*, 2017, Woodhead Publishing, 1-44
2. Al-awar R. S., Ray J. E., Schultz R. M., Andis S. L., Kennedy J. H., Moore R. E., Liang J., Golakoti T., Subbaraju G. V., Corbett T. H., A Convergent Approach to Cryptophycin-52 Analogues: Synthesis and Biological Evaluation of a Novel Series of Fragment A Epoxides and Chlorohydrins, 2003, *J. Med. Chem.*, 46, 2985–3007
3. Allen E.J., Nelson E.W., On the artificial culture of marine plankton organisms., 1910, *J. Mar. Biol. Assoc. U.K.*, 8, 421–74
4. Allen M.M., Smith A.J., Nitrogen chlorosis in blue-green algae., 1969, *Archiv für Mikrobiologie*, 69, 2, 114-120
5. Allen, M. M., Cyanobacterial cell inclusions., 1984, *Annu. Rev. Microbiol.*, 38, 1, 1-25
6. Anahas A.M.P., Muralitharan G., Characterization of heterocystous cyanobacterial strains for biodiesel production based on fatty acid content analysis and hydrocarbon production., 2018, *Energy Convers. Manag.*, 157, 423-437
7. Andersen R.A., The Microalgal Cell., 2002, In *Handbook of Microalgal Culture*, John Wiley & Sons, 3-21

### B

8. Back S., Liang J., Production of cryptophycin from blue-green algae., 2005, *J. Young Investig.*, 12
9. Bai R., Schwartz R.E., Kepler J.A., Pettit G.R., Hamel E., Characterization of the Interaction of Cryptophycin 1 with Tubulin: Binding in the *Vinca Domain*, Competitive Inhibition of Dolastatin 10 Binding, and an Unusual Aggregation Reaction, 1996, *Cancer Res.*, 56, 4398-4406
10. Bajaj I.B., Lele S.S., Singhal R.S., A statistical approach to optimization of fermentative production of poly ( $\gamma$ -glutamic acid) from *Bacillus licheniformis* NCIM 2324., 2009, *Bioresour. Technol.*, 100, 2, 826-832
11. Barbosa M.J., Wijffels R.H., Biofuels from microalgae., 2013, In *Handbook of Microalgal Culture*, John Wiley & Sons, 566-577
12. Beversdorf L.J., Weirich C.A, Bartlett S.L., Miller T.R., Variable Cyanobacterial Toxin and Metabolite Profiles across Six Eutrophic Lakes of Differing Physiochemical Characteristics, 2017, *Toxins*, 9, 62, 1-21
13. Bi Y.H, Hu Z.Y., Influence of Temperature, Nutrients and Light Intensity on the Growth of *Nostoc flagelliforme*, 2004, *CJPE*, 4, 3, 245-249
14. Biondi N., Piccardi R., Margheri M.C., Rodolfi L., Smith G.D., Tredici M.R., Evaluation of *Nostoc* strain ATCC 53789 as a potential source of natural pesticides., 2004, *Appl. Environ. Microbiol.*, 70, 6, 3313-3320
15. Bláha L., Babica P., Maršálek B., Toxins produced in cyanobacterial water blooms-toxicity and risks., 2009, *Interdiscip. Toxicol.*, 2, 2, 36-41
16. Blankenship R.E., Origin and evolution of photosynthesis, In *Molecular mechanisms of photosynthesis*, 2002, John Wiley & Sons., 220-257
17. Borowitzka M.A., Biology of Microalgae., 2018, In *Microalgae in Health and Disease Prevention*, Academic Press., 23-72
18. Botos I., Wlodawer A., Cyanovirin-N: a sugar-binding antiviral protein with a new twist., 2003, *Cell. Mol. Life Sci.*, 60, 2, 277-287
19. Briand J.F., Jacquet S., Flinois C., Avois-Jacquet C., Maissonnette C., Leberre B., Humbert J.F., Variations in the microcystin production of *Planktothrix rubescens* (Cyanobacteria) assessed from a four-year survey of Lac du Bourget (France) and from laboratory experiments, 2005, *Microb. Ecol.*, 50, 418–428.

**C**

20. Campíns-Falcó P., Herráez-Hernández R., Serra-Mora P., Liquid Chromatography Instrumentation, 2019, In *Encyclopedia of Analytical Science (3rd Ed.)*, Academic Press, ,108-116
21. Campos A., Vasconcelos V., Molecular mechanisms of microcystin toxicity in animal cells., 2010, *Int. J. Mol.*, 11, 1, 268-287
22. Chaganty S., Golakoti T., Heltzel C., Moore R.E., Yoshida W.Y., Isolation and structure determination of cryptophycins 38, 326, and 327 from the terrestrial cyanobacterium *Nostoc* sp. GSV 224., 2004, *J. Nat. Prod.*, 67, 8, 1403-1406
23. Chen M., Li Y., Birch D., Willows R.D., A cyanobacterium that contains chlorophyll f—a red-absorbing photopigment., 2012, *FEBS Lett.*, 586, 3249-3254
24. Chernushevich I.V., Loboda A.V., Thomson B. A., An introduction to quadrupole–time-of-flight mass spectrometry., 2001, *J. Mass Spectrom.*, 36, 8, 849-865.
25. Chmelík D., Hrouzek P., Fedorko J., Vu D.L., Urajová P., Mareš J., Červený J., Accumulation of cyanobacterial oxadiazine nocuolin A is enhanced by temperature shift during cultivation and is promoted by bacterial co-habitants in the culture, 2019, *Algal Res.*, 44, 101673, 1-8
26. Choi C.Y., Kim N.N., Shin H.S., Park H.G., Cheon S, Kil G., The effect of various wavelengths of light from light-emitting diodes on the antioxidant system of marine cyanobacteria, *Synechococcus* sp., 2013, *Mol. Cell. Toxicol.*, 9, 295
27. Cirés S., Delgado A. González-Pleiter M., Quesada A., Temperature Influences the Production and Transport of Saxitoxin and the Expression of sxt Genes in the Cyanobacterium *Aphanizomenon gracile*., 2017, *Toxins*, 9, 322-337

**D**

28. d' Agostino G., del Campo J., Mellado B., Izquierdo M.A., Minrik T., Cirri L., Marini L., Perez-Gracia J.L., Scmbia G., A multicenter phase II study of the cryptophycin analog LY355703 in patients with platinum-resistant ovarian cancer, 2006, *Int. J. Gynecol. Cancer*, 16, 71–76
29. da Fontoura Prates D., Radmann E.M., Duarte J.H., de Moraes M.G., Costa J.A.V., Spirulina cultivated under different light emitting diodes: Enhanced cell growth and phycocyanin production., 2018, *Bioresour. Technol.*, 256, 38-43.
30. da Rocha A.B., Lopes R.M., Schwartzmann G., Natural products in anticancer therapy., 2001, *Curr. Opin. Pharmacol.*, 1, 4, 364-369
31. Dai Y.J, Li J., Wei S.M., Chen N., Xiao Y.P., Tan Z.L., Jia S.R., Yuan N.N., Tan N., Song Y.J., Effect of Light with Different Wavelengths on *Nostoc* flagelliforme Cells in Liquid Culture, 2013, *J. Microbiol. Biotechnol.*, 23, 4, 534-538
32. Das A., Christ B., Hörtensteiner S., Characterization of the pheophorbide a oxygenase/phyllobilin pathway of chlorophyll breakdown in grasses., 2018, *Planta*, 248, 4, 875-892
33. de Muys J.M., Rej R., Nguyen D., Go B., Fortin S., Lavallée J.F., Synthesis and in vitro cytotoxicity of cryptophycins and related analogs, 1996, *Bioorg. Med. Chem. Lett.*, 6, 10, 1111-1116
34. Dembitsky V.M., Rezanka T., Metabolites produced by nitrogen-fixing *Nostoc* species., 2005, *Folia microbiol.*, 50, 5, 363-391
35. Desikachary T.V., Cyanophyta., 1959, In *I.C.A.R. monographs on algae.*, New Delhi: Indian Council of Agricultural Research, 1-72
36. Dong M.W., HPLC Instrumentation in Pharmaceutical Analysis: Status, Advances, and Trends., 2005, In *Separation Science and Technology* (Vol. 6), Academic Press. ,47-75
37. Duy T.N., Lam P.K., Shaw G.R., Connell D.W., Toxicology and risk assessment of freshwater cyanobacterial (blue-green algal) toxins in water., 2000, In *Reviews of environmental contamination and toxicology*, Springer, 113-185
38. Dzhambazov B., Moten D., Basheva D., Belkinova D., Teneva I., The allelopathetic effects of toxin-producing cyanobacteria are pH-dependent, 2018, In *18th International Multidisciplinary Scientific GeoConference SGEM 2018*, SGEM, 905-912
39. Dziallas C., Grossart H.-P., Increasing Oxygen Radicals and Water Temperature Select for Toxic *Microcystis* sp., 2011, *PLoS ONE*, 6, 9, e25569

**E**

40. Edelman M.J., Gandara D.R., Hausner P., Israel V., Thornton D., DeSanto J., Doyle L.A., Phase 2 study of cryptophycin 52 (LY355703) in patients previously treated with platinum-based chemotherapy for advanced non-small cell lung cancer, 2003, *Lung Cancer*, 39, 197-199
41. Eggen M., Georg G.I., The cryptophycins: Their synthesis and anticancer activity., 2002, *Med. Res. Rev.*, 22, 85-101
42. Ehira S., Ohmori M., Sato N., Genome-wide expression analysis of the responses to nitrogen deprivation in the heterocyst-forming cyanobacterium *Anabaena* sp. strain PCC 7120, 2003, *DNA Res.*, 10, 97-113
43. Ehrenreich I. M., Waterbury J.B., Webb E.A., Distribution and diversity of natural product genes in marine and freshwater cyanobacterial cultures and genomes., 2005, *Appl. Environ. Microbiol.*, 71, 11, 7401-7413
44. Eldin M.J., Kanhaiya K., Debabrata D., Physicochemical parameters optimization, and purification of phycobiliproteins from the isolated *Nostoc* sp., 2014, *Bioresour. Technol.*, 166, 541-547

**F**

45. Falconer I.R., Health effects associated with controlled exposures to cyanobacterial toxins., 2008, In *Cyanobacterial Harmful Algal Blooms: State of the Science and Research Needs*, Springer, 607-612
46. Falkowski P.G, La Roche J., Acclimation to spectral irradiance in algae, 1991, *J. Phycol.*, 27, 8-14
47. Fay P., Oxygen relations of nitrogen fixation in cyanobacteria, 1992, *Microbiol Rev.*, 56, 340-373
48. Fenn J.B., Mann M., Meng C.K., Wong S.F., Whitehouse C.M., Electrospray ionization for mass spectrometry of large biomolecules., 1989, *Science*, 246, 4926, 64-71.
49. Ferrão-Filho A.S., Kozlowsky-Suzuki B., Cyanotoxins: bioaccumulation and effects on aquatic animals., 2011, *Mar. drugs*, 9, 12, 2729-2772
50. Ferrão-Filho A.S., Azevedo S.M., DeMott W.R., Effects of toxic and non-toxic cyanobacteria on the life history of tropical and temperate cladocerans., 2000, *Freshw. Biol.*, 45, 1, 1-19
51. Fidor A., Konkel R., Mazur-Marzec H., Bioactive peptides produced by cyanobacteria of the genus *Nostoc*: a review., 2019, *Mar. drugs*, 17, 10, 561
52. Flores E., Herrero A., Wolk C.P., Maldener I., Is the periplasm continuous in filamentous multicellular cyanobacteria?, 2006, *Trends Microbiol.*, 14, 439-443
53. Foy R.H, Gibson C.E., The influence of irradiance, photoperiod and temperature on the growth kinetics of three planktonic diatoms, 1993, *Eur. J. Phycol.*, 28, 4, 203-212

**G**

54. Gabdulkhakov A.G., Dontsova M.V., Structural studies on photosystem II of cyanobacteria., 2013, *Biochemistry*, 78, 13, 1524-1538
55. Garcia-Pichel F., Cyanobacteria, 2009, In *Encyclopedia of Microbiology (Third Edition)*, Academic Press, 2009, 107-124
56. Geider R., La Roche J., Redfield revisited: variability of C: N: P in marine microalgae and its biochemical basis., 2002, *Eur. J. Phycol.*, 37, 1, 1-17
57. Golakoti T., Ogino J., Heltzel C.E., Le Husebo T., Jensen C.M., Larsen L.K., Patterson G.M.L., Moore R.E., Mooberry S.L., Corbett T.H., Valeriote, F. A., Structure determination, conformational analysis, chemical stability studies, and antitumor evaluation of the cryptophycins. Isolation of 18 new analogs from *Nostoc* sp. strain GSV 224., 1995, *J. Am. Chem. Soc.*, 117, 49, 12030-12049
58. Golakoti T., Ohtani I., Patterson G. M., Moore R. E., Corbett T.H., Valeriote F.A., Demchik L., Total structures of cryptophycins, potent antitumor depsipeptides from the blue-green alga *Nostoc* sp. strain GSV 224., 1994, *J. Am. Chem. Soc.*, 116, 11, 4729-4737
59. Golakoti T., Yoshida W.Y., Chaganty S., Moore R.E., Isolation and structure determination of nostocyclopeptides A1 and A2 from the terrestrial cyanobacterium *Nostoc* sp. ATCC53789., 2001, *J. Nat. Prod.*, 64, 54 -59

60. Golakoti T., Yoshida W.Y., Chaganty S., Moore R.E., Isolation and structures of nostopeptolides A1, A2 and A3 from the cyanobacterium *Nostoc* sp. GSV224., 2000, *Tetrahedron*, 56, 46, 9093-9102
61. Gordaliza M., Natural products as leads to anticancer drugs., 2007, *Clin. Transl. Oncol.*, 9, 12, 767-776
62. Granata T., Dependency of Microalgal Production on Biomass and the Relationship to Yield and Bioreactor Scale-up for Biofuels: a Statistical Analysis of 60+ Years of Algal Bioreactor Data., 2017, *Bionergy Res.*, 10, 1, 267-287
63. Gressel J., Transgenic marine microalgae: a value-enhanced fishmeal and fish oil replacement., 2013, *Handbook of Microalgal Culture: Applied Phycology and Biotechnology*, Wiley-Blackwell, 653-670
64. Grobbelaar J.U., Inorganic algal nutrition., 2013, In *Handbook of Microalgal Culture: Biotechnology and Applied Phycology*, Blackwell publishing, 123-133
65. Groth G., Schott K., Ohnmacht U., Manegold C., Gatzemeier U., A phase II study of LY355703 (cryptophycine) as first-line therapy for stage IIIb or IV NSCLC subjects: preliminary analysis., 2012, *Eur J. Cancer*, 37, 6, 48
66. Grotjohann I., Fromme P., Structure of cyanobacterial photosystem I., 2005, *Photosynth Res.*, 85, 1, 51-72
67. Guckert J.B., Cooksey K.E., Triglyceride accumulation and fatty acid profile changes in *Chlorella* (Chlorophyta) during high pH-induced cell cycle inhibition, 1990, *J. Phycol.*, 26, 72-79
68. Gupta P.L., Lee S.M., Choi H.J., A mini review: photobioreactors for large scale algal cultivation., 2015, *World J. Microbiol. Biotechnol.*, 31, 9, 1409-1411

## H

69. Hansson L.A., Gustafsson S., Rengefors K., Bomark L. Cyanobacterial chemical warfare affects zooplankton community composition., 2007, *Freshw. Biol.*, 52, 7, 1290-1301
70. Harrison P.J., Berges J.A., Marine culture media., 2005, In *Algal culturing techniques*, Academic Press, 21-33
71. Hartonen K., Laitinen T., Riekkola M.L., Current instrumentation for aerosol mass spectrometry., 2011, *Trends Analyt. Chem. TrAC*, 30, 9, 1486-1496.
72. Hayes W., Rannard S., Controlled/'living' polymerization methods, 2004, In *Polymer Chemistry, a practical approach*, Oxford University Press, 99-125
73. Hemlata Fatma T., Screening of Cyanobacteria for Phycobiliproteins and Effect of Different Environmental Stress on Its Yield, 2009, *Bull. Environ. Contam. Toxicol.*, 83, 509
74. Hernández J.M., López-Rodas V., Costas E., Microcystins from tap water could be a risk factor for liver and colorectal cancer: A risk intensified by global change., 2009, *Med. Hypotheses*, 72, 539-540
75. Herrero A., Flores E., Imperial Ródenas J., In *Nitrogen assimilation in bacteria.*, 2019, SCIC
76. Hirsch C.F., Liesch J.M., Salvatore M.J., Schwartz R.E., Sesin D.F., U.S. Patent No. 4,946,835., 1990, Washington, DC: U.S. Patent and Trademark Office.
77. Hitzfeld B.C., Höger S.J., Dietrich D.R., Cyanobacterial toxins: removal during drinking water treatment, and human risk assessment., 2000, *Environ. Health Perspect.*, 108, 1, 113-122
78. Hoiczuk E., Hansel A., Cyanobacterial cell walls: news from an unusual prokaryotic envelope., 2000, *J. Bacteriol.*, 182, 5, 1191-1199.
79. Hongsthong A., Bunnag B., Overview of Spirulina: biotechnological, biochemical and molecular biological aspects., 2009, In *Handbook on Cyanobacteria: Biochemistry, Biotechnology and Applications*, Nova Science Publishers, 51-103
80. Hori K., Ishibashi G., Okita T., Hypocholesterolemic effect of blue-green alga, *ishikurage* (*Nostoc commune*) in rats fed atherogenic diet., 1994, *Plant Foods Hum Nutr.*, 45, 1, 63-70
81. Huang Z., Liu Y., Paulsen B. S., & Klaveness D., Studies on polysaccharides from three edible species of *Nostoc* (Cyanobacteria) with different colony morphologies: comparison of monosaccharide compositions and viscosities of polysaccharides from field colonies and suspension cultures., 1998, *J. Phycol.*, 34, 6, 962-968

**I**

82. Ingall E., Jahnke R., Influence of watercolumn anoxia on the elemental fractionation of carbon and phosphorus during sediment diagenesis. 1997, *Mar. Geol.*, 139, 219–229

**J**

83. Jacob-Lopes E., Scoparo C.H.G, Lacerda L.M.C.F, Franco T.T, Effect of light cycles (night/day) on CO<sub>2</sub> fixation and biomass production by microalgae in photobioreactors, 2009, *Chem. Eng. process*, 48, 1, 306-310
84. Jaki B., Orjala J., Sticher O., A novel extracellular diterpenoid with antibacterial activity from the cyanobacterium *Nostoc commune.*, 1999, *J. Nat. Prod.*, 62, 3, 502-503
85. Johnson S.R., Lange B.M., Open-access metabolomics databases for natural product research: present capabilities and future potential., 2015, *Front. Bioeng. Biotechnol.*, 3, 22.
86. Johnson W., Nier A., Atomic Masses in the Region Xenon to Europium., 1957, *Phys. Rev.*, 105, 3, 1014-1023
87. Jokela J., Herfindal L., Wahlsten M., Permi P., Selheim F., Vasconcelos V., Døskeland S.O., Sivonen K., A novel cyanobacterial nostocyclopeptide is a potent antitoxin against microcystins., 2010, *ChemBioChem*, 11, 1594-1599
88. Jordan M.A., Mechanism of action of antitumor drugs that interact with microtubules and tubulin., 2002, *Curr. Med. Chem. Anticancer Agents*, 2, 1, 1-17
89. Jungkon K., Jung-Kwan S., Hyojung Y., Pil-Je K., Kyunghee C., Combined effects of the cyanobacterial toxin microcystin\_LR and environmental factors on life-history traits of indigenous cladoceran *Moina Macrocopa*, 2014, *Environ. Toxicol. Chem.*, 33, 11, 2560–2565

**K**

90. Kaebernick M., Neilan B.A., Börner T., Dittmann E., Light and the transcriptional response of the microcystin biosynthesis gene cluster., 2000, *Appl. Environ. Microbiol.*, 66, 8, 3387–3392
91. Kakimoto M., Ishikawa T., Miyagi A., Saito K., Miyazaki M., Asaeda T., Yamaguchi M., Uchimiya H., Kawai-Yamada M., Culture temperature affects gene expression and metabolic pathways in the 2-methylisoborneol-producing cyanobacterium *Pseudanabaena galeata*. 2014, *J. Plant Physiol.*, 171, 292-300
92. Kaklamanos G., Aprea E., Theodoridis G., Mass spectrometry: principles and instrumentation, 2020, In *Chemical Analysis of Food*, Academic Press, 525-552
93. Kana T.M., Glibert P.M., Effect of irradiances up to 2000  $\mu\text{E m}^{-2} \text{s}^{-1}$  on marine *Synechococcus* WH7803—I. Growth, pigmentation, and cell composition., 1987, *Deep Sea Res. Part I Oceanogr. Res. Pap.*, 34, 4, 479-495
94. Kanekiyo K., Lee J.B., Hayashi K., Takenaka H., Hayakawa Y., Endo S., Hayashi T., Isolation of an antiviral polysaccharide, nostoflan, from a terrestrial cyanobacterium, *Nostoc flagelliforme.*, 2005, *J. Nat. Prod.*, 68, 7, 1037-1041
95. Kaplan-Levy R.N., Hadas O., Summers M.L., Rücker J., Sukenik A., Akinetes: dormant cells of cyanobacteria., 2010, In *Dormancy and resistance in harsh environments*, Springer, 5-27
96. Kawachi M., Noël M.-H., Steriliation and sterile technique, 2005, In *Algal Culturing Techniques*, Academic Press, 65-81
97. Kehr J.C., Picchi D.G., Dittmann E., Natural product biosyntheses in cyanobacteria: a treasure trove of unique enzymes., 2011, *Beilstein J. Org. Chem.*, 7, 1, 1622-1635
98. Kerksiek K., Mejillano M.R., Schwartz R.E., Georg G.I., Himes R.H., Interaction of cryptophycin 1 with tubulin and microtubules, 1995, *FEBS Lett.*, 377, 59-61
99. Khajepour F., Hosseini S.A., Nasrabadi R.G., Effect of Light Intensity and Photoperiod on Growth and Biochemical Composition of a Local Isolate of *Nostoc calcicole.*, 2015, *Appl. Biochem. Biotechnol.*, 176, 8, 2279-2289

100. Kim N.N., Shin H.S., Park H.G., Lee J., Kil G., Choi C.Y., Profiles of Photosynthetic Pigment Accumulation and Expression of Photosynthesis-related Genes in the Marine Cyanobacteria *Synechococcus* sp.: Effects of LED Wavelengths, 2014, *Biotechnol. Bioproc. Eng.*, 19, 2, 250-256
  101. King J.M., Spotte S.H., *Marine Aquariums in the Research Laboratory.*, 1974, Eastlake, Ohio: Aquarium Systems, 1-34
  102. Klausmeier C.A., Litchman E., Daufresne T., Levin S.A., Optimal nitrogen-to-phosphorus stoichiometry of phytoplankton., 2004, *Nature*, 429, 6988, 171-174
  103. Knaul F.M., Arreola-Ornelas H., Méndez O., Alsan M., Seinfeld J., Marx A., Atun R., The global economic burden of cancer, 2014, In *World cancer report 2014*, International Agency for Research on Cancer, 676-583
  104. Kobayashi M., Kurosu M., Ohyabu N., Wang W., Fujii S., Kitagawa I., The absolute stereostructure of arenastatin A, a potent cytotoxic depsipeptide from the Okinawan marine sponge *Dysidea Arenaria*, 1994, *Chem. Pharm. Bull.*, 42, 10, 2196-2198
  105. Kobayashi M., Kurosu M., Wang W., Kitagawa I., A total synthesis of Arenastatin A, an extremely potent cytotoxic depsipeptide, from the Okinawan marine sponge *Dysidea Arenaria.*, 1994, *Chem. Pharm. Bull.*, 42, 11, 2394-6
  106. Krumbein W.E., Cyanobakterien-Bakterien oder Algen. In *Oldenburger Symposium über Cynobakterien.*, 1979, Oldenburg, Universität Oldenburg: 107-112
  107. Kuan D., Duff S., Posarac D., Bi X., Growth optimization of *Synechococcus elongatus* PCC7942 in lab flasks and a 2-D photobioreactor., 2015, *Can. J. Chem. Eng.*, 93, 4, 640-647
  108. Kumar K., Banerjee D., Das D., Carbon dioxide sequestration from industrial flue gas by *Chlorella sorokiniana.*, 2014, *Bioresour. Technol.*, 152, 225-233
  109. Kumar K., Das D., Growth characteristics of *Chlorella sorokiniana* in airlift and bubble column photobioreactors., 2012, *Bioresour. Technol.*, 116, 307-313
  110. Kumar K., Mella-Herrera R.A., Golden J.W., Cyanobacterial heterocysts., 2010, *Cold Spring Harb. Perspect. Biol.*, 2, 4
  111. Kurmayer R., The toxic cyanobacterium *Nostoc* sp. strain 152 produces highest amounts of microcystin and nostophycin under stress conditions, 2011, *J. Phycol.*, 47, 1, 200-207
- L**
112. LaCourse M.E., LaCourse W.R., General instrumentation in HPLC., 2017, In *Liquid Chromatography*, Elsevier, 417-429
  113. LaCourse W.R., Column liquid chromatography: Equipment and instrumentation, 2002, *Anal. Chem.*, 74, 12, 2813-2831
  114. Lambein F., Wolk C.P., Structural studies on the glycolipids from the envelope of the heterocyst of *Anabaena cylindrica.*, 1973, *Biochemistry*, 12, 5, 791-798
  115. Lazaroff N., Vishniac W., The Effect of Light on the Developmental Cycle of *Nostoc muscorum*, a Filamentous Blue-Green Alga., 1961, *J. gen. Microbiol.*, 25, 365-374
  116. Levring T., Some culture experiments with *Ulva lactuca.*, 1946, *Kgl. Fysiogr., Sällsk. Hdl.*, 16, 7, 45-56
  117. Lewis S.W., Lenehan C.E., Liquid and Thin-Layer Chromatography., 2013, In *Encyclopedia of Forensic Sciences*, Academic Press, 586-589
  118. Liang J., Biosynthesis of the anticancer drug cryptophycin, 2006, *Research, Education, and Economics Information System (REEIS)*, HAW00504-1020S
  119. Lloyd L., Ball S., Mapp K., The Influence of Silica Pore Size on Efficiency, Resolution and Loading in Reversed-Phase HPLC, 2011, In *5990-8298EN*, Agilent Technologies, Inc.
  120. Lönneporge, A., Lind L.K., Kalla S.R., Gustafsson P., Öquist G., Acclimation process in the light-harvesting system of cyanobacterium *Anacystis nidulans* following a light shift from white to red light., 1985, *Plant Physiol.*, 78, 110-114
  121. Ludwig F., Medger A., Börnick H., Opitz M., Lang K., Göttfert M., Röske I., Identification and expression analysis of putative sesquiterpene synthase genes in *Phormidium* sp. and prevalence of *geoA*-like genes in a drinking water reservoir., 2007, *Appl. Environ. Microbiol.*, 73, 6988-6993

122. Luesch H., Harrigan G.G., Goetz G., Horgen F.D., The cyanobacterial origin of potent anticancer agents originally isolated from sea hares., 2002, *Curr. Med. Chem.*, 9, 20, 1791-1806
123. Luimstra V.M., Schuurmans J.M., Verschoor A.M., Hellingwerf K.J., Huisman J., Matthijs H.C.P., Blue light reduces photosynthetic efficiency of cyanobacteria through an imbalance between photosystems I and II., 2018, *Photosynth. Res.*, 138, 177-189

## M

124. Ma R., Lu F., Bi Y., Effects of light intensity and quality on phycobiliprotein accumulation in the cyanobacterium *Nostoc sphaeroides* Kützing, 2015, *Biotechnol. Lett.*, 37, 8, 1663-1669
125. MacIntyre H.L., Kana T.M., Anning T., Geider R.J., Photoacclimation of photosynthesis irradiance response curves and photosynthetic pigments in microalgae and cyanobacteria, 2002, *J. Phycol.*, 38, 17-38
126. MacKintosh C., Beattie K.A., Klumpp S., Cohen P., Codd G.A., Cyanobacterial microcystin-LR is a potent and specific inhibitor of protein phosphatases 1 and 2A from both mammals and higher plants., 1990, *FEBS Lett.*, 264, 2, 187-192
127. Magarvey N. A., Beck Z.Q., Golakoti T., Ding Y., Huber U., Hemscheidt T.K., Abelson D., Moore R.E., Sherman D. H., Biosynthetic characterization and chemoenzymatic assembly of the cryptophycins. Potent anticancer agents from *Nostoc* cyanobionts., 2006, *ACS chem. biol.*, 1, 12, 766-779
128. Malviya R., Bansal V., Pal O.P., Sharma P.K., High performance liquid chromatography: a short review., 2010, *J. Glob. Pharma Technol.*, 2, 5, 22-26
129. Mankiewicz J., Tarczyska M., Walter Z., Zalewski M., Natural toxins from cyanobacteria, 2003, *Acta Biol Cracov Bot*, 45, 9-20
130. Masukawa H., Sakurai H., Hausinger R.P., Increased heterocyst frequency by *patN* disruption in *Anabaena* leads to enhanced photobiological hydrogen production at high light intensity and high cell density, 2017, *Appl. Microbiol. Biotechnol.*, 101, 5, 2177-2188
131. Matlock B.C., "Differences in bacterial optical density measurements between UV-Visible spectrophotometers", Thermo-Scientific, Technical note No.52236
132. Méjean A., Ploux O., A genomic view of secondary metabolite production in cyanobacteria., 2013, In *Advances in botanical research*, Academic Press., 65, 189-234
133. Melis A., Spectroscopic methods in photosynthesis: photosystem stoichiometry and chlorophyll antenna size., 1989, In *Philosophical Transactions of the Royal Society of London. B, Biological Sciences*, 323, 1216, 397-409
134. Miller S.R., Castenholz R.W., Evolution of Thermotolerance in Hot Spring Cyanobacteria of the Genus *Synechococcus*, 2000, *Appl. Environ. Microbiol.*, 66, 10, 4222-4229
135. Mitra A., Sept D., Localization of the Antimitotic Peptide and Depsipeptide Binding Site on  $\beta$ -Tubulin, 2004, *Biochemistry*, 43, 13955-13962
136. Mollenhauer D., Bengtsson R., Lindstrøm E.A., Macroscopic cyanobacteria of the genus *Nostoc*: a neglected and endangered constituent of European inland aquatic biodiversity., 1999, *Eur. J. Phycol.*, 34, 4, 349-360
137. Moore R.E., Barrow R.A., Corbett T.H., Valeriote F.A., Hemscheidt T.K., 1996, International Patent WO 96/40184
138. Mullineaux C.W., Mariscal V., Nenninger A., Khanum H., Herrero A., Flores E., Adams D.G., Mechanism of intercellular molecular exchange in heterocyst-forming cyanobacteria., 2008, *EMBO J.*, 27, 1299-1308
139. Murakami N., Wang W., Ohyabu N., Ito T., Tamura S., Aoki S., Kobayashi M., Kitagawa I., Synthesis of Amide Analogs of Arenastatin A, 2000, *Tetrahedron*, 56, 46, 9121-9128
140. Myers O.D., Sumner S.J., Li S., Barnes S., Du X., One Step Forward for Reducing False Positive and False Negative Compound Identifications from Mass Spectrometry Metabolomics Data: New Algorithms for Constructing Extracted Ion Chromatograms and Detecting Chromatographic Peaks., 2017, *Anal. Chem.*, 89, 17, 8696-8703



**N**

141. Nahrwold M., b 2-Aminosäuren als Bausteine, funktionalisierter Cryptophycin-Analoga, 2009, Dissertation, universität Bielefeld
142. Nicklisch A., Growth and light absorption of some planktonic cyanobacteria, diatoms and Chlorophyceae under simulated natural light fluctuations, 1998, *J. Plankton Res.*, 20, 1, 105–119
143. Nicolaisen K, Hahn A, Schleiff E., The cell wall in heterocyst formation by *Anabaena* sp. PCC 7120, 2009, *J. Basic Microbiol.*, 49, 5–24
144. Niedermeyer T.H., Strohalm M., mMass as a software tool for the annotation of cyclic peptide tandem mass spectra., 2012, *PLoS one*, 7, 9, e44913.
145. Nogales E., Wang H.W., Niederstrasser H., Tubulin rings: which way do they curve?, 2003, *Curr. Opin. Struct. Biol.*, 13, 256–261
146. Norman B.H., Hemscheidt T., Richard M., Schultz R.M., Sherri L. Andis S.L., Total Synthesis of Cryptophycin Analogues. Isosteric Replacement of the C–D Ester, 1998, *J. Org. Chem.*, 1998, 63, 15, 5288-5294
147. Nothias L.F., Petras D., Schmid R., Dührkop K., Rainer J., Sarvepalli A., ... & Aicheler F., Feature-based molecular networking in the GNPS analysis environment., 2020, *Nat. Methods*, 17, 9, 905-908
148. Nowruzzi B., Khavari-Nejad R., Sivonen K., Kazemi B., Najafi F., Nejadstattari T. Identification and toxigenic potential of *Nostoc* sp., 2012, *Algae.*, 27:303–313
149. Nozzi N.E., Oliver J.W., Atsumi S., Cyanobacteria as a platform for biofuel production., 2013, *Front. Bioeng. Biotechnol.*, 1, 7, 1-6

**O**

150. Oh H.S., Lee C.S., Srivastava A., Oh H.M., Ahn C.Y., Effects of Environmental Factors on Cyanobacterial Production of Odorous Compounds: Geosmin and 2-Methylisoborneol., 2017, *J. Microbiol. Biotechnol.*, 7, 1316-1323
151. Ohtani I., Moore R.E., Runnegar M.T., Cylindrospermopsin: a potent hepatotoxin from the blue-green alga *Cylindrospermopsis raciborskii*., 1992, *J. Am. Chem. Soc.*, 114, 20, 7941-7942
152. Olivon F., Allard P.M., Koval A., Righi D., Genta-Jouve G., Neyts J.,...& Katanaev V.L., Touboul D., Wolfender J.-L., Litaudon M., Bioactive natural products prioritization using massive multi-informational molecular networks., 2017, *ACS Chem. Biol.*, 12, 10, 2644-2651.
153. Orr P.T., Jones G.J., Relationship between microcystin production and cell division rates in nitrogen limited *Microcystis aeruginosa* cultures., 1998, *Limnol. Oceanogr.*, 43, 1604–1614

**P**

154. Paerl H.W., Paul V.J., Climate change: links to global expansion of harmful cyanobacteria., 2012, *Water Res.*, 46, 5, 1349-1363.
155. Palamareva M.D., Liquid chromatography Overview, 2005, In *Encyclopedia of Analytical Science*, Elsevier, 106-112
156. Paliwal C., Mitra M., Bhayani K., Bharadwaj V.S.V., Ghosh T., Dubey S., Mishra S., Abiotic stresses as tools for metabolites in microalgae, 2017, *Bioresour. Technol.*, 244, 1216-1226
157. Paliwal C., Pancha I., Ghosh T., Maurya R., Chokshi K., Bharadwaj S.V.V., Ram S., Mishra S., Selective carotenoid accumulation by varying nutrient media and salinity in *Synechocystis* sp. CCNM 2501., 2015, *Bioresour. Technol.*, 197, 363-368
158. Panda D., Ananthnarayan V., Larson G., Shih C., Jordan M.A., Wilson L., Interaction of the antitumor compound cryptophycin-52 with tubulin., 2000, *Biochemistry*, 39, 46, 14121-14127
159. Panda D., Himes R.H., Moore R.E., Wilson L., Jordan M.A., Mechanism of Action of the Unusually Potent Microtubule Inhibitor Cryptophycin, 1997, *Biochemistry*, 36, 12948-12953
160. Pansare S.K., Patel S.M., Lyophilization Process Design and Development: A Single-Step Drying Approach, 2019, *J. Rep. Pharm. Sci.*, 108, 1423-1433
161. Park H.D., Yokoyama A., Okino T., Fate of microcystin in Lake Suwa., 2001, *Japanese J. Limnology*, 62, 3, 229-248.

162. Patel V.F., Andis S.L., Kennedy J.H., Ray J.E., Schultz R.E., Novel Cryptophycin Antitumor Agents: Synthesis and Cytotoxicity of Fragment "B" Analogues, 1999, *J. Med. Chem.*, 42, 14, 2588-2603
163. Patterson P., Antiviral activity of blue-green algae cultures., 1993, *J. phycol.*, 29, 125-30.
164. Percival S.L., Williams D.W., Cyanobacteria, 2014 In *Microbiology of Waterborne Diseases*, Academic Press., 79-88
165. Pereira S., Micheletti E., Zille A., Santos A., Moradas-Ferreira P., Tamagnini P., De Philippis R., Using extracellular polymeric substances (EPS)-producing cyanobacteria for the bioremediation of heavy metals: do cations compete for the EPS functional groups and also accumulate inside the cell?, 2011, *Microbiology*, 157, 2, 451-458
166. Pitt J.J., Principles and Applications of Liquid Chromatography-Mass Spectrometry in Clinical Biochemistry, 2009, *Clin Biochem Rev*, 30, 19-34
167. Pluskal T., Castillo S., Villar-Briones A., Orešič M., MZmine 2: Modular framework for processing, visualizing, and analyzing mass spectrometry-based molecular profile data., 2010, *BMC Bioinform.*, 11, 395
168. Post A.F., Loogman J.G., Mur L.R., Photosynthesis, carbon flows and growth of *Oscillatoria agardhii* Gomont in environments with a periodic supply of light., 1986, *J. Gen. Microbiol.*, 132, 2129–2136

## Q

169. Qian F., Dixon D.R., Newcombe G., Ho L., Dreyfus J., Scales P.J., The effect of pH on the release of metabolites by cyanobacteria in conventional water treatment processes, 2014, *Harmful Algae*, 39, 253–258
170. Qiu B., Liu J., Liu Z., Liu S., Distribution and ecology of the edible cyanobacterium Ge-Xian-Mi (*Nostoc*) in rice fields of Hefeng County in China., 2002, *J. Appl. Phycol.*, 14, 5, 423-429.

## R

171. Rahimpour M.R., Biniiaz P., Makarem M.A., Integration of microalgae into an existing biofuel industry., 2017, In *Bioenergy Systems for the Future*, Woodhead Publishing, 481-519
172. Rapala J., Sivonen K., Lyra C., Niemelä S.I., Variation of microcystins, cyanobacterial hepatotoxins, in *Anabaena* spp. as a function of growth stimuli., 1997, *Appl. Environ. Microbiol.*, 63, 6, 2206–2212
173. Ray S., Bagchi S.N., Nutrients and pH regulate algicide accumulation in cultures of the cyanobacterium *Oscillatoria laetevirens*, 2001, *New Phytol.*, 149, 455–460
174. Regenstein J.M., Regenstein C.E., Column Chromatography, 1984, In *Food protein Chemistry*, Academic Press, 144-167
175. Rippka R., Deruelles J., Waterbury J.B., Herdman M., Stanier R.Y., Generic assignments, strain histories and properties of pure cultures of cyanobacteria., 1979, *Microbiology*, 111, 1, 1-61
176. Robert A.B., Calvyn S., Fitje L., Remmy E.M., Jimmy P., Stefan K., Alexander B., Ekaterina E., Gabrielle K., Terrein and Butyrolacton VII, Ant. biotically Active Compounds from Symbiotic Fungus *Aspergillus Terreus* Isolated from Ascidian *Didemnum*, 2018, *Molle. Biomed. J. Sci&Tech. Res.*, 9, 4, 7288-7292

## S

177. Saide A., Lauritano C., Ianora A., Pheophorbide a: State of the Art., 2020, *Marine Drugs*, 18, 5, 257
178. Sang M., Wang M., Liu J., Zhang C., Li A., Effects of Temperature, Salinity, Light Intensity, and pH on the Eicosapentaenoic Acid Production of *Pinguicoccus pyrenoidosus*, 2012, *J. Ocean Univ. China*, 11, 2, 181-186
179. Sarker S.D., Nahar L., Applications of high performance liquid chromatography in the analysis of herbal products., 2015, In *Evidence-Based Validation of Herbal Medicine*, Elsevier, 405-425
180. Sato N., Murata N., Studies on the temperature shift-induced desaturation of fatty acids in monogalactosyl diacylglycerol in the blue-green alga (cyanobacterium), *Anabaena variabilis*., 1981, *Plant Cell Physiol.*, 22, 6, 1043-1050
181. Schäfer M., Mass Spectrometry| Fundamentals and Instrumentation., 2019, In *Encyclopedia of Analytical Science (3<sup>rd</sup> edition)*, Elsevier, 358-365

- 182.Schatz D., Keren Y., Vardi A., Sukenik A., Carmeli S., Börner T., Dittman E., Kaplan A., Towards clarification of the biological role of microcystins, a family of cyanobacterial toxins., 2007, *Environ. Microbiol.*, 9, 4, 965-970
- 183.Schreiber E., Die Reinkultur von marinen Phytoplankton und deren Bedeutung für die Erforschung der Produktionsfähigkeit des Meerwassers., 1927, *Wiss. Meeresuntersuch.*, 16, 1–34
- 184.Schüßler A., The Geosiphon–Nostoc endosymbiosis and its role as a model for arbuscular mycorrhiza research., 2012, In *Fungal associations*, Springer, 77-91
- 185.Schwartz R.E., Hirsch C.F., Sesin D.F., Flor J.E., Chartrain M., Fromtling R. E., Harris G.H., Salvatore M.J., Liesch J.M., Yudin, K., Pharmaceuticals from cultured algae., 1990 *J. Ind. Microbiol.*, 5, 113-123
- 186.Sessa C., Weigang-Köhler K., Pagani O., Greim G., Mora O., De Pas T., Burgess M., Weimer I., Johnson R., Phase I and pharmacological studies of the cryptophycin analogue LY355703 administered on a single intermittent or weekly schedule, 2002, *Eur. J. Cancer.*, 38,18, 2388-2396.
- 187.Sharma L., Mallick N., Accumulation of poly- $\beta$ -hydroxybutyrate in *Nostoc muscorum*: regulation by pH, light–dark cycles, N and P status and carbon sources., 2005, *Bioresour. Technol.*, 96, 11, 1304-1310
- 188.Shatwell T., Nicklisch A., Köhler J., Temperature and photoperiod effects on phytoplankton growing under simulated mixed layer light fluctuations, 2012, *Limnol. Oceanogr.*, 57, 2, 541-553
- 189.Sheehan J., Dunahay T., Benemann J., Roessler P., A look back at the US Department of Energy's aquatic species program: biodiesel from algae., 1998, *National Renewable Energy Laboratory*, 328, 1-294
- 190.Shevela D., Pishchalnikov R.Y., Eichacker L.A, Govindjee, Oxygenic Photosynthesis in Cyanobacteria, 2013, In *Stress Biology of Cyanobacteria*, Boca Raton: CRC Press, 3-40
- 191.Siegel R.L., Miller K.D., Jemal A., Cancer statistics, 2019., 2019, *CA Cancer J. Clin.*, 69, 7-34
- 192.Simmons T.L., Andrianasolo E., McPhail K., Flatt P., Gerwick W.H., Marine natural products as anticancer drugs., 2005, *Mol. Cancer Ther.*, 4, 2, 333-342
- 193.Singh J.S., Kumar A., Rai A.N., Singh D.P., Cyanobacteria: a precious bio-resource in agriculture, ecosystem, and environmental sustainability., 2016, *Front. Microbiol.*, 7, 529
- 194.Singh R.K., Tiwari S.P., Rai A.K., Mohapatra T.M., Cyanobacteria: an emerging source for drug discovery., 2011, *J. Antibiot.*, 64, 6, 401-412
- 195.Singh S.M., Elster J., Cyanobacteria in Antarctic lake environments., 2007, In *Algae and cyanobacteria in extreme environments*, Springer, 303-320
- 196.Sivonen K., Effects of light, temperature, nitrate, orthophosphate, and bacteria on growth of and hepatotoxin production by *Oscillatoria agardhii* strains., 1990, *Appl. Environ. Microbiol.*, 56, 9, 2658–2666
- 197.Smith C.D., Zhang X., Mechanism of Action of Cryptophycin: Interaction with the Vinca alkaloid domain of tubulin, 1996, *J. Biol. Chem.*, 271, 6192-6198
- 198.Smith C.D., Zhang X., Mooberry S.L., Patterson G.M.L, Moore R.E., Cryptophycin: A New Antimicrotubule Agent Active against Drug-resistant Cells, 1994, *Cancer Research* 54, 3779-3784
- 199.Solter P.F., Beasley V.R., Phycotoxins., 2013, In *Haschek and Rousseaux's Handbook of Toxicologic Pathology*, Academic Press., 1155-1186
- 200.Somogyi Á., Mass spectrometry instrumentation and techniques., 2008, In *Medical applications of mass spectrometry*, Elsevier, 93-140
- 201.Song L., Sano T., Li R., Watanabe M.M., Liu Y., Kaya K., Microcystin production of *Microcystis viridis* (cyanobacteria) under different culture conditions., 1998, *Phycological Res.*, 46, 19-23
- 202.Sparkman O.D., Penton Z.E., Kitson F.G., In *Mass Spectrometry Instrumentation.*, 2011, Academic Press, 89-148
- 203.Stanier R.Y., Cohen-Bazire G., Phototrophic prokaryotes: the cyanobacteria., 1977, *Annu. Rev. Microbiol.*, 31, 1, 225-274
- 204.Stevenson J.P., Sun W., Gallagher M., Johnson R., Vaughn D., Schuchter L., Algazy K., Hahn S., Enas N., Ellis D., Thornton D., O'Dwyer P.J., Phase I Trial of the Cryptophycin Analogue LY355703 Administered as an Intravenous Infusion on a Day 1 and 8 Schedule Every 21 Days, 2002, *Nat. Prod. Res.*, 8, 2524–2529
- 205.Straka L., Rittmann B.E., Effect of culture density on biomass production and light utilization efficiency of *Synechocystis* sp. PCC 6803., 2018, *Biotechnol. Bioengin.*, 115, 2, 507-511

206. Subbaraju G.V., Golakoti T., Patterson G.M., Moore R.E., Three new cryptophycins from *Nostoc* sp. GSV 224., 1997, *J. Nat. Prod.*, 60, 3, 302-305
207. Sukenik A., Bennett J., Falkowski P., Light-saturated photosynthesis — Limitation by electron transport or carbon fixation?, 1987, *Biochim. Biophys. Acta Biomembr.*, 891, 3, 205-215
208. Sutherland J.M., Herdman M., Stewart W.D., Akinetes of the cyanobacterium *Nostoc* PCC 7524: macromolecular composition, structure and control of differentiation., 1979, *Microbiology*, 115, 2, 273-287

## T

209. Takenaka H., Yamaguchi Y., Hibino T., Effects of the edible blue-green alga *Nostoc flagelliforme* (Facai) on 1,2-dimethylhydrazine-induced colon tumorigenesis in Sprague-Dawley male rats, 2015, *Algal Resources*, 8, 143-146
210. Tang E., Vincent W., Effects of daylength and temperature on the growth and photosynthesis of an Arctic cyanobacterium, *Schizothrix calcicola* (Oscillatoriaceae), 2000, *Eur. J. Phycol.*, 35, 3, 263-272
211. Thiel T., Pratte B., Effect on heterocyst differentiation of nitrogen fixation in vegetative cells of the cyanobacterium *Anabaena variabilis* ATCC 29413., 2001, *J. Bacteriol.*, 183, 280–286
212. Tippelt A., Busche T., Rückert C., Nett M., Complete Genome Sequence of the Cryptophycin-Producing Cyanobacterium *Nostoc* sp. Strain ATCC 53789., 2020, *Microbiol. Resour. Announc.*, 9, 14
213. Tiwari O.N., Khangembam R., Shamjetshabam M., Sharma A. S., Oinam G., Brand J.J., Characterization and Optimization of Biofloculant Exopolysaccharide Production by Cyanobacteria *Nostoc* sp. BTA97 and *Anabaena* sp. BTA990 in Culture Conditions, 2015, *Appl. Biochem. Biotechnol.*, 176, 7, 1950-1963
214. Toepel J., Welsh E., Summerfield T.C., Pakrasi H.B., Sherman L.A., Differential transcriptional analysis of the cyanobacterium *Cyanothece* sp. strain ATCC 51142 during light-dark and continuous-light growth, 2008, *J. Bacteriol.*, 190, 3904–3913.
215. Tonk L., Visser P.M., Christiansen G., Dittmann E., Snelder E.O.F.M., Wiedner C., The microcystin composition of the cyanobacterium *Planktothrix agardhii* changes toward a more toxic variant with increasing light intensity., 2005, *Appl. Environ. Microbiol.*, 71, 5177–5181.
216. Tsai K.P, Effects of two copper compounds on *Microcystis aeruginosa* cell density, membrane integrity, and microcystin release, 2015, *Ecotox. Environ. Safe.*, 120, 428-435

## V

217. van Alphen P., Abedini Najafabadi H., Branco dos Santos F., Hellingwerf K.J., Increasing the photoautotrophic growth rate of *Synechocystis* sp. PCC 6803 by identifying the limitations of its cultivation., 2018, *Biotechnol. J.*, 13, 8, 1700764
218. van Apeldoorn M.E., Van Egmond H.P., Speijers G.J., Bakker G.J., Toxins of cyanobacteria, 2007, *Mol. Nutr. Food. Res.*, 51, 1, 7-60
219. van der Westhuizen A.J., Eloff J.N, Effect of temperature and light on the toxicity and growth of the blue-green alga *Microcystis aeruginosa* (UV-006), 1985, *Planta*, 163, 1, 55-59
220. Vargas M.A., Rodriguez H., Moreno J., Olivares H., Campo J.D., Rivas J., Guerrero M.G., Biochemical composition and fatty acid content of filamentous nitrogen-fixing cyanobacteria., 1998, *J. Phycol.*, 34, 5, 812-817
221. Varie D.L., Shih C., Hay D.A., Andis S.L., Corbett T.H., Gossett L.S., Janisse S.K., Martinelli M.J., Moher E.D., Schultz R.M., Toth J.E., Synthesis and biological evaluation of cryptophycin analogs with substitution at C-6 (fragment C region), 1999, *Bioorg. Med. Chem. Lett.*, 9, 3, 369-374
222. Vermaas W.F., Photosynthesis and respiration in cyanobacteria., 2001, In *eLS*
223. Vijayakumar S., Menakha M., Pharmaceutical applications of cyanobacteria—A review., 2015, *J. Acute Med.*, 5, 1, 15-23

**W**

224. Waksmundzka-Hajnos M., Hawrył M.A., Cieśla Ł., Analysis of plant material, 2015, In *Instrumental Thin-Layer Chromatography*, Elsevier, 505-553
225. Walton K., Berry J.P., Indole alkaloids of the Stigonematales (Cyanophyta): Chemical diversity, biosynthesis and biological activity., 2016, *Mar. Drugs*, 14, 4, 73.
226. Wang M., Carver J.J., Phelan V.V., Sanchez L.M., Garg N., Peng Y., ... & Porto C., Sharing and community curation of mass spectrometry data with Global Natural Products Social Molecular Networking., 2016, *Nat. biotechnol.*, 34, 8, 828-837.
227. Watanabe M.F., A highly toxic strain of the blue-green alga *Microcystis aeruginosa* isolated from Lake Suwa., 1983, *Nippon Suisan Gakkaishi*, 49, 1759-1765
228. Watanabe M.F., Oishi S., Effects of environmental factors on toxicity of a cyanobacterium (*Microcystis aeruginosa*) under culture conditions., 1985, *Appl. Environ. Microbiol.*, 49, 5, 1342-1344
229. Waterbury J.B., Watson S.W., Guillard R.R., Brand L.E., Widespread occurrence of a unicellular, marine, planktonic, cyanobacterium., 1979, *Nature*, 277, 5694, 293-294
230. Watts N.R., Cheng N., West W., Steven A.C., Dan L., Sackett D.L., The Cryptophycin-Tubulin Ring Structure Indicates Two Points of Curvature in the Tubulin Dimer, 2002, *Biochemistry*, 41, 12662-12669
231. Weiss C., Sammet B., Sewald N., Recent approaches for the synthesis of modified cryptophycins., 2013, *Nat. Prod. Rep.*, 30, 7, 924-940
232. White Paper; "OD600 Measurements Using Different Photometers. Why does the absorbance value of turbidity measurements vary using different photometers?", Eppendorf AG, 2015
233. Wijffels R.H., Barbosa M.J., Eppink M.H., Microalgae for the production of bulk chemicals and biofuels., 2010, *Biofuel Bioprod. Biorefin.*, 4, 3, 287-295
234. Wilhelm C., Jakob T., From photons to biomass and biofuels: evaluation of different strategies for the improvement of algal biotechnology based on comparative energy balances., 2011, *Appl. Microbiol. Biotechnol.*, 92, 5, 909-919
235. Woese C.R., Kandler O., Wheelis M.L., Towards a natural system of organisms: proposal for the domains Archaea, Bacteria, and Eucarya, 1990, *Proc. Natl. Acad. Sci. U.S.A.*, 87, 12, 4576-4579

**Y**

236. Yang J.Y., Sanchez L.M., Rath C.M., Liu X., Boudreau P.D., Bruns N., Glukhov E., Wodtke A., de Felicio R., Fenner A., Wong W.R., Lington R.G., Zhang L., Debonsi H.M., Gerwick W.H., Dorrestein P.C., Molecular networking as a dereplication strategy., 2013, *J. Nat. Prod.*, 76, 9, 1686-1699
237. Yen H.K., Lin T.F., Liao P.C., Simultaneous detection of nine cyanotoxins in drinking water using dual solid-phase extraction and liquid chromatography-mass spectrometry., 2011, *Toxicon*, 58, 2, 209-218

**Z**

238. Zahra Z., Choo D.H., Lee H., Parveen A., Cyanobacteria: Review of Current Potentials and Applications., 2020, *Environments*, 7, 2, 13
239. Zanchett G., Oliveira-Filho E.C., Cyanobacteria and cyanotoxins: from impacts on aquatic ecosystems and human health to anticarcinogenic effects., 2013, *Toxins*, 5, 10, 1896-1917
240. Zapomělová E., Hrouzek P., Řeháková K., Morphological variability in selected heterocystous cyanobacterial strains as a response to varied temperature, light intensity and medium composition, 2008, *Folia Microbiol.*, 53, 333-341
241. Zevenboom W., Mur L.R., Growth and photosynthetic response of the cyanobacterium *Microcystis aeruginosa* in relation to photoperiodicity and irradiance, 1984, *Arch. Microbiol.*, 139, 232-239
242. Zhang L., Pakrasi H.B., Whitmarsh J., Photoautotrophic growth of the cyanobacterium *Synechocystis* sp. PCC 6803 in the absence of cytochrome c553 and plastocyanin., 1994, *J. Biol. Chem.*, 269, 7, 5036-5042
243. Zheng T., Zhou M., Yang L., Wang Y., Wang Y., Meng Y., Liu J., Zuo Z., Effects of high light and temperature on *Microcystis aeruginosa* cell growth and  $\beta$ -cyclocitral emission, 2020, *Ecotoxicol. Environ. Saf.*, 192, 110313, 1-8

Thèse de l'Université de Paris  
M. Alexandros POLYZOIS

Amélioration de la production d'un métabolite ayant une puissante activité anticancéreuse chez la cyanobactérie *Nostoc* sp. ATCC 53789, en utilisant le stress abiotique. Etude phytochimique de cette souche

Soutenance prévue le 16 décembre 2020

## Résumé des travaux

Aujourd'hui, le cancer est la deuxième cause de décès dans le monde. En particulier, il a été responsable de plus de 6.000 décès aux États-Unis en 2019, alors qu'on estime qu'un décès sur six est dû au cancer (Siegel R.L. 2019). Ceci a stimulé la recherche de nouveaux traitements. Parmi les molécules d'origine naturelle, de nombreux produits marins et plusieurs composés cyanobactériens ont été examinés pour ce but (Luesch H. *et al.* 2002, Simmons T.L. *et al.* 2005). Un de ces composés présentant une activité remarquable est une toxine cyanobactérienne appelée cryptophycine.

### Chapitre 1 : Mises au point sur le sujet.

#### Cyanobactéries, cyanotoxines

Les cyanobactéries sont un vaste groupe de microorganismes qui produisent divers composés, des métabolites primaires comme des acides gras, des sucres ou des métabolites secondaires comme les caroténoïdes (Hitzfeld B.C. *et al.* 2000, Paerl H.W and Paul V.J. 2012). Ces composés peuvent présenter différents intérêts pour l'Homme : utilisations nutritionnelles, biocarburants, et même biofertilisants.

En ce qui concerne le domaine pharmaceutique, les activités biologiques de plusieurs métabolites secondaires de cyanobactéries et d'algues ont fait l'objet d'études. Des agents antiviraux et antifongiques ainsi que des composés ayant une activité anticancéreuse ont été développés (Singh R.K. *et al.* 2011, Vijayakumar S. and Menakha M. 2015). Par exemple, la noscomine de *Nostoc commune* a montré une puissante activité antibactérienne contre *Bacillus cereus* et *Escherichia coli* (Jaki B. *et al.* 1999). Un polysaccharide, le nostoflan, isolé de *Nostoc flagelliforme* (Patterson P. *et al.* 1993) possède des propriétés antivirales contre plusieurs virus enveloppés comme le virus de l'immunodéficience humaine (VIH) et l'herpès simplex (HSV).

En ce qui concerne les biocarburants, la forte teneur en lipides des cyanobactéries a jeté les bases du développement de carburants de substitution provenant de la biomasse (Barbosa M.J and Wijffels

R.H. 2017, Nozzi N.E *et al.* 2013). La surconsommation de combustibles fossiles et la crise du changement climatique qui en résulte ont conduit la recherche scientifique à se concentrer sur ce domaine au cours des cinq dernières décennies avec des projets de premier plan tels que le programme sur les espèces aquatiques, qui a débuté aux États-Unis dès 1978 (Sheehan J. *et al.* 1998). Cependant, le faible rendement lipidique et les installations actuelles augmentent considérablement le prix de revient actuel de la biomasse sèche. Par ailleurs, les surfaces nécessaires pour produire du biodiesel sont considérables (équivalentes à la superficie du Portugal pour l'Europe) (Wijffels R.H. *et al.* 2010). Des études ont prouvé que le stress abiotique, tel que la privation d'azote, pouvait augmenter la teneur en lipides cyanobactériens (Wilhelm C. and Jakob T. 2011). Ainsi, des conditions de stress combinées à de nouvelles installations optimales pourraient rendre le biodiesel rentable.

Enfin, plusieurs métabolites primaires, des polysaccharides, des pigments et complexes pigmentaires-protéiques, la chlorophylle et la phycocyanine sont utilisés comme compléments alimentaires. Un exemple caractéristique est celui de la "spiruline" qui est obtenue principalement à partir de la culture d'*Arthrospira maxima* et d' *A. platensis*. Elle contient des quantités importantes d'acide  $\gamma$ -linoléique (GLA), de phycocyanine, de  $\beta$ -carotène et de polysaccharides. En raison de cette composition, la "spiruline" est utilisée comme complément alimentaire pour son activité antioxydante et anti-inflammatoire ainsi que pour sa capacité à prévenir l'hypercholestérolémie (Hongsthong A. and Bunnag B. 2009, da Fontoura Prates *et al.* 2018).

Cependant, la production par les cyanobactéries de composés nocifs pour l'homme, les animaux et l'environnement est également observée. Ces produits toxiques sont des métabolites secondaires produits par des cyanobactéries et sont connus sous le nom de cyanotoxines. Les cyanotoxines sont considérées comme les toxines naturelles les plus répandues dans l'environnement. Certains facteurs environnementaux pourraient favoriser la formation d'efflorescences, comme l'eutrophisation, les concentrations élevées qui en résultent dans les eaux représentent des risques sanitaires et écologiques pour les animaux et les humains (Bláha L. *et al.* 2009).

Ces toxines peuvent avoir un impact néfaste sur la santé des personnes et des animaux. La variété des symptômes dépend du type de toxine, de la souche du producteur ainsi que de la concentration à laquelle la victime est exposée. Les principales voies d'infection sont la voie orale, l'exposition cutanée et l'inhalation. L'infection par ingestion peut être directe, lorsque de l'eau contaminée est consommée, ou indirecte, lorsque des aliments (comme le poisson et les légumes), qui ont été exposés aux cyanotoxines, sont consommés. La voie indirecte provoque le phénomène de bioaccumulation chez les consommateurs secondaires (comme l'homme) dans la chaîne alimentaire, avec de multiples impacts sur eux. Enfin, l'exposition cutanée et l'inhalation constituent une autre menace potentielle, lorsque la victime nage dans des eaux contaminées ou vit à proximité d'efflorescences toxiques. Les symptômes peuvent apparaître rapidement en quelques jours sous la

forme de lésions principalement au niveau du foie, des reins et du côlon. Cependant, des symptômes à plus long terme peuvent également se manifester sous forme de tumeurs et de cancer lorsque le patient est exposé de manière chronique à des doses de la toxine (Zanchett G. and Oliveira-Filho E.C. 2013). Ferrão-Filho A.S. and Kozlowsky-Suzuki B. 2011 établissent la classification des cyanotoxines sur la base de deux méthodes. Dans le premier cas, les cyanotoxines sont regroupées en fonction de l'effet qu'elles provoquent sur la victime et peuvent ainsi être caractérisées comme des neurotoxines, des hépatotoxines et des dermatotoxines. Dans la seconde méthode, les toxines sont identifiées sur la base de leur structure chimique principale, par exemple les peptides cycliques, les alcaloïdes et les lipopolysaccharides (LPS) (Zanchett G. and Oliveira-Filho E.C. 2013).

### Physiologie et phytochimie des cyanobactéries

Les cyanobactéries basent leurs sources de nutriments sur deux processus principaux, la photosynthèse oxygénée et la fixation de l'azote. La photosynthèse oxygénée, qui est la principale source d'énergie pour la cellule cyanobactérienne, a lieu dans les cellules végétatives. Certaines souches de cyanobactéries ont développé des types de cellules différenciées, autres que les cellules végétatives dans lesquelles se produit la photosynthèse, pour servir à divers processus tels que la fixation de l'azote et la propagation de nouveaux organismes. En fonction du besoin à couvrir, les cyanobactéries peuvent transformer une cellule végétative en d'autres cellules spécialisées, qui sont les hétérocystes, les akinètes et l'hormogonie (Hoiczuk E. and Hansel A. 2000). Dans les hétérocystes, la fixation de l'azote, qui est un processus dépendant de l'ATP, a lieu dans des conditions de privation d'azote (Nicolaisen K. *et al.* 2009). Ce processus est responsable de la réduction du diazote N<sub>2</sub> en ammonium, qui serait assimilé par le microorganisme. Les akinètes pourraient ressembler à des endospores bactériennes, car elles sont toutes deux résistantes aux conditions de culture difficiles. Elles jouent un rôle dans la survie du micro-organisme dans un environnement défavorable et de sa re-germination lorsque les conditions seraient meilleures (Kaplan-Levy R.N. *et al.* 2010). Enfin, les hormogonies sont des filaments mobiles courts qui sont constitués de quelques cellules de taille inférieure à celle des cellules végétatives. La formation de l'hormogonie est une méthode de propagation de la souche et est le résultat d'une combinaison de changements environnementaux qui signalent un état de stress (Liaimer A. *et al.* 2011, Meeks J.C *et al.* 2002).

Le profil biochimique des cyanobactéries peut être divisé en trois groupes principaux de métabolites primaires : les lipides, les glucides et les protéines. Plus précisément, un résumé de 12 souches *Nostoc* montre que le rapport protéines/poids sec varie de 37 % à 52 %, le rapport glucides de 15 à 30% et, les lipides de 8% à 13% respectivement (Vargas M.A. *et al.* 1998). Les phycobiliprotéines constituent le plus grand groupe de protéines, avec jusqu'à 50 % de la quantité totale. Une autre quantité importante de protéines est détectée dans les parois cellulaires des peptidoglycane. Ainsi,



on remarque une grande diversité de protéines et leur rôle dans une variété de mécanismes cellulaires (Vargas M.A *et al.* 1998, Andersen R.A 2013). Les hydrates de carbone des cellules cyanobactériennes ont une formation semblable à celle de l'amidon. Les laminarines sont des polysaccharides de glucose ayant un squelette de glucane lié à  $\beta$ -1,3 et des chaînes latérales liées à  $\beta$ -D-1,6. Ces formations varient en taille. Les plus petites, comme la chrysolaminarine avec 30 résidus de glucose, et qui est une substance de réserve est rencontrée dans une lignée majeure d'Eucaryotes, les Hétérocontes photosynthétiques. Des formations nettement plus grandes, que l'on peut voir même au microscope optique (Andersen R.A 2013) sont également présentes.

Les lipides de la cellule cyanobactérienne se trouvent principalement dans deux formations. Ils sont détectés : a) dans la structure bicouche des biomembranes, b) dans les membranes photosynthétiques combinées à des protéines. Dans les cyanobactéries, la proportion la plus élevée de lipides - jusqu'à 80 % - se trouve sous forme de triacylglycérols. Le deuxième groupe le plus important est celui des lipides polaires, tandis que les lipides neutres (comme les esters de stérol, les cires et les stérols libres) existent en quantités mineures (Dembitsky V.M. and Rezanka T. 2005). Enfin, il existe un petit groupe de composés divers où l'on peut trouver des depsipeptides. Deux groupes représentatifs de depsipeptides sont les nostocyclopeptides et les cryptophycines. Il existe trois analogues des nostocyclopeptides ; A1, A2, A3, qui sont exprimés dans un rapport de 10:1:1. Malgré leur présence unique dans le *Nostoc* sp. ATCC 53789, ces composés n'ont montré aucune activité biologique significative jusqu'à aujourd'hui. Plus précisément, ils n'ont montré aucune toxicité contre les lignées de cellules LoVo et KB, ni activité antifongique ou antibactérienne. Enfin, ils n'ont eu aucune inhibition contre l'activité des protéases. (Golakoti T. *et al.* 2000, 2001).

## Cryptophycine - analogues et activité biologique

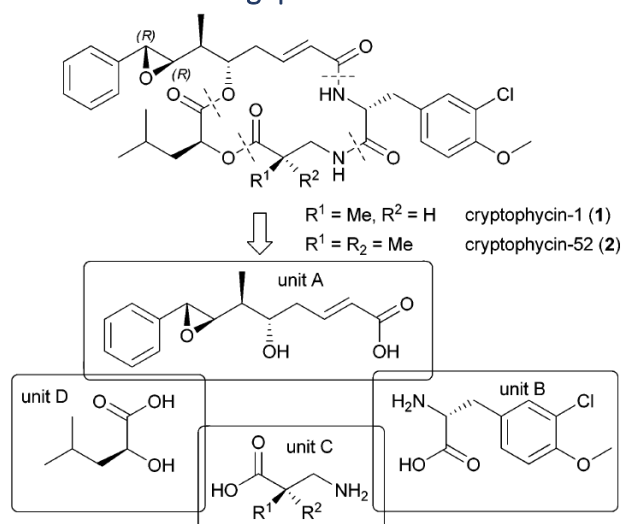


Figure : Deux des analogues les plus représentatifs de série cryptophycine sont la Cry-1 qui est un analogue naturel et a été le premier analogue détecté, tandis que Cry-52 est un analogue synthétique qui a connu un développement important et est entré en phase clinique II. La cryptophycine est composée de 4 unités dans la séquence cyclique A, B, C, D. L'unité A comprend un acide phényl-octénoïque, l'unité B, une 3-chloro-O-méthyl-D-tyrosine, l'unité C une méthyl-β-alanine, et l'unité, un acide L-leucique (Adapté de Weiss C. *et al.* 2013).

L'article de Schwartz R.E *et al.* 1990 et plus tard le brevet de Hirsch F.H *et al.* 1990, des laboratoires Merck, et Ocean genetics décrivaient d'abord la Cry-1 et le microorganisme producteur, *Nostoc* sp. MB5357 qui est maintenant connu sous le code ATCC 53789 (American Type Culture Collection - ATCC). La souche a d'abord été collectée sur un lichen de l'île d'Arron en Écosse. Plus précisément, 3 mm carrés du thalle du lichen mentionné ont été incubés avec 2,5 ml de BG-13 à 25 °C pendant 3-4 semaines. À partir de la culture obtenue, la souche souhaitée a été isolée puis stockée dans le milieu BG-13. Cependant, en ce qui concerne son activité biologique, seule son activité antifongique a été décrite dans un premier temps.

Son activité a été caractérisée contre les champignons filamenteux et la levure de *Cryptococcus* sp.. L'activité contre *Cryptococcus* sp. était si importante que le composé nouvellement découvert a été nommé "cryptophycine" selon le nom d'espèce du champignon.

Plus tard, Cry a été isolée à partir d'une autre souche, *Nostoc* sp. GSV 224 (Golakoti T. *et al.* 1994), qui a été initialement isolée à partir d'un échantillon terrestre en Inde par un botaniste indien, Gopalasmudram Sitaraman Venkataraman, directeur du département de biotechnologie - Centre des algues bleues de l'Université Madurai Kamaraj, et qui portait donc l'abréviation GSV. À partir de cette souche, 7 analogues de Cry ont été isolés et caractérisés : Cry-1, -2, -3, -4, -5 ester méthylique, -6 ester méthylique et -7, et ils ont été soumis pour la première fois à des essais cytotoxiques (sur des lignées cellulaires KB et LoVo) (Golakoti T. *et al.* 1994). Ensuite, pour des recherches plus approfondies, il a été fourni par le professeur Wolk C.P., du laboratoire de recherche sur les plantes de la MSU-DOE, de l'université de l'État du Michigan, mais il n'était pas disponible dans le commerce. La même année, l'arénastatine A a été isolée et évaluée (Kobayashi M. *et al.* 1994). Elle a été isolée de l'éponge d'Okinawa *Dysidea arenaria*. Il est à noter que la valeur de la CI<sub>50</sub> -5 pg/ml- sur la lignée

cellulaire KB est similaire à celle de Cry-1 et -2. Il a été démontré plus tard que l'arénastatine A était identique à la Cry-24, ce composé était dû à un symbiote cyanobactérien (Robert A.B *et al.* 2018).

Enfin, Nowruzi B. *et al.* 2012 ont examiné les morts suspectes de chiens et de souris dans les environs des rizières en Iran. Les auteurs ont prélevé des échantillons de sol dans les rizières et les ont avec un milieu BG110. La souche cultivée de cyanobactéries avec des hétérocystes a été caractérisée comme *Nostoc* sp. ASN\_M. Parmi les composés isolés de la souche, trois classes de composés peptidiques ont été identifiées : anabaenopeptides, cryptophycines et nostocyclopeptides. À ce stade, il a été affirmé que la toxicité et la mort de la faune environnante étaient dues aux cyanotoxines, mais peu de recherches supplémentaires ont été menées sur cette espèce (Nowruzi B. *et al.* 2012).

Le projet qui a été envisagé pour ce travail de thèse, s'est concentré sur la souche *Nostoc* sp. ATCC 53789, qui est actuellement la seule disponible dans le commerce. Ce projet, visant initialement au développement d'une application industrielle, il était donc nécessaire de disposer d'une souche disponible dans le commerce.

Les cryptophycines représentent un large groupe de peptolides, naturellement produits par les cyanobactéries du genre *Nostoc* sp. En série cryptophycine, vingt-huit composés chimiquement définis ont été isolés, ils sont complétés par de nombreux analogues obtenus par synthèse. La Cry-1 est l'analogue qui a été isolé et étudié pour la première fois. Cry-1 est également le composé majoritaire dans le microorganisme producteur de type sauvage. Pour ces raisons, nous avons choisi cet analogue comme étude de cas et exemple représentatif du groupe des cryptophycines. Cry-1 a une formule moléculaire de C<sub>35</sub>H<sub>43</sub>ClN<sub>2</sub>O<sub>8</sub> et son nom chimique selon IUPAC est : (3*S*,6*R*,10*R*,13*E*,16*S*)-10-[(3-chloro-4-methoxyphenyl)methyl]-6-methyl-3-(2-methylpropyl)-16-[(1*S*)-1-[(2*R*,3*R*)-3-phenyloxiran-2-yl]ethyl]-1,4-dioxa-8,11-diazacyclohexadec-13-ene-2,5,9,12-tetrone.

Cry-1 est un depsipeptide circulaire dont le poids moléculaire est de 655,2 g/mole et la masse molaire de 655,2 Da.

Sa structure peut être divisée en quatre sous-unités. L'unité A comprend un acide phénylocténoïque, avec un groupe époxyde qui joue un rôle essentiel pour la puissante activité de la molécule. L'unité B comprend la 3-chloro-O-méthyl-D-tyrosine, l'unité C comprend la méthyl β-alanine, et l'unité D comprend l'acide L-leucique. Ces unités sont liées dans une séquence cyclique ABCD.

Comme mentionné, Cry-1 peut être produit par trois souches de *Nostoc* sp. Cependant, les cryptophycines ont été principalement étudiée chez *Nostoc* sp. GSV 224 en raison d'une production plus élevée dans cette souche par rapport aux deux autres. L'étude chimique d'une grande culture de *Nostoc* sp. GSV 224 a permis d'identifier 28 analogues naturels de Cry. Les premiers analogues Cry isolés étaient : cry -2, -3, -4, -5, -6, -7, alors que parmi ces analogues, seul Cry-2 a montré une forte puissance, similaire à l'activité de Cry-1 (Golakoti T. *et al.* 1994). Cependant, il a été mis en évidence

que Cry-5, -6, -7 n'étaient pas à l'origine des analogues de naturels de Cry mais des artefacts qui se sont formés en présence du méthanol utilisé processus d'isolation (Golakoti T. *et al.* 1995).

Ensuite, 18 autres analogues ont été caractérisés, ils présentent des modifications dans une unité A-D. Cry-24 est le seul à présenter des modifications dans deux unités (B et C) (Golakoti T. *et al.* 1995). La plupart des analogues présentent des modifications dans l'unité B, et il n'y avait que deux analogues (Cry-21 et -29) avec des modifications dans l'unité C (Golakoti T. *et al.* 1995). Parmi les analogues naturels de Cry naturels identifiés, Cry-1 est le plus puissant. Seuls quelques autres analogues, ont montré une activité toxique notable. Cry-21, est très puissant, et présente une activité biologique proche de celle de Cry-1 (Golakoti T. *et al.* 1995).

### Cryptophycine – mécanisme d'action et relations structure-activité

On a découvert que Cry était un puissant perturbateur de l'équilibre dynamique microtubules/tubuline. Les microtubules sont impliqués dans la régulation de nombreux processus cellulaires et du fuseau mitotique. Ainsi, les microtubules sont la cible d'un grand nombre de médicaments anticancéreux à base de produits naturels. L'incubation de cellules leucémiques L 1210 avec de la cryptophycine a entraîné une inhibition de la prolifération cellulaire proportionnellement à la dose. En parallèle, le pourcentage de cellules en mitose est augmenté. Le traitement par Cry ou par la vinblastine induit une polymérisation, cependant le prétraitement des cellules avec du taxol a empêché la dépolymérisation des microtubules en réponse à la vinblastine ou à la Cry, car le prétraitement a fortement stabilisé les microtubules (Panda D. *et al.* 1997, Jordan M.A. 2002).

En ce qui concerne le site de liaison, il a été constaté que même si Cry semble interagir avec la position de fixation des *Vinca*, il ne s'attache probablement pas exactement sur ce site, mais il recouvre cette position, car il a peu de similarités structurales avec les alcaloïdes de la *Vinca* (Panda D. *et al.* 1997). L'avantage le plus significatif de Cry, par rapport aux alcaloïdes du genre *Vinca*, est qu'il semble être un mauvais substrat pour la glycoprotéine P, pompe d'efflux qui induit une résistance aux traitements (Smith C.D. *et al.* 1994). Cette propriété est répertoriée comme son point majeur dans le développement d'un nouveau composé pharmaceutique actif (Smith C.D. *et al.* 1996). La dernière spécificité importante de l'action est le haut niveau d'irréversibilité de la liaison Cry (Smith C.D. *et al.* 1994, 1996) due à la présence d'un cycle époxyde réactif, permettant la formation d'une liaison covalente avec des acides aminés de la tubuline.

Les relations structure-activité dans cette série mettent en évidence que l'oxygène de l'époxyde peut également être ouvert par HCl en chlorhydrate (Cry-8), les deux composés, Cry-1 et Cry-8 ont une puissance similaire (Golakoti T. *et al.* 1994). La méthanolyse (Cry-9), conduit à un composé dénué d'activité (Golakoti T. *et al.* 1994, Biondi N. *et al.* 2004). Aucune activité n'est également observée pour les analogues Cry-3 et -4, où il y a une élimination totale du groupe hydroxyle ou de l'époxyde

respectivement. Tout ce qui précède met en évidence le rôle significatif de l'oxygène sur l'unité A sous forme de groupe hydroxy ou d'époxyde. D'autres caractéristiques importantes sont la présence de l'acide leucique et la liaison ester entre les unités C et D. En ce qui concerne l'acide leucique, en cas d'absence de celui-ci, les analogues Cry-6, -7, -10, -12 ont une activité sensiblement plus faible. L'absence de la liaison ester conduit à la Cry-5 qui est inactive (Golakoti T. *et al.* 1994).

## Chapitre 2 – Effets du stress abiotique sur la production de cryptophycine

Les conditions environnementales de culture affectent souvent la croissance et la physiologie de la souche ainsi que sa production en cyanotoxines. Ainsi, le réglage des conditions de culture est un moyen indirect de modifier la croissance et la production de Cry-1. Les principaux paramètres de la culture objet de cette étude sont le pH, la température, la composition du milieu et le paramètre de la lumière. Plus précisément, le principal processus métabolique des cyanobactéries est la photosynthèse oxygénée. On peut donc comprendre qu'une modification du paramètre lumière pourrait avoir un impact significatif sur le taux de croissance et la physiologie des cyanobactéries. Les principales conditions relatives à la lumière sont la photopériode, l'intensité et la longueur d'onde de la lumière.

### Matériel et méthodes

Afin de tester les conditions environnementales décrites, les expériences sont réalisées sur 10 jours en triple exemplaire pour évaluer les conditions biologiques et techniques. Nous avons tout d'abord, dû développer des méthodes pour observer la croissance de la culture et mesurer la quantité de Cry produite. Une détermination de la quantité de biomasse sèche permet d'apprécier la croissance des bactéries, l'hémocytomètre n'étant pas applicable avec précision aux cyanobactéries filamenteuses et la DO différant selon les spectromètres. Toutes les mesures sont effectuées en triplicat.

### Mesure de la croissance

Il y a principalement deux façons d'observer la croissance de la culture : a) par la densité optique et b) par le calcul de la biomasse sèche. La densité optique est le moyen indirect le plus courant de calculer la biomasse des microorganismes en suspension. Les formations cellulaires du microorganisme, comme les pigments photosynthétiques, peuvent absorber la lumière à des longueurs d'onde spécifiques. Cependant, au-delà d'une valeur d'environ 700 nm, la longueur d'onde ne peut être absorbée par aucune de ces formations et le faisceau lumineux traverse la suspension sans être absorbé. D'autre part, cette quantité de lumière est diffusée lors de son passage à travers l'échantillon, et à la fin, seule une partie de ce faisceau atteint le détecteur. Une deuxième méthode est le calcul de la biomasse sèche. La biomasse sèche a été calculée comme la moyenne de trois

échantillons. Étant donné que l'hémocytomètre n'est pas applicable avec précision aux cyanobactéries filamenteuses et que la DO diffère selon les spectromètres, cette technique est la plus appropriée pour le projet. Cependant, la mesure de la biomasse sèche prend beaucoup de temps par rapport à la DO. Une courbe d'étalonnage a donc été établie pour faire correspondre la DO à des mg de biomasse sèche.

### Quantification de petites quantités de cryptophycine

Un processus d'extraction a été mis au point à partir du prélèvement de 20 mL d'échantillon de biomasse des conditions stérile. Il fait intervenir un homogénéisateur de tissu "PRECELLYS® 24". La quantité de Cry-1 dans la biomasse est mesurée par HPLC afin d'établir l'aire sous la courbe. Là aussi une courbe permet de calculer la concentration dans chaque échantillon.

### Travaux personnels

En suivant les méthodes développées ci-dessus, nous traçons trois courbes pour chaque expérience. Premièrement, nous avons observé la croissance de la culture en nous basant sur la méthode de calcul de la biomasse sèche développée, qui est exprimée en mg de biomasse sèche dans 10 mL de culture. Ensuite, avec la méthode de calcul de la concentration de la cryptophycine mise au point précédemment, la quantité réelle de Cry dans un échantillon de 20 mL est calculée. Cela est mentionné comme "quantité de Cry par culture". Enfin, le quotient de Cry produit par 10 mL de culture par rapport à la biomasse sèche calculée, est donné.

### Expériences sur l'intensité lumineuse

La souche a été cultivée dans un multi-cultivateur MC 1000 (PSI- Photon System Instruments) en utilisant des tubes de 5 cm de diamètre. Dans nos conditions expérimentales, les intensités lumineuses utilisées correspondaient à des intensités moyennes, élevées et très élevées.

En ce qui concerne la croissance de la culture, dans la plus faible intensité lumineuse, la biomasse sèche a doublé après trois jours et triplé en dix jours. Sous des intensités lumineuses plus élevées, les cellules se sont développées plus lentement et la biomasse a donc doublé seulement après 8 jours de croissance. Ces résultats suggèrent que ces intensités lumineuses plus élevées stressent les cellules. Ceci était conforme aux observations microscopiques. Les fragmentations observées dans les cultures soumises à un stress lumineux se sont développées à des intensités élevées et très élevées. Le nombre de fragments augmentait avec l'intensité lumineuse. La culture cultivée à une intensité lumineuse moyenne avait le taux de croissance le plus élevé. En même temps, les intensités lumineuses très élevées entraînaient la mort des cellules par photoinhibition. La production de Cry par biomasse sèche a également été affectée par l'intensité lumineuse.

Dans nos conditions expérimentales, les intensités lumineuses allant de 80 à 120  $\mu\text{mol photon m}^{-2} \text{s}^{-1}$  sont les plus adaptées pour la production de Cry. Plus généralement, le stress lumineux n'est pas bon pour augmenter la production de Cry. Le résultat de la production du métabolite est en accord avec les données bibliographiques (Khajepour F. *et al.* 2015, Ma R. *et al.* 2015, Kurmayer R. *et al.* 2011, Eldin M.J. *et al.* 2014, Chmelík D. *et al.* 2019, Zheng T. *et al.* 2020, Oh H.S. *et al.* 2017) qui proposent que des intensités lumineuses moyennement faibles seraient optimales. Pour résumer les trois graphiques sur l'intensité lumineuse, nous pouvons dire que, conformément aux données bibliographiques, *Nostoc* sp. préfère des intensités lumineuses moyennes pour la croissance et la production de Cry.

### Expériences sur la photopériode

La souche a été cultivée dans un erlenmeyer de 500 mL avec un volume de travail de 300 mL. Un inoculum correspondant à 4,0 mg de biomasse sèche/10mL a été dilué avec du milieu BG11 frais et ajusté à une concentration finale de 2,5 mg de biomasse sèche/10mL, ce qui donne un volume final de 300 mL. La culture a été réalisée dans un "Brunswick Innova 4340 Refrigerated Incubator Shaker" sous aération constante. La température a été réglée à  $25 \pm 1$  °C par une ventilation d'air. La lumière était fournie à une intensité de 45  $\mu\text{mol photon m}^{-2} \text{s}^{-1}$  et 50 mbar de  $\text{CO}_2$  étaient fournis en permanence dans la chambre d'incubation.

Nous avons comparé la lumière continue (24:0) à une photopériode de 16 heures de lumière et 8 heures d'obscurité (16:8). Le taux de croissance était similaire dans les deux conditions, même si la croissance des cellules dans l'incubateur avec table d'agitation était complètement différente de celle dans le bioréacteur utilisé pour l'expérience sur l'intensité lumineuse. Ce résultat suggère qu'une période lumineuse de 16 heures est suffisante pour stocker assez d'énergie pour maintenir la croissance des cellules pendant une période non lumineuse allant jusqu'à 8 heures. Une deuxième explication est que *Nostoc* sp. comme d'autres souches de cyanobactéries montrent une préférence pour la photopériode de leur habitat naturel d'où elles ont été initialement isolées (Jacob-Lopes E. *et al.* 2009). La souche a été initialement isolée de l'île d'Aaron, en Écosse, où la photopériode naturelle ressemble à la photopériode 16:8 (L:D). En revanche, la période d'obscurité a eu un effet très négatif sur la production de Cry. Sous une lumière continue, la production de Cry par biomasse sèche a augmenté jusqu'au quatrième jour (la production a doublé), puis a diminué avec l'augmentation de la concentration cellulaire. Lorsque la photopériode 16:8 était utilisée, la production de Cry restait faible et ensuite, lorsque les cellules étaient concentrées, la production diminuait. La concentration de Cry dans la culture augmente plus rapidement sous une lumière continue (24:0). Nous avons conclu que la lumière continue est favorable à la production de Cry. Cette observation indique deux hypothèses pour la production de la cyanotoxine. Premièrement, la production pourrait être

photodépendante et donc la lumière est un facteur nécessaire pour le processus. Deuxièmement, dans des conditions non lumineuses, le micro-organisme fournit une énergie limitée qui doit être utilisée pour la survie et non pour la production de métabolites secondaires.

### Expériences sur la longueur d'onde

Les conditions de culture étaient identiques à celles de l'expérience sur la photopériode. Afin d'évaluer l'effet d'une longueur d'onde spécifique de la lumière, des films en couleur (Eurolite, Toronto, Canada) ont été placés le long de la surface externe de chaque flacon. Les courbes de transmission des filtres ont été tracées à l'aide d'un spectrophotomètre UV-Vis (Beckman, DU 640). Sur la base de ces courbes, le pic d'émission du filtre rouge était de 590-700 nm et celui du filtre bleu de 410-490 nm.

En ce qui concerne la croissance de la culture, une absence de développement a été observée pendant les deux premiers jours, puis la croissance a été plus rapide. La biomasse a triplé sous lumière orange et a doublé sous lumière bleue après 10 jours de croissance. Comme cela a été observé précédemment dans d'autres laboratoires, la croissance cellulaire a été largement plus lente sous lumière bleue que sous lumière rouge-orange. Par rapport à la lumière rouge-orange, la lumière bleue n'a pas amélioré la production de Cry par cellule. Plus précisément, la lumière bleue a conduit à une baisse pendant les deux premiers jours, puis une légère augmentation jusqu'à son maximum le quatrième jour. Au contraire, la lumière rouge-orange a conduit à une augmentation constante jusqu'au quatrième jour. Ainsi, après 4 jours de croissance, la production de Cry a triplé sous la lumière rouge-orange et n'a fait que doubler sous la lumière bleue. Enfin, comme dans le reste des expériences où les cellules sont devenues plus concentrées, la production de Cry par cellule a diminué.

Lorsque la concentration en Cry de la culture a été suivie, on a observé sous une lumière rouge-orange une augmentation de la concentration en Cry pendant 7 jours due à la combinaison d'une concentration cellulaire plus élevée et d'une production plus importante de Cry par mg de biomasse. Ensuite, la concentration totale de Cry a diminué en raison de la production plus faible de Cry par cellule. Sous lumière bleue, la concentration de Cry a augmenté entre les jours 2 et 4, principalement en raison d'une meilleure production de Cry par cellule. La lente croissance des cellules sous lumière bleue est liée au fait que la lumière bleue est principalement absorbée par le PSI, ce qui entraîne un déséquilibre des activités du photosystème et une diminution de l'efficacité de la photosynthèse. La lumière bleue affecte également la production de Cry, très probablement liée à une faible efficacité photosynthétique diminuant la puissance de synthèse des métabolites.



### Expériences sur le pH

Comme mentionné ci-dessus, la photosynthèse oxygénée, qui est la conversion du CO<sub>2</sub> et de l'eau en sucre grâce à l'énergie lumineuse, est le principal processus métabolique des cyanobactéries (Vermaas W.F 2001, Blankenship R.E. 2002). La consommation de CO<sub>2</sub>, entraîne automatiquement une augmentation de la valeur du pH. Afin d'examiner l'effet du pH sur la culture, nous avons essayé de stabiliser la valeur du pH et d'arrêter son augmentation. Les valeurs de pH que nous voulions examiner sur la base de recherches bibliographiques (Ray S. *et al.* 2001, Sang M. *et al.* 2012, Guckert J.B. *et al.* 1990) et de l'expérience du laboratoire étaient de pH 7,5 et pH 8,0. Nous avons testé différents tampons chimiques dans une gamme de concentrations afin de trouver celui qui ne serait pas toxique pour la souche, et qui serait en même temps capable de maintenir le pH à la valeur souhaitée. Parmi les tests comparés, le Tris à 10 mM présentait la meilleure combinaison de faible toxicité et de contrôle relativement bon du pH.

L'augmentation constante du pH n'a pas permis d'extraire un résultat clair pour l'effet du pH. Pendant les 6 premiers jours, une culture était toujours à un pH plus bas (culture "à pH plus bas") que l'autre (culture "à pH plus élevé"). La production de Cry par cellule était plus élevée dans la culture "à pH élevé". Le "pH élevé" a atteint son maximum de production par cellule le deuxième jour, lorsque son pH était de 8,36. Son maximum était 1,5 fois plus élevé que le maximum du "pH faible". Le "pH inférieur" a atteint son maximum par production cellulaire le troisième jour, lorsque la valeur du pH était de 7,76. Ainsi, en raison des variations du pH, nous ne pouvons généralement faire qu'une première hypothèse, à savoir qu'un pH supérieur à 8,3 est favorable à la fois à la croissance et à la production de Cry. De cette expérience, nous ne pouvons qu'émettre l'hypothèse que la synthèse de Cry est favorisée à un pH de 8 à 8,5.

### Expériences portant sur la composition du milieu de culture

Afin de tester l'effet du stress lié à la privation de nitrates et l'implication des hétérocystes dans le processus d'expression de Cry, deux milieux de culture différents ont été comparés. La différence entre les deux milieux de culture était la présence ou l'absence de nitrate comme source d'azote. Dans une culture, NaNO<sub>3</sub> a été remplacé par NaCl, avec une quantité proportionnelle de Na. Les autres conditions de culture (température, intensité lumineuse, agitation, CO<sub>2</sub>, récipient de culture et volume de travail) étaient identiques à celles des expériences sur la photopériode.

En l'absence d'azote combiné, la formation d'hétérocystes, dans lesquels l'azote est converti en ammoniacque par l'azotéase, est induite. Dans l'expérience, l'inoculum des deux ensembles provenait d'une culture mère cultivée en milieu BG11. Ce milieu contient du nitrate, et donc les filaments de *Nostoc* sp. étaient constitués uniquement de cellules végétatives. Dans la culture BG11o sans nitrate, des processus métaboliques ont été induits et des hétérocystes ont été formés. Ainsi, la production

de Cry par cellule est restée stable pendant les deux premiers jours où il n'y avait pas encore d'hétérocyste.

Suite à l'apparition des premiers hétérocystes sur la BG110-culture, la production de Cry par cellule a chuté, car a) la quantité d'hétérocystes développés n'était pas encore suffisante, et b) les réserves d'azote décomposées ne répondaient qu'aux besoins primaires ou avaient déjà été consommées. À partir du sixième jour, où une quantité suffisante d'hétérocystes avait été développée, la production par cellule de la culture BG110 a augmenté de manière significative, et son taux a légèrement baissé seulement le neuvième jour. En revanche, la production par cellule de la culture BG11 a lentement augmenté jusqu'à atteindre son maximum le 7<sup>e</sup> jour, avec une densité d'environ 6 mg de biomasse sèche/20 mL.

En ce qui concerne la croissance, les deux cultures ont suivi des schémas similaires jusqu'au sixième jour. À partir de ce moment, la culture du BG11 a continué sa croissance tandis que la culture du BG110 a cessé de croître au septième jour. Ce plateau se traduit par une densité cellulaire nettement inférieure à celle de la culture BG11.

L'effet combiné de la croissance et de la "production de Cry par cellule" est représenté sur le graphique de la production totale de Cry. Dans un milieu pauvre en nitrate, la culture reste presque au même niveau jusqu'au septième jour. Ensuite, en raison de la production élevée de Cry par biomasse sèche (par cellule), la concentration de Cry a rapidement augmenté pour atteindre un niveau encore plus élevé que la culture contenant du nitrate. La culture BG11 produit Cry proportionnellement à son taux de croissance et atteint son maximum le septième jour, ce qui correspond à la phase exponentielle tardive.

#### Expériences sur la température

Les conditions de culture étaient identiques à celles de l'expérience sur la photopériode. La seule différence était que la température était de 25, 30 et 35 °C.

Les taux de croissance à 25 et 30 °C étaient similaires. La culture à 35 °C a eu un taux de croissance plus élevé jusqu'au troisième jour, où elle a ralenti et est devenue plus basse que celle à 25 et 30 °C. Le résultat significatif de cette expérience a été l'observation de l'effet de la température sur la production de Cry par mg de biomasse. La production par cellule du métabolite à température ambiante (25 °C) a légèrement augmenté pendant les deux premiers jours, puis elle a fortement augmenté jusqu'au troisième jour et a atteint son maximum le sixième jour. Fait remarquable, les températures supérieures à 25 °C ont eu un impact important sur le profil métabolomique des cellules : les cellules ont largement diminué la production de Cry dès le début et après 3 jours à 35 °C, elles ont presque cessé de produire la toxine.

La concentration de Cry de la culture a suivi un schéma similaire. À 25 °C, la concentration est restée stable pendant les deux premiers jours, puis a doublé du troisième au quatrième jour. La

concentration de Cry dans la culture a continué à augmenter pendant les 10 jours de l'expérience, bien que le taux d'augmentation ait été légèrement plus faible au cours des deux derniers jours. En revanche, à 30 et 35 °C, la concentration n'a pas augmenté. À 30 °C, le niveau de la toxine a légèrement diminué pendant les 6 premiers jours, et a légèrement augmenté jusqu'au niveau initial bas. À 35 °C, la concentration de Cry a rapidement diminué et à partir du troisième jour, il n'y avait presque plus de toxine dans la culture. Le résultat ci-dessus indique que la production de métabolites est fortement influencée par la température, comme cela a été mentionné précédemment pour d'autres cyanotoxines telles que la MC (Kurmayer R. 2011, van der Westhuizen A.J. and Eloff J.N. 1985, Sivonen K. 1990).

### Effet synergique des conditions optimales

Il serait utile de préciser le résultat global des conditions optimales développées et leur éventuel effet synergique. Tous les paramètres de culture optimaux sont repris et pour le pH nous visons à maintenir pendant une période prolongée la culture à la gamme optimale de pH 8,5-9,0. Ainsi, nous choisissons le pH 7,5, car nous nous attendions à une croissance rapide et à une élévation du pH en raison des conditions optimales. Un deuxième groupe de conditions, qui serait défini comme "blanc", était nécessaire pour comparer et valider les résultats. Ainsi, nous avons défini comme "blanc" l'expérience qui a été menée à un pH de 7,5.

Les deux ensembles ne diffèrent pas de manière significative en ce qui concerne leur croissance pendant les six premiers jours, et ils ont des taux de croissance approximativement similaires jusqu'à ce moment. Toutefois, par la suite, l'ensemble optimal a eu des performances légèrement meilleures. En ce qui concerne la production de Cry, le pic de "l'ensemble optimal" est presque 30 % plus élevé que le pic de l'ensemble "pH 7,5". Lorsque nous comparons les "conditions combinées" avec chaque expérience qui les compose, dans le flacon d'Erlenmeyer, nous observons que les "conditions combinées" ont un effet synergique car la souche est plus performante. En récapitulant les paramètres examinés sur la culture en flacons, on peut noter que dans toutes les expériences, la production maximale de Cry par mg de biomasse se situe dans la phase exponentielle tardive (5,15 à 8,0 mg de biomasse sèche/10 mL). La valeur de ce maximum varie en fonction de l'état physiologique de la souche et des paramètres expérimentaux. Cependant, sur la base des expériences ci-dessus, quelles que soient la taille et le type de vaisselle utilisé, le maximum de Cry par cellule devrait être attendu sur une phase exponentielle moyennement tardive, même si la valeur réelle de croissance ne serait pas la même. Cela est conforme aux données bibliographiques sur la production des cyanotoxines, qui mentionnent que, par exemple, la production de MC est optimale entre la phase exponentielle et la phase stationnaire, alors qu'en phase stationnaire, sa concentration est 6 fois

moindre par rapport à la phase exponentielle (Watanabe M.F 1983, Watanabe M.F and Oishi S. 1985).

### Adaptation à l'échelle

L'optimisation des conditions de culture entraînerait une surproduction de métabolites. Dans un premier temps, l'industrie pharmaceutique tirerait profit de ces conditions pour développer davantage le composant anticancéreux potentiel. Dans une dernière étape, la souche a donc été testée dans des conditions à plus grande échelle afin de noter l'effet des conditions de mise à l'échelle sur la croissance et la production du métabolite. La souche a été cultivée dans un photobioréacteur (PRB) avec un volume de travail de 12 L avec un milieu BG11 sous  $25 \pm 1$  °C et un pH de 7,5-8. L'intensité lumineuse a été fixée à  $145 \mu\text{mol photon m}^{-2} \text{s}^{-1}$  (intensité lumineuse moyenne), et la photopériode était de 16:8 (L:D). L'expérience a été menée en une seule série de PRB avec 4 répétitions techniques chaque jour d'échantillonnage. Les mêmes conditions de culture ont été adaptées dans l'expérience de culture en flacon également. Les conditions de culture étaient les mêmes que dans l'expérience sur la photopériode 16:8 (L :D). Les deux cultures ont commencé à une densité de 2,5 mg de biomasse sèche/10 mL, qui a été inoculée à partir d'une culture mère de 4,0 mg de biomasse sèche/10 mL. En ce qui concerne l'expérience en flacon, chaque réplique biologique était composée de trois cultures Erlenmeyer, qui étaient les trois répliques techniques.

Premièrement, il y a une grande différence dans les taux de croissance. La culture du PBR est passée par une phase de latence jusqu'au septième jour. La phase logarithmique a été suivie d'une phase exponentielle, qui a presque doublé la densité des cyanobactéries du septième au dixième jour. D'autre part, la culture en flacon a connu une augmentation plus précoce avec un taux de croissance d'environ 20 % par jour jusqu'au septième jour.

Cela peut se produire d'abord en raison de l'effet de flash léger auquel les cellules sont confrontées, ensuite en raison du stress de cisaillement causé par une forte agitation (van Alphen P. *et al.* 2018) et enfin en raison de l'injection de CO<sub>2</sub> non exacte qui fait souvent chuter le pH hors de sa zone optimale (Kuan D. *et al.* 2015). Dans les faibles densités, les cellules pourraient être davantage exposées au phénomène de stress de cisaillement et de photoinhibition. La différence la plus importante est notée dans la production par cellule. La production par cellule de la culture PBR augmente constamment, et a été multipliée par 4 environ en dix jours. Au contraire, la culture en flacon ne présente pas de grandes variations de sa production par cellule. Par exemple, sa production cellulaire la plus élevée, qui est enregistrée le septième jour, n'est supérieure à ses valeurs initiales que de 1,3 fois. Une conséquence de cette grande différence entre les deux cultures est le fait que lorsque le PBR est en phase exponentielle, il produit presque 5 fois plus de Cry au total que la culture en flacon.

### Chapitre 3 : exploration phytochimique de la souche *Nostoc* sp. ATCC 53789 par réseaux moléculaires

Suite à l'optimisation des conditions de culture, nous visons à étudier a) le profil phytochimique de *Nostoc* sp. ATCC 53789, b) comment les conditions de culture affectent ce profil, c) comment ce profil change pendant la croissance de la culture. Pour ce faire, nous avons dû mettre au point des techniques d'extraction et de purification pour des volumes importants. Ensuite, ces extraits et fractions bruts ont été étudiés à travers la création de "réseaux moléculaires" pour obtenir une vue d'ensemble de leur profil.

#### Procédé d'extraction de la biomasse sèche

La partie actuelle du projet se concentre sur l'étude de la biomasse de la culture. Nous nous sommes concentrés sur la biomasse et non sur le milieu pour deux raisons. Premièrement, en général, la portion extracellulaire des cyanotoxines est mineure par rapport à la portion intracellulaire pendant la phase exponentielle (Park H.D. *et al.* 2001, Qian F. *et al.* 2014). Deuxièmement, le projet vise à l'échelle industrielle, de sorte que le traitement de grands volumes de liquide, provenant du milieu de culture, est beaucoup plus compliqué et coûteux que le traitement de la phase solide de la biomasse sèche. Pour ces deux raisons, c'est la biomasse et non le milieu de culture qui sera étudié. La première étape est le développement de la culture dans le PBR et la séparation du milieu de culture de la biomasse. La croissance de la culture dans le réacteur est contrôlée tous les deux jours par mesure de la densité optique et détermination de la quantité de biomasse sèche, comme décrit au chapitre 2. Sur la base de ces mesures, au point de croissance souhaité, une quantité de culture est sortie du réacteur pour être récoltée.

Simultanément, un nouveau milieu frais est ajouté dans des conditions stériles dans la culture restante sur PBR pour poursuivre la culture. La quantité de culture obtenue est placée dans un flacon de décantation de 6 L et est laissée pendant la nuit pour la séparation gravitationnelle de la biomasse du milieu. La biomasse humide est centrifugée à 2 000 tours/minute pendant 15 minutes pour une séparation supplémentaire du milieu. La dernière étape comprend la lyophilisation de cette quantité pour obtenir la biomasse sèche finale. Cette biomasse est ensuite pulvérisée à l'aide d'un mortier et d'un pilon, et le poids de la poudre finale est calculé.

Pour l'extraction de cette biomasse sèche, nous avons comparé 4 systèmes de solvants MeCN:DCM 4:1, MeCN:DCM 5:1, MeOH 100% et DCM 100%. Sur la base du rendement Cry, mesuré selon la méthode HPLC décrite ci-dessus, nous avons choisi le système de solvant MeCN:DCM 4:1.

### Purification de la cryptophycine-1

Dans le but d'étudier le profil phytochimique de la souche, nous avons développé et appliqué deux techniques chromatographiques.

La première méthode se concentre sur la purification de Cry-1 et comprend deux étapes. À chaque étape, nous appliquons une chromatographie sur colonne ouverte pour la purification progressive de l'extrait brut jusqu'à ce que nous obtenions les fractions enrichies en Cry-1. 25 g de biomasse sèche, provenant d'environ 36,7 L de culture, ont été soumis au processus d'extraction décrit ci-dessus et ont donné 1,14 g d'extrait brut. L'extrait a été dilué dans 35 mL de DCM et a été soumis à une chromatographie flash sur colonne de 2,5 cm sous forme de dépôt liquide. Pour la phase stationnaire, on a utilisé 32,7 g de silice de granulométrie 15 à 40 µm.

Sur la base de la méthode de Back S. 2005, on a d'abord ajouté 3 volumes de DCM dans la colonne (CV) puis la polarité est brusquement augmentée en passant à une phase mobile AcOEt:Isopropanol 4:1 v:v. Le but de ce changement brusque est de fractionner rapidement l'extrait brut en trois parties. Plus tard le groupe qui contient les composés d'intérêt sera soumis à une purification supplémentaire. Le second groupe est donc obtenu avec 1,5 CV du système du mélange de solvants suivant : AcOEt:Isopropanol 4:1 v:v.

Ce second extrait est soumis à une seconde chromatographie sur colonne ouverte. Ainsi, 295,3 mg de ce groupe ont été ajoutés en charge sèche au sommet de la phase stationnaire comportant 11,0 g de silice, de granulométrie 15-40 µm. La phase mobile de cette seconde colonne est un gradient de Cyclohexane:EtOAc.

Sur la base de la chromatographie couche mince (Cyclohexane:AcOEt 30:70 v:v) et de l'HPLC, la fraction qui contient la Cry-1 est isolée. A partir de 25 g de biomasse sèche initiale, provenant de 36,7 L de culture, 23,3 mg de Cry-1 sont ainsi obtenus.

Un second protocole de fractionnement que nous avons développé est basé sur une méthode en une seule étape par chromatographie sur colonne flash. 1,17 L de culture dans des conditions optimales, telles que développées au chapitre 2, conduisent à un extrait de 0,8 g de biomasse sèche. Cet extrait a été soumis à une chromatographie sur colonne flash système "Isolera TM One (Biotage). Le fractionnement sur colonne est couplé à un auto-collecteur basé sur un spectromètre UV, qui a détecté les composés élués. Le spectromètre UV a été réglé pour balayer de 235 nm à 245 nm, qui sont les longueurs d'onde où Cry-1 est détecté. Le mode de gradient était basé sur une phase mobile Cyclohexane:EtOAc qui a été développée ci-dessus.

### Investigation phytochimique par analyse UHPLC-ESI-Q-TOF-HRMS<sup>2</sup> et mise en réseau moléculaire

La fraction obtenue à partir des deux méthodes développées a été soumise à une analyse ESI-Q-TOF-HRMS<sup>2</sup>. Un spectromètre de masse ESI-Q-TOF-HRMS<sup>2</sup> a été sélectionné, ce qui permet de combiner un quadripôle avec un analyseur de temps de vol. Le premier analyseur (Q) crée un champ électrostatique, qui permet aux ions de se déplacer en raison du changement de charge de l'électrode. Ce changement entraîne une séparation des ions par rapport à leur masse. Ensuite, les ions sont déplacés dans la cellule de collision, et sont soumis à une dissociation induite par la collision (CID). Pour illustrer mon propos, les paramètres utilisés pour notre étude sur la SEP/SM seront brièvement décrits ci-après.

La collecte des données a été effectuée en mode d'analyse dépendante des données (DDA) dans une fenêtre de masse de  $m/z$  150 à 1.200. Seuls trois ions précurseurs ont été sélectionnés parmi les ions les plus intenses et transmis dans la DDA où une énergie de collision moyenne de 30 eV a été appliquée. Sur la base des paramètres pertinents, nous avons développé une méthode UHPLC en phase inversée adaptée aux études par MS/MS d'extraits bruts de la souche *Nostoc* ou de fractions enrichies. Cette méthode est adaptée de celle utilisée pour la quantification de cryptophycine et utilise un gradient de solvants similaire. Le débit et la température de la colonne ont été fixés respectivement à 40 °C et 500  $\mu$ L/min. Le système de solvants était un mode à gradient de H<sub>2</sub>O/ACN. En ce qui concerne les réglages MS/MS, le mode était ESI positive-AutoMS/MS.

Les paramètres sur Auto-MS/MS étaient la sélection des 3 ions précurseurs les plus intenses dans la gamme de 150-1.200  $m/z$ , alors que l'énergie de collision était de 30 eV. La tension au capillaire était de 4.500 V. La pression au nébuliseur de gaz était de 2 bars, le débit de gaz sec était de 9 L/min à 200 °C. Concernant les réglages de détection, la gamme de masse était de 50-1650  $m/z$ , la fréquence d'acquisition était de 2 Hz (MS et MS/MS). Ensuite, nous avons paramétré une série de paramètres en relation avec le logiciel MZmine et le GNPS. MZmine est le logiciel pour le traitement des données obtenues tandis que le GNPS est lié à la construction des réseaux et à la correspondance des composés avec les bibliothèques d'extraits existantes en ligne.

### Étude des analogues de Cry et du profil phytochimique de *Nostoc* sp. à travers les réseaux moléculaires obtenus.

Cry-1 a d'abord été découverte dans la souche *Nostoc* sp. ATCC<sup>®</sup> 53789<sup>™</sup> (Schwartz R.E. *et al.* 1990, Hirsch C.F. *et al.* 1990) bien que par la suite tous les autres analogues aient été étudiés dans la souche *Nostoc* sp. GSV 224 en raison des rendements plus élevés en dérivés de série cryptophycine. Jusqu'à aujourd'hui, 28 analogues de Cry ont été caractérisés dans la souche *Nostoc* sp. GSV 224. Donc, comme *Nostoc* sp. ATCC 53789 est le seul producteur de cryptophycine disponible dans le

commerce, nous avons voulu examiner son profil phytochimique, et surtout examiner si elle produit d'autres analogues en série cryptophycine.

Un travail préliminaire sur les analogues potentiels de série cryptophycine produits par la souche pourrait être établie grâce aux réseaux moléculaires. La première étape, est d'étudier le fractionnement de témoins pour savoir à quels fragments nous devons nous attendre et leurs masses moléculaires respectives.

Pour la Cry-1 la fragmentation, qui aboutirait à la libération de l'acide carboxylique, pourrait se faire principalement de deux manières possibles, par une ouverture directe ou par un autre processus en deux étapes. La première voie est un clivage direct, tandis que la seconde est suivie d'un transfert d'hydroxyle (Golakoti T. *et al.* 1994, Niedermeyer T.H. and Strohm M. 2012). À partir de cette fragmentation, les principaux ions observés sont les unités C-D avec un adduit H<sub>2</sub>O à m/z 218 (selon les substrats des analogues dans ces unités), et les unités B-C-D à m/z 412, qui varient également selon les substrats des analogues. Ces valeurs concernent des fragments de Cry-1, de sorte que les valeurs réelles des analogues peuvent varier en raison de leurs différents substrats. (Golakoti T. *et al.* 1994, Nowruzi B. *et al.* 2012, Niedermeyer T.H. and Strohm M. 2012)

Sur la base des fragmentations proposées, nous faisons l'hypothèse que dans *Nostoc* sp. ATCC 53789, il y a neuf analogues série cryptophycine en plus de Cry-1. Il s'agit de Cry-2, -3, -4, -24, -176. De plus, il y a un des composés suivants : Cry-26,-39, 2 des Cry-50, -40, -16, -21, et un des composés parmi Cry-19, -28, 29. L'aire du pic des analogues de Cry dans l'extrait brut oriente sur les proportions des analogues. Ces proportions sont pertinentes avec les concentrations des analogues dans *Nostoc* sp. GSV 224.

Les analogues Cry -21,-16,-50,-40 sont des stéréo-isomères, ils ont donc la même masse moléculaire et leur identification ne peut se faire uniquement par les données de masse. Il en va de même pour les analogues Cry-30, -26 et les analogues Cry-29,-28,-19. Cependant, leurs proportions attendues, compte tenu de leurs pourcentages déjà connus dans *Nostoc* sp. GSV 224, orientent vers certains analogues. Ainsi, nous supposons qu'au n° 4 devrait se trouver Cry-21, au n° 5 Cry-30 et au n° 9 Cry-28. En ce qui concerne les variations des analogues de cryptophycine, nous avons comparé leurs proportions dans différentes phases de croissance et différentes conditions de culture. Comme prévu, en phase logarithmique, nous n'avons détecté pratiquement aucune production de cryptophycine, car la production de métabolites secondaires est attendue plus tard dans la courbe de croissance. En comparant les différentes conditions, nous avons noté que dans des conditions combinées -optimales- il y avait une production plus élevée des principaux analogues, comme Cry-1, -2, -4. Il faut remarquer que le réseau ne fournit qu'une première représentation semi-quantitative avec un faible niveau de



précision, donc des recherches supplémentaires sont nécessaires pour obtenir des données plus précises.

Cependant, nous avons réussi à annoter plus de noeuds à partir de la base des résultats du GNPS et des recherches bibliographiques. Nous identifions les nostocyclopeptides d'abord en fonction du m/z des ions, et dans un deuxième temps en fonction de leur temps de rétention. Plus précisément, ils ont été élués de 1,06 à 1,86, ce qui est conforme au fait qu'il s'agit de composés polaires.

En outre, les consultations de la bibliothèque en ligne sur le site du GNPS sont également un outil qui a contribué à l'annotation. Ainsi, nous avons obtenu un résultat pour le phéophorbide A. Le phéophorbide A (PPBa) est un tetrapyrrole. C'est un produit de dégradation de la chlorophylle. Plus précisément, le PPBa est un produit de déphytylation et de la démétallation de la chlorophylle a. Le cluster PPBa est relié à un ensemble de grappes multiples. Ce vaste complexe contient probablement des composés moins polaires tels que les chlorophylles et les lipides. Nous formulons cette hypothèse pour plusieurs raisons. Premièrement, le complexe est relié à l'amas de PPBa par de multiples arêtes, ce qui révèle sa proximité avec les composés de la chlorophylle. Ensuite, sur la base du temps de rétention des noeuds de 12,00 à 17,30 min, nous supposons qu'il s'agit de composés moins polaires qui ont été élués avec la "phase de lavage" en UHPLC. De plus, une autre raison qui justifie la caractérisation générale de ce complexe est la comparaison des extraits bruts de la phase logarithmique et de la phase exponentielle tardive. Ici, nous avons observé un rapport élevé de ces noeuds dans la phase logarithmique, ce qui signifie que les composés sont principalement des métabolites primaires.

## Conclusion générale et perspectives d'avenir

Pour récapituler, en examinant tout d'abord les paramètres de la lumière, nous avons montré que les intensités lumineuses élevées entraînent la mort des cellules, tandis qu'une intensité lumineuse moyenne convient à la croissance et à la production de métabolites. Ensuite, en comparant différentes longueurs d'onde, il a été mis en évidence que la lumière rouge-orange était optimale pour la production de Cry. Cela peut se produire car la lumière rouge-orange peut être absorbée par les deux photosystèmes PSI et PSII. Elle a une activité photosynthétique significativement plus élevée que le spectre bleu, qui n'est absorbé que par le PSI. Concernant la photopériode de la lumière, nous remarquons que même si le 16:8 (L:D) et la lumière constante ont un effet similaire sur les modèles de croissance, la lumière continue produit une quantité sensiblement plus élevée de métabolites. Cela indique que la production de Cry pourrait être un processus dépendant de la lumière. Dans des conditions non lumineuses, le micro-organisme fournit l'énergie limitée produite pour répondre à ses priorités de survie et non à la production de métabolites secondaires.

Les niveaux de nitrates dans la composition du milieu ont également été examinés pour étudier l'implication des hétérocystes sur le processus d'expression de Cry. Il a été montré que, en l'absence d'azote, la formation d'hétérocystes. Les cellules assurent les besoins primaires et consomment les quelques réserves d'azote, de sorte que le niveau de production de Cry dans la culture est nettement inférieur. La plage optimale de pH est indiquée comme étant de 8,5 à 9,0, tandis que la production de Cry est significativement inhibée à  $T > 30^{\circ}\text{C}$ . Il a également été démontré que l'application d'une combinaison des conditions optimales développées avait un effet synergique positif. Enfin, nous avons comparé les cultures en flacon aux conditions de mise à l'échelle en photobioréacteur (culture dans 15 L de PBR) qui a une conséquence positive sur la production de Cry-1. Un autre résultat important a été la mise au point de méthodes de quantification des métabolites à partir de petits volumes de cultures. Comme nous avons examiné des échantillons biologiques, la méthode de quantification devrait être : a) rapide (nous devrions avoir les données quantitatives le même jour que l'échantillonnage), b) précise (le volume de l'échantillon était petit en raison de la culture en flacon et de la concentration de métabolites significativement faible), c) répétitive (chaque test consiste en trois répliques biologiques et techniques, qui acquièrent une répétabilité). Ces techniques d'extraction-quantification développées pourraient être appliquées à l'examen de toute une série d'échantillons biologiques, avec une adaptation appropriée de la méthode CLHP.

Enfin, le profil phytochimique de la souche a été étudié, car seuls des nostocyclopeptides et de la cryptophycine 1 ont été identifiés sur la souche à ce jour. La souche a été cultivée en photobioréacteur, et les méthodes d'isolement et de purification ont été développées. Les extraits obtenus ont été soumis à une analyse UHPLC-ESI-Q-TOF-HRMS<sup>2</sup>. Les résultats ont été traités par les logiciels MZmine et GNPS, et présentés dans des réseaux moléculaires. Concernant l'empreinte moléculaire générale, nous avons identifié les produits de dégradation de la chlorophylle et vérifié la présence de nostocyclopeptides. La découverte des analogues de Cry a été particulièrement intéressante, car nous avons réussi à identifier et à préciser les proportions relatives de 9 analogues non détectés auparavant dans cette souche. L'approche des réseaux moléculaires ainsi que les expériences sur les conditions de culture ont montré que la concentration de Cry atteint son maximum entre le milieu et la fin de la phase exponentielle. En outre, des données sur l'activité biologique pourraient être incluses dans le réseau actuel pour indiquer les composés actifs potentiels. Plus précisément, Cry-1 a démontré de faibles valeurs de la CI50 sur les lignées cellulaires KB, LoVo et SKOV3. Des essais, comme ceux mentionnés, pourraient aider à l'annotation des composés potentiellement cytotoxiques, et contribuer à la poursuite de l'analyse ciblée.

Plusieurs perspectives pourraient être examinées sur la base des résultats obtenus et des méthodes développées. Comme mentionné ci-dessus, la combinaison des conditions développées a permis

d'obtenir le rendement maximal de Cry, tandis que la culture à grande échelle a permis d'augmenter encore plus la production. Ces résultats sont compatibles avec une exploitation industrielle.

## Références bibliographiques

1. Andersen R.A., The Microalgal Cell., 2002, In *Handbook of Microalgal Culture*, John Wiley & Sons, 3-21
2. Barbosa M.J., Wijffels R.H., Biofuels from microalgae., 2013, In *Handbook of Microalgal Culture*, John Wiley & Sons, 566-577
3. Biondi N., Piccardi R., Margheri M.C., Rodolfi L., Smith G.D., Tredici M.R., Evaluation of Nostoc strain ATCC 53789 as a potential source of natural pesticides., 2004, *Appl. Environ. Microbiol.*, 70, 6, 3313-3320
4. Bláha L., Babica P., Maršálek B., Toxins produced in cyanobacterial water blooms-toxicity and risks., 2009, *Interdiscip. Toxicol.*, 2, 2, 36-41
5. Blankenship R.E., Origin and evolution of photosynthesis, In *Molecular Mechanisms of Photosynthesis*, 2002, John Wiley & Sons., 220-257
6. Chmelík D., Hrouzek P., Fedorko J., Vu D.L., Urajová P., Mareš J., Červený J., Accumulation of cyanobacterial oxadiazinenucolin A is enhanced by temperature shift during cultivation and is promoted by bacterial co-habitants in the culture, 2019, *Algal Res.*, 44, 101673, 1-8
7. da Fontoura Prates D., Radmann E.M., Duarte J.H., de Moraes M.G., Costa J.A.V., Spirulina cultivated under different light emitting diodes: Enhanced cell growth and phycocyanin production., 2018, *Bioresour. Technol.*, 256, 38-43.
8. Dembitsky V.M., Rezanka T., Metabolites produced by nitrogen-fixing Nostoc species., 2005, *Folia Microbiol.*, 50, 5, 363-391
9. Eldin M.J., Kanhaiya K., Debabrata D., Physicochemical parameters optimization, and purification of phycobiliproteins from the isolated Nostoc sp., 2014, *Bioresour. Technol.*, 166, 541-547
10. Ferrão-Filho A.S., Kozłowski-Suzuki B., Cyanotoxins: bioaccumulation and effects on aquatic animals., 2011, *Mar. Drugs*, 9, 12, 2729-2772
11. Golakoti T., Ogino J., Heltzel C.E., Le Husebo T., Jensen C.M., Larsen L.K., Patterson G.M.L., Moore R.E., Mooberry S.L., Corbett T.H., Valeriote, F. A., Structure determination, conformational analysis, chemical stability studies, and antitumor evaluation of the cryptophycins. Isolation of 18 new analogs from Nostoc sp. strain GSV 224., 1995, *J. Am. Chem. Soc.*, 117, 49, 12030-12049
12. Golakoti T., Ohtani I., Patterson G. M., Moore R. E., Corbett T.H., Valeriote F.A., Demchik L., Total structures of cryptophycins, potent antitumor depsipeptides from the blue-green alga Nostoc sp. strain GSV 224., 1994, *J. Am. Chem. Soc.*, 116, 11, 4729-4737
13. Golakoti T., Yoshida W.Y., Chaganty S., Moore R.E., Isolation and structure determination of nostocyclopeptides A1 and A2 from the terrestrial cyanobacterium Nostoc sp. ATCC53789., 2001, *J. Nat. Prod.*, 64, 54-59
14. Golakoti T., Yoshida W.Y., Chaganty S., Moore R.E., Isolation and structures of nostopeptolides A1, A2 and A3 from the cyanobacterium Nostoc sp. GSV224., 2000, *Tetrahedron*, 56, 46, 9093-9102
15. Guckert J.B., Cooksey K.E., Triglyceride accumulation and fatty acid profile changes in Chlorella (Chlorophyta) during high pH-induced cell cycle inhibition, 1990, *J. Phycol.*, 26, 72-79
16. Hirsch C.F., Liesch J.M., Salvatore M.J., Schwartz R.E., Sesin D.F., U.S. Patent No. 4,946,835., 1990, Washington, DC: U.S. Patent and Trademark Office.
17. Hitzfeld B.C., Höger S.J., Dietrich D.R., Cyanobacterial toxins: removal during drinking water treatment, and human risk assessment., 2000, *Environ. Health Perspect.*, 108, 1, 113-122
18. Hoiczky E., Hansel A., Cyanobacterial cell walls: news from an unusual prokaryotic envelope., 2000, *J. Bacteriol.*, 182, 5, 1191-1199.
19. Hongsthong A., Bunnag B., Overview of Spirulina: biotechnological, biochemical and molecular biological aspects., 2009, In *Handbook on Cyanobacteria: Biochemistry, Biotechnology and Applications*, Nova Science Publishers, 51-103

20. Jacob-Lopes E., Scoparo C.H.G, Lacerda L.M.C.F, Franco T.T, Effect of light cycles (night/day) on CO<sub>2</sub> fixation and biomass production by microalgae in photobioreactors, 2009, *Chem. Eng. process*, 48, 1, 306-310
21. Jaki B., Orjala J., Sticher O., A novel extracellular diterpenoid with antibacterial activity from the cyanobacterium *Nostoc commune*., 1999, *J. Nat. Prod.*, 62, 3, 502-503
22. Jordan M.A., Mechanism of action of antitumor drug that interact with microtubules and tubulin., 2002, *Curr. Med. Chem. Anticancer Agents*, 2, 1, 1-17
23. Kaplan-Levy R.N., Hadas O., Summers M.L., Rücker J., Sukenik A., Akinetes: dormant cells of cyanobacteria., 2010, *In Dormancy and resistance in harsh environments*, Springer, 5-27
24. Khajepour F., Hosseini S.A., Nasrabadi R.G., Effect of Light Intensity and Photoperiod on Growth and Biochemical Composition of a Local Isolate of *Nostoc calcicole*., 2015, *Appl. Biochem. Biotechnol.*, 176, 8, 2279-2289
25. Kobayashi M., Kurosu M., Ohyabu N., Wang W., Fujii S., Kitagawa I., The absolute stereostructure of arenastatin A, a potent cytotoxic depsipeptide from the Okinawan marine sponge *Dysidea Arenaria*, 1994, *Chem. Pharm. Bull.*, 42, 10, 2196-2198
26. Kobayashi M., Kurosu M., Wang W., Kitagawa I., A total synthesis of Arenastatin A, an extremely potent cytotoxic depsipeptide, from the Okinawan marine sponge *Dysidea Arenaria*., 1994, *Chem. Pharm. Bull.*, 42, 11, 2394-6
27. Kuan D., Duff S., Posarac D., Bi X., Growth optimization of *Synechococcus elongatus* PCC7942 in lab flasks and a 2-D photobioreactor., 2015, *Can. J. Chem. Eng.*, 93, 4, 640-647
28. Kurmayer R., The toxic cyanobacterium *Nostoc* sp. strain 152 produces highest amounts of microcystin and nostophycin under stress conditions, 2011, *J. Phycol.*, 47, 1, 200-207
29. Liaimer A., Jenke-Kodama H., Ishida K., Hinrichs K., Stangeland J., Hertweck C., Dittmann E. A polyketide interferes with cellular differentiation in the symbiotic cyanobacterium *Nostoc punctiforme*., 2011, *Environ. Microbiol. Rep.*, 3, 5, 550-558
30. Luesch H., Harrigan G.G., Goetz G., Horgen F.D., The cyanobacterial origin of potent anticancer agents originally isolated from sea hares., 2002, *Curr. Med. Chem.*, 9, 20, 1791-1806
31. Ma R., Lu F., Bi Y., Effects of light intensity and quality on phycobiliprotein accumulation in the cyanobacterium *Nostoc sphaeroides* Kütz., 2015, *Biotechnol. Lett.*, 37, 8, 1663-1669
32. Meeks J.C., Campbell E.L., Summers M.L., Wong F.C., Cellular differentiation in the cyanobacterium *Nostoc punctiforme*., 2002, *Arch. Microbiol.*, 178, 6, 395-403
33. Nicolaisen K, Hahn A, Schleiff E., The cell wall in heterocyst formation by *Anabaena* sp. PCC 7120, 2009, *J. Basic Microbiol.*, 49, 5-24
34. Niedermeyer T.H., Strohalm M., mMass as a software tool for the annotation of cyclic peptide tandem mass spectra., 2012, *PLoS one*, 7, 9, e44913.
35. Nowruzi B., Khavari-Nejad R., Sivonen K., Kazemi B., Najafi F., Nejad Sattari T. Identification and toxigenic potential of *Nostoc* sp., 2012, *Algae*, 27:303-313
36. Nozzi N.E., Oliver J.W., Atsumi S., Cyanobacteria as a platform for biofuel production., 2013, *Front. Bioeng. Biotechnol.*, 1, 7, 1-6
37. Oh H.S., Lee C.S., Srivastava A., Oh H.M., Ahn C.Y., Effects of Environmental Factors on Cyanobacterial Production of Odorous Compounds: Geosmin and 2-Methylisoborneol., 2017, *J. Microbiol. Biotechnol.*, 7, 1316-1323
38. Paerl H.W., Paul V.J., Climate change: links to global expansion of harmful cyanobacteria., 2012, *Water Res.*, 46, 5, 1349-1363
39. Panda D., Himes R.H., Moore R.E., Wilson L., Jordan M.A., Mechanism of Action of the Unusually Potent Microtubule Inhibitor Cryptophycin, 1997, *Biochemistry*, 36, 12948-12953
40. Park H.D., Yokoyama A., Okino T., Fate of microcystin in Lake Suwa., 2001, *Japanese J. Limnology*, 62, 3, 229-248.
41. Patterson P., Antiviral activity of blue-green algae cultures., 1993, *J. phycol.*, 29, 125-30.
42. Qian F., Dixon D.R., Newcombe G., Ho L., Dreyfus J., Scales P.J., The effect of pH on the release of metabolites by cyanobacteria in conventional water treatment processes, 2014, *Harmful Algae*, 39, 253-258
43. Ray S., Bagchi S.N., Nutrients and pH regulate algicide accumulation in cultures of the cyanobacterium *Oscillatoria aetivirens*, 2001, *New Phytol.*, 149, 455-460

44. Robert A.B., Calvyn S., Fitje L., Remmy E.M., Jimmy P., Stefan K., Alexander B., Ekaterina E., Gabrielle K., Terrein and Butyrolacton VII, Ant. biotically Active Compounds from Symbiotic Fungus *Aspergillus Terreus* Isolated from *Ascidian Didemnum*, 2018, *Molle. Biomed. J. Sci&Tech. Res.*, 9, 4, 7288-7292
45. Sang M., Wang M., Liu J., Zhang C., Li A., Effects of Temperature, Salinity, Light Intensity, and pH on the Eicosapentaenoic Acid Production of *Pinguicoccus pyrenoidosus*, 2012, *J. Ocean Univ. China*, 11, 2, 181-186
46. Schwartz R.E., Hirsch C.F., Sesin D.F., Flor J.E., Chartrain M., Fromtling R. E., Harris G.H., Salvatore M.J., Liesch J.M., Yudin, K., Pharmaceuticals from cultured algae., 1990 *J. Ind. Microbiol.*, 5, 113-123
47. Sheehan J., Dunahay T., Benemann J., Roessler P., A look back at the US Department of Energy's aquatic species program: biodiesel from algae., 1998, *National Renewable Energy Laboratory*, 328, 1-294
48. Siegel R.L., Miller K.D., Jemal A., Cancer statistics, 2019., 2019, *CA Cancer J. Clin.*, 69, 7-34
49. Simmons T.L., Andrianasolo E., McPhail K., Flatt P., Gerwick W.H., Marine natural products as anticancer drugs., 2005, *Mol. Cancer Ther.*, 4, 2, 333-342
50. Singh R.K., Tiwari S.P., Rai A.K., Mohapatra T.M., Cyanobacteria: an emerging source for drug discovery., 2011, *J. Antibiot.*, 64, 6, 401-412
51. Sivonen K., Effects of light, temperature, nitrate, orthophosphate, and bacteria on growth of and hepatotoxin production by *Oscillatoria agardhii* strains., 1990, *Appl. Environ. Microbiol.*, 56, 9, 2658-2666
52. Smith C.D., Zhang X., Mechanism of Action of Cryptophycin: Interaction with the Vinca alkaloid domain of tubulin, 1996, *J. Biol. Chem.*, 271, 6192-6198
53. Smith C.D., Zhang X., Mooberry S.L., Patterson G.M.L, Moore R.E., Cryptophycin: A New Antimicrotubule Agent Active against Drug-resistant Cells, 1994, *Cancer Research* 54, 3779-3784
54. van Alphen P., Abedini Najafabadi H., Branco dos Santos F., Hellingwerf K.J., Increasing the photoautotrophic growth rate of *Synechocystis* sp. PCC 6803 by identifying the limitations of its cultivation., 2018, *Biotechnol. J.*, 13, 8, 1700764
55. van der Westhuizen A.J., Eloff J.N, Effect of temperature and light on the toxicity and growth of the blue-green alga *Microcystis aeruginosa* (UV-006), 1985, *Planta*, 163, 1, 55-59
56. Vargas M.A., Rodriguez H., Moreno J., Olivares H., Campo J.D., Rivas J., Guerrero M.G., Biochemical composition and fatty acid content of filamentous nitrogen-fixing cyanobacteria., 1998, *J. Phycol.*, 34, 5, 812-817
57. Vermaas W.F., Photosynthesis and respiration in cyanobacteria., 2001, In *eLS*
58. Vijayakumar S., Menakha M., Pharmaceutical applications of cyanobacteria—A review., 2015, *J. Acute Med.*, 5, 1, 15-23
59. Watanabe M.F., A highly toxic strain of the blue-green alga *Microcystis aeruginosa* isolated from Lake Suwa., 1983, *Nippon Suisan Gakkaishi*, 49, 1759-1765
60. Watanabe M.F., Oishi S., Effects of environmental factors on toxicity of a cyanobacterium (*Microcystis aeruginosa*) under culture conditions., 1985, *Appl. Environ. Microbiol.*, 49, 5, 1342-1344
61. Weiss C., Sammet B., Sewald N., Recent approaches for the synthesis of modified cryptophycins., 2013, *Nat. Prod. Rep.*, 30, 7, 924-940
62. Wijffels R.H., Barbosa M.J., Eppink M.H., Microalgae for the production of bulk chemicals and biofuels., 2010, *Biofuel Bioprod. Biorefin.*, 4, 3, 287-295
63. Wilhelm C., Jakob T., From photons to biomass and biofuels: evaluation of different strategies for the improvement of algal biotechnology based on comparative energy balances., 2011, *Appl. Microbiol. Biotechnol.*, 92, 5, 909-919
64. Zanchett G., Oliveira-Filho E.C., Cyanobacteria and cyanotoxins: from impacts on aquatic ecosystems and human health to anticarcinogenic effects., 2013, *Toxins*, 5, 10, 1896-1917
65. Zheng T., Zhou M., Yang L., Wang Y., Wang Y., Meng Y., Liu J., Zuo Z., Effects of high light and temperature on *Microcystis aeruginosa* cell growth and  $\beta$ -cyclocitral emission, 2020, *Ecotoxicol. Environ. Saf.*, 192, 110313, 1-8

Improvement of the production of a secondary metabolite with potent anticancer activity in cyanobacterium *Nostoc* sp. ATCC 53789, using abiotic stress. Phytochemical investigation of this strain.

Cyanobacteria is one of the most ancient and largest groups of bacteria on Earth. They produce a range of compounds useful for human and its activities, from biofuels to nutrition. They also, however, produce secondary metabolites with toxic effect, the cyanotoxins. The study of these toxins may lead to novel pharmaceutical agents. We examined the cyanotoxin cryptophycin-1, as it has been reported to possess significant anticancer properties. It interacts with tubulin's *Vinca* domain and disrupts the microtubule's dynamics leading to apoptosis. Unfortunately, despite its high potency, its synthesis provides insufficient yield for industrial use. However, stressing cyanobacteria by modification of the culture's environmental conditions, can be a means for increasing metabolite's production yield. Our work was performed with *Nostoc* sp. ATCC 53789 which is currently the only commercially available strain among the three species producing this metabolite. We examined a range of abiotic culture parameters in relation to light conditions (photoperiod, intensity, wavelength), pH, temperature and medium composition. Then, the synergic effect of combined conditions was evaluated, as well as the effect of high-scale cultivation in a photobioreactor. Growth was measured and metabolite concentration was calculated through an HPLC method, developed for small-volumes quantification. Growth and toxin's productivity curves were then drawn. It was concluded that orange-red constant light of medium intensities provided the optimum yield. Nitrates were also needed in medium, while the strain performed better at 25 °C and in a pH range 8.5-9.0. Moreover, the combined conditions were shown to have a positive synergic effect, while the cultivation in a photobioreactor increased significantly the obtained yield, even if the growth rate was lower. In addition to the examination of cryptophycin-1, the total molecular fingerprint of the strain was examined by molecular networks from UHPLC-ESI-Q-TOF-HRMS<sup>2</sup> analysis. Finally, these results indicate the presence of 9 cryptophycin-analogues and their respective proportions in *Nostoc* sp. ATCC 53789, unidentified in this strain to this date. Through the molecular networks' aspect, the analogues were observed to be mostly expressed in the late exponential phase and under the developed combined optimal culture conditions, the major analogues seemed to be overexpressed. The results of this work set the grounds for further research and industrial exploitation in the field of novel cyanobacterial anticancer agents.

**Keywords:** Cryptophycin; *Nostoc* sp. ATCC 53789; cyanotoxin; abiotic stress; photobioreactor; molecular networking; UHPLC-HRMS<sup>2</sup>